



**HAL**  
open science

# Dimères d'acides résiniques et de dérivés de la lignine : nouveaux précurseurs pour la synthèse de polymères bio-sourcés

Audrey Llevot

► **To cite this version:**

Audrey Llevot. Dimères d'acides résiniques et de dérivés de la lignine : nouveaux précurseurs pour la synthèse de polymères bio-sourcés. Polymères. Université de Bordeaux, 2014. Français. NNT : 2015BORD0323 . tel-01171452

**HAL Id: tel-01171452**

**<https://theses.hal.science/tel-01171452>**

Submitted on 3 Jul 2015

**HAL** is a multi-disciplinary open access archive for the deposit and dissemination of scientific research documents, whether they are published or not. The documents may come from teaching and research institutions in France or abroad, or from public or private research centers.

L'archive ouverte pluridisciplinaire **HAL**, est destinée au dépôt et à la diffusion de documents scientifiques de niveau recherche, publiés ou non, émanant des établissements d'enseignement et de recherche français ou étrangers, des laboratoires publics ou privés.

THÈSE PRÉSENTÉE  
POUR OBTENIR LE GRADE DE  
**DOCTEUR DE**  
**L'UNIVERSITÉ DE BORDEAUX**

ÉCOLE DOCTORALE DES SCIENCES CHIMIQUES

SPÉCIALITÉ : POLYMÈRES

Par Audrey, LLEVOT

**Dimères d'acides résiniques et de dérivés de la lignine :  
nouveaux précurseurs pour la synthèse de polymères bio-  
sourcés**

**Resinic acid and lignin derivative dimers : new precursors for the synthesis of  
biobased polymers**

Sous la direction de : Pr. Henri, CRAMAIL  
co-directeur : Pr. Stéphane, CARLOTTI et Prof. Stéphane GRELIER

Soutenance prévue le 10 décembre 2014

Membres du jury :

M. COQUERET, Xavier  
Mme. BAUMBERGER, Stéphanie  
M. CAILLOL, Sylvain  
M. CRAMAIL, Henri  
M. CARLOTTI, Stéphane  
M. GRELIER, Stéphane

Professeur, Université Reims  
Professeur, AgroParisTech  
Ingénieur de recherches, ENSCM-CNRS  
Professeur, Université Bordeaux  
Professeur, Université Bordeaux  
Professeur, Université Bordeaux

Président du jury  
Rapporteur  
Rapporteur  
Directeur de thèse  
Directeur de thèse  
Directeur de thèse



« Votre succès et votre bonheur reposent en vous-mêmes. Prenez la résolution de rester heureux, et votre joie formera un véritable bouclier contre les difficultés »

« Quand on y croit, on a plus de chance de réussir »

Hellen Keller



# Remerciements

---

La réalisation de ses travaux n'aurait pas été possible sans de nombreuses personnes que je tiens à remercier.

Tout d'abord un immense merci à mes trois directeurs de thèse, les professeurs Henri Cramail, Stéphane Carlotti et Stéphane Grelier pour leur encadrement, leur enthousiasme et leur motivation au quotidien. Travailler auprès de vous a confirmé et même augmenté mon intérêt pour la recherche académique. Plus particulièrement, je remercie le Pr Henri Cramail pour la confiance qu'il m'a accordée, depuis l'instant où il m'a accepté en thèse dans son groupe de recherche, jusqu'à l'obtention de mon post doc ! Je remercie le Pr Stéphane Carlotti pour son écoute, son soutien et ses conseils tout au long de ma thèse, qui ont su me maintenir motivée. Et enfin, je remercie le Pr Stéphane Grelier (avec qui j'ai eu la chance de partager son bureau) pour ses nombreuses idées, sa simplicité, son sourire quotidien et ses conseils pour ma future carrière. La Laccase est entre de bonnes mains et n'a pas fini de faire parler d'elle !

Je tiens également à remercier le Dr Etienne Grau qui est arrivé au cours de ma thèse et qui a été disponible pour m'aider avec l'acide abiétique, pour réaliser des calculs DFT et corriger mes différents travaux.

Ensuite, je suis très reconnaissante au Dr Sylvain Caillol et au professeur Stéphanie Baumberger d'avoir accepté d'être les rapporteurs de cette thèse ainsi qu'au professeur Xavier Coqueret d'avoir accepté d'examiner ses travaux.

Je tiens à souligner la participation à ces travaux de mes stagiaires, Licences, Masters ou Ingénieurs : notamment Léa Bonnot et Thibaud Geoffroy qui ont eu la lourde tâche de travailler avec l'acide abiétique, merci pour vos efforts et surtout votre bonne humeur qui a survécu à tous les isomères, mais aussi Adeline Miquelot pour son aide pour l'optimisation des conditions réactionnelles employant la Laccase et Thomas Lesgourgues pour la synthèse de résines époxy.

Je tiens également à exprimer ma sympathie à l'ensemble du personnel permanent du LCPO, notamment à Catherine, Corinne, Mimi, Bernadette, Nicole et Loic qui participent quotidiennement au bon fonctionnement du laboratoire, ainsi qu'à toutes les personnes que j'ai eu la chance d'avoir en tant qu'enseignants et qui m'ont donné l'envie de me spécialiser

dans les polymères et finalement, ceux avec qui je suis partie en congrès et que j'ai pu apprécier dans un contexte différent.

A mes yeux, il est indispensable de remercier toutes les personnes qui sont responsables des appareils de mesures, qui les entretiennent et qui ont eu la gentillesse de me former : Anne-Laure pour la RMN, Nico pour la SEC (mais aussi la pelote et pour ton énergie débordante), Eric et Yannick dont j'admire la patience dont ils font preuve respectivement avec la HPLC et la Flash, puis la GC. Enfin, j'exprime toute ma gratitude à la Dream team, Cédric, Manu et Gégé pour tous les éclats de rire qu'ils ont provoqué mais surtout pour les multiples caractérisations thermo-mécaniques parfois de l'extrême, sur des quantités microscopiques, je m'excuse d'avoir autant insisté...

Enfin un grand merci à tous les post doctorants, ex doctorants, doctorants et stagiaires qui j'ai rencontré au LCPO pendant mes 3 années de thèses : Chris, Vincent, Katerina, Antoine, Maréva, Célia, Jules, Paul, Estelle, Blandine, Maud, Olivia, Alex, Carine, Elise, Eleni, Efty, Chrystilla, Samira, Anne-Laure, Arvind, Yuki, Winnie, Romain, Silvia, Charlotte, Camille, Jun, Na, Feifei, Mathilde, Coraline, Giordano, Romain, Edgar, Déborah, Laurie, Jérémie, Tapas, Dounia et bien d'autres encore...). Une mention spéciale au labo N0-36, Lise et Thomas qui m'ont bien intégré à mon arrivée et qui m'ont montré la route à suivre, Prakash, Océane, Geoffrey et PL qui je suis sûre vont conserver le dynamisme du labo, l'esprit du tabouret et des colonnes... Enfin un grand merci à la Carlotti team : Christos, Kévin, Maéva (??? c'est sa place la plus appropriée dans les remerciements), Junior et Clément qui ont toujours su me redonner le sourire sur qui j'ai pu compter (et j'espère que ça va durer) et à Enrique, arrivé tardivement mais que j'ai beaucoup apprécié côtoyer.

Enfin, je remercie toute ma famille, mes amis (Boucau city) et particulièrement mes parents qui m'ont toujours soutenu.



« Votre succès et votre bonheur reposent en vous-mêmes. Prenez la résolution de rester heureux, et votre joie formera un véritable bouclier contre les difficultés »

« Quand on y croit, on a plus de chance de réussir »

Hellen Keller

# Remerciements

---

La réalisation de ses travaux n'aurait pas été possible sans de nombreuses personnes que je tiens à remercier.

Tout d'abord un immense merci à mes trois directeurs de thèse, les professeurs Henri Cramail, Stéphane Carlotti et Stéphane Grelier pour leur encadrement, leur enthousiasme et leur motivation au quotidien. Travailler auprès de vous a confirmé et même augmenté mon intérêt pour la recherche académique. Plus particulièrement, je remercie le Pr Henri Cramail pour la confiance qu'il m'a accordée, depuis l'instant où il m'a accepté en thèse dans son groupe de recherche, jusqu'à l'obtention de mon post doc ! Je remercie le Pr Stéphane Carlotti pour son écoute, son soutien et ses conseils tout au long de ma thèse, qui ont su me maintenir motivée. Et enfin, je remercie le Pr Stéphane Grelier (avec qui j'ai eu la chance de partager son bureau) pour ses nombreuses idées, sa simplicité, son sourire quotidien et ses conseils pour ma future carrière. La Laccase est entre de bonnes mains et n'a pas fini de faire parler d'elle !

Je tiens également à remercier le Dr Etienne Grau qui est arrivé au cours de ma thèse et qui a été disponible pour m'aider avec l'acide abiétique, pour réaliser des calculs DFT et corriger mes différents travaux.

Ensuite, je suis très reconnaissante au Dr Sylvain Caillol et au professeur Stéphanie Baumberger d'avoir accepté d'être les rapporteurs de cette thèse ainsi qu'au professeur Xavier Coqueret d'avoir accepté d'examiner ses travaux.

Je tiens à souligner la participation à ces travaux de mes stagiaires, Licences, Masters ou Ingénieurs : notamment Léa Bonnot et Thibaud Geoffroy qui ont eu la lourde tâche de travailler avec l'acide abiétique, merci pour vos efforts et surtout votre bonne humeur qui a survécu à tous les isomères, mais aussi Adeline Miquelot pour son aide pour l'optimisation des conditions réactionnelles employant la Laccase et Thomas Lesgourgues pour la synthèse de résines époxy.

Je tiens également à exprimer ma sympathie à l'ensemble du personnel permanent du LCPO, notamment à Catherine, Corinne, Mimi, Bernadette, Nicole et Loic qui participent quotidiennement au bon fonctionnement du laboratoire, ainsi qu'à toutes les personnes que j'ai eu la chance d'avoir en tant qu'enseignants et qui m'ont donné l'envie de me spécialiser

dans les polymères et finalement, ceux avec qui je suis partie en congrès et que j'ai pu apprécier dans un contexte différent.

A mes yeux, il est indispensable de remercier toutes les personnes qui sont responsables des appareils de mesures, qui les entretiennent et qui ont eu la gentillesse de me former : Anne-Laure pour la RMN, Nico pour la SEC (mais aussi la pelote et pour ton énergie débordante), Eric et Yannick dont j'admire la patience dont ils font preuve respectivement avec la HPLC et la Flash, puis la GC. Enfin, j'exprime toute ma gratitude à la Dream team, Cédric, Manu et Gégé pour tous les éclats de rire qu'ils ont provoqué mais surtout pour les multiples caractérisations thermo-mécaniques parfois de l'extrême, sur des quantités microscopiques, je m'excuse d'avoir autant insisté...

Enfin un grand merci à tous les post doctorants, ex doctorants, doctorants et stagiaires qui j'ai rencontré au LCPO pendant mes 3 années de thèses : Chris, Vincent, Katerina, Antoine, Maréva, Célia, Jules, Paul, Estelle, Blandine, Maud, Olivia, Alex, Carine, Elise, Eleni, Efty, Chrystilla, Samira, Anne-Laure, Arvind, Yuki, Winnie, Romain, Silvia, Charlotte, Camille, Jun, Na, Feifei, Mathilde, Coraline, Giordano, Romain, Edgar, Déborah, Laurie, Jérémie, Tapas, Dounia et bien d'autres encore...). Une mention spéciale au labo N0-36, Lise et Thomas qui m'ont bien intégré à mon arrivée et qui m'ont montré la route à suivre, Prakash, Océane, Geoffrey et PL qui je suis sûre vont conserver le dynamisme du labo, l'esprit du tabouret et des colonnes... Enfin un grand merci à la Carlotti team : Christos, Kévin, Maéva (??? c'est sa place la plus appropriée dans les remerciements), Junior et Clément qui ont toujours su me redonner le sourire sur qui j'ai pu compter (et j'espère que ça va durer) et à Enrique, arrivé tardivement mais que j'ai beaucoup apprécié côtoyer.

Enfin, je remercie toute ma famille, mes amis (Boucau city) et particulièrement mes parents qui m'ont toujours soutenu.

## GENERAL TABLE OF CONTENTS

<b>Résumé en français.....</b>	<b>1</b>
<b>Scientific production .....</b>	<b>9</b>
<b>List of abreviations.....</b>	<b>11</b>
<b>General introduction.....</b>	<b>13</b>

### **Chapitre 1: Polymerization and dimerization of resinic acids and phenolic compounds potentially derived from lignin: state of the art**

<b>I Resinic acids, polycyclic biobased synthons.....</b>	<b>26</b>
<b>1. Abietic acid extraction, production and use .....</b>	<b>26</b>
<b>2. Abietic acid thermoset polymers.....</b>	<b>27</b>
1) Synthesis and properties of rosin vinyl ester resins.....	28
2) Synthesis and properties of epoxy resin curing agents from rosin .....	30
3) Synthesis of epoxy compounds from abietic acid derivatives and used in epoxy resin formulations .....	33
<b>3. Abietic acid thermoplastic polymers .....</b>	<b>37</b>
1) Synthesis and properties of rosin pendant chain polymers.....	38
2) Synthesis and properties of polymers with rosin derivatives in the main chain.....	46
<b>4. Abietic acid dimerization.....</b>	<b>52</b>
<b>II Chemical modification and polymerization of aromatic synthons potentially derived from lignin.....</b>	<b>55</b>
<b>1. Vanillin extraction, production and utilization .....</b>	<b>56</b>
<b>2. Synthesis and properties of thermoset polymers from vanillin and eugenol.....</b>	<b>57</b>
1) Synthesis and properties of vinyl ester resins derived from vanillin.....	57
2) Synthesis and properties of cyanate ester thermosets derived from vanillin.....	58

3) Synthesis of epoxy resins from compounds potentially derived from lignin .....	59
<b>3. Synthesis and properties of thermoplastic polymers from phenol potentially derived from lignin.....</b>	<b>62</b>
1) Synthesis of thermotropic polymers from vanillic acid.....	63
2) Synthesis of fully biobased poyesters from vanillin, syringaldehyde and ferulic acid.....	67
3) Synthesis and properties of vanillin-based polyoxalate.....	71
4) Coupling of lignin derivatives, building blocks for polymer synthesis.....	71
<b>4. Vanillin dimer synthesis: promising synthon for polymer synthesis.....</b>	<b>75</b>
1) Synthesis of divanillin <i>via</i> chemical methods.....	76
2) Synthesis of divanillin <i>via</i> enzymatic coupling .....	76
<b>5. Laccase-catalyzed oxidative phenolic coupling .....</b>	<b>77</b>
1) Biochemical, structural characteristic and reaction mechanism of laccases .....	77
2) Laccases-catalyzed oxidative coupling phenolic compound .....	79
<b>III REFERENCES.....</b>	<b>87</b>

## CHAPTER 2: Abietic acid dimer synthesis and purification towards new biobased polymers

<b>I Introduction .....</b>	<b>95</b>
<b>II Abietic acid dimer synthesis .....</b>	<b>95</b>
<b>1. Abietic acid dimerization, purification and characterization .....</b>	<b>96</b>
1) Dimerization of abietic acid.....	96
2) Isolation of abietic acid dimers .....	97
3) Characterization of the abietic acid dimers.....	101
<b>2. Investigation of the dimerization mechanism of abietic acid .....</b>	<b>102</b>
<b>3. Optimization of the dimerization of abietic acid .....</b>	<b>105</b>
1) Influence of the monomer purity on the dimerization of abietic acid .....	105



2) Experimental condition screening of abietic acid dimerization.....	107
<b>III Synthesis of polyesters from abietic acid dimers via direct polycondensation .....</b>	<b>109</b>
1. Polycondensation of abietic acid dimers .....	109
2. Thermomechanical properties of abietic acid dimer copolymers.....	111
<b>IV Synthesis of unsaturated polyester via ADMET polymerization.....</b>	<b>113</b>
1. Bis-unsaturated abietic ester dimer synthesis and characterization .....	113
2. ADMET polymerization of bis-unsaturated abietic ester dimers.....	114
1) Chemical structure and molar mass of the unsaturated polyesters .....	114
2) Thermomechanical properties of the unsaturated polymers .....	117
<b>V Conclusion and perspectives .....</b>	<b>119</b>
<b>VI References .....</b>	<b>121</b>
<b>VII Experimental .....</b>	<b>122</b>

## **Chapter 3: Laccase-catalyzed coupling of potentially biobased phenyl compounds**

<b>I Introduction .....</b>	<b>127</b>
<b>II Laccase-catalyzed vanillin dimerization .....</b>	<b>127</b>
1. Dimerization procedure and dimer characterization .....	127
2. Optimization of the experimental conditions.....	130
1) Enzyme quantity .....	131
2) Kinetic study: time, co-solvent and gas solution saturation influence .....	131
3) Refill procedure: re-use of the filtrate.....	134
<b>III Laccase-catalyzed oxidative coupling: substrate screening .....</b>	<b>135</b>
1. Synthesis of oligomer mixtures catalyzed by laccase .....	135
1) Laccase-catalyzed coupling of <i>ortho</i> unsubstituted phenols .....	136
2) Laccase-catalyzed coupling of <i>ortho</i> disubstituted phenols .....	139
3) Laccase-catalyzed coupling of <i>ortho</i> monosubstituted phenol.....	143
4) Laccase-catalyzed coupling of aniline derivatives .....	153

2. Laccase-catalyzed selective coupling leading to single dimer formation .....	156
1) An aniline derivative: 2,6-dimethoxyaniline .....	156
2) Laccase-catalyzed synthesis of bisphenols in high yield.....	157
<b>IV Chemical modifications of the biphenyl compounds .....</b>	<b>165</b>
1. Chemical modifications of divanillin (1).....	165
2. Chemical modifications of methyl vanillate dimer (4) .....	167
3. Chemical modifications of 2-methoxy-4-methylphenol dimer (5).....	169
4. Chemical modifications of 2,6-dimethoxyphenol dimer (6).....	170
5. Chemical modifications of dieugenol (7) .....	171
<b>V Conclusion and perspectives .....</b>	<b>172</b>
<b>VI References.....</b>	<b>174</b>
<b>VII Experimental .....</b>	<b>175</b>
<b>VIII Supporting information.....</b>	<b>179</b>

## **Chapter 4: Synthesis and structure-property investigations of polymers from biphenyl building blocks**

<b>I Introduction .....</b>	<b>199</b>
<b>II Synthesis and characterization of thermoplastic polymers from biphenyl precursors via polycondensation .....</b>	<b>199</b>
<b>1. Synthesis and characterization of biphenyl polyesters .....</b>	<b>200</b>
1) Optimization of the polymerization conditions .....	200
2) Synthesis of a series of copolyester .....	204
3) Thermomechanical properties of the copolymers.....	206
<b>2. Preliminary study on polyamide synthesis from biphenyl precursors .....</b>	<b>209</b>
<b>III Synthesis and characterization of thermoplastic polymers from biphenyl precursors via ADMET polymerization .....</b>	<b>212</b>

1. Synthesis, chemical structure and molar mass determination .....	212
2. Thermomechanical properties of the unsaturated polymers .....	217
<b>IV Synthesis and characterization of epoxy resin from biphenyl precursors .....</b>	<b>220</b>
1. Synthesis of epoxy resins from 2,6-dimethoxy phenol dimer .....	221
2. Swelling properties .....	223
3. Thermomechanical properties of the epoxy resins .....	224
4. Comparison of the thermomechanical properties of several biobased epoxy resins.	228
<b>V Conclusion and perspectives .....</b>	<b>229</b>
<b>VI References .....</b>	<b>231</b>
<b>VII Experimental .....</b>	<b>233</b>
<b>General conclusion and perspectives.....</b>	<b>239</b>
<b>Materials and methods.....</b>	<b>243</b>



# Résumé en français

---

Les polymères, largement utilisés dans notre vie quotidienne (emballage, transport, cosmétique, bâtiment, etc.) ont connu un essor très important dans les 60 dernières années passant d'une production mondiale de 2 millions de tonnes en 1950 à 280 millions de tonnes en 2011. Les monomères traditionnels à partir desquels les polymères sont synthétisés sont presque tous dérivés du pétrole et représentent 7% de sa consommation annuelle (environ 4 Gtonnes/an).<sup>1</sup> Cependant, la demande grandissante de ressources fossiles, pétrole et gaz, utilisées majoritairement pour la production d'énergie, ajoutée à leur diminution, entraînent inexorablement une tension de plus en plus forte sur leurs prix. A cela, se rajoutent des problématiques environnementales (émission croissante de CO<sub>2</sub> dans l'atmosphère) et de santé publique qui incitent à la recherche de solutions plus durables, plus respectueuses de l'Homme et de son environnement.<sup>2</sup> La biomasse constitue la seule source abondante de structures carbonées. En effet, le temps de régénération du carbone issu de ressources renouvelables se compte en années (ou dizaine d'années) alors que celui des ressources fossiles en millions d'années! Notre société n'a donc plus le choix que de créer des bioraffineries, pour produire des carburants, de l'énergie et les produits chimiques indispensables à notre vie moderne. En sélectionnant la bio-ressource et la transformation appropriée (extraction, fermentation, pyrolyse), une grande variété de molécules est accessible. De plus en plus de travaux traitent du développement de telles bio-plateformes.<sup>3</sup> Les polymères biosourcés nouveaux, tel le polylactide, ou identiques aux polymères pétro-sourcés, tel le bio-polyéthylène, font désormais partie de l'économie avec une production globale de 1,1 millions de tonnes en 2011. Leur développement se poursuit et leur production mondiale en 2016 devrait atteindre 5,8 millions de tonnes.<sup>4</sup>

Parmi les ressources issues du végétal, les huiles végétales permettent l'accès à une large gamme de molécules aliphatiques et sont considérées comme une biomasse majeure pour le développement de polymères biosourcés. Cette bio-ressource permet ainsi de mimer une grande partie des polymères aliphatiques issus du pétrole.<sup>5,6</sup> La recherche de molécules cycliques et aromatiques, issues de la biomasse, est également un défi majeur aujourd'hui, car de telles structures confèrent généralement de bonnes propriétés mécaniques et thermiques aux matériaux polymères qui en dérivent. Les sucres et les dérivés du bois (terpènes, tanins, polyphénols, polysaccharides) sont des sources majeures donnant accès à ces substrats

(poly)cycliques et/ou aromatiques. Dans ce contexte, ces travaux de thèse visent la valorisation d'une molécule polycyclique, l'acide abiétique, issu de la colophane, et de dérivés phénoliques potentiellement dérivés de la lignine, pour la synthèse de polymères rigides bio-sourcés. Dans les deux cas, des monomères symétriques et difonctionnels sont élaborés par réaction de dimérisation des précurseurs bio-sourcés puis testés en polymérisation.

La colophane est obtenue par distillation de la résine de pin ou du tall oil (sous-produit de l'industrie papetière); sa production est supérieure à 1 million de tonnes par an. Elle est traditionnellement utilisée pour des applications biomédicales ou dans les peintures, encres et adhésifs. Elle contient 10% de composés neutres (terpènes) et 90% d'un mélange d'acides organiques, principalement de l'acide abiétique. La structure tricyclique des acides résiniques confère à ces composés des caractéristiques intéressantes pour la synthèse de polymères biosourcés rigides et semi-rigides.

Dans la littérature, deux types de polymères thermoplastiques ont été synthétisés à partir d'acide abiétique : les polymères possédant le motif abiétique comme groupe pendent et ceux possédant le motif abiétique dans la chaîne principale. Les polymères possédant le motif abiétique comme groupe pendent sont généralement des polymères bien définis, de hautes masses molaires, synthétisés par polymérisation radicalaire. Le motif abiétique n'étant pas dans la chaîne principale, la température de transition vitreuse de ces matériaux n'est pas très élevée. Les polymères possédant le motif abiétique dans la chaîne principale sont communément synthétisés par polycondensation. Seulement de faibles masses molaires sont atteintes en raison de l'encombrement stérique ou d'une pureté insuffisante des monomères.<sup>7</sup> La polymérisation par métathèse (ADMET) de dérivés de l'acide abiétique a permis d'augmenter la masse molaire des polymères synthétisés. Ces matériaux présentent des températures de transition vitreuse plus élevées que les polymères possédant le motif abiétique comme groupe pendent et conservent une bonne stabilité thermique.<sup>8</sup>

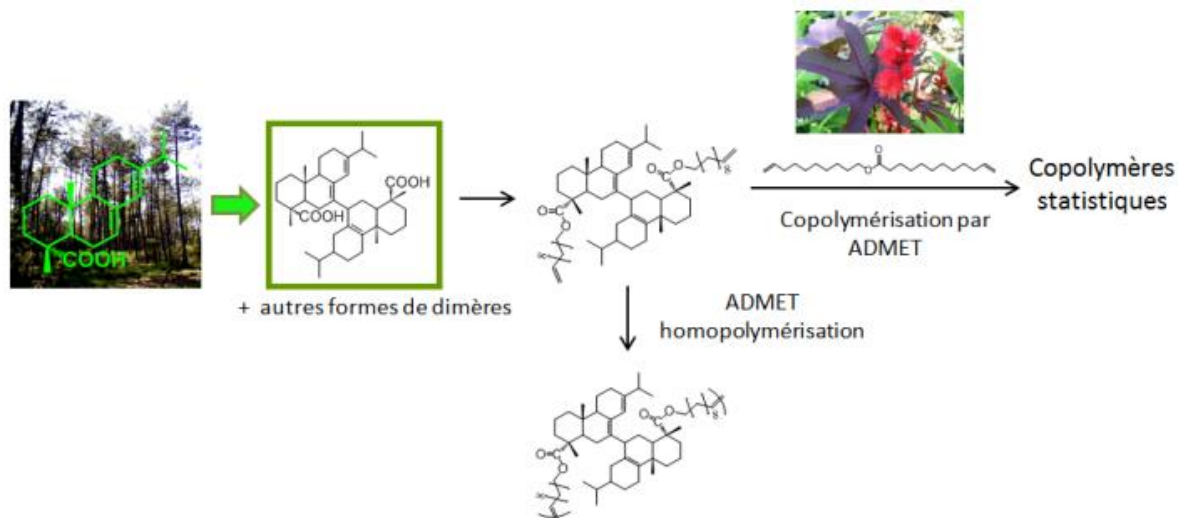
Dans le cadre de ce travail de thèse, la stratégie développée a consisté à préparer des polymères thermoplastiques possédant le motif abiétique intracaténaire à partir du dimère de l'acide abiétique.

Ainsi, l'acide abiétique a été dimérisé en utilisant de l'acide sulfurique dans le chloroforme à 45 °C pendant 5 h, selon la méthode développée par Sinclair *et al.* Cette réaction produit un mélange de 30% de monomères, 60% de dimères et 10% de trimères. Les conditions de séparation de ces constituants ont été déterminées par des études de chromatographie sur couche mince et de chromatographie liquide à haute performance. Le

produit issu de la dimérisation de l'acide abiétique a alors été purifié par chromatographie Flash sur colonne de silice greffée C18 en employant un gradient méthanol/eau comme éluant. Trois fractions ont été collectées. Les deux premières fractions contiennent respectivement de l'acide déhydroabiétique et un mélange d'acide abiétique et de ses isomères (acide lévopimarique et acide palustrique). La troisième fraction contient 2% de monomères, 90% de dimères et 8% de trimères. Sa fonctionnalité en fonctions acide, mesurée par dosage acido-basique, a été estimée à 2,0. Cependant, l'analyse de ces dimères par chromatographie gazeuse a révélé la présence de plusieurs dimères possédant différentes structures. En effet, dans la littérature, une vingtaine de structures de dimères ont été proposées car la dimérisation de l'acide abiétique se produit selon un mécanisme cationique qui n'a pas été élucidé. Dans notre cas, l'une des structures a été identifiée par spectroscopie IRFT comme étant une lactone. Des variations de paramètres de réaction (température, temps, catalyseur) n'ont pas permis d'améliorer le rendement et la sélectivité de la dimérisation. La troisième fraction isolée après la dimérisation de l'acide abiétique selon la méthode développée par Sinclair a donc été utilisée pour la synthèse de polyesters.

Les dimères de l'acide abiétique ont d'abord été polymérisés par polycondensation avec du PEG 600 et du 1,10-decanediol, mais seuls des oligomères ont été obtenus. Ces faibles masses molaires peuvent être attribuées à l'encombrement stérique et à la présence de lactones modifiant la stoechiométrie du système. Cependant, les propriétés thermomécaniques de ces polymères étant prometteuses, une autre méthode de polymérisation a été développée. En effet, les dimères ont été estérifiés avec de l'undécénol (dérivé des huiles végétales) afin d'obtenir des composés bis-insaturés, qui ont ensuite été (co)polymérisés par polymérisation par métathèse selon le procédé ADMET (Acyclic Diene METathesis) avec l'undécénoate d'undécényle (également synthétisé à partir d'huiles végétales). Cette modification chimique a permis de diminuer l'encombrement stérique autour des fonctions réactives pour la polymérisation et d'éviter l'impact négatif de la fonction hydroxyle sur la stoechiométrie du système. La copolymérisation statistique des deux monomères a permis de moduler les propriétés thermomécaniques des polymères ainsi obtenus. Une série de polyesters thermoplastiques insaturés totalement amorphes (100% acide abiétique) ou semi-cristallins (100% undécénoate d'undécényle), et présentant une température de dégradation supérieure à 300°C a été synthétisée. L'analyse enthalpique différentielle (AED) des différents copolymères (AB) ainsi obtenus montre une diminution de l'enthalpie de fusion avec l'incorporation progressive de dimères d'acide abiétique (de 10 à 90%) dans les chaînes

polymères. Les propriétés thermomécaniques de l'homopolymère d'acide abiétique révèlent une température de transition vitreuse de 102°C pour ce matériau.



Suite à cette étude, nous nous sommes intéressés à la dimérisation et polymérisation de composés phénoliques, mieux définis, potentiellement issus de la lignine. La lignine, un des principaux composés du bois, est le second biopolymère le plus abondant après la cellulose. Elle est biosynthétisée à partir de trois phénylpropanoïdes appelés monolignols qui diffèrent par le degré de méthylation de leur noyau aromatique.<sup>9</sup> La maîtrise de la déconstruction de la lignine permettrait d'en faire une ressource à grande échelle pour la production de molécules aromatiques bio-sourcées.<sup>10</sup> Actuellement, la vanilline est le seul phénol industriellement produit à partir de lignine. La majorité des travaux décrits dans la littérature traitant de la polymérisation de dérivés de la lignine sont récents et montrent ainsi l'intérêt grandissant qui est porté à cette bio-ressource. Dans ces exemples, les dérivés de la lignine confèrent de bonnes propriétés thermomécaniques aux polymères qui en dérivent. Dans nos travaux, des composés phénoliques potentiellement issus de la lignine ont été dimérisés. Les composés biphenyles alors produits sont ensuite polymérisés. Peu d'exemples de polymérisation de composés biphenyles potentiellement issus de la lignine ont été décrits dans la littérature, puisque seulement des polymères base de *Schiff* et de la polyvanilline ont été produits à partir de divanilline et des résines esters de cyanates ont été préparés à partir du dimère du 4-méthyl-2-méthoxyphénol.<sup>11-13</sup>

Lors de cette thèse le couplage oxydatif de molécules phénoliques potentiellement issues de la lignine a été étudié par catalyse enzymatique par une laccase. Les laccases, glycoprotéines présentes dans de nombreuses plantes, insectes et champignons, font parties de la famille des oxydoréductases. De nombreuses études traitent de l'utilisation de la laccase en tant que biocatalyseur pour des réactions d'oxydation de groupements fonctionnels ou de



couplages oxydatifs de molécules phénoliques. En effet, les laccases génèrent des intermédiaires radicalaires sur les composés phénoliques qui subissent des réactions de couplages produisant des dimères, des oligomères ou des polymères. Les conditions réactionnelles telles que l'origine de la laccase, le co-solvant, la quantité d'oxygène et de laccase en solution influencent la sélectivité et le rendement des produits formés lors du couplage.

Nous avons développé un procédé de dimérisation de molécules phénoliques sur l'exemple de la vanilline. Ce procédé 'vert' emploie des solvants non toxiques, l'acétone et un tampon d'acétate de sodium, à température ambiante, pendant 24 h, dans un milieu saturé en oxygène. L'avantage majeur de ce procédé réside dans la séparation très simple entre la vanilline, soluble, et son dimère, la divanilline, insoluble. Après filtration, la divanilline récupérée présente une très grande pureté et le milieu réactionnel peut être rechargé en oxygène et en vanilline (sans rajouter de laccase). Les rendements restent élevés, aux alentours de 95%, au moins pour les 8 premiers cycles. Ce procédé a été utilisé pour différents substrats qui, selon la substitution du noyau aromatique, produisent des oligomères, des mélanges de dimères ou sélectivement un seul dimère. Sept phénols (le 4-hydroxy-3-méthoxybenzotrile, le vanillate de méthyle, le 4-méthyl-2-méthoxyphénol, le 2,6-diméthoxyphénol et l'eugénol) ont permis l'obtention de dimères purs avec des rendements supérieurs à 80%. Ces dimères ont ensuite été modifiés chimiquement en diols, diacides, diesters, bis-époxydes et en composés divinylés afin de constituer une bio-plateforme de composés biphényles polymérisables.

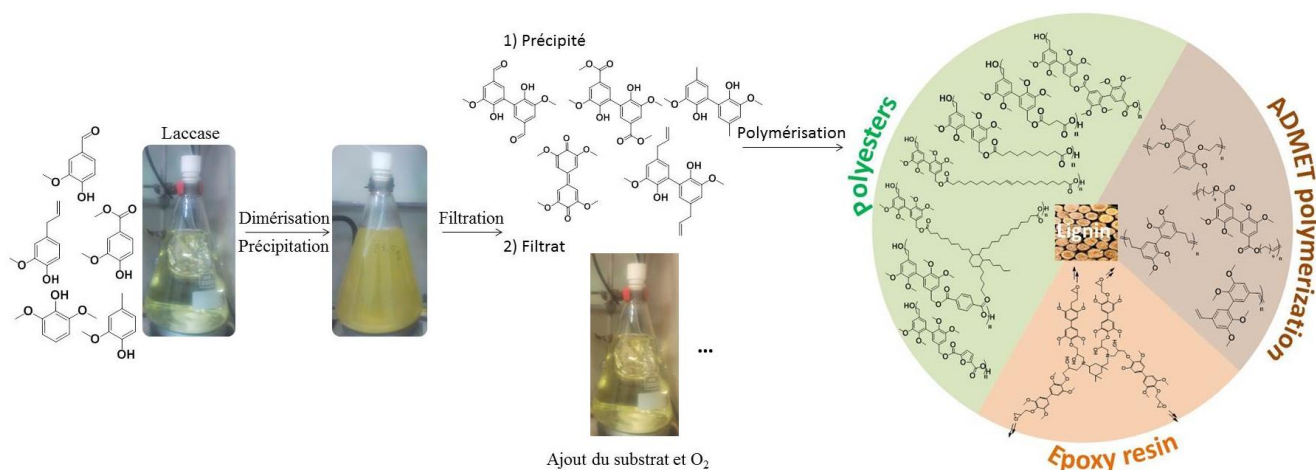
Ces composés biphényles ont ensuite été polymérisés par différentes techniques. Le diol et le diester de méthyle possédant les phénols protégés ont été polymérisés par polycondensation. Les conditions optimales de polymérisation ont été déterminées par polymérisation du diol avec le diméthyl sebaçate et l'acide sébacique. Un polymère de haute masse molaire, 65 000 g/mol a été obtenu par transestérification utilisant 0.5 mol% de butoxyde de titane comme catalyseur. Ces conditions ont été appliquées pour la polymérisation du diol avec plusieurs diesters, de structures aliphatiques possédant des longueurs de chaînes différentes et avec des diesters aromatiques et le diester de méthyle issus de la divanilline. Ainsi, des polymères possédant des transitions vitreuses, couvrant une gamme de température de -4 °C à 140 °C ont été synthétisés. Tous ces polymères sont stables thermiquement, au-delà de 300 °C. Ces propriétés thermiques sont similaires à celles des polymères de commodité tels que le poly(téréphtalate d'éthylène) et le polystyrène qui ont des températures de transition vitreuses de 70 et 100 °C respectivement. Une étude préliminaire a

également été réalisée sur la synthèse de polyamides. Le diacide vanillique méthylé a été polymérisé avec le 1,10-diaminodécane, le 1,6-diaminohexane et la 4,4'-diaminodianiline pour former des polyamides possédant des températures de transitions vitreuses de 124 °C, 136 °C et 157 °C respectivement. Cette étude nécessite une optimisation des conditions réactionnelles mais les résultats obtenus sont dans la gamme de température des polyphthalamides synthétisés à partir des acides téréphtalique ou isophtalique.

Quatre composés bis-insaturés ont également été polymérisés par ADMET. Ils sont issus du dieugenol méthylé, de la réaction de Wittig de la divanilline, de l'allylation du dimère du 4-méthyl-2-méthoxyphénol et de la transestérification entre le diester vanillique et l'undécénol. La polymérisation par ADMET de chaque composé a été effectuée en solution dans le *Polarclean* (méthyl-5-(diméthylamino)-2-méthyl-5-oxopentanoate), avec les catalyseurs de Grubbs I, Grubbs II, Hoveyda Grubbs I and Hoveyda Grubbs II. La mesure des masses molaires des polymères ainsi préparés a permis de déterminer le catalyseur le mieux adapté à chaque substrat. Globalement, les catalyseurs d'Hoveyda Grubbs se sont montrés plus efficaces que les catalyseurs de Grubbs. Selon leur structure, les polymères synthétisés possèdent des masses molaires comprises entre 7 000 g/mol et 40 000 g/mol et des températures de transitions vitreuses comprises entre 4 et 160 °C. En particulier, le composé divinylque préparé à partir de la divanilline a permis la synthèse d'un polymère conjugué de haute stabilité thermique, autour de 380 °C, et possédant une haute transition vitreuse, entre 160 et 200 °C et de masse molaire de 30 000 g/mol.

Enfin, les résines époxy font partie des matières plastiques les plus courantes. Elles sont employées dans de multiples domaines tels que l'industrie aéronautique et spatiale, la construction, les pièces électroniques et également les loisirs. Actuellement, l'éther diglycidique du bisphénol-A (DGEBA), synthétisé à partir du bisphénol-A, est le réactif époxydé commercial le plus répandu et entre dans 95% des résines. Le bisphénol-A est considéré comme toxique pour le corps humain et a été classé cancérigène, mutagène et reprotoxique (CMR). Son utilisation étant controversée et même interdite dans certains cas, son remplacement (partiel ou total) représente un enjeu majeur. Les dimères que nous avons synthétisés présentent des structures proches de celles du bisphénol-A. Le bisphénol produit par la dimérisation du 2,6-diméthoxyphénol a été modifié avec l'épichloridrine pour former un bis-époxyde utilisé pour la synthèse de résines époxy. Les résines époxy ont été formulées avec différentes quantités d'isophorone diamine (IPDA) afin d'observer l'influence du rapport époxyde/amine sur les propriétés thermomécaniques du réseau. Les meilleures propriétés ont été obtenues pour un ratio molaire 1/1. Ces résines époxy présentent une température de

transition vitreuse de 123 °C et une perte de masse de 5% à 312 °C. Ces valeurs sont légèrement inférieures mais néanmoins proches de celles des résines DGEBA/IPDA qui présentent une Tg de 142 °C et une perte de masse de 5% à 330 °C. Pour comparaison, les mêmes résines synthétisées à partir de l'isosorbide qui est également biosourcé, possèdent une Tg de 100 °C et une perte de masse de 5% à 305 °C.



L'objectif de cette thèse était l'investigation de nouvelles ressources biosourcées rigides et leur utilisation dans les polymères biosourcés. La première partie de ce travail, traitant de la dimérisation de l'acide abiétique a permis l'isolation de dimères d'acide abiétique qui apportent rigidité et stabilité thermique aux matériaux qui en résultent. Cependant, la structure mal définie de ces dimères limite leur utilisation pour la synthèse de polymères de hautes masses molaires. Dans un second temps, des composés biphenyles ont été synthétisés avec une grande pureté et de bons rendements par dimérisation enzymatique de molécules phénoliques dérivées de la lignine selon un procédé 'vert'. Une bio-plateforme de composés biphenyles a été constituée. Ces molécules ont permis la synthèse de matériaux possédant diverses propriétés thermomécaniques et sont intéressantes pour substituer l'acide téréphtalique pour la synthèse de polyesters et polyamides et le bisphénol-A pour la synthèse de résines epoxy, par exemple.

## Références :

1. R. Mülhaupt, *Macromolecular Chemistry and Physics*, **2012**, 214, 159-174.
2. S. Sorrell, J. Speirs, R. Bentley, R. Miller and E. Thompson, *Energy*, **2012**, 37, 709-724.
3. J. H. Clark, F. E. I. Deswarte and T. J. Farmer, *Biofuels, Bioproducts and Biorefining*, **2009**, 3, 72-90.
4. G.-Q. Chen and M. K. Patel, *Chemical Reviews*, **2011**, 112, 2082-2099.
5. L. Maisonneuve, T. Lebarbe, E. Grau and H. Cramail, *Polymer Chemistry*, **2013**, 4, 5472-5517.
6. G. Lligadas, J. C. Ronda, M. Galià and V. Cádiz, *Materials Today*, **2013**, 16, 337-343.
7. P. A. Wilbon, F. Chu and C. Tang, *Macromolecular Rapid Communications*, **2012**, 34, 8-37.
8. P. A. Wilbon, A. L. Gullledge, B. C. Benicewicz and C. Tang, *Green materials*, **2013**, 1, 96-104.
9. S. Laurichesse and L. Avérous, *Progress in Polymer Science*, **2014**, 39, 1266-1290.
10. C. Xu, R. A. D. Arancon, J. Labidi and R. Luque, *Chemical Society Reviews*, **2014**, 43, 7485-7500.
11. A. S. Amarasekara and A. Razzaq, *Polymer Science*, **2012**, 2012, 1-6.
12. A. S. Amarasekara, B. Wiredu and A. Razzaq, *Green Chemistry*, **2012**, 14, 2395-2397.
13. B. G. Harvey, M. E. Wright, S. Compel, A. J. Guenther, K. Lamison, L. R. Cambrea, H. A. Meylemans and S. McCormick, *polymer preprint*, **2011**, 52, 282-283.

# Scientific production

---

## Publications and patents:

Mantzaridis, C., Brocas, AL., Llevot, A., Cendejas Santana, G., Auvergne, R., Caillol, S., Carlotti, S., Cramail, H., Rosin acid oligomers as precursors of DGEBA-free epoxy resins, *Green Chemistry*, **2013**, 15, 3091-3098

Brocas, AL., Llevot, A., Mantzaridis, C., Cendejas Santana, G., Auvergne, R., Caillol, S., Carlotti, S. and Cramail, H., Epoxidized rosin acids as co-precursors for epoxy resins, *Designed Monomers and Polymers*, **2014**, 17, 301-310.

Llevot, A., Grau, G., Carlotti, S., Grelier, S., Cramail, H. Dimerization of Abietic Acid for the Design of Renewable Polymers from ADMET, accepted in *European polymer journal*.

Llevot, A., Grau, G., Carlotti, S., Grelier, S., Cramail, H., La résine de pin, source de nouveaux polymères?, *Actualité chimique*, novembre 2014 n°390.

Llevot, A., Cramail, H., Carlotti, S., Grau, G., Grelier, S. New phenolic polymers and preparation processes thereof 2014, EP14306563.9

Llevot, A., Cramail, H., Carlotti, S., Grau, G., Grelier, S. New process for preparing biphenyl compounds, 2014, EP14306566.2

## Communications:

### Posters

Llevot, A., Grau, G., Carlotti, S., Grelier, S., Cramail, H., *Synthesis, purification and modification of abietic acid dimer, an interesting source of (co)monomers for the design of novel renewable polymers*

- 6th workshop on fats and oils as renewable feedstock for the chemical industry, Karlsruhe Germany, March 17-19 (2013). **Poster price**
- EPF congress, Pisa Italy, June 16-21 (2013). **2<sup>nd</sup> poster price**
- 4ème colloque recherche de la Federation Gay Lussac, Paris France, December 4-6 (2013)

### Oral presentations

Llevot, A., Grau, G., Carlotti, S., Grelier, S., Cramail, H., *Abietic Acid Dimers: a Promising Source of Monomers for the Design of Novel Renewable Polymers*

- 41ème Journée d'Etudes des Polymères (JEPO), Aussois France, September 15-20 (2013)
- Journée Thèse des Bois, Bordeaux, France July 2 (2014)
- Macro IUPAC, Chiang Mai Thailand, July 6-11 (2014)



# List of abbreviations

---

## Techniques:

DMA: dynamic mechanical analysis  
DSC: differential scanning calorimetry  
FTIR: Fourier transform infrared  
GC: gas chromatography  
HMBC: heteronuclear multiple bond correlation  
HPLC: high performance liquid chromatography  
HSQC: heteronuclear single quantum coherence  
NMR: nuclear magnetic resonance  
SEC: size exclusion chromatography  
TGA: thermogravimetric analysis  
TLC: thin layer chromatography

## Chemicals

APTS: *para*-toluene sulfonic acid  
BTCA: 1,2,4-benzenetricarboxylic anhydride  
CHDA: 1,2-cyclohexanedicarboxylic anhydride  
DBTO: dibutyltin oxide  
DCM: dichloromethane  
DER332: diglycidyl ether oligomer epoxy resin  
DER6224: low molar mass product of bisphenol A and epichlorohydrine  
DIPC: diisopropylcarbodiimide  
DGEBA: diglycidyl ether of bisphenol A  
DMAP: 4-dimethylaminopyridine  
DMF: dimethylformamide  
DMSO: dimethylsulfoxide  
DVB: divinylbenzene  
E44: diglycidyl ether oligomer epoxy resin  
EG: ethylene glycol  
IPDA: isophorone diamine  
IPDI: isophorone diisocyanate  
m-CPBA: *meta*-chloroperbenzoic acid  
MMA: methylmethacrylate  
MeOH: methanol  
NCTP: N-(4-carboxyphenyl)trimellitimide  
NMP: N-methyl-pyrrolidone  
PEG: polyethylene glycol  
PG: propylene glycol  
PTMG: polytetramethyleneglycol  
TBABr : tetrabutylammonium bromide  
TBD: 1,5,7-triazabicyclododecene

TBT: tetrabutyl titanate  
TCE: tetrachloroethane  
TEA: triethylamine  
TEBAC: benzyltriethylammonium chloride  
THF: tetrahydrofuran  
Ti(OBu)<sub>4</sub>: titanium n-butoxide  
VA: vanillic acid  
ZnAc<sub>2</sub>: zinc acetate  
Polarclean: methyl-5-(dimethylamino)-2-methyl-5-oxopentanoate

## Characteristic parameters

D: dispersity  
DP<sub>n</sub>: polymerization degree  
E: Young's modulus  
E': storage modulus  
E'': loss modulus  
E<sub>a</sub>: activation energy  
G': storage modulus  
G'': loss modulus  
M<sub>n</sub>: number average molar mass  
M<sub>w</sub>: mass average molar mass  
R: gas constant  
T: temperature  
Td5%: temperature corresponding to 5 wt% loss  
tanδ: loss factor  
T<sub>g</sub>: glass transition temperature  
T<sub>m</sub>: melting temperature  
T<sub>α</sub>: α-relaxation temperature  
ΔH: enthalpy

## Polymerization techniques

ADMET: acyclic diene metathesis  
ATRP: atom transfer radical polymerization  
CRP: controlled radical polymerization  
RAFT: reversible addition-fragmentation chain transfer  
ROP: ring-opening polymerization





# **GENERAL INTRODUCTION**

# General introduction

Polymers are widely used in our daily life (packaging, cosmetics, housing, constructions, transportation, etc). Within the last 60 years, their production increased from 2 million tons in 1950 to 300 million tons in 2013. Nowadays, synthetic polymers represent 7% of petroleum annual production.<sup>1</sup> However, the growing demand of petroleum along with the decrease of its economically available amount lead to a rise of its price.<sup>2</sup> In addition to this cost and finite availability issues, environmental concerns such as greenhouse gas emission motivate researchers to develop sustainable solutions.

Biomass constitutes the only source of available renewable carbon. Indeed, the regeneration time of carbon from biomass is measured in decades whereas the one of fossil resources reaches several million years.<sup>3</sup> From these observations, the concept of biorefinery was imagined in the respect of the twelve principles of green chemistry.<sup>4</sup> A biorefinery is a facility that integrates biomass conversion processes and equipment to produce fuels, heat and value-added chemicals from biomass (Figure 1).<sup>5-10</sup>

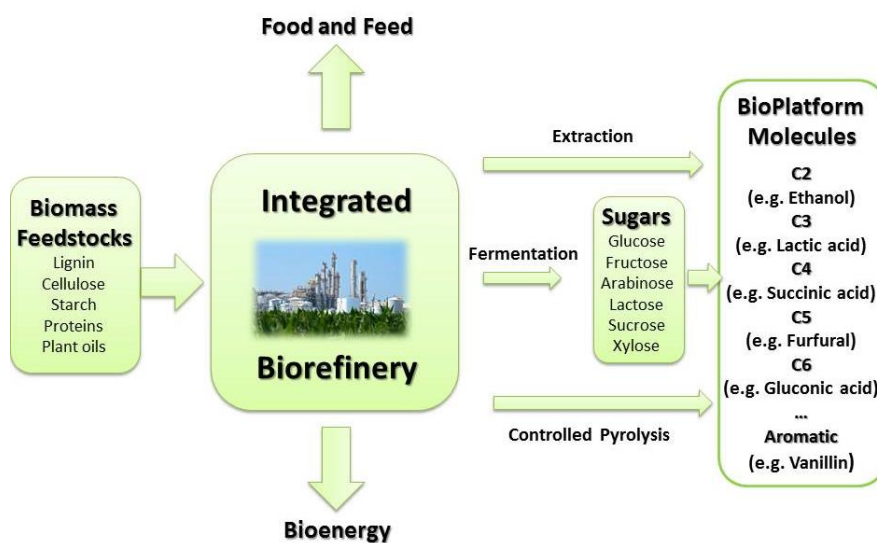


Figure 1: Schematic idealized concept of an integrated biorefinery.

In tandem with the conception of biorefinery, over the two last decades, scientists have targeted the development of green and sustainable polymers.<sup>11-19</sup> Green plastics can be produced in three ways: (i) direct use or modification of natural polymers such as lignin, cellulose, starch etc.<sup>20,21</sup> (ii) polymerization of building blocks obtained from biomass deconstruction or extraction,<sup>22,23</sup> (iii) polymerization *via* microorganism fermentation of sugars or lipids found in nature (poly(hydroxyalkanoate)s, etc.).<sup>24</sup> Nowadays, new biobased polymers, such as polylactides and mimic of petroleum-based polymers, such as bioethylene,

are part of our economy with a global production of 1.1 million tons in 2011. With their current development, their production is expected to reach 6.1 million tons in 2017 (Figure 2).<sup>25</sup>

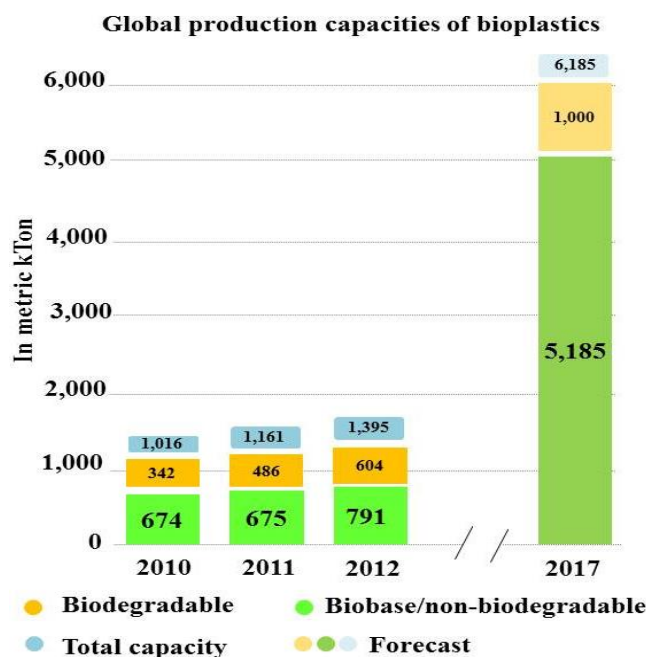


Figure 2: Biobased polymers: evolution of production capacities from 2011 to 2020.<sup>25</sup>

Among the available bioresources, vegetable oils, already used for the manufacture of surfactants, lubricants, cosmetics, paints and coatings, have been intensively studied for the synthesis of biobased polymers because of their good availability. Indeed, the annual global production of the major vegetable oils in 2011/2012 amounted 156 million tons.<sup>26</sup> This bioresource leads to a large platform of aliphatic molecules and wide range of thermoplastic and thermoset polymers after modifications (Figure 3).<sup>22,27-32</sup>

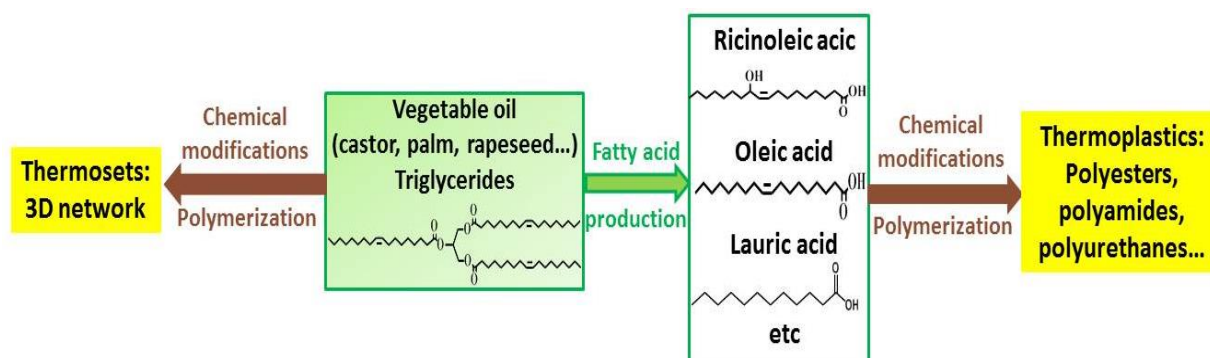


Figure 3: Strategy to synthesize renewable polymers from vegetable oils.

In order to broaden the palette of renewable polymers, other molecules need to be investigated in order to modify the thermomechanical properties of the vegetable oil aliphatic polymers or

to enable the synthesis of polymers with different thermomechanical. Cycloaliphatic and aromatic compounds are two categories of molecules which can enable the synthesis of polymers with high thermal stability and rigidity (Figure 4). For instance, high transition temperature polymers are greatly appreciated for packaging under heating. These classes of petroleum-based molecules have also to be substituted.

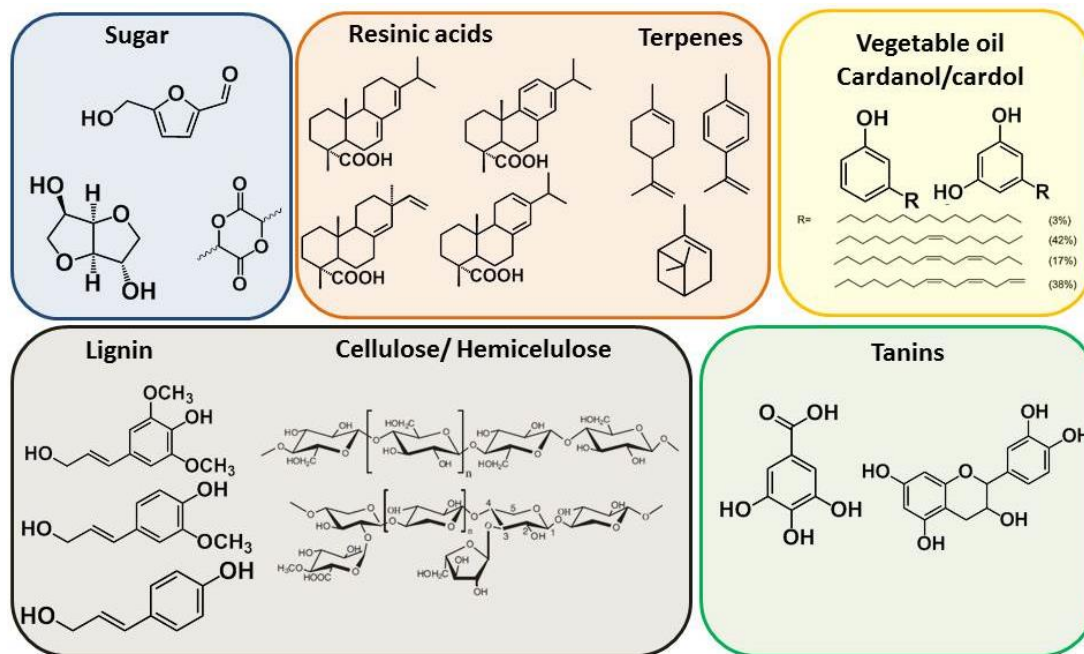


Figure 4: Cycloaliphatic and aromatic biobased molecules.

Cycloaliphatic compounds are constituents of several natural resources. Among the naturally occurring feedstocks, carbohydrates, which include polysaccharides as well as sugars, are interesting sources of cycloaliphatic molecules due to their abundance, diversity and accessibility. Indeed, cellulose and hemicellulose constitute the most abundant part of plant biomass (production of 50 to 100 billion ton/year). They are suitable to build a sustainable platform of chemicals and the derived polymers. These compounds have key applications in the field of biomedicine due to their degradability.<sup>33,34</sup> Bicyclic sugar derivatives, such as isosorbide, isomannide and isoidide were highlighted in several studies for being useful reinforcing agents in polymer synthesis due to their bicyclic structure.<sup>35</sup> Terpenes represent another class of cyclic versatile chemical feedstock.<sup>36</sup> Among them, limonene, a byproduct of citrus industry with an annual production of 70 000 tons, was studied for the synthesis of polyesters, polyamides, polyurethanes, thermosets, by step polymerization or using cationic or radical polymerization.<sup>37-43</sup> The studies of these cycloaliphatic natural resources are not described in this thesis as these molecules were not investigated in the present work. Bioresources derived from wood and especially pines have aroused interest due to their

abundance, low cost and easy chemical modifications. Rosin, which total annual production is superior to 1 million ton, contains mainly abietic acid and few other resinic acids. Abietic acid with its rigid tricyclic skeleton possessing two double bonds and a carboxylic functional group appears to be an interesting platform towards stiff biobased polymers.<sup>23</sup> Examples of rosin derivative polymerizations have been reported and will be described in the first chapter.

Aromatic compounds constitute basic chemicals to manufacture everyday life items. Indeed, they play a key role in pharmaceuticals, perfumes, dyestuff and polymer industries.<sup>44</sup> In plastic industry, aromatic units offer rigidity, hydrophobicity and fire resistance to the respective polymers. For instance, aromatic polyesters, such as poly(alkyleneterephthalate)s are widely commercially used (global PET production over 28 million tons in 2012), especially in food packaging and textile field due to their good thermomechanical and barrier properties.<sup>45,46</sup> Aromatic polyamides, such as *Kevlar* constitute high performance polymers due to their high stability and rigidity. Phenolic compounds are also widely used as raw materials. For instance, Bisphenol-A (BPA) is an important monomer for the synthesis of polycarbonates, epoxy resins and a popular plasticizer for thermoplastic polymers. BPA production reached 4.4 million tons in 2012. All these aromatic compounds are mainly petroleum-based and derived from benzene, xylene and cumene. Thus, the development of aromatic renewable polymers is drawing an enormous interest.

Some aromatic structures can be synthesized from natural compounds or are directly found in limited quantity in Nature. For instance, *p*-cymene can be easily synthesized from terpenes (mainly used for pharmaceutical and fragrance)<sup>47</sup> and transformed into terephthalic acid.<sup>48</sup> Some polyphenol contained in tannin are used for the synthesis of epoxy resins.<sup>49</sup> Cardanol, extracted from cashew nut shell liquid<sup>50</sup> (which potential production 450 000 metric tons per year<sup>51</sup>) is used into polymers,<sup>52,53</sup> surfactants,<sup>54</sup> nanomaterials. Finally, hydroxymethyl furfural synthesized from sugar dehydration, is an important aromatic building block for a wide range of applications<sup>55,56</sup> and even used for the synthesis of biobased PET after several modifications.<sup>57</sup> However, the main source of phenolic and so aromatic compounds is lignin. Isolated from wood or annual plant, this biopolymer constitutes the second most abundant renewable polymer after cellulose, with a world production of 40-50 million tons per year.<sup>58</sup> Lignin is composed of three primary monolignols: sinapyl alcohol, coniferyl alcohol and *p*-coumaryl alcohol and can potentially be depolymerized leading to monophenols such as phenol, guaiacol or syringol and their derivatives.<sup>59-62</sup> Vanillin, a phenol commercially available, can be extracted from lignin and also obtained by biosynthetic pathway from

abundant glucose.<sup>63</sup> This aromatic compound, very interesting due to its availability and difunctionality, has already been used as biobased building blocks.

This thesis focuses on the study of polycyclic biobased molecules, i.e resinic acids, and phenolic compounds potentially derived from lignin, such as vanillin and other *o*-methoxy or *o*-dimethoxy phenols (Figure 5). In order to get symmetric synthons, both classes of substrates were dimerized. Then, several aromatic and polycyclic thermoplastic polymers were synthesized either by polycondensation or acyclic diene metathesis (ADMET) method. Epoxy resins were also investigated from the biphenyl synthons.

This manuscript is organized into four chapters.

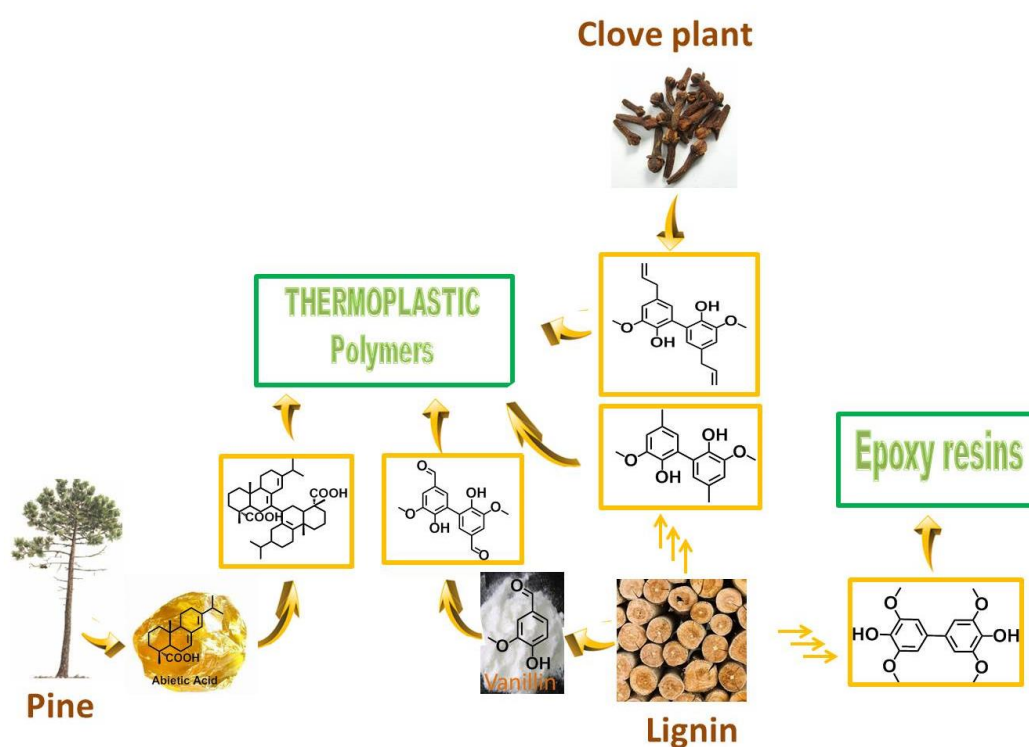


Figure 5: Schematization of our strategy.

In the first chapter, the state of the art regarding the polymerization and dimerization of resinic acids and phenolic molecules potentially derived from lignin will be reviewed. First, the wide use of rosin as epoxy or curing agent sources of thermoset polymers will be presented, before focusing on the synthesis of rosin-based thermoplastic polymers. The radical (co)polymerization of rosin derivatives, leads to pendant abietic acid moieties which thermomechanical properties and applications will be discussed. Then, the different strategies to synthesize abietic acid main chain polymers *via* polycondensation will be presented and compared in terms of polymer molar masses. Finally, the investigations on the abietic acid

dimerization will be discussed. In a second part, the synthesis and properties of thermoset and thermoplastic polymers prepared from phenols potentially derived from lignin will be described. Biobased phenols are mainly used in thermoplastics and their description includes thermotropic polymers, PET mimics, copolymers with fatty acid derivatives and the synthesis and polymerization of symmetric building blocks. Since mainly vanillin will be dimerized using laccase in the third chapter, the different routes of dimerizing vanillin *via* chemical or enzymatic pathway, already reported in literature, will be discussed before ending with the presentation of the studies on laccase-catalyzed phenolic oxidative coupling.

The second chapter of this manuscript is dedicated to the dimerization of abietic acid and to the polymerization of the resulting dimers. The reaction conditions of the dimerization will be investigated by varying the abietic acid purity, the catalyst, as well as the reaction time and temperature. The purification and characterization of the dimers will be also an important part of this chapter. Because low molar mass polyesters will be obtained by polycondensation of the abietic acid dimers, the latter will be esterified with undecenol to perform ADMET polymerization on the bis-unsaturated substrates. Homopolymer and copolymers with different composition of undecenyl undecenoate will be prepared and characterized.

The third chapter of this manuscript is dedicated to the enzymatic dimerization of vanillin and other lignin derivatives catalyzed by laccase. First, the process of dimerization will be described and optimized on the example of vanillin. Then, this process will be investigated on different substrates yielding oligomers, mixture of dimers or pure dimers. The pure dimers will be fully characterized and chemically modified leading to a broad platform of biphenyl compounds.

In the fourth chapter, the resulting diols and diesters will be used in polycondensation with other biobased monomers to obtain polyesters with a wide range of thermomechanical properties. ADMET polymerization will be performed on the bis-unsaturated dimers yielding polymers with high glass transition temperatures and excellent thermal stability. Epoxy resins will be synthesized from the bisepoxy dimers and IPDA. Their thermomechanical properties will be compared with the ones of DGEBA-based equivalents.



## REFERENCES

1. R. Mülhaupt, *Macromolecular Chemistry and Physics*, **2013**, 214, 159-174.
2. S. Sorrell, J. Speirs, R. Bentley, R. Miller and E. Thompson, *Energy*, **2012**, 37, 709-724.
3. C. Okkerse and H. van Bekkum, *Green Chemistry*, **1999**, 1, 107-114.
4. P. Anastas and N. Eghbali, *Chemical Society Reviews*, **2010**, 39, 301-312.
5. J. H. Clark, F. E. I. Deswarte and T. J. Farmer, *Biofuels, Bioproducts and Biorefining*, **2009**, 3, 72-90.
6. <http://www.nrel.gov/biomass/biorefinery.html>.
7. A. Corma, S. Iborra and A. Velty, *Chemical Reviews*, **2007**, 107, 2411-2502.
8. P. Gallezot, *Chemical Society Reviews*, **2012**, 41, 1538-1558.
9. Y. Pu, M. Kosa, U. Kalluri, G. Tuskan and A. Ragauskas, *Appl Microbiol Biotechnol*, **2011**, 91, 1525-1536.
10. R. A. Sheldon, *Green Chemistry*, **2014**, 16, 950-963.
11. M. J. L. Tschan, E. Brule, P. Haquette and C. M. Thomas, *Polymer Chemistry*, **2012**, 3, 836-851.
12. A. Gandini, *Macromolecules*, **2008**, 41, 9491-9504.
13. A. Gandini, *Green Chemistry*, **2011**, 13, 1061-1083.
14. K. Madhavan Nampoothiri, N. R. Nair and R. P. John, *Bioresource Technology*, **2010**, 101, 8493-8501.
15. G.-Q. Chen and M. K. Patel, *Chemical Reviews*, **2011**, 112, 2082-2099.
16. R. T. Mathers, *Journal of Polymer Science Part A: Polymer Chemistry*, **2012**, 50, 1-15.
17. N. Peelman, P. Ragaert, B. De Meulenaer, D. Adons, R. Peeters, L. Cardon, F. Van Impe and F. Devlieghere, *Trends in Food Science & Technology*, **2013**, 32, 128-141.
18. C. Vilela, A. F. Sousa, A. C. Fonseca, A. C. Serra, J. F. J. Coelho, C. S. R. Freire and A. J. D. Silvestre, *Polymer Chemistry*, **2014**, 5, 3119-3141.
19. N. Hernández, R. C. Williams and E. W. Cochran, *Organic and Biomolecular Chemistry*, **2014**, 12, 2834-2849.
20. S. Laurichesse and L. Avérous, *Progress in Polymer Science*, **2014**, 39, 1266-1290.
21. R. Deutschmann and R. F. H. Dekker, *Biotechnology Advances*, **2012**, 30, 1627-1640.
22. M. A. R. Meier, J. O. Metzger and U. S. Schubert, *Chemical Society Reviews*, **2007**, 36, 1788-1802.
23. P. A. Wilbon, F. Chu and C. Tang, *Macromolecular Rapid Communications*, **2012**, 34, 8-37.
24. G.-Q. Chen, *Chemical Society Reviews*, **2009**, 38, 2434-2446.
25. <http://en.european-bioplastics.org/>.
26. PlasticsEurope, <http://www.plasticseurope.fr/>.
27. M. Desroches, R. Auvergne, B. Boutevin and S. Caillol, *OCL-oleagineux Corps Gras Lipides*, **2013**, 20, 16-22.
28. L. Montero De Espinosa and M. A. R. Meier, *European Polymer Journal*, **2011**, 47, 837-852.
29. L. Maisonneuve, T. Lebarbe, E. Grau and H. Cramail, *Polymer Chemistry*, **2013**, 4, 5472-5517.
30. M. R. Islam, M. D. H. Beg and S. S. Jamari, *Journal of Applied Polymer Science*, **2014**, 131, 9016-9028.
31. S. Miao, P. Wang, Z. Su and S. Zhang, *Acta Biomaterialia*, **2014**, 10, 1692-1704.
32. G. Lligadas, J. C. Ronda, M. Galià and V. Cádiz, *Materials Today*, **2013**, 16, 337-343.
33. N. B. Shelke, R. James, C. T. Laurencin and S. G. Kumbar, *Polymers for Advanced Technologies*, **2014**, 25, 448-460.
34. R. K. Shukla and A. Tiwari, *Carbohydrate Polymers*, **2012**, 88, 399-416.
35. F. Fenouillot, A. Rousseau, G. Colomines, R. Saint-Loup and J. P. Pascault, *Progress in Polymer Science*, **2010**, 35, 578-622.
36. W. Schwab, C. Fuchs and F.-C. Huang, *European Journal of Lipid Science and Technology*, **2012**, 115, 3-8.
37. M. Firdaus, M. A. R. Meier, U. Biermann and J. O. Metzger, *European Journal of Lipid Science and Technology*, **2013**, 116, 31-36.



38. M. Firdaus, L. Montero de Espinosa and M. A. R. Meier, *Macromolecules*, **2011**, 44, 7253-7262.
39. M. Shibata and M. Asano, *Journal of Applied Polymer Science*, **2013**, 129, 301-309.
40. S. Sharma and A. K. Srivastava, *Polymer-Plastics Technology and Engineering*, **2003**, 42, 485-502.
41. K. Satoh, M. Matsuda, K. Nagai and M. Kamigaito, *Journal of the American Chemical Society*, **2010**, 132, 10003-10005.
42. K. Satoh, A. Nakahara, K. Mukunoki, H. Sugiyama, H. Saito and M. Kamigaito, *Polymer Chemistry*, **2014**, 5, 3222-3230.
43. K. Yao and C. Tang, *Macromolecules*, **2013**, 46, 1689-1712.
44. M. Granda, C. Blanco, P. Alvarez, J. W. Patrick and R. Menéndez, *Chemical Reviews*, **2013**, 114, 1608-1636.
45. <http://www.specialchem4polymers.com/resources/latest/displaynews.aspx?id=10364>.
46. S. Munoz-Guerra, C. Lavilla, C. Japu and A. Martinez de Ilarduya, *Green Chemistry*, **2014**, 16, 1716-1739.
47. S. Burt, *International Journal of Food Microbiology*, **2004**, 94, 223-253.
48. M. Colonna, C. Berti, M. Fiorini, E. Binassi, M. Mazzacurati, M. Vannini and S. Karanam, *Green Chemistry*, **2011**, 13, 2543-2548.
49. R. Auvergne, S. Caillol, G. David, B. Boutevin and J.-P. Pascault, *Chemical Reviews*, **2013**, 114, 1082-1115.
50. A. H. Tullo, *Chemical & Engineering News Archive*, **2008**, 86, 26-27.
51. V. S. Balachandran, S. R. Jadhav, P. K. Vemula and G. John, *Chemical Society Reviews*, **2013**, 42, 427-438.
52. C. Voirin, S. Caillol, N. V. Sadavarte, B. V. Tawade, B. Boutevin and P. P. Wadgaonkar, *Polymer Chemistry*, **2013**, 3142-3162.
53. E. Darroman, L. Bonnot, R. Auvergne, B. Boutevin and S. Caillol, *European Journal of Lipid Science and Technology*, **2014**, n/a-n/a.
54. X. H. Yang, G. M. Xiao, Z. M. Wang, F. Jing, Y. H. Zhou and J. C. Jiang, *Chemistry and Industry of Forest Products*, **2013**, 33, 144-148.
55. R.-J. van Putten, J. C. van der Waal, E. de Jong, C. B. Rasrendra, H. J. Heeres and J. G. de Vries, *Chemical Reviews*, **2013**, 113, 1499-1597.
56. C. H. R. M. Wilsens, B. A. J. Noordover and S. Rastogi, *Polymer (United Kingdom)*, **2014**, 55, 2432-2439.
57. M. Shiramizu and F. D. Toste, *Chemistry – A European Journal*, **2011**, 17, 12452-12457.
58. S. Laurichesse and L. Avérous, *Progress in Polymer Science*, 39, 3119-3141.
59. J. Zakzeski, P. C. A. Bruijninx, A. L. Jongerius and B. M. Weckhuysen, *Chemical Reviews*, **2010**, 110, 3552-3599.
60. M. Kleinert and T. Barth, *Chemical Engineering & Technology*, **2008**, 31, 736-745.
61. T. Yoshikawa, T. Yagi, S. Shinohara, T. Fukunaga, Y. Nakasaka, T. Tago and T. Masuda, *Fuel Processing Technology*, **2013**, 108, 69-75.
62. T. Yoshikawa, S. Shinohara, T. Yagi, N. Ryumon, Y. Nakasaka, T. Tago and T. Masuda, *Applied Catalysis B: Environmental*, **2014**, 146, 289-297.
63. K. Li and J. W. Frost, *Journal of the American Chemical Society*, **1998**, 120, 10545-10546.



# CHAPTER 1:

## Polymerization and dimerization of resinic acids and phenolic compounds potentially derived from lignin: state of the art

**Key words:** rosin, abietic acid, vanillin, potentially biobased phenols, thermosets, thermoplastics, dimerization, enzymatic coupling, laccase.

**Mots clés:** colophane, acide abiétique, phénol potentiellement bio-sourcés, polymères thermodurcissables, polymères thermoplastiques, dimérisation, couplage enzymatique, Laccase.

## TABLE OF CONTENTS

<b>I</b>	<b>Resinic acids, polycyclic biobased synthons.....</b>	<b>26</b>
1.	Abietic acid extraction, production and use.....	26
2.	Abietic acid thermoset polymers .....	27
1)	Synthesis and properties of rosin vinyl ester resins .....	28
2)	Synthesis and properties of epoxy resin curing agents from rosin .....	30
3)	Synthesis of epoxy compounds from abietic acid derivatives and used in epoxy resin formulations.....	33
3.	Abietic acid thermoplastic polymers.....	37
1)	Synthesis and properties of rosin pendant chain polymers.....	38
a)	Free radical polymerization of rosin derivatives.....	38
b)	Controlled radical polymerization of rosin derivatives.....	39
2)	Synthesis and properties of polymers with rosin derivatives in the main chain	46
a)	Synthesis of maleopimarate main chain thermoplastic polymers .....	46
b)	Synthesis of acrylopimarate main chain thermoplastic polymers.....	48
c)	Synthesis of polyamides and poly(amide-imide)s from abietic acid ketones ...	50
4.	Abietic acid dimerization .....	52
<b>II</b>	<b>Chemical modifications and polymerization of aromatic synthons potentially derived from lignin.....</b>	<b>55</b>
1.	Vanillin extraction, production and use .....	56
2.	Synthesis and properties of thermoset polymers from vanillin and eugenol .....	57
1)	Synthesis and properties of vinyl ester resins derived from vanillin.....	57
2)	Synthesis and properties of cyanate ester thermosets derived from vanillin	58
3)	Synthesis of epoxy resins from compounds potentially derived from lignin .	59
a)	Synthesis of bisepoxides from vanillin .....	59
b)	Synthesis and properties of eugenol-based epoxy resins .....	62
3.	Synthesis and properties of thermoplastic polymers from phenols potentially derived from lignin .....	62
1)	Synthesis of thermotropic polymers from vanillic acid .....	64
2)	Synthesis of fully biobased poyesters from vanillin, syringaldehyde and ferulic acid .....	67

a) Copolyesters of vanillin or ferulic acid and vegetable oil derivatives .....	67
b) Synthesis of PET mimic polymers from vanillin, 4-hydroxybenzoic acid and syringaldehyde.....	70
<b>3) Synthesis and properties of vanillin-based polyoxalate .....</b>	<b>71</b>
<b>4) Coupling of lignin derivatives, building blocks for polymer synthesis.....</b>	<b>71</b>
a) Synthesis of symmetric building blocks from lignin derivatives .....	72
b) Polymerization of the lignin derivatives with symmetric structure .....	73
<b>4. Vanillin dimer synthesis: promising synthon for polymer synthesis .....</b>	<b>75</b>
<b>1) Synthesis of divanillin <i>via</i> chemical methods .....</b>	<b>76</b>
<b>2) Synthesis of divanillin <i>via</i> enzymatic coupling .....</b>	<b>76</b>
<b>5. Laccase-catalyzed oxidative phenolic coupling.....</b>	<b>77</b>
<b>1) Biochemical, structural characteristics and reaction mechanism of laccases</b>	<b>77</b>
<b>2) Laccase-catalyzed oxidative coupling phenolic compounds.....</b>	<b>79</b>
a) Synthesis of ill-defined oligomers from polyphenols .....	79
b) Synthesis of ill-defined oligomers from <i>ortho</i> unsubstituted phenolic compounds.....	80
c) Synthesis of dimers from <i>ortho</i> unsubstituted phenols .....	81
d) Synthesis of ill-defined oligomers from <i>ortho,para</i> -unsubstituted phenols .....	81
e) Laccase-catalyzed synthesis of well-defined polymers and dimers from <i>ortho</i> -disubstituted phenols .....	82
f) Laccase-catalyzed oxidative coupling of <i>ortho</i> methoxy <i>para</i> substituted phenols.....	84
<b>III REFERENCES .....</b>	<b>87</b>

## I Resinic acids, polycyclic biobased synthons

### 1. Abietic acid extraction, production and use

Rosin, also known as colophony, is obtained either by the process of distillation of the conifer tree resin or of tall oil, a by-product of the *Kraft* process, or from aged pine stumps. Rosin world production is estimated over 1 million ton per year. Thereof, gum rosin represents 60% of this production and tall oil rosin 35%. The chief region of gum rosin harvesting is Southeast Asia. USA and Europe produce tall oil rosin, recovered during chemical pulping, to try to meet their own demand, but still need to import Asian gum rosin (Figure 1).<sup>1</sup> The main sources of supply in Europe are Northern Europe and France, where Maritime Pine is extensively cultivated in the district of Landes.

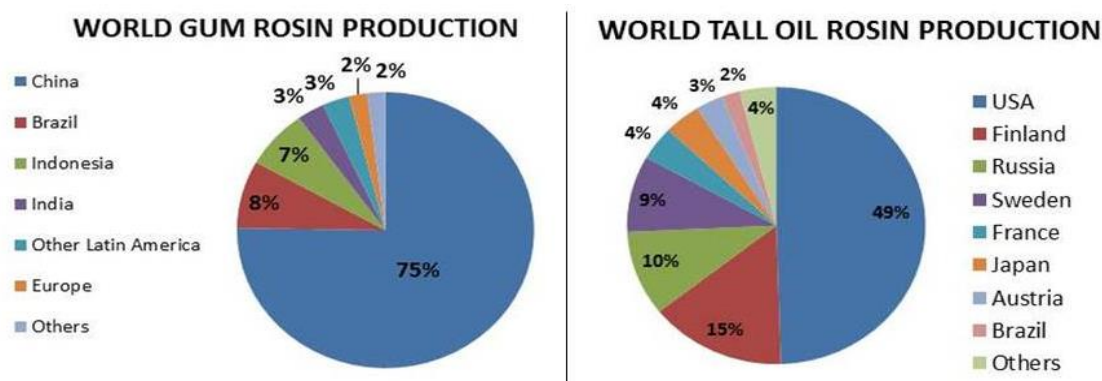
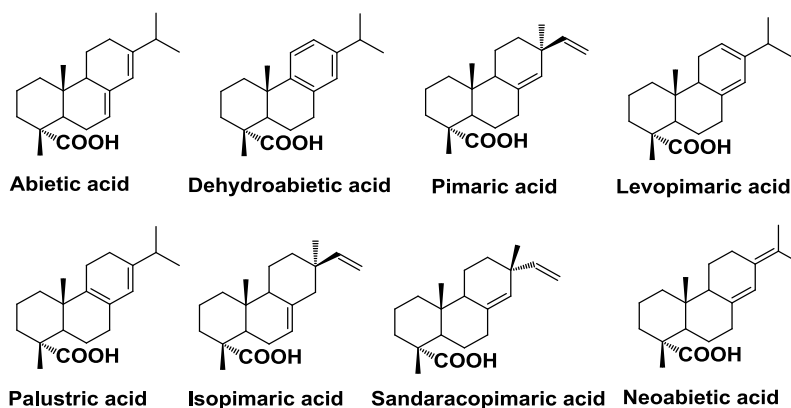


Figure 1: Repartition of world rosin production (2011).

Rosin is composed of 10% of neutral compounds (terpenes) and 90% of diterpenic monocarboxylic acids commonly named resinic acids whose formula is  $C_{19}H_{29}COOH$  (Scheme 1). This mixture of isomeric organic acids has a variable composition depending on its source. In all cases, abietic acid, which represents 40% to 60% of the mixture, is the main compound.



Scheme 1: Resinic acid structures.

Rosin possesses interesting properties such as hydrophobicity, good thermal properties and biocompatibility. Its rigid tricyclic skeleton possessing double bonds and a carboxylic functional group allows this compound to be used for many applications, as coatings, printing inks, food additives, adhesives and for biomedical purposes (e.g. ointment, glazing agent), (Figure 2).<sup>2,3</sup>

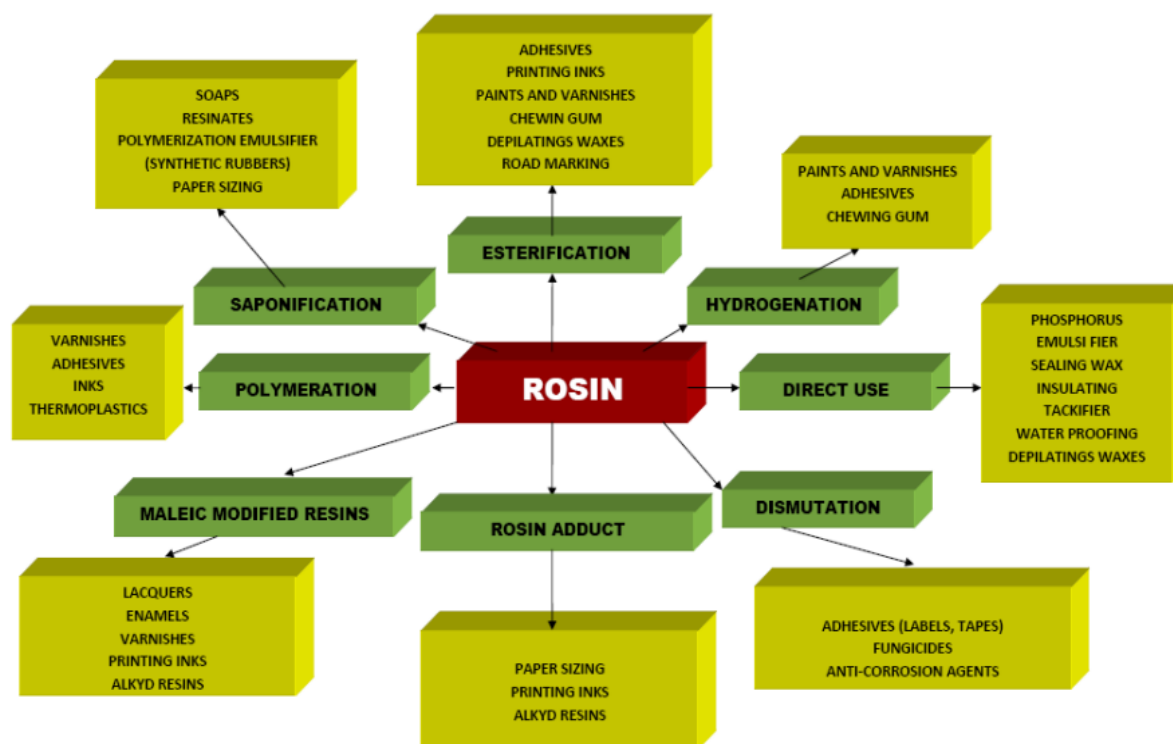
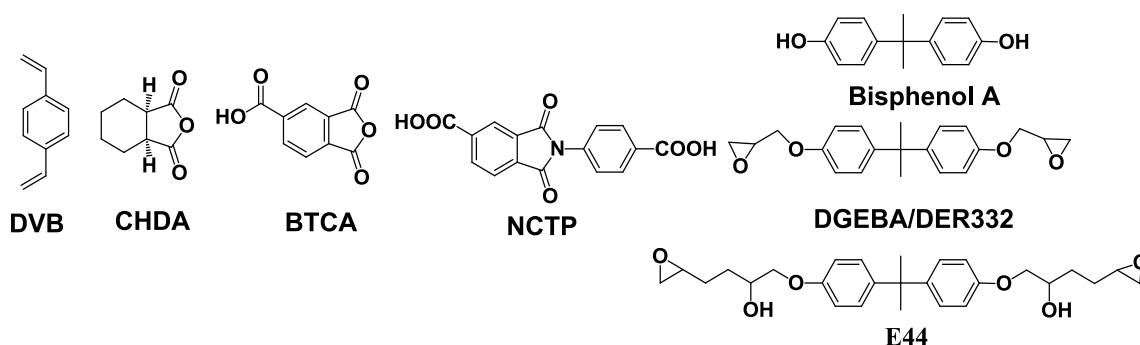


Figure 2 : Chemical modifications of rosin and main applications.

As abietic acid is the most abundant resinic acid, our study will focus on its use for the synthesis of thermoset and thermoplastic polymers.

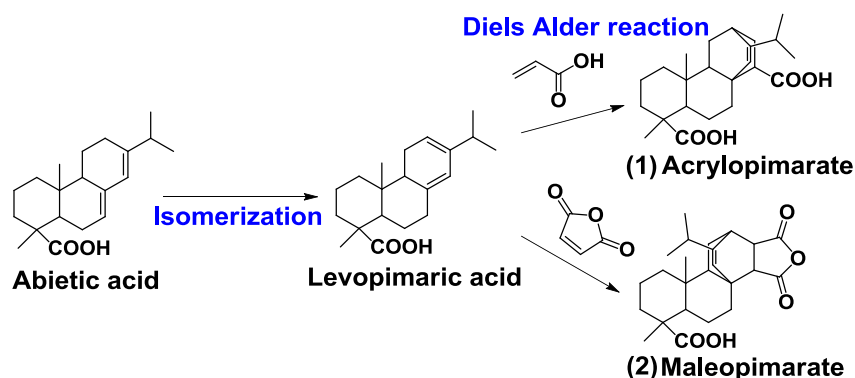
## 2. Abietic acid thermoset polymers

Thermosetting resins are polymeric materials in a preliminary soft solid or viscous state that change irreversibly into an insoluble, infusible polymer network by curing. Thermosetting polymers represent 20% of the plastic production. Typical examples are phenolic or urea formaldehyde resins, unsaturated polyesters, and mainly epoxy resins. A lot of efforts were recently reported on the synthesis of biobased thermosets from rosin.<sup>4</sup> Thus, rosin was investigated for the substitution of aromatic or cyclic petroleum-based compounds such as divinylbenzene (DVB), 1,2-cyclohexanedicarboxylic anhydride (CHDA) and 1,2,4-benzenetricarboxylic anhydride (BTCA), N-(4-carboxyphenyl)trimellitimide (NCTP) used as curing agent or glycidyl ether of bisphenol-A (DGEBA) as bisepoxide (Scheme 2).



Scheme 2: Common petroleum-based compounds used for thermoset synthesis.

Most of the polymers described in this chapter are synthesized from two abietic acid derivatives: acrylopimarate (1) and maleopimarate (2). (1) and (2) are prepared from levopimaric adduct, which is easily obtained by heating abietic acid to high temperature. The Diels-Alder reaction between rosin (levopimaric acid) and acrylic acid or maleic anhydride as dienophile leads to difunctional monomers, (1) and (2) (Scheme 3)<sup>5</sup>

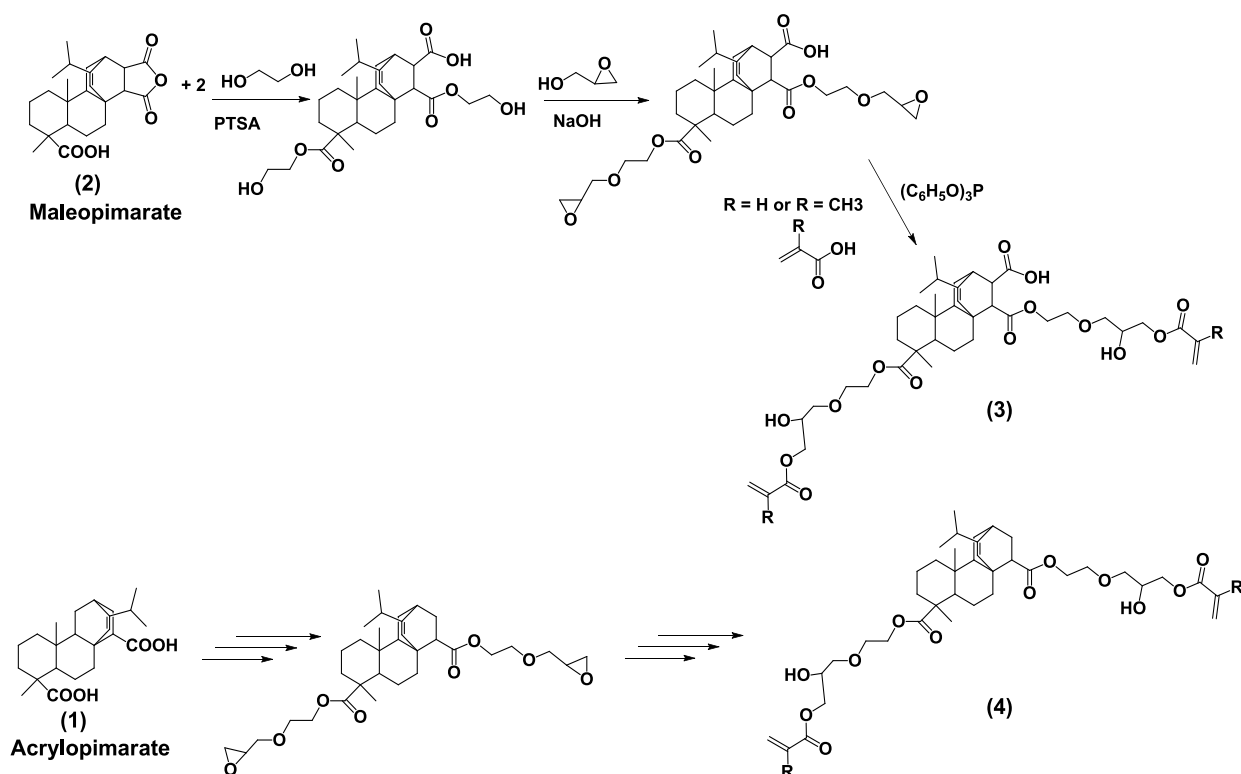


Scheme 3: Synthesis of acrylopimarate (1) and maleopimarate (2) from abietic acid.

### 1) Synthesis and properties of rosin vinyl ester resins

Two examples of synthesis of vinyl ester resins were found in literature. First, vinyl ester resins were produced from acrylopimarate (1) and maleopimarate (2) and cured with styrene, for coating applications.<sup>6</sup> (1) and (2) were modified with ethylene glycol to increase the solubility in styrene monomer and the flexibility of the cured resins. The reaction of the resulting hydroxyl rosin derivatives with epichlorohydrin leads to epoxy compounds which can react with acrylic or methacrylic acids to produce the divinyl ester cross-linkers (3), (4) (Scheme 4).



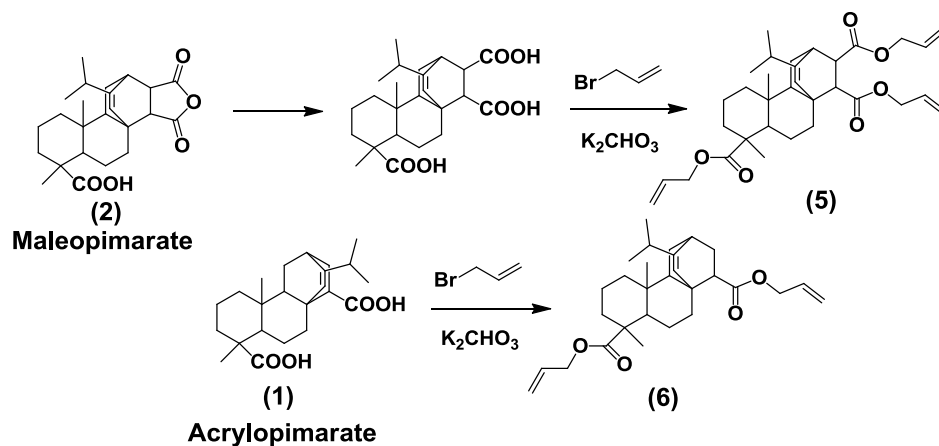


**Scheme 4: Synthesis of vinyl ester resins from acrylopimarate (1) and maleopimarate (2).**

The acrylate and methacrylate compounds were dissolved in styrene and cured by free radical initiated polymerization. Curing data indicate that styrene has a better ability to react with acrylates than with methacrylates. After curing, the glass transition temperature ( $T_g$ ) of the resin produced from maleopimarate **(3)** and acrylopimarate **(4)** derivatives are around 90 °C and 100 °C respectively. The chemical resistance of the coated vinyl ester resins was evaluated. The good results make this material suitable for linings for petroleum tanks, salt barges and ships, general chemical tankers and exterior coatings for the bottoms, boot-topping and decks.

Recently, a rosin derivative was tested for substitution of divinylbenzene.<sup>7</sup> Indeed, allyl rosin derivatives were used as rigid co-monomers with soybean oil derivatives (Scheme 5) and compared to the same resins synthesized from petroleum-based divinylbenzene. Maleopimarate **(2)** and acrylopimarate **(1)** were esterified with allyl bromide, yielding **(5)** and **(6)** and polymerized by radical polymerization with soybean derivatives. The reactivity of electron poor vinyl group of rosin derivative is a little lower than the one of divinylbenzene but maximum curing was successfully achieved screening curing times and temperatures. The thermomechanical analyses showed that rosin derivatives were more effective than divinylbenzene in enhancing the thermal and mechanical properties of cured soybean oil derivatives. Indeed, glass transition, elongation at break and tensile modulus are respectively

35.4 °C, 7.8%, 1.9 MPa, for 20% divinylbenzene, and 46.5 °C, 7.8%, 2.6 MPa for 20% rosin. T<sub>g</sub> was increased to 81 °C with 60% of incorporation of (6) and to 86 °C for the adduct containing three vinyl groups (5). Finally, the replacement of divinylbenzene by rosin does not influence the thermal stability of the resulting resins. In this study, rosin was proven to be a good substitute to divinylbenzene.

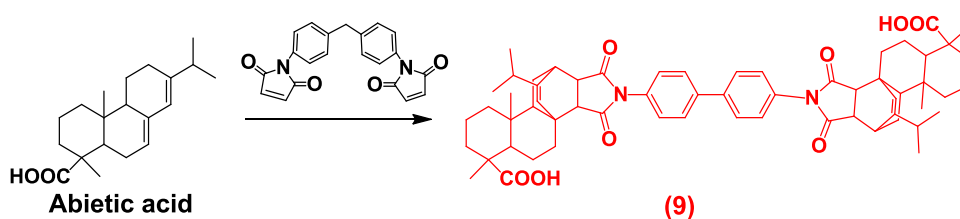
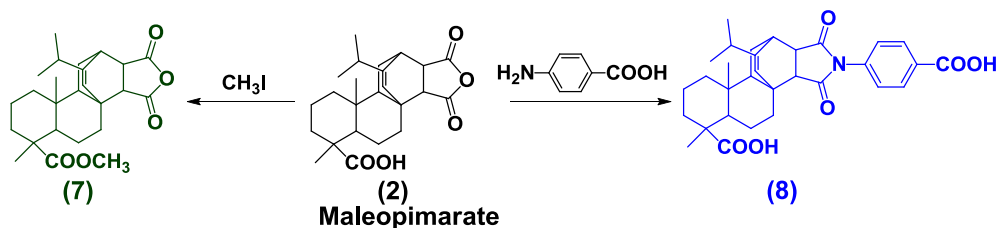


Scheme 5: Synthesis of vinyl esters from acrylopimarate (1) and maleopimarate (2).

## 2) Synthesis and properties of epoxy resin curing agents from rosin

Several studies investigated the use of acrylopimarate (1) or maleopimarate (2) derivatives as curing agents for epoxy resins (Scheme 6-7-8). Zhang and coll. compared maleopimarate (2) and methylmaleopimarate (7) to their petroleum-based analogues 1,2-cyclohexanedicarboxylic anhydride (CHDA) and 1,2,4-benzenetricarboxylic anhydride (BTCA) as curing agent for a high purity bisphenol-A diglycidyl ether, called DER332 epoxy resins and for eugenol epoxy derivatives (Scheme 6).<sup>8,9</sup> In each case, the epoxies cured with different curing agents, showed similar activation energy values indicating that rosin curing agent has similar reactivity and energy consumption to the commercial one. The resins cured with (2) and (7) possess the highest glass transition temperature due to the tricyclic structure of rosin. However, rosin-based resins exhibit slightly lower degradation temperature than the petroleum-based ones (Table 1). Thus, the curing agents based on maleopimarate (2) and (7), which are simpler to synthesize and more environmentally friendly, have great potential to replace aromatic or cycloaliphatic epoxy curing agents (Table 1). The synthesis imide-diacids to cure epoxy is a strategy to increase the thermal stability of the resulting epoxy resin.<sup>10</sup> The first curing agent (8) was prepared by reacting maleopimarate (2) with 4-aminobenzoic acid (Scheme 6). The second imide-diacid curing agent (9) was obtained by Diels Alder reaction

between abietic acid and 1,1'-(methylenedi-4,16phenylene)bismaleimide, in a 2:1 molar ratio (Scheme 7).



The imide-diacids (8) and (9) were compared to N-(4-carboxyphenyl)trimellitamide (NCPT) (Scheme 2) for curing DER6224 epoxy system which is a low molar mass product of bisphenol-A and epichlorohydrin, in a molar epoxy/diacid ratio of 2:1. Similar activation energies were calculated for curing with petroleum-based and rosin-based curing agents (Table 1).

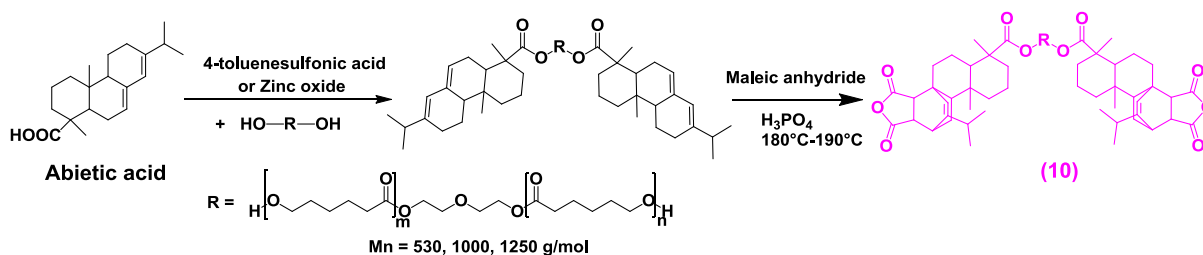
**Table 1: Comparison of the properties of rosin cured epoxy resins and petroleum cured ones.**

Epoxy resin	Curing agent	Ea (Kissinger) (kJ/mol)	Tg (°C)	Td5% (C°)
<b>DER332</b>	CHDA	74.8	114	330
	BTCA	67.5	178	340
	(2)	72.9, 73.3	186	320
	(7)	73.3	124	312
<b>Eugenol</b>	CHDA	65.7, 73.4	114	320
	(2)	63.2, 68.1, 71.2	155	317
<b>DER6224</b>	NCPT	81.9	107	350
	(8)	84.1	141	363
	(9)	88/07	152	355

The rosin-based epoxy resins prepared from (8) and (9) exhibit higher Tg, (141 and 151 °C), tensile strengths (63.4 and 57.9 MPa) and elastic modulus (4.6 and 4.5 MPa) than the petroleum-based one (Tg of 106 °C, tensile strength of 50.2 MPa, elastic modulus of

3.6 MPa) and similar thermal degradation. This study shows that rosin constitutes a good substitute to replace NCPT, as imide-diacid curing agent (Table 1).

In order to increase the flexibility of the materials, Zhang and coll. developed rosin-based curing agents with caprolactone segment (OH-R-OH) between two rosin units (**10**) (Scheme 8).<sup>10</sup> In a first step, abietic acid was esterified with polycaprolactone diol of different length (530, 1 000, 1 250 g/mol) in a ratio 2:1. Then, maleic anhydride was added to the ester through Diels Alder reaction. These dianhydride cured DER332 epoxy resins. The length of the soft segment increases the distance between cross-links and thus from 530 g/mol to 1 000 g/mol to 1 250 g/mol, the elongation increases of 73% and 44% and the tensile strength decreases of 44% and 75%. The thermal stability of the resins is also affected by the chain length. Indeed, the 5% thermal degradation temperature decreases from 353 to 334 °C with the increase of the chain length. This drop is attributed to the presence of less cross-links.

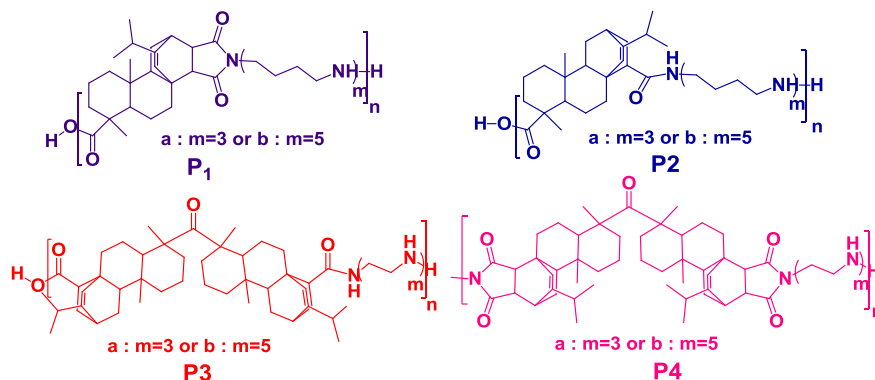


**Scheme 8: Synthesis of epoxy resin curing agents from abietic acid and caprolactone**

Finally, polyamides represent also good curing agent as they can be used at any ratio and they are inexpensive. The polyamide-imides **P1**, **P2**, **P3** and **P4** were synthesized as hardeners for rosin epoxy resins (Scheme 9). Their synthesis and properties will be described in the main chain rosin-based polymer section.<sup>11</sup> The condensation of epichlorohydrin and rosin-acid formaldehyde leads to multifunctional cycloaliphatic glycidyl ester and ether epoxy resins which are cured by **P1**, **P2**, **P3** and **P4**. Varying the ratio abietic acid/formaldehyde changes the structure of the resin and so, the epoxy functionality, which is between 2.7 and 4.0. As the thermomechanical properties of the epoxy resins are affected by the cross-linking density, the theoretical mixing ratio ( $r$ ) were calculated by the following equation to reach the stoichiometric quantity of amine activated hydrogen and epoxy groups:

$$r = \frac{M_w \text{ of polyamide} \cdot 100}{\text{Epoxy equivalent weight} \cdot \text{number of activated hydrogen}}$$

The structure of the hardener influences the curing temperature. All the resins exhibit good chemical and corrosive resistance due to cycloaliphatic structure. The coating adhesion is increased with the number of hydroxyl groups, so with the number of starting epoxy groups.

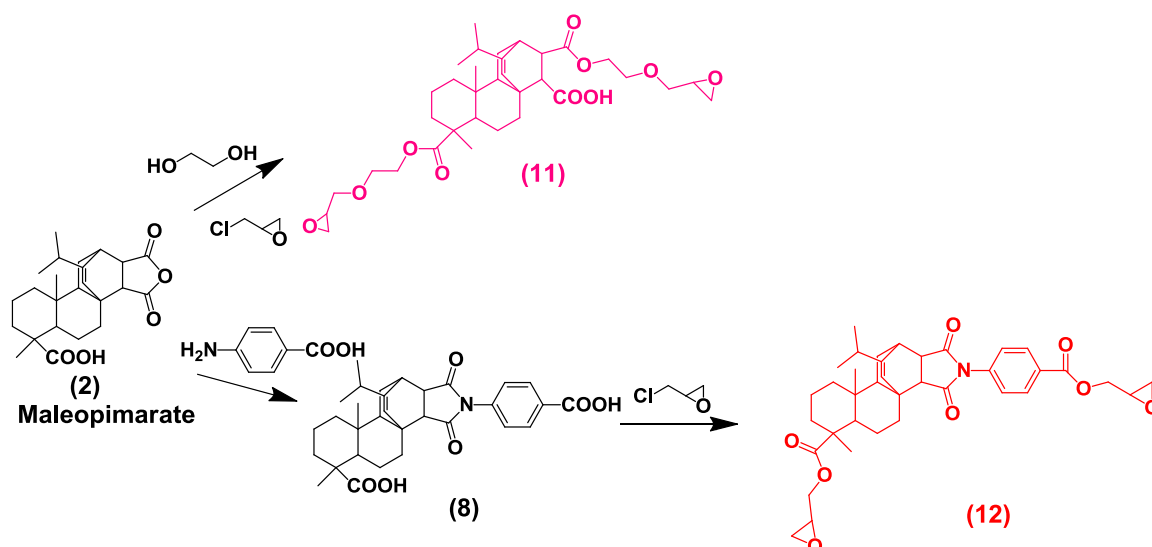


Scheme 9: Abietic acid-based polyamides used as curing agent for epoxy resins.

### 3) Synthesis of epoxy compounds from abietic acid derivatives and used in epoxy resin formulations

Several bisepoxides and multi-epoxides were synthesized from rosin or abietic acid and used for the preparation of epoxy resins.

First, maleopimarate (**2**) was esterified with ethylene glycol. The resulting hydroxymethylated derivative reacted with epichlorohydrin to form a bisepoxide (**11**) (Scheme 10).<sup>12</sup> Then, Zhang and coll. investigated the synthesis of epoxy resins from glycidyl ester of rosin-maleic anhydride imidodicarboxylic acid (**12**) (Scheme 10).<sup>13</sup>

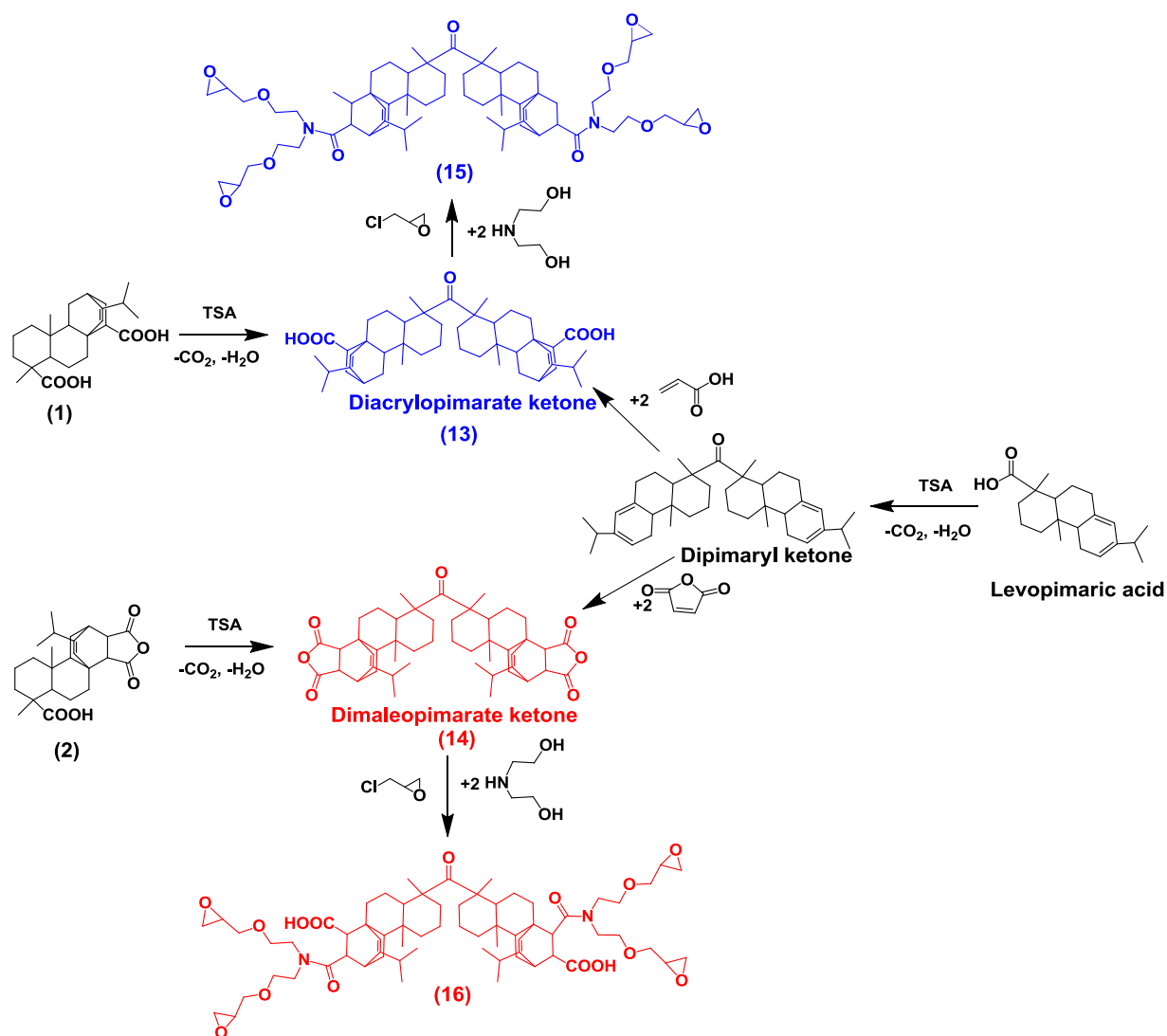


Scheme 10: Synthesis of bisepoxides compounds for epoxy resin synthesis.

The reaction of maleopimarate (**2**) with aminobenzoic acid yields a diacid (**8**) which was esterified with epichlorohydrin, yielding (**12**). (**12**) was cured with 1,2-

cyclohexanedicarboxylic anhydride (CHDA) and compared to commercial epoxy resin DER332 which was cured on the same way. Compared to commercial epoxy resin, rosin-based polymer exhibits a higher Tg (156 °C against 144 °C), slightly lower storage modulus at 30 °C and 5% degradation temperature (respectively 2.5 MPa against 3.3 MPa and 311 °C against 330 °C). Given the magnitude of these values, all these data are comparable. In comparison to epoxy resin from vegetable oils (Tg of 12 °C, and 5% degradation temperature between 200 °C and 300 °C), the thermomechanical properties of rosin-based epoxy resins are higher due to its polycyclic structure.

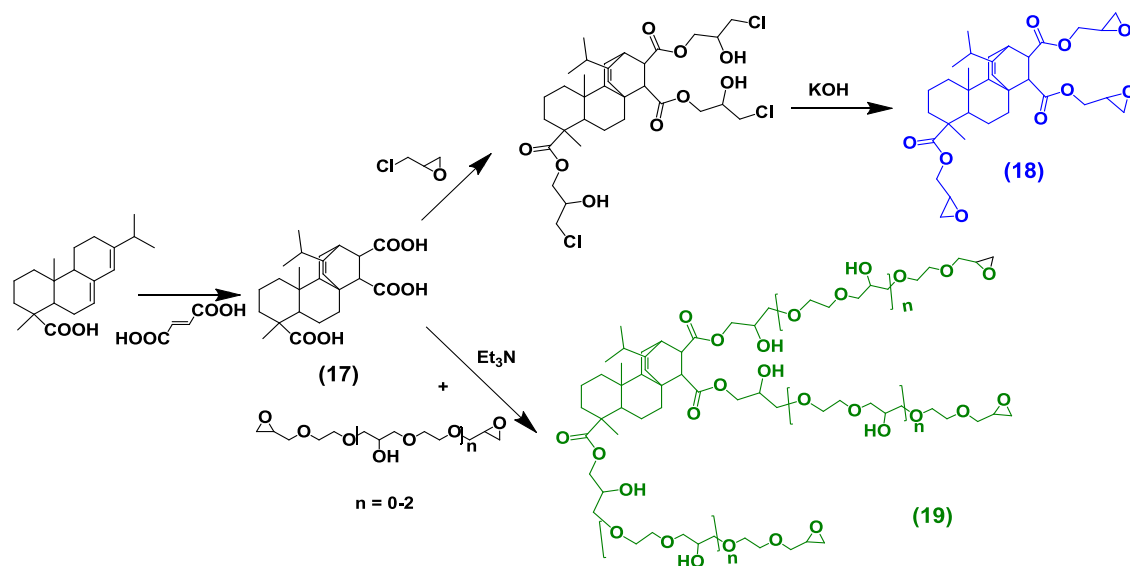
Other abietic acid derivatives can be synthesized by the dehydrodecarboxylation of abietic acid (or levopimaric acid) catalyzed by *p*-toluenesulfonic acid at 210 °C yielding ketones (13), (14). (Scheme 11)<sup>14,15</sup>



Scheme 11: Synthesis of diacrylopimarate ketone (13) and dimaleopimarate ketone (14) and derived bisepoxides.

Two synthetic pathways were explored. The ketones can be obtained directly by dehydrodecarboxylation of acrylopimarate (**1**) and maleopimarate (**2**) or by cycloaddition of acrylic acid and maleic anhydride on dipymaryl ketone (Scheme 11). The first strategy gave the highest yield (63%). These ketones reacted with diethanolamine to produce multifunctional hydroxyl derivatives, which become tetraglycidyl ether after reaction with epichlorohydrin (**15**) and (**16**).<sup>16</sup> Curing was performed with poly(amide-imide)s hardener already described as **P1**, **P2**, **P3** and **P4** in the previous section. The obtained resins showed high chemical and solvent resistance for coating application on steel.

Several epoxy resins were synthesized from abietic acid. In 2013, Mo and coll. synthesized a tricarboxylic acid (**17**) by performing a Diels Alder reaction between abietic acid and fumaric acid (Scheme 12). In the one hand, the esterification of (**17**) with epichlorohydrin leads to triglycidyl ester (**18**). In the other hand, the reaction of (**17**) with ethylene glycol diglycidyl ether of different chain length and triethylamine yields triglycidyl ethers (**19**) with spacers of different lengths. The resins were cured with methylhexahydrophthalic anhydride. The thermomechanical properties of each abietic acid-based resin and of commercial bisphenol-A-based resin, E44, were compared. As expected, the tensile strength, modulus and breaking elongation increase and the brittleness of the material decreases with increasing ethylene glycol spacer chain length. All these data were similar to the ones of the petroleum-based E44 resin (Table 2). The thermal properties of the triglycidyl ester (**18**) are higher than the triglycidyl ether ones (**19**) due to less flexible chains. The resin based on (**18**) exhibited glass transition, degradation temperature, resistance to water and acetone similar to the commercial equivalent.

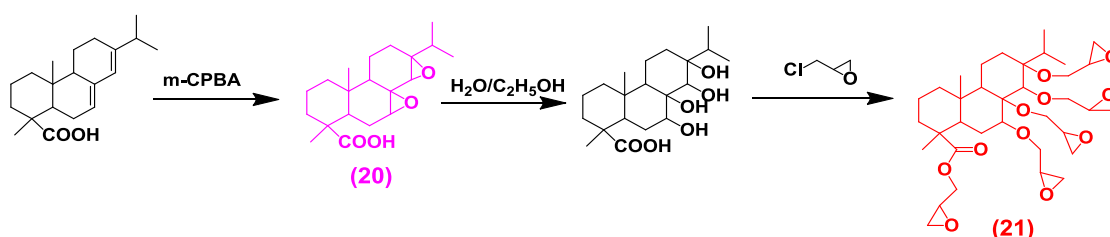


Scheme 12: Synthesis of multi-epoxides compounds from abietic acid.

**Table 2: Thermomechanical properties of rosin-based epoxy resins from (17).**

Monomer	T <sub>g</sub> (°C)	Td5% (°C)	Modulus (GPa)	Breaking elongation (%)
E44	140	342	0.29	12.3
(18)	167	328	0.471	13.3
(19) n=0	81	239	0.495	17.3
(19) n=1	79	234	0.300	20.5
(19) n=2	75	230	0.270	13.6

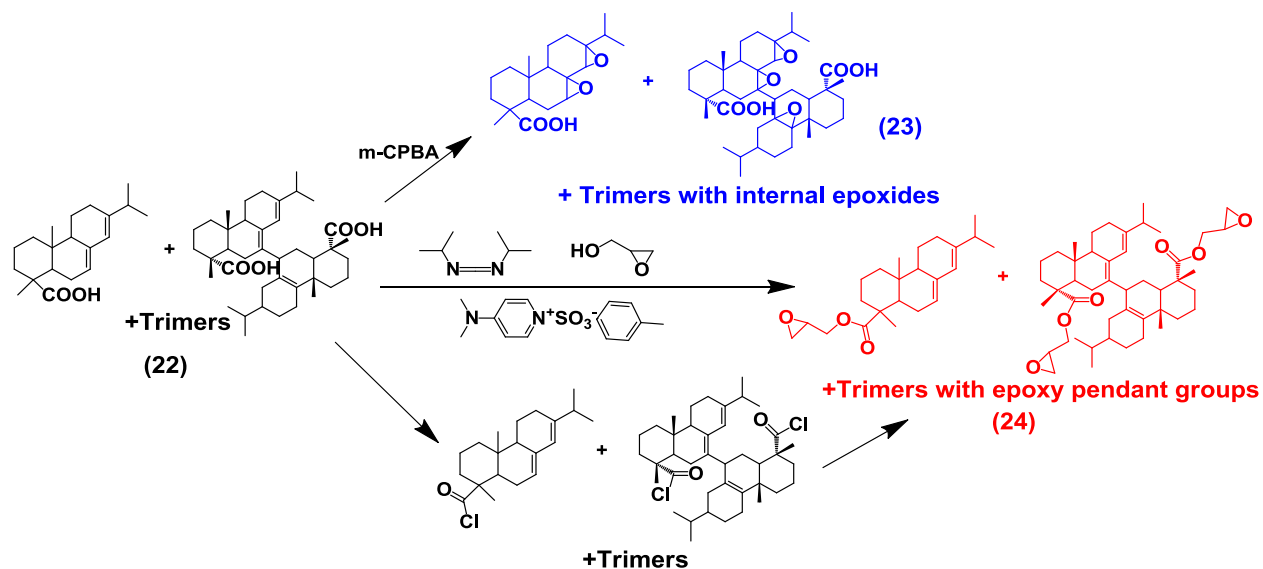
We recently developed epoxidized abietic acid as co-precursors for epoxy resins.<sup>17</sup> Abietic acid was epoxidized with 3-chloroperbenzoic acid yielding internally epoxidized abietic acid (20) (Scheme 13). The epoxide moieties of (20) were opened after dissolution and heating in a water/ethanol mixture. The resulting tetrahydroxyl abietic acid reacted with epichlorohydrin to produce epoxy abietic acid with five pendant epoxy groups (21). (20) was mixed with DGEBA in a 10% and 20% ratio of (20) and cured with isophorone diamine. The partial replacement of DGEBA by (20) leads to a slight decrease of the T<sub>g</sub> (from 140 °C to 130 °C) and of the elastic modulus (from 1 to 0.4 GPa). The same study was achieved with incorporation up to 40% of (21), due to the viscous aspect of this compound. Lower thermomechanical values than the previous system were obtained due to a flexible spacer arm. However, the T<sub>g</sub> remains high, 110 °C and the modulus equal to 0.2 MPa.

**Scheme 13: Synthesis of epoxidized abietic acid and of abietic acid with pendant epoxide groups.**

Following this work, we developed the use of rosin acid oligomers as precursors of DGEBA-free epoxy resins.<sup>18</sup> *Polygral* (22), a commercial by-product of paper and forestry industry, is a mixture of abietic acid and isomers (50%), abietic acid dimers (40%) and trimers (10%). First, *Polygral* was epoxidized using *m*CPBA leading to compounds with internal epoxides (23) (Scheme 14). 60% DGEBA, 40% of (23) in epoxy resins cured with IPDA were produced. A slight decrease of the T<sub>g</sub> (from 140 °C to 114 °C) and of the elastic modulus (from 1 to 0.4 GPa) in comparison to the 100% DGEBA epoxy resin was observed. Then, DGEBA free-epoxy resins were also synthesized. *Polygral* was esterified with glycidol using



carbodiimide or acid chloride chemistry yielding (24). Both methodologies proved to be efficient. As the compound was a viscous liquid, it was homogeneously mixed with IPDA to synthesize DGEBA-free epoxy resins. The  $T_g$  of 93 °C was lower than the DGEBA-based epoxy resin but the modulus of 1.2 GPa is similar.



Scheme 14: Synthesis of epoxy compounds from *Polygral*.

### Conclusion:

The Diels Alder reaction of rosin and acrylic acid or maleic acid leads to acrylopimarate (1) and maleopimarate (2), which constitute the precursors of rosin polymerization. Acrylate, methacrylate and allyl rosin derivatives were synthesized from acrylopimarate (1) and maleopimarate (2), employed as curing agents for the synthesis of vinyl ester resins and proved to good substitutes for commercial petroleum-based divinylbenzene. Diacids, dianhydrides and polyamides were produced from rosin and revealed to be efficient curing agents for epoxy resins. Finally, bisepoxides and multi-epoxides rosin derivatives were cured by classical curing agents to yield epoxy resins with thermomechanical properties similar to DGEBA-based epoxy resins.

### 3. Abietic acid thermoplastic polymers

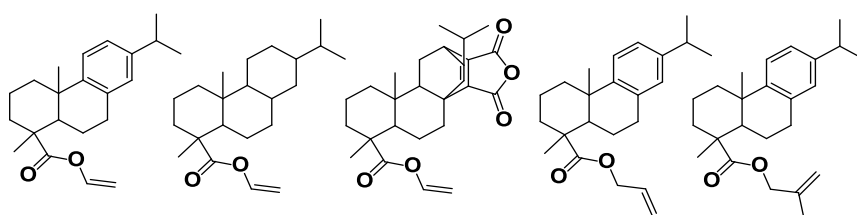
Thermoplastic polymers are also produced from resinic acids either after conversion of resinic acid to vinyl, allyl ester or acrylic group which can undergo radical polymerization to prepare well-defined side chain rosin-based polymers or *via* the Diels-Alder reaction between levopimaric acid and maleic anhydride (or acrylic acid), to yield difunctional monomers and the main chain rosin derived polymers thereof.

### 1) Synthesis and properties of rosin pendant chain polymers

Within the last decade, several studies investigated the radical polymerization of rosin derivatives leading to rosin pendant chain polymers and copolymers used for a large range of applications.

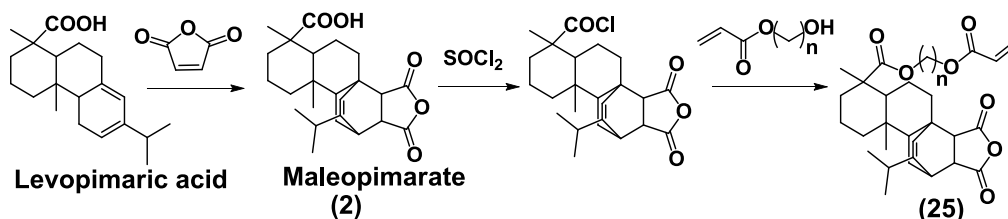
#### a) Free radical polymerization of rosin derivatives

First, vinyl ester, allyl ester and acrylic monomers were polymerized by free radical polymerization. Vinyl and allyl moieties only led to low molar mass polymers but the acrylic moiety increases the reactivity of the double bond and gives promising results (Scheme 15).<sup>19,20</sup>



**Scheme 15: Rosin derived vinyl and allyl ester monomers.**

Lee and Hong published a study on the synthesis of acrylic rosin derivatives and their application as negative photoresist.<sup>21</sup> Rosin moiety was selected for its adhesion, solubility and transparency properties and its incorporation into the photoresist polymer backbone enhanced the processability compared to the conventional photoresist material. Monofunctional acrylic rosin derivatives were synthesized by esterification of maleopimarate (**2**) and various acrylates and copolymerized by radical polymerization with methylmethacrylate (Scheme 16).



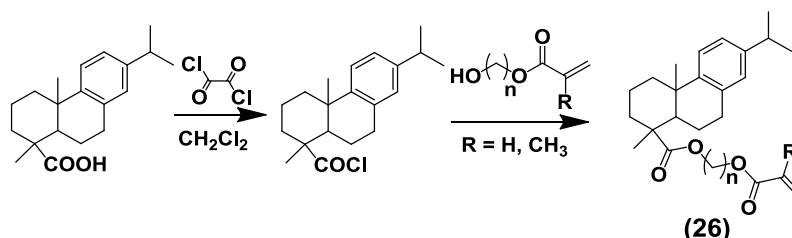
**Scheme 16: Synthesis of maleopimarate acrylate for negative photoresist application.**

The increase of the spacer length of the acrylate increased the molar mass, due to a decrease in steric hindrance, and decreased the glass transition temperature (Table 3). Then, the rosin double bond contributed to photocross-linking by the reaction with nitrene produced from bis-arylazide type photoinitiator by UV radiation. As expected, the obtained copolymers finally showed good solubility, transparency, adhesion, sensitivity, contrast and resolution.

**Table 3: Properties of the copolymers containing maleopimarate acrylate (25).**

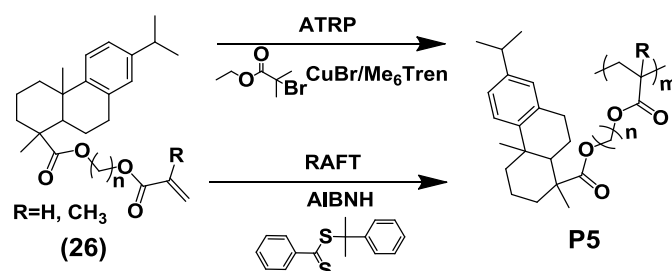
n	Monomer/MMA		T <sub>g</sub> (°C)	$\bar{M}_n$ (g/mol)	$\mathcal{D}$
	Feed	Result			
1	1/1	1/1.2	122	9 300	2.32
2	1/1	1/1.4	114	9 600	2.45
3	1/1	1/1.3	97	13 400	2.29

Chu and coll. further investigated, by DSC, the kinetic of free radical polymerization of dehydroabietic  $\beta$ -acryloxyl ethyl ester (**26**) (Scheme 17) in the presence of AIBN, at different temperatures. The obtained polymers showed a T<sub>g</sub> around 25 °C, a molar mass around 5 000 g/mol with a dispersity of 1.1.<sup>22</sup> This reaction led to well-defined low molar mass polymers. In order to increase the molar mass value, controlled radical polymerization was developed.

**Scheme 17: Synthetic route of dehydroabietic acid acrylate derivatives.**

#### b) Controlled radical polymerization of rosin derivatives

Controlled radical polymerization (CRP) of the dehydroabietic acrylic esters (chosen for the high stability of the aromatic group) leads to well-defined polymers with controlled molar mass, narrow dispersity and well-defined functionalities and architectures, **P5** (Scheme 18).

**Scheme 18: Polymerization of dehydroabietic acrylic ester by ATRP and RAFT methodologies.**

Tang and coll. developed a series of these polymers for different applications. First, they studied the properties of the methacrylate and acrylate rosin-based polymers (**P5**-acrylate, **P5**-methacrylate) synthesized from (**26**) by ATRP using ethyl 2-bromoisobutyrate as initiator, copper bromide (CuBr) as catalyst, tris(2-(dimethylamino)ethyl)amine (Me<sub>6</sub>Tren) as ligand in tetrahydrofuran (THF). The use of less polar solvent such as anisole leads to a better control

of **P5**-methacrylate polymerization. The increase in the acrylate spacer length yielded higher molar masses and lower glass transition temperatures. The polymerization of methacrylate monomer was faster, led to higher molar masses and higher glass transition temperatures (Table 4). These polymers showed a two-step degradation profile with a first slight loss at 220 °C and a second complete decomposition with the onset at 325 °C.<sup>23</sup>

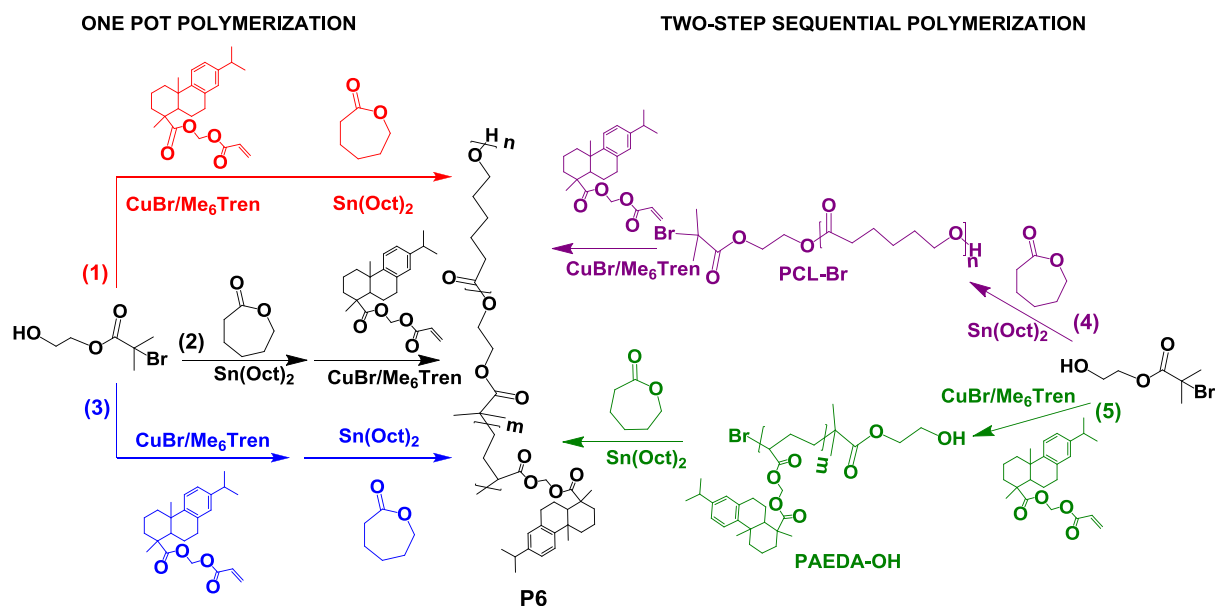
**Table 4: Properties of the polymers containing rosin moieties (P5) prepared by ATRP and RAFT methodologies from (26).**

Polymerization method	Solvent	Monomer	n	$\bar{M}_n$ (g/mol)	$\mathcal{D}$	Tg (°C)
ATRP	THF	Acrylate	2	11 500	1.20	50
	THF	Acrylate	4	21 500	1.25	22
	Anisole	Methacrylate	2	31 000	1.33	90
RAFT	THF	Acrylate	2	29 100	1.30	
	Toluene	Methacrylate	2	20 000	<1.3	

The authors extended the study of dehydroabiatic  $\beta$ -acryloxyl ethyl ester (**26**) polymerization to RAFT polymerization (reversible addition-fragmentation chain transfer polymerization), using cumyl dithiobenzoate as transfer agent and AIBN as radical initiator, yielding **P5** (Scheme 18).<sup>24</sup> The polymerization of methacrylate monomer in toluene showed a living character but led to lower molar mass than ATRP. Under the same conditions, acrylate polymers possessed high dispersity, over 1.5. The replacement of toluene by THF leads to a better control, dispersity of 1.3 but the reaction was very slow (Table 4). For this reason, in the following studies, all the copolymers of dehydroabiatic acid acrylate or methacrylate (**26**), with cellulose, lignin, polyethylene glycol and fatty acids were synthesized by ATRP. These copolymerizations enable to broaden the characteristic of the dehydroabiatic-based polymers and to target a wide range of applications.

The same group combined ring opening polymerization (ROP) and ATRP to synthesize renewable resinic acid degradable  $\epsilon$ -caprolactone block polymers **P6** (Scheme 19).<sup>25</sup> This work was driven by two reasons: increasing the amount of renewable compound in degradable materials that are not renewable as well as accessing new properties due to dehydroabiatic moieties. Two strategies were developed. The one pot polymerization involved the difunctional initiator (hydroxyethylbromoisobutyrate, HEBiB) and simultaneously or successively, addition of caprolactone and dehydroabiatic ethyl acrylate without any workup in between (Route 1, 2, 3 Scheme19). For the simultaneous polymerization (Route 1), the polymerization ( $\mathcal{D} = 1.26$ ) was well-controlled for a

composition in caprolactone up to 32 units and in dehydroabietic ethyl acrylate of 70 units. The sequential addition of dehydroabietic compound first, followed by caprolactone (Route (2)) led to a poor control of polymerization and almost no caprolactone was polymerized, probably because of the deactivation of Sn(II) catalyst after accumulation of Cu catalyst. Finally, the addition of caprolactone first, to avoid the problem of catalyst deactivation (Route (3)), results in the synthesis of a diblock copolymer with 200 units of caprolactone and 20 of dehydroabietic ethyl acrylate and a reasonable dispersity of 1.38. A higher block of dehydroabietic ethyl acrylate can be obtained by varying the ratio acrylate/macroinitiator. The two-step sequential polymerization employed difunctional initiator (hydroxyethylbromoisobutyrate, HEBiB) yielding PCL-Br (Route (4)) or PAEDA-OH (Route (5)) by ROP or ATRP respectively. This first reaction was stopped and the so-formed macroinitiators reprecipitated. They show narrow SEC distributions and dispersities below 1.3 meaning that they are well defined. Then, ROP or ATRP from these macroinitiator was performed.



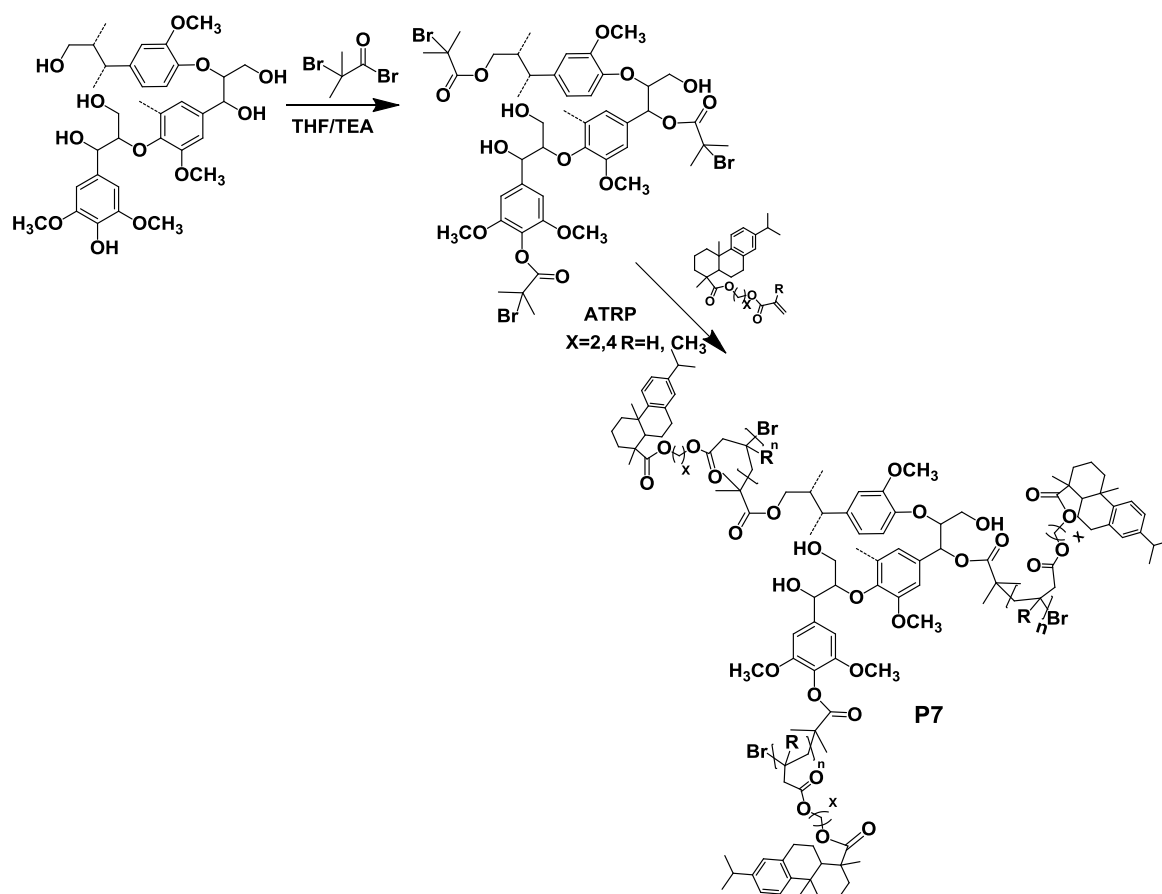
**Scheme 19: Preparation of diblock copolymers containing caprolactone and dehydroabietic ethyl acrylate.**

$^1\text{H}$  NMR and SEC analyses indicate, in both cases, the diblock formation with narrow molar mass distributions. Route (4) led to a polymer composition of 41 units of each compounds whereas route (5) yields 50 units of dehydroabietic compound and 500 units of caprolactone. Polycaprolactone segments exhibited excellent degradability under acidic condition.

The dehydroabietic polymer does not show any degradability under these conditions but is potentially degradable by microbials.<sup>26,27</sup> The successful synthesis of rosin caprolactone block

copolymer could be extended to other degradable materials and could be used for advanced applications.

The “grafting from” ATRP methodology was used for the synthesis of biocomposites. First, Tang and coll. provided the synthesis of rosin polymer-grafted lignin biocomposites with modified lignin as macroinitiators, **P7** (Scheme 20).<sup>28</sup> Macroinitiators were prepared by partial esterification of the lignin OH groups. Both phenolic and aliphatic alcohols participated in the esterification, but phenolic is preferentially converted. The macroinitiator contained 2.47 mmol/g of bromine.



**Scheme 20: Synthesis of rosin polymer-grafted lignin biocomposites.**

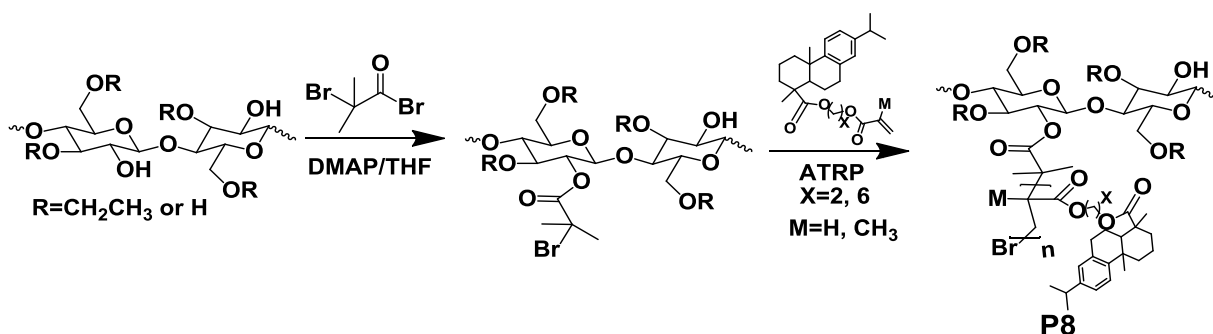
The kinetic studies of the ATRP polymerization of the dehydroabiatic acid derivative revealed the living and controlled character of the polymerization. High molar masses, up to 186 000 g/mol for methacrylate derivative were reached. The structure of the acrylic monomers allows the synthesis of biocomposites with a T<sub>g</sub> ranging from 20 °C to 100 °C. The incorporation of these moieties into lignin increased significantly the hydrophobicity of the materials, as the contact angle reached 90° instead of 75° in lignin. Moreover, as rosin moieties dominated at the surface of the composite, its water uptake decreased from

18 weight% to below 1 wt% (Table 5). This study highlighted the interesting synthesis of a hydrophobic, high water resistant lignin composite.

Table 5: Properties of the rosin-grafted lignin composites (P7).

Monomer	X	Conversion (%)	$\bar{M}_w$ (g/mol)	$\bar{M}_n$ (g/mol)	$D$	Tg (°C)	Contact angle (°)	Water uptake (weight%)
Lignin			1 700	870	1.95	98	75	>18
Acrylate	4	65	52 100	16 600	3.13	20	91	<1
Acrylate	2	62	19 100	11 600	1.65	70	89	<1
Methacrylate	2	88	186 000	56 400	3.31	95	91	<1

Later, the same strategy was adopted on ethyl cellulose (Scheme 21).<sup>29</sup> Macroinitiators with various amounts of bromine were synthesized by partial esterification of the ethyl cellulose hydroxyl groups. The higher bromine content macroinitiators led to the lower molar mass polymers, probably due to steric hindrance. In this context, the macroinitiator used for all the acrylic ester contained 0.5 mmol/g of bromine.



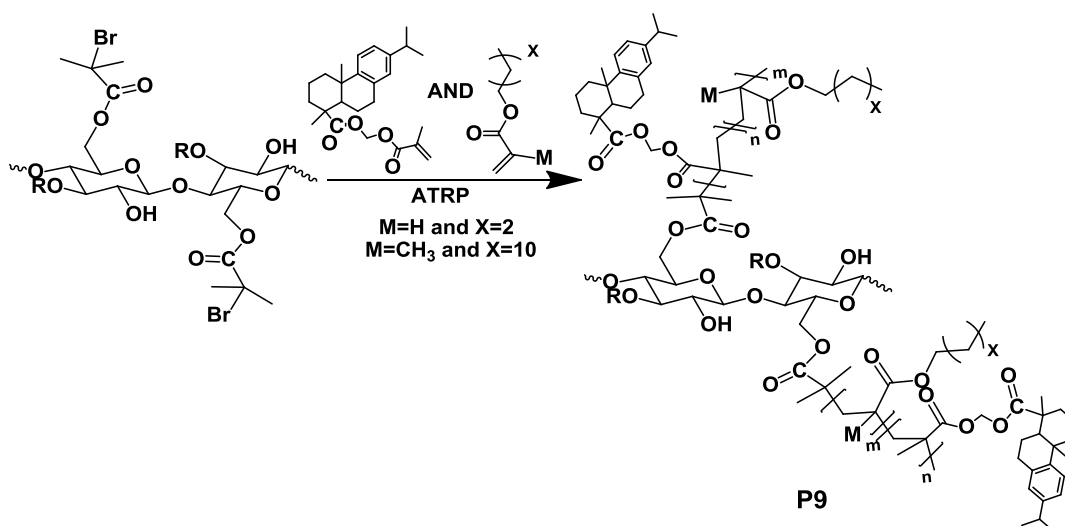
Scheme 21: Synthesis of rosin polymer-grafted cellulose composites.

The polymerization of all the dehydroabiestic derivatives was living and controlled. The molar masses of the polymers, **P8** were measured by both NMR and SEC (Table 6). First, the thermostability of the polymers increased in comparison with cellulose. Indeed, the ethyl cellulose 5% degradation temperature is 264 °C although after modification, this temperature ranges from 395 to 417 °C. As described previously with lignin composites, these polymers show tunable glass transition and their hydrophobicity is remarkably enhanced (Table 6). Finally, the surface morphology studied by AFM indicates good film forming properties and UV absorption. The transmittance of ethylmethacrylate dehydroabiestic polymer grafted cellulose in the visible region was over 80% while in the UV range (200-315 nm), it decreased to 0%. This phenomenon was not observed with unmodified ethylcellulose. All these characteristics make them good candidates for UV absorbent coating materials.

**Table 6: Properties of the ethyl cellulose-grafted lignin composites.**

Monomer	X	Conversion (%)	$\bar{M}_n$ (NMR) (g/mol)	$\bar{M}_n$ (SEC) (g/mol)	$\bar{D}$ (SEC)	Tg (°C)	Contact angle (°)
Ethylcellulose						102.5	75
Acrylate	2	10	3 900	1 900	1.39	48.4	98
Acrylate	6	15	6 800	2 300	1.16	14.3	96
Methacrylate	2	56	23 000	6 400	2.07	82.5	96
Methacrylate	6	40	18 700	5 900	1.18	27.6	97

The replacement of rosin only, by copolymers of rosin and butyl acrylate or fatty acid (lauryl methacrylate) in this cellulose-based copolymer, allowed Tang and coll. to synthesize thermoplastic elastomers, **P9**.<sup>30</sup> Dehydroabietic ethylmethacrylate was used in this study (Scheme 22).

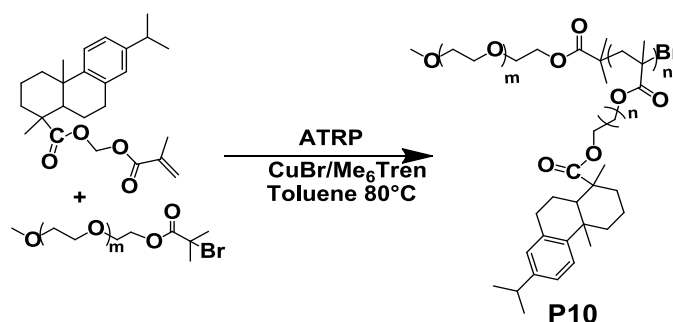
**Scheme 22: Synthesis of rosin/fatty acid polymer-grafted cellulose composites.**

Higher molar mass polymers than in the previous study were prepared (the ratio of dehydroabietic ethylmethacrylate never exceeded 50%). Indeed, using butylacrylate, the copolymer molar masses ranged between 30 000 and 50 000 g/mol while using laurylmethacrylate they are between 83 000 and 242 000 g/mol depending on the dehydroabietic ethylmethacrylate/butylacrylate or laurylmethacrylate ratio. The glass transition temperature could also be tuned from -15 °C to 60 °C by increasing the dehydroabietic ethylmethacrylate content in butylacrylate copolymers and from -48 °C to 27 °C in laurylmethacrylate copolymers. As mentioned in the previous example, the thermal stability of cellulose is increased due to the grafted copolymers. The thermal stability of butylacrylate copolymers is higher than the one of laurylmethacrylate copolymers which remains high



because of the tricyclic structure of dehydroabietic acid. These samples exhibit excellent hydrophobicity with contact angles between 89 and 105°. The samples with 25-40% of dehydroabietic ethylmethacrylate, meaning the ones with Tg between 10 and 30 °C manifest good elastomeric properties with elasticity at strain over 500%. These polymers are good candidates for applications requiring material with high elasticity without rupture at high strength.

Finally, Jiang and coll. synthesized well-defined amphiphilic poly(ethylene glycol) and poly(dehydroabietic ethyl methacrylate) block copolymers, **P10**, by ATRP for drug delivery applications (Scheme 23).<sup>31</sup> Poly(dehydroabietic ethyl methacrylate), which is biocompatible, was chosen for its hydrophobicity which facilitates the drug loading, here, the water insoluble piperlongumine (PLGM). A PEG of 5 000 g/mol was used in this study. A copolymer **P10** of 31 300 g/mol with a dispersity of 1.26 was synthesized. The copolymer and the drug were dissolved in THF and a nanoencapsulation method in water led to the formation of PLGM encapsulated PEG-b-PDAEMA nanoparticles with hydrodynamic diameters of 110 nm and narrow size distribution. These nanoparticles are stable in loading with 19.5% of drug. This value is higher than common nanoparticles, which good loading is generally around 10%, due to the excellent hydrophobicity of dehydroabietic moieties. In tumor bearing mice, the nanoparticles show passive targeting accumulation in the tumor site and long blood circulation time. *In vivo* antitumor examination shows that PLGM-loaded **P10** nanoparticles have superior antitumor activity to free PLGM. Thus, the dehydroabietic ethyl methacrylate can be considered as a promising hydrophobic compound for the synthesis of copolymer drug delivery systems.



Scheme 23: Synthesis of poly(ethylene glycol)-poly(dehydroabietic ethyl methacrylate) copolymer.

### Conclusion:

In the previous examples CRP allowed the synthesis of well-defined (co)polymers from resinic acids with relatively high molar masses. All the (co)polymers bear resinic acid as

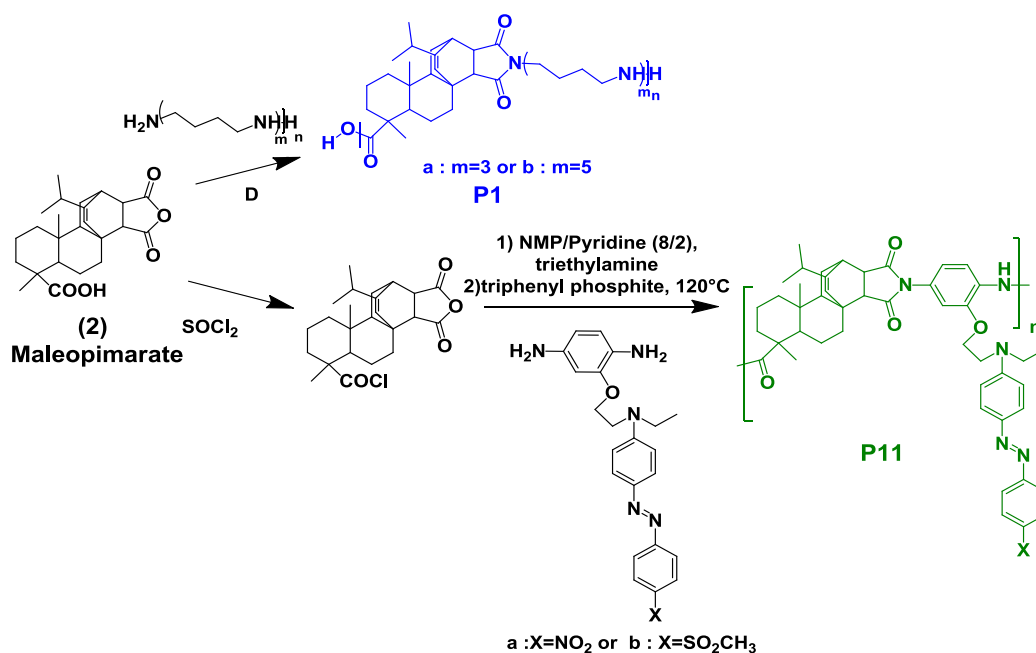
pendant groups. The copolymerization of resinic acid with various monomers enables the tuning of the thermomechanical properties and so, the target of a wide range of applications. This part highlighted the interesting characteristics of resinic acid monomers in terms of thermal stability, rigidity, hydrophobicity and film forming.

## **2) Synthesis and properties of polymers with rosin derivatives in the main chain**

The synthesis of main chain rosin-based polymers is more difficult, mainly because of steric hindrance. The multiple following examples illustrate this problem. The characteristics and thermomechanical properties of the main chain abietic acid polymers are summarized in Table 7 p 52. The main chain rosin-based polymers are synthesized from acrylopinarate (**1**) and maleopinarate (**2**) adducts. The step growth polymerizations of these monomers with diols, diacids, diesters, diamines lead to the synthesis of main chain rosin-based polyesters, polyamides, polyamide-imides which are described below.

### a) Synthesis of maleopinarate main chain thermoplastic polymers

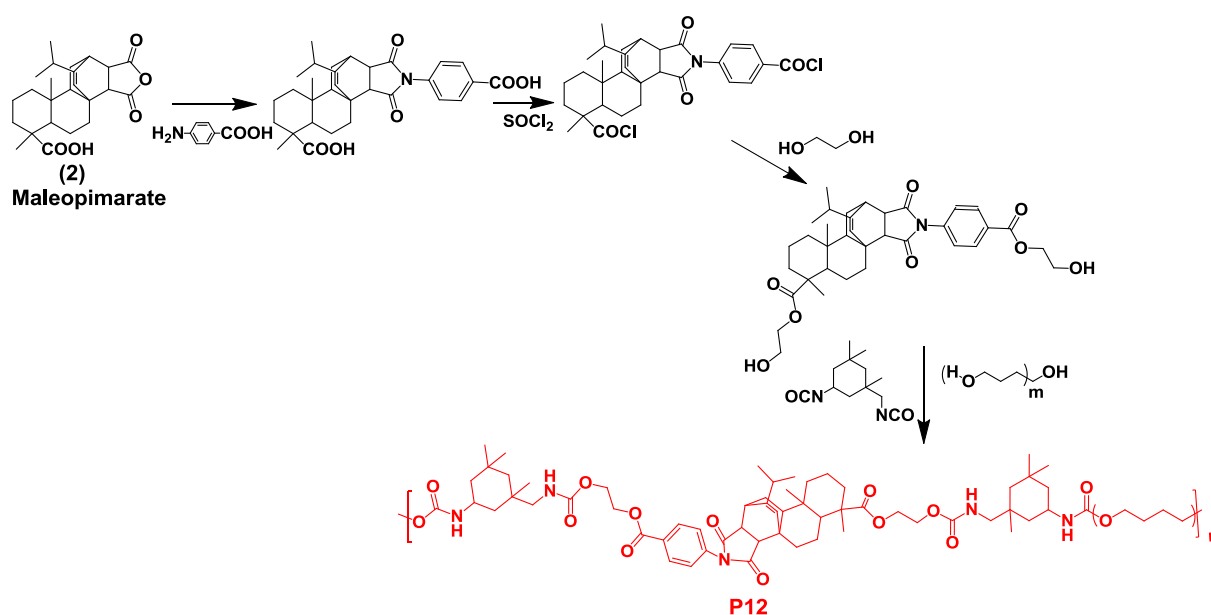
The polymers synthesized from maleopinarate (**2**) will be first described. Poly(amide-imide) is a category of polymers well known for its excellent thermal stability and high rigidity. Two kinds of rosin poly(amide-imide) were developed. Kim and coll. provided new rosin-based photoactive poly(amide-imide)s by the polycondensation of maleopinarate (**2**) with azo-dye diamines, **P11** (Scheme 24).<sup>32,33</sup> The cycloaliphatic structure of rosin into the polymer chain gives excellent solubility in organic solvent and, in this manner, easy process ability for the formation of thin films by spin coating. The films display excellent properties including a smooth surface, toughness, adhesion to the substrate and high optical quality.



**Scheme 24: Synthesis of poly(amide-imide)s from maleopimarate monomer.**

Atta and coll. developed a series of poly(amide-imide) by polycondensation of maleopimarate, **P1** (Scheme 24) with triethylene tetramine and pentaethylene hexamine in order to be used as hardener for epoxy resins.<sup>11</sup> The properties of the resulting epoxy resins have already been described in the previous section. Low molar mass polymers, with a degree of polymerization between 3 and 6, but high Tg at around 150 °C, were obtained.

Recoverable rosin-based polyurethanes **P12** were recently synthesized by Zhu and coll.<sup>34</sup> Maleopimarate (**2**) was modified into a diol by the successive reaction with aminobenzoic acid and ethylene glycol (Scheme 25).

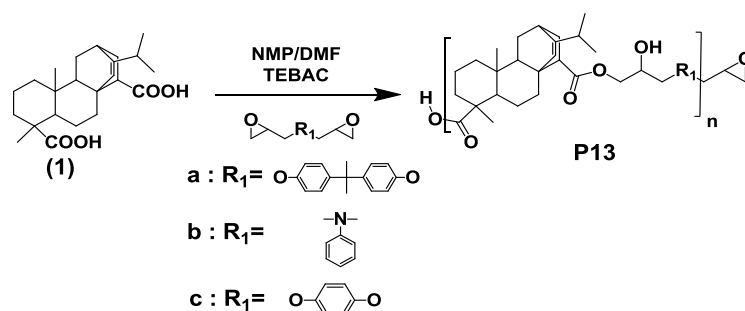


**Scheme 25: Synthesis of polyurethanes from maleopimarate monomer.**

In their study, polyurethanes were synthesized by a step polymerization between isophorone diisocyanate (IPDI), polytetramethyleneglycol 2 000 (PTMG) and rosin derivative in 2:1:1 molar ratio. Rosin was selected because the micro-phase separation (formation of hard segment and soft segment domains) and thermal stability of the hard segment are both key factors that influence the recovery properties. Only mechanical properties were investigated. The shape recovery with more than 1 000% strain reaches up to 96% at room temperature in 3 min and the recoverable strain is more than 960%, which was 2.5 times better than the best value previously reported.

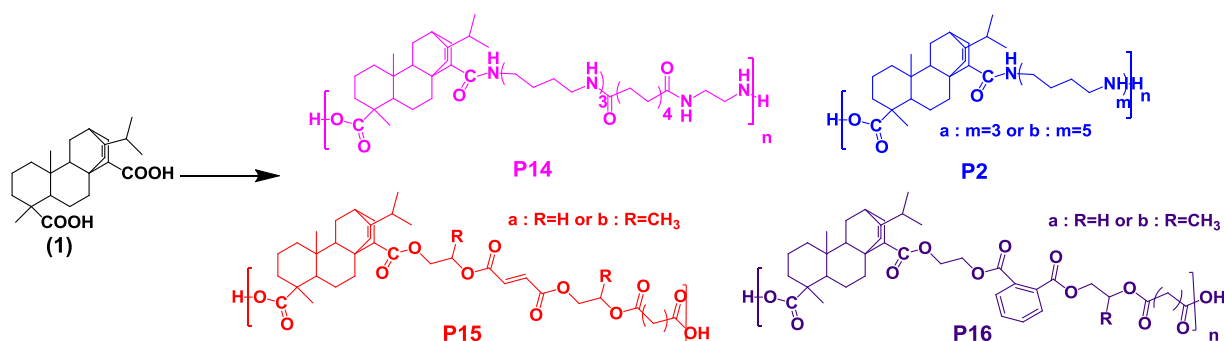
#### b) Synthesis of acrylopinarate main chain thermoplastic polymers

Most of the main chain rosin-based polymers were synthesized from the acrylopinarate (**1**). In 2005, Bicu and coll. developed, first, a series of polyhydroxyesters from acrylopinarate (**1**) and various bisepoxides (a, diglycidylether of bisphenol-A, b, diglycidylaniline and c, diglycidyl ether of hydroquinone) (Scheme 26).<sup>35</sup> The obtained polymers, **P13** (a, b, c), show relatively high Tg, at around 70 °C, and good thermostability, over 280 °C.



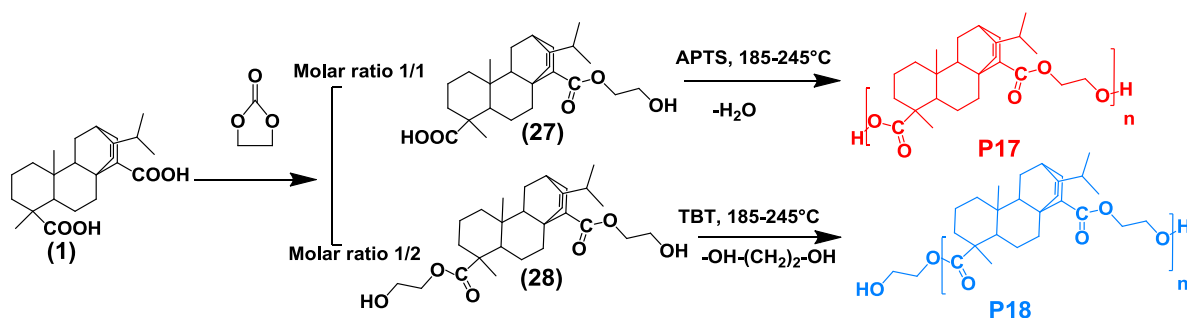
**Scheme 26: Synthesis of main chain abietic acid polyhydroxyester from acrylopinarate.**

Subsequently, main chain abietic acid polyamides were synthesized (Scheme 27). The same group provided water soluble polyamides from acrylopinarate (**1**), triethylenetetramine and adipic acid, **P14**.<sup>36</sup> After reaction with epichlorohydrin, these polymers are able to cross-link under heating and can be used in the paper industry. Atta and coll. developed another series of poly(amide)s by polycondensation of acrylopinarate (**1**), **P2** with triethylene tetramine or pentaethylene hexamine in order to be used as hardener for epoxy resins.<sup>11</sup> The properties of the resulting epoxy resins have already been described in the previous section. The same authors reacted the propylene or ethylene glycol, PG or EG, with different adducts following by acrylic acid or maleic anhydride to introduce double bond in the chain. These unsaturated polyesters, **P15**, **P16**, after curing with styrene, can be used as corrosion protection of steel.<sup>37,12</sup> All these synthetic pathways led to oligomers, up to nine units (Table 7).



**Scheme 27: Synthesis of main chain abietic acid polyamides from acrylicopimarate.**

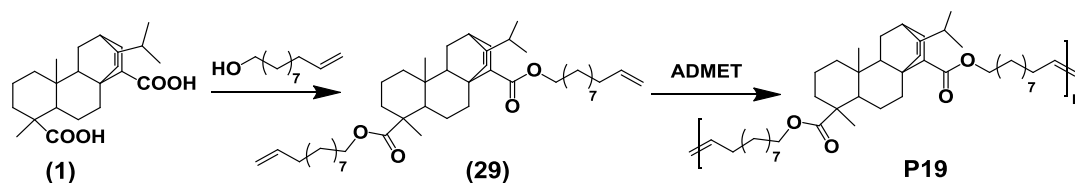
Recently, Bicu and coll. developed a new route for the synthesis of polyesters from acrylicopimarate exhibiting relatively high molar mass.<sup>38</sup> A condensation reaction of the adduct with a cyclic carbonate ester (1,3-dioxolan-2-one) catalyzed by an efficient amine (triethylamine) yield hydroxyalkyl esters (**27**), (**28**) (Scheme 28). A molar carbonate/rosin ratio of 1/1 leads to an AB monomer, (**27**), with an alcohol and a carboxylic acid terminal group, whereas a molar carbonate/rosin ratio of 2/1 yields an A<sub>2</sub> monomer, (**28**), with two alcohol terminal groups. The monomers were homopolymerized yielding **P17** and **P18**. Degrees of polymerization of 30 were reached and **P17** and **P18** possess high T<sub>g</sub>, at around 110 °C, and degradation temperature over 300 °C. The polyesters synthesized by polycondensation of these molecules showed good thermal stability and high dielectric properties.



**Scheme 28: Synthesis of main chain abietic acid polyesters from acrylicopimarate.**

Special attention should be given on the last example as the same strategy but based on the abietic acid dimer is adopted in our work. Indeed, recently, Tang and coll. synthesized novel polyesters from castor oil and rosin, through metathesis chemistry **P19** (Scheme 29).<sup>39</sup> They esterified acrylicopimaric acid with undecenol to yield a bis-unsaturated monomer (**29**). The esterification was performed in two steps. First acrylicopimarate (**1**) reacted with oxalyl chloride before adding a second mixture of triethylamine and undecenol. The resulting product was purified by silica gel column chromatography to obtain a yield of 44%. Finally,

acyclic diene metathesis (ADMET) polymerization in bulk was carried out employing Hoveyda Grubbs catalyst, yielding **P18**. Polyesters with molar mass up to 9 200 g/mol, corresponding to 19 units, were produced (Scheme 29). The polyester shows a low glass transition temperature of  $-5\text{ }^{\circ}\text{C}$ , due to the undecenol in the main chain and a good thermal stability, around  $300\text{ }^{\circ}\text{C}$  for 5% of degradation temperature.

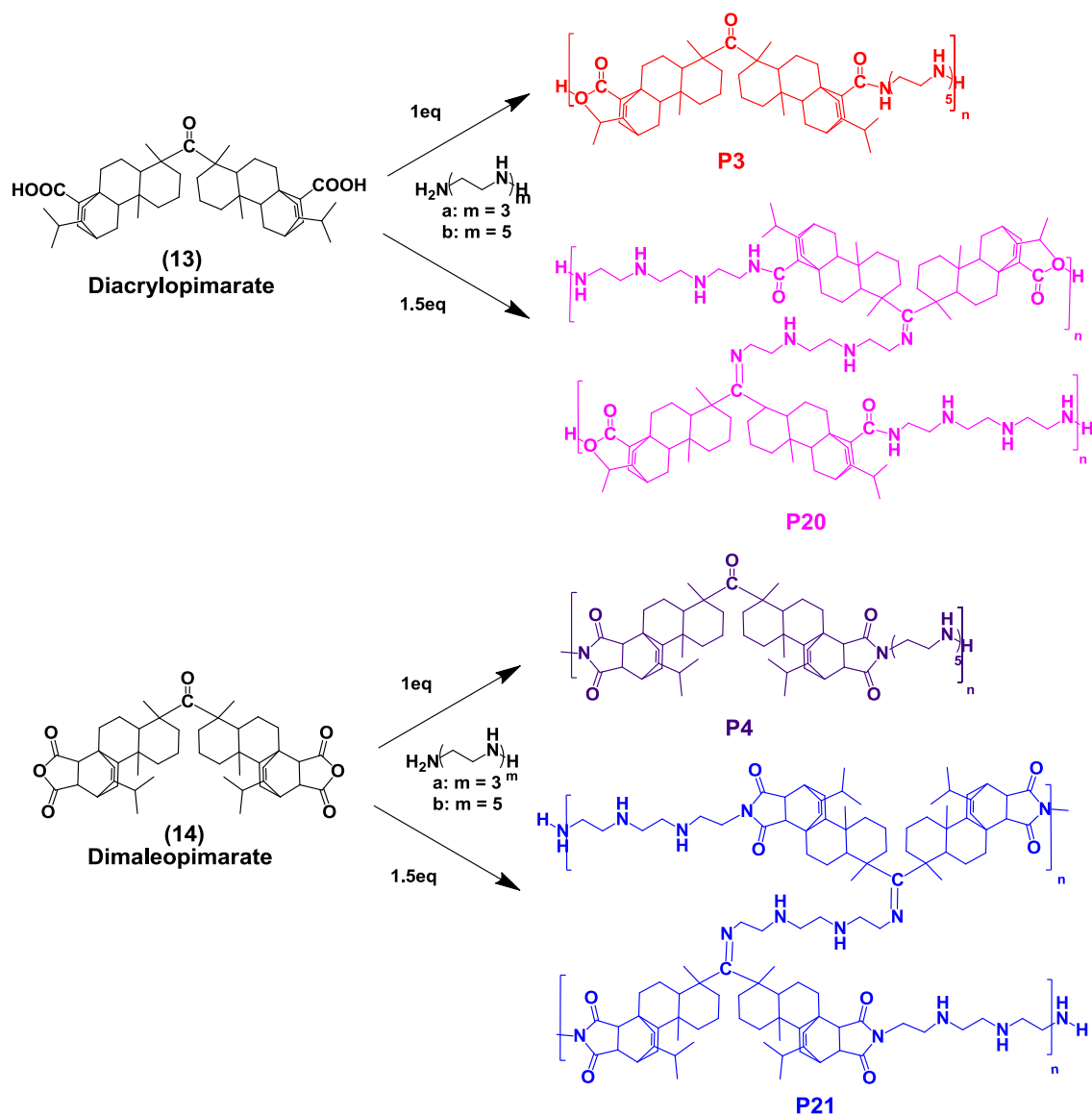


**Scheme 29:** Synthesis of bis-unsaturated acrylopimarate and polymerization *via* ADMET methodology.

c) Synthesis of polyamides and poly(amide-imide)s from abietic acid ketones

Another way to obtain difunctional monomers is the synthesis of abietic acid ketone (Scheme 30). Diacrylopimarate ketone (**13**) and dimaleopimarate ketone (**14**) were synthesized, as described in the previous section and polymerized.<sup>40</sup>

The ketone-diacid monomers (**13**) and (**14**) were copolymerized with triethylene tetramine or pentaethylene hexamine leading to polyamides, **P3** and **P20** or poly(amide-imide)s, **P4** and **P21**. **P3** and **P4**, synthesized with 1 eq of diamine are linear polymers. **P20** and **21** are synthesized with 1.5 eq of diamine and present some branching. All these polymers exhibit good thermal properties. 10% degradation temperature ranged from 275 to 360  $^{\circ}\text{C}$ . Again, the degree of polymerization ranged from 2 to 10, meaning that only oligomers are formed. These polymers can be cross-linked with epichlorohydrin and used as consolidating agent for network fibrous structures, or used as curing agent for epoxy resins, as already described in the first section.



**Scheme 30: Synthesis of polyamides and poly(amide-imide)s from ketone diacid monomers and triethylene tetramine and pentaethylene hexamine.**

### Conclusion:

Main chain rosin polymers were synthesized from acrylopimarate (1) and maleopimarate (2) adduct or derived ketones (13) and (14). High thermal properties are achieved but almost all the polymers exhibit low molar masses. The highest degrees of polymerization (highlighted in green in table 7) were achieved adopting ADMET polymerization and polycondensation of the hydroxyalkyl esters (27) and (28). The similarity between these reactions is that the carboxylic acid moieties were first esterified with a spacer and then polymerized. This strategy enables the reduction of the steric hindrance around the reactive functions allowing higher molar masses to be reached.

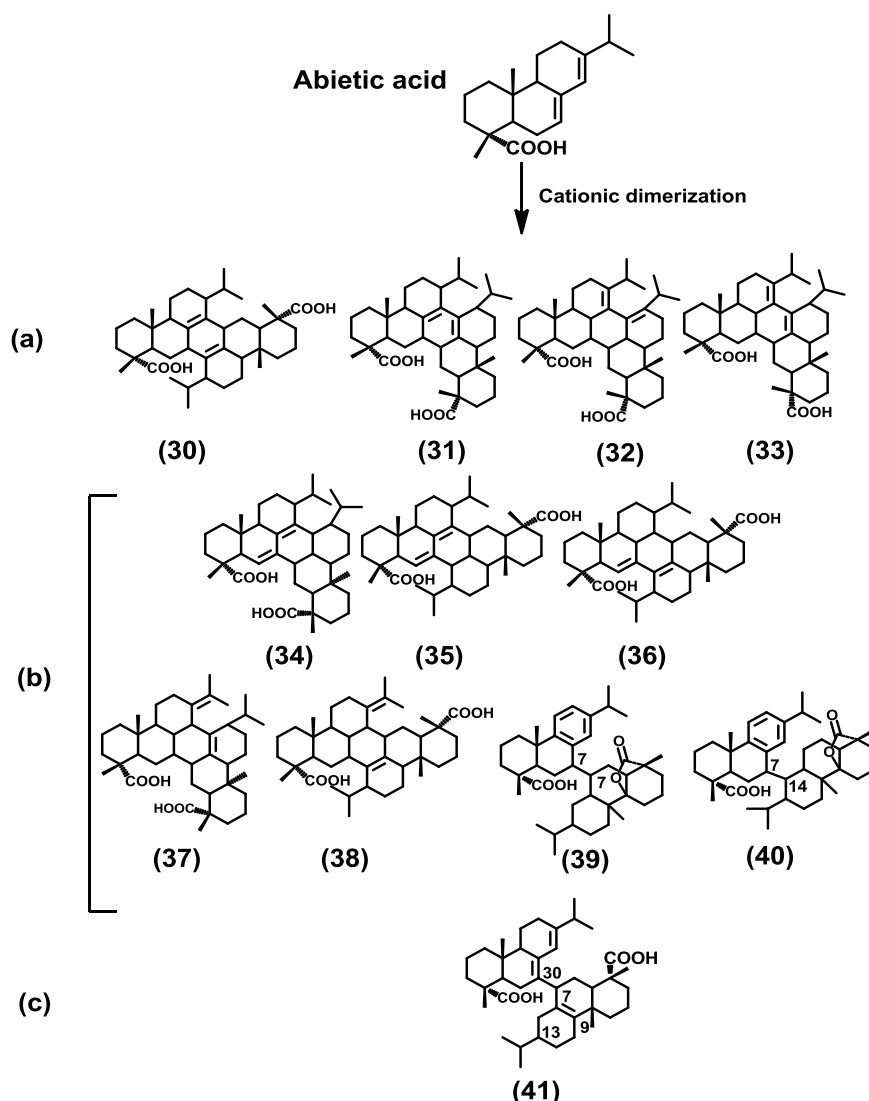
Table 7: Characteristic and thermomechanical properties of abietic acid main chain polymers.

Monomer	Polymer	Structure	$\bar{M}_n$ (g/mol)	$\bar{D}$	$\overline{DP}_n$	Tg (°C)	Tm (°C)	Td
Maleopimarate	P1	Poly(amide-imide)	a: 2 095 b: 1 995	/ /	4 3	/ /	170 205	/ /
	P10	Polyesterimide	a: 4 200 b: 2 100	1.95 1.91	6 3	146	/ /	250
Acrylopimarate	P12	Polyhydroxyester	a: 5 000 b: 4 000 c: 3 200	/ / /	9 8 6	82 75 66	/ / /	10%: 337 10%: 300 10%: 280
	P2	Polyamide	a: 1 560 b: 1 160	/ /	3 2	/ /	160 195	/ /
	P14	Unsaturated polyester	a: 6 000 b: 5 200	/ /	8 7	/ /	/ /	/ /
	P15	Unsaturated polyester	a: 5 600 b: 4 800	/ /	7 5	/ /	/ /	/ /
	P16	Polyester	11 600	2.63	29	107	181	305
	P17	Polyester	12 200	1.97	31	118	168	315
	P18	Unsaturated polyester	9 200	/	19	-5	/	5%: 303
Ketones	P3a	Polyamide	7 800	/	10	/	192	10%: 340
	P4a	Poly(amide-imide)	8 400	/	10	/	172	10%: 275
	P19	Polyimide	7 800	/	/	/	262	10%: 360
	P20	Poly(amide-imide)	10 200	/	/	/	209	10%: 340

#### 4. Abietic acid dimerization

Another interesting way to obtain polymerizable abietic acid-based monomer concerns its dimerization. Indeed, under strong acidic conditions and high temperature, abietic acid can undergo dimerization. The resulting mixture is composed of dimers with small amounts of trimers. Such dimerized rosin is a commercially important product which finds application in adhesives, films, varnishes and even into formulation of transdermal drug delivery system, because of its excellent film forming.<sup>41</sup> However to the best of our knowledge, no report of synthesis of thermoplastic polymers from the dimer mixture has been found in the literature yet.



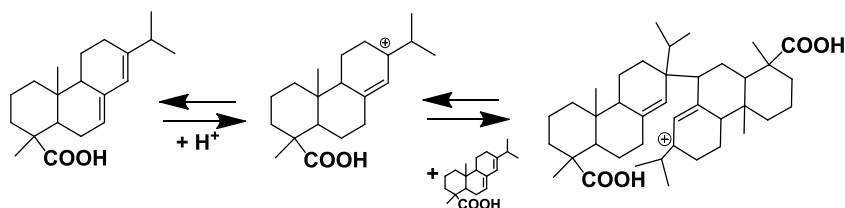


**Scheme 31: Abietic dimer structures suggested in literature: (a) abietic acid structures previously suggested by Brus<sup>42</sup>, Morillon<sup>43</sup> and Bardyshev<sup>44</sup> (b) abietic dimers proposed by Zinkel from NMR and IR data<sup>45</sup> and (c) dimer structure partially characterized by X-ray by Zinkel<sup>46</sup>.**

In 1919, Grun and coll. reported for the first time the “polymerization” of rosin using sulfuric acid.<sup>47</sup> During 40 years, this work was followed by several patents in which the dimers were only characterized by color, softening point and acid number. This little information was sufficient for conventional uses. In 1953, 1958 and 1964, Brus, Bardyshev and Morillon and coll., directed attention to the structures of the dimers. After an isolation work with a yield below 10%, they postulated the structures of the dimers employing to spectral investigations. Brus, first suggested **(30)**, Morillon added **(31)** and Bardyshev assigned different structures, **(32)** and **(33)** with a preference for structure **(33)** (Scheme 31). In 1965, Leonard studied the impact of the dimer content on the crystallization of tall oil rosin.<sup>48</sup> Their gas chromatography investigations detected 15 components. In this study, the dimerization was performed with

Brønsted ( $\text{H}_2\text{SO}_4$ ) and Lewis acid ( $\text{BF}_3$ ) catalysts. The two resulting mixtures showed peaks with the same retention time but different intensities, meaning that the dimers have the same structure but not the same relative ratio. No structure was proposed for the dimers.

In 1969, Schuller and coll. worked on the influence of the reaction conditions on the yield of dimerization of abietic acid and a mechanism was postulated (Scheme 32).<sup>49</sup> Parameters such as catalyst, solvent and concentration were studied separately. With a yield of 91%, sulfuric acid proved to be the most efficient catalyst over the ten tried. Only, anhydrous 4-toluene sulfonic acid, borontrifluoride diethyletherate and difluorophosphoric acid gave yield over 50%. Over the thirteen solvents investigated, the best one was chloroform. The reaction was completed within 5 h. Another interesting parameter is the purity of the starting material. Indeed, this reaction was performed on gum rosin, wood rosin, tall oil rosin, pure abietic acid, levopimaric and isopimaric acids. Whereas abietic acid reached 91% yield, the three rosins yield is around 50%. Concerning the isomers, levopimaric acid reached a yield of 75 %, while isopimaric showed only 30% yield meaning that some isomer contained in rosin disfavor dimerization.



**Scheme 32: Proposed mechanism for abietic acid dimerization.**

Later, Zinkel and coll. detected by capillary gas-liquid chromatography the presence of 40 dimeric components.<sup>45</sup> Six dimers were isolated, in milligram quantity and their structure was partially elucidated. The dimerization product was prefractionated on silica gel, using 10-50% diethylether/petroleum ether followed by methanol. After esterification of the fractions with diazomethane, purification was accomplished by silica gel using 0-10% diethylether/petroleum ether gradient with supplemental argentation chromatography. Three major components had molar mass of 632 g/mol ( $\text{C}_{42}\text{H}_{64}\text{O}_4$ ), in agreement with heptacyclic structures. Three minor compounds possess molar mass of 616 g/mol, indicating that one of the carboxylic groups is present as a lactone.  $^1\text{H}$  NMR studies reveal that two of the major dimers have conjugated double bonds. The authors could not determine if the coupling was “head-to-head” or “head-to-tail”. Based on these data, thermodynamical simulations and  $^{13}\text{C}$  NMR observations, two of the major dimers have the structures (34), (35) or (36). The third main dimer with non-conjugated double bonds could be identified as structures (37) or

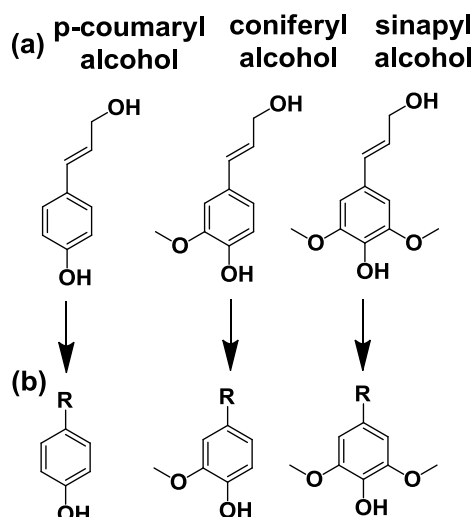
(38). The three other components, besides the lactone, possess an aromatic structure and their mass spectrum displays a monomer to monomer cleavage. The dehydroabietic unit is probably linked to the 7 or 14 position of the abietane lactone. In this context, the proposed structures for these compounds are structures (39) and (40). The same group reported the molecular structure of a dimer isolated from 4-toluene sulfonic acid catalyzed dimerization of methyl levopimarate in chloroform at room temperature. A very fast isomerization of abietic acid into levopimaric acid was observed following by a slow dimerization with 10% yield. After purification, the dimer was isolated as a crystalline compound (41). The single crystal X-ray analysis reveals the formation of only one new C-C bond between C7 and C30, of two chiral centers at C7 and C13 and the loss of one at C9. The broad signal of C13 can be assigned to the presence of epimers, confirmed by NMR.

### Conclusion:

Dimerization of abietic acid remains a complicated process which mechanism is still blurring, as proved the formation of more than 40 structures. Some of them could be isolated in milligram quantity, but not enough to synthesize polymers.

## II Chemical modifications and polymerization of aromatic synthons potentially derived from lignin

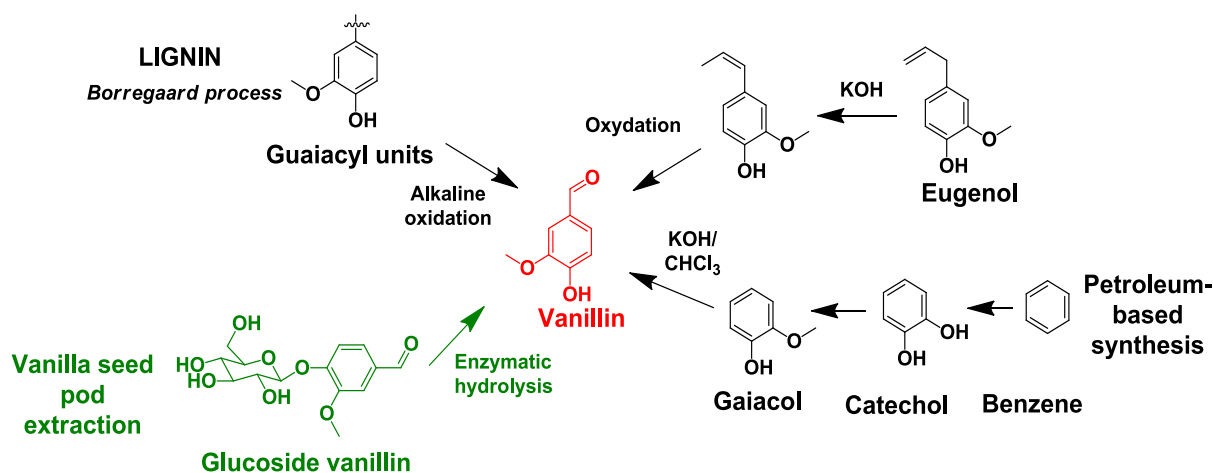
Lignin is the only large scale renewable feedstock which contains aromatic units.<sup>50</sup> The chemical structure of lignin consists of phenylpropane units originating from three aromatic alcohols (monolignol): *p*-coumaryl, coniferyl and sinapyl alcohols (Scheme 33). The amount of monolignol depends on the biological specie. Lignin deconstruction, could lead to different phenolic molecules such as 4-substituted phenol, 4-substituted-2-methoxy phenol, 4-substituted-2,6-dimethoxy phenol. Despite extensive research, there are only very few reports of efficient ways of recovering such aromatic products.<sup>51</sup> The only notable commercial process is the production of vanillin from lignosulfonates, formed as by-product of the sulfite pulping industry.<sup>52,53</sup> Most of the polymers produced from lignin derivatives are based on vanillin or ferulic acid, which is easily obtained from vanillin.<sup>54,55</sup> Moreover, some examples of polymerization of benzaldehyde and syringaldehyde are often described to show the influence of the *o*-methoxy group on the polymer properties.



Scheme 33: Structure of (a) monolignol, (b) molecules potentially extracted from lignin.

### 1. Vanillin extraction, production and use

Vanillin (4-hydroxy-3-methoxybenzaldehyde) is the major constituent flavor of vanilla. Several ways of production or extraction have been developed over the years (Scheme 34). Historically, it has been extracted from vanilla beans. Native from Mexico, it now grows in tropical area all around the world. Vanilla seed pods contain 2% by dry weight of vanillin in the form of  $\beta$ -D-glucoside vanillin. The beans are first immersed in hot water before sun drying. This curing process results in enzymatic hydrolysis, releasing vanillin. Due to the high price of natural vanillin, at the end of the 19<sup>th</sup> century, vanillin was synthesized from eugenol, extracted from oil of clove.<sup>56</sup> Later, in 1936, vanillin was synthesized, in the US and Canada, in a production scale, from lignin of waste sulfite liquor, a by-product of pulping paper industry. Indeed, lignin is sulfonated and solubilized during the pulping of wood. The alkaline oxidation of gaiacyl units (up to 25% of the lignin structure depending on the raw wood used) leads to vanillin.<sup>57</sup> Today, this process is not popular anymore because of environmental concerns. The only large producer of vanillin from lignin is *Borregaard Industries*, located in Norway. It represents 15% of the global vanillin production but this process attracts more and more interest due to continuous technical improvements.<sup>58,59</sup> In 2010, 15 000 tons were produced from petrol and 2 000 tons from lignin. Indeed, synthetic vanillin is easily obtained from petroleum-based gaiacol. Solvay dominates the market as 85% of vanillin production derived from petroleum resources.



Scheme 34: Routes of vanillin production from lignin, benzene, eugenol and natural extraction

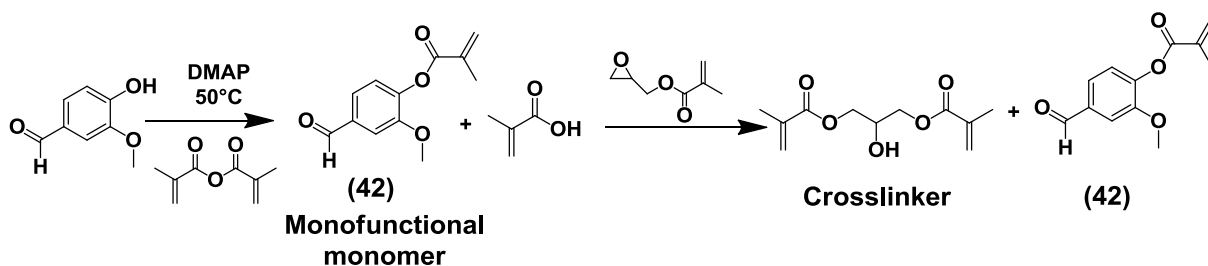
Vanillin is widely used in food flavor formulations (chocolate, baking, beverage), perfumery and fragrances, odor masking (tires, plastics) and for the synthesis of several pharmaceuticals, chemicals and agrochemical intermediates.

## 2. Synthesis and properties of thermoset polymers from vanillin and eugenol

Very few examples of thermoset polymers using lignin derivatives were reported. All of them are very recent works which describe the polymerization of vanillin or eugenol. Eugenol is extracted out of clove oil but could potentially be obtained from lignin moieties.

### 1) Synthesis and properties of vinyl ester resins derived from vanillin

In 2012, 100% biobased vinyl ester resins from vanillin methacrylate and glycerol dimethacrylate were prepared in a highly sustainable way.<sup>60</sup> The monomers were synthesized in a one pot two-step reaction without generating waste since the by-product of step one, methacrylic acid is a reactant of step two (Scheme 35). Cured resin was prepared by free radical polymerization of (42). The conversion reached 60% after reaction and 80% after post curing.

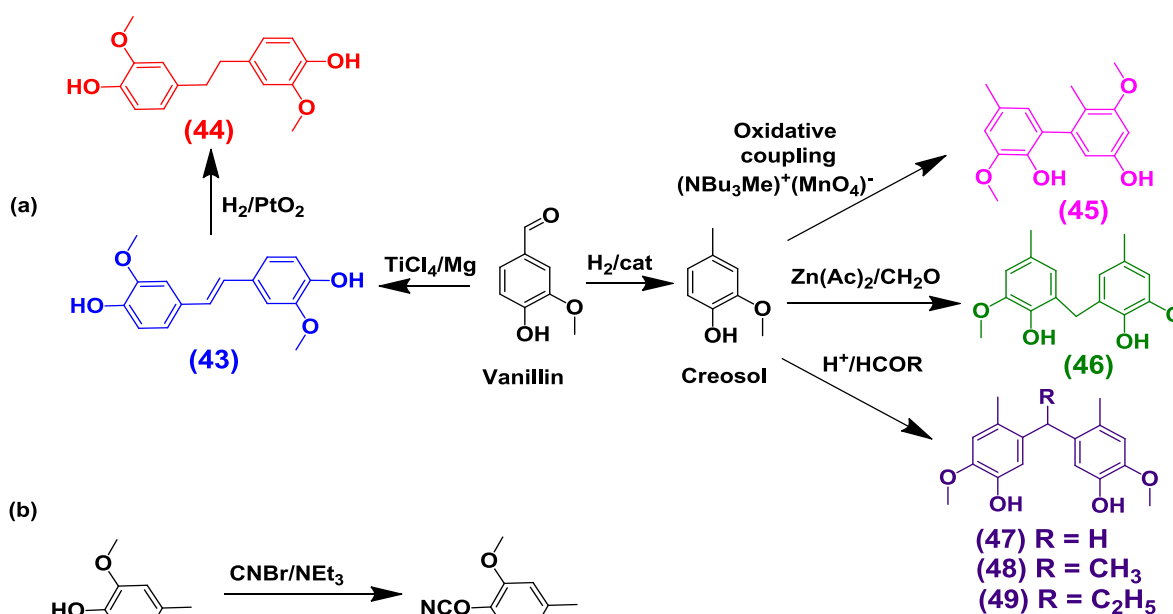


Scheme 35: Synthesis of vanillin methacrylate and glycerol dimethacrylate.

The resulting resin is a hard transparent thermoset which exhibits a  $T_g$  of 155 °C, a storage modulus of 3.6 GPa at 25 °C and a 50% degradation temperature of 405 °C. These values are comparable to the ones of the typical vinyl ester resins synthesized with 45% of styrene ( $T_g$  of 145 °C, storage modulus of 2.7 GPa and 50% thermal degradation over 400 °C). In this example, vanillin methacrylate, (42), was a good substitute for styrene moiety in vinyl ester resins.

## 2) Synthesis and properties of cyanate ester thermosets derived from vanillin

Recently, Harvey and coll. reported two studies on the synthesis of cyanate ester thermosets from vanillin.<sup>61,62</sup> Seven bisphenols were produced from vanillin (Scheme 36). On one hand, reductive coupling (MacMurry coupling) of the vanillin aldehyde in presence of titanium tetrachloride leads to (43) with a yield of 41%. This bisphenol was hydrogenated to give the saturated compound (44). On the other hand, vanillin was hydrogenated to obtain creosol. From creosol, several bisphenols were synthesized.<sup>63</sup> The first method consisted in oxidative coupling creosol to produce the 2,2-biphenyl derivative (45) because the phenol group directed the coupling to the *ortho* position. The product was isolated in a 50% yield. The second route employed the condensation reaction of creosol with formaldehyde, acetaldehyde or propionaldehyde. Zinc acetate was shown to be a selective catalyst for the *ortho*-coupling of formaldehyde (46).



Scheme 36: Synthesis of bisphenols from vanillin (a), synthesis of cyanate from phenol moiety (b).

Dilute HCl and HBr solutions were shown to be effective catalysts for the selective coupling of aldehydes in the *meta* position to the hydroxyl group (47), (48), (49). The bisphenols were

readily converted to cyanate with cyanogen bromide under basic conditions. Bis(cyanate esters) were cured at high temperature to produce cyanate ester thermosets. The bis(cyanate esters) exhibited different behaviors and some of them were not suitable for this application. DSC measurements showed that the bis(cyanate esters) derived from (45) and (46) were not able to complete efficiently their curing due to the rigidity of the structure and the steric hindrance around the cyanate group. The bis(cyanate esters) derived from (43) has a too high melting point, over 220 °C, which makes it unsuitable to be used by itself. In contrast, the curing of the bis(cyanate esters) derived from (44), (47), (48) and (49) was complete. The resulting thermosets exhibit glass temperature over 200 °C and 5% degradation temperature of 300 °C (Table 8). Most commercial resins which derived from bisphenol do not exhibit heteroatoms. The *ortho* methoxy group of the vanillin-based resins leads to different properties in curing and to different thermal decomposition. Despite a slightly decrease in thermal stability, the vanillin-based resins present properties comparable to the petroleum-based commercial ones.

**Table 8: Thermomechanical properties of vanillin-based cyanate thermoset.**

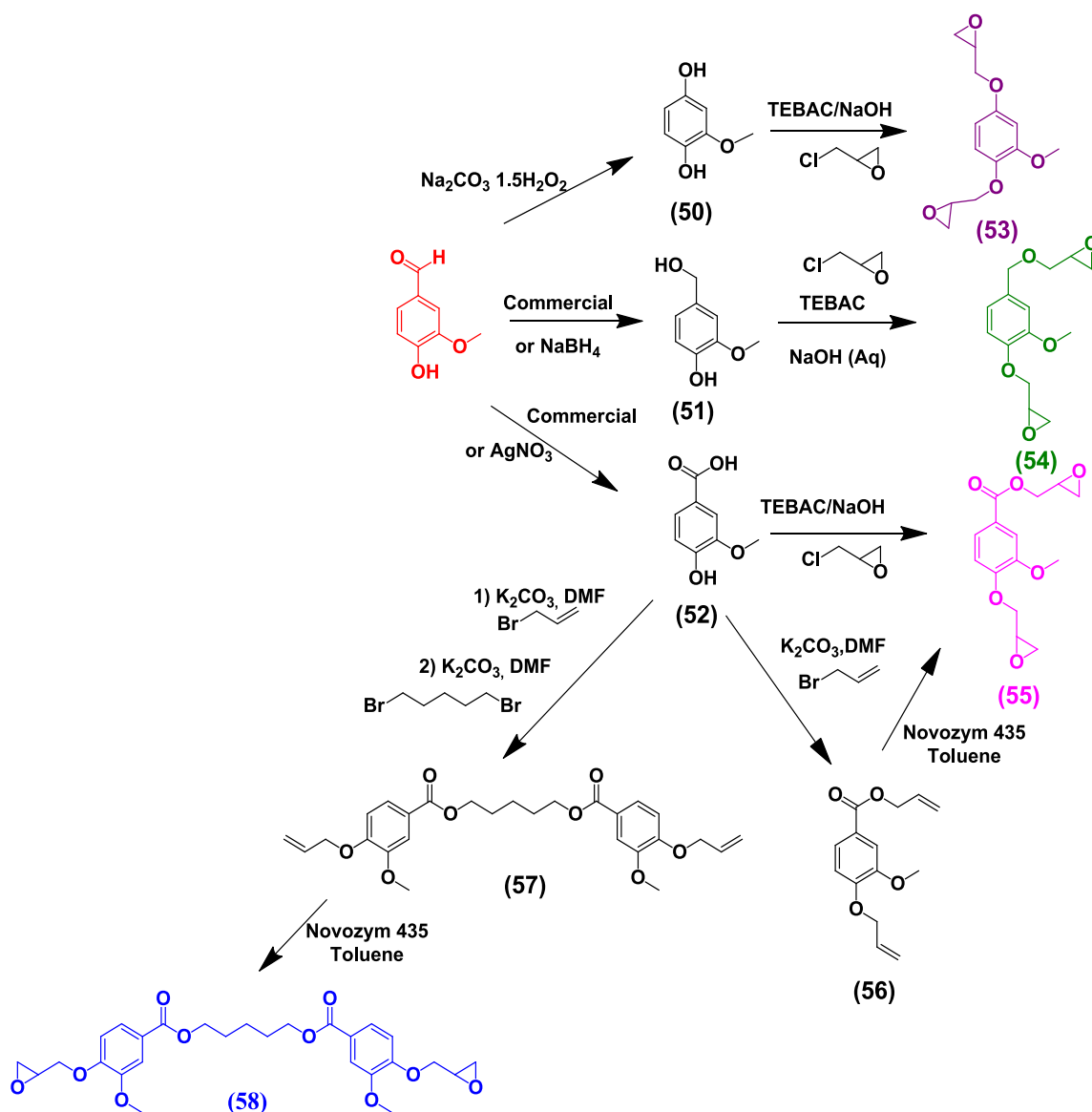
Monomer	T <sub>g</sub> (°C)	T <sub>d</sub> % (°C)	Annotation
(44)	202	340	
(46)	178	326	Not totally cured
(47)	248	357	
(48)	214	337	
(49)	214	348	

### 3) Synthesis of epoxy resins from compounds potentially derived from lignin

#### a) Synthesis of bisepoxides from vanillin

Recently, Caillol and coll. reported the synthesis of several bisepoxides from vanillin (Scheme 37).<sup>64</sup> Vanillyl alcohol, (51), and vanillic acid, (53), are common commercial compounds easily produced from vanillin, typically with NaBH<sub>4</sub> reduction and AgNO<sub>3</sub> oxidation. 2-Methoxyhydroquinone (50) was prepared from vanillin by Dakin reaction. Compounds (50) and (52) underwent glycidylation reactions under solvent free conditions, using a phase transfer catalyst, triethylbenzyl ammonium chloride, and NaOH, yielding (53) and (55), respectively.<sup>65</sup> The benzyl alcohol of (51) was not reactive under these conditions so the bisepoxide (54) was synthesized employing a biphasic phase transfer catalyst system.<sup>66</sup>

Moreover, Fulcrand and coll. developed another strategy to synthesize bisepoxide compounds from vanillic acid. They studied its chemo-enzymatic functionalization (Scheme 37).<sup>67</sup> On one hand, vanillic acid was allylated using allyl bromide and potassium carbonate in DMF, yielding **(56)**.



Scheme 37: Synthesis of bisepoxides by chemical modification of vanillin.

The double bonds of the diallylated compounds were epoxidized by immobilized Lipase B from *Candida antarctica* (Novozym 435) in toluene, caprylic acid as active oxygen carrier and hydrogen peroxide as oxygen donor. The optimal conditions ( $\text{C}_8:\text{H}_2\text{O}_2$  ratio, time and temperature) led to the formation of bisepoxide (**55**) with 70% yield, and 17% of monoepoxide. This result is better than the one obtained using *m*CPBA as oxidative agent, where only 53% of bisepoxides are produced. On the other hand, in order to design a compound

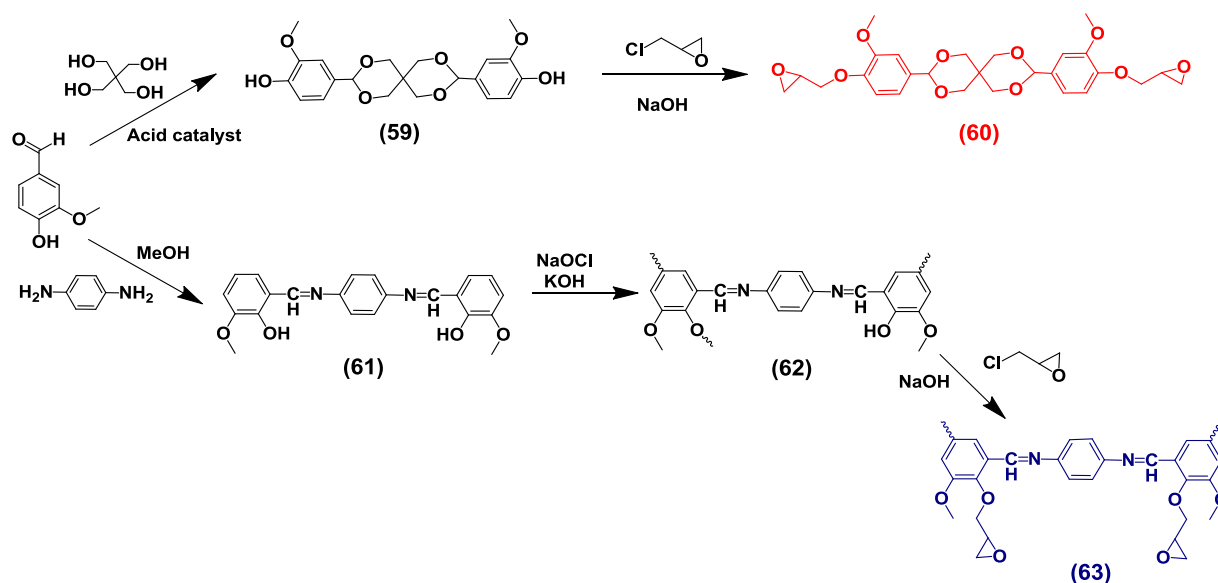


close to bisphenol-A, an excess of vanillic acid was reacted with 1,5-dibromopentane to obtain a bisphenol. This bisphenol underwent allylation, (**57**), and epoxidation following the methodology described before. The bisepoxide (**58**) was obtained with 66% yield while 19% of mono-epoxide is produced (Scheme 37).

From these bisepoxides, only a first epoxy resin was produced from (**53**) and isophorone diamine. This system shows a Tg of 117 °C. Improving its formulation, this value is expected to reach the one of the DGEBA equivalent system (Tg = 158 °C). Vanillic bisepoxides are promising compounds as bio-based alternative to DGEBA.

Another bisepoxide (**60**) has been synthesized from dehydration condensation between vanillin and pentaerythritol, yielding the bisphenol (**59**), followed by reaction with epichlorohydrin (Scheme 38).<sup>68</sup> The acetal linkage is pH sensitive and can be degraded under acidic conditions. This compound reacted with diaminodiphenylmethane to obtain cross-linked epoxy resin. The relaxation caused by the hydrogen bonding between the methoxy and the hydroxyl group of the resin was studied. This phenomenon improved the impact and tensile strength and is found in all lignin-based epoxy resins. No further characterizations of the polymer were described.

Finally, a vanillic multi-epoxide compound (**63**) was synthesized by Gül and coll. (Scheme 38).<sup>69</sup> First the bisphenol (**61**) was produced by reaction between 2 equivalents of vanillin and one of phenylene diamine.

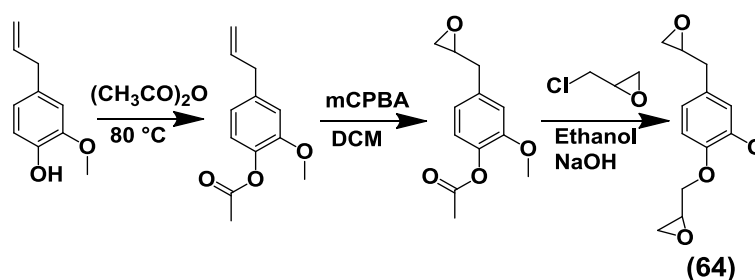


**Scheme 38: Synthesis of vanillic bisepoxide and multi-epoxides by coupling with pentaerythritol and with phenylene diamine, respectively.**

Oligomers (**62**) were formed by oxidative polycondensation. The remaining phenols (**62**) reacted with epichlorohydrin resulting in a *Schiff* base epoxy oligomer resin. The formation of *Schiff* base from an aldehyde or ketone is a reversible reaction. Heating or hydrolysis by aqueous acid or base can lead to the originating aldehydes and amines.

#### b) Synthesis and properties of eugenol-based epoxy resins

The best proof that aromatic molecules potentially derived from lignin are good substitutes of current commercial epoxy resin from bisphenol-A was described by Zhang and coll. in 2013.<sup>9</sup> Eugenol bisepoxide (**64**) was synthesized first by epoxidation of the double bond with *m*CPBA, after protection of the phenol by acetylation, followed by glycidylation with epichlorohydrin (Scheme 39). Curing was achieved with hexahydrophthalic acid. The curing and thermomechanical properties of this new biobased epoxy resin were compared to a commercial one from DGEBA, the epoxy resin DER353. Both resins present similar values of peak curing and activation energy. Eugenol-based resin exhibits a higher T<sub>g</sub> (114 °C versus 106 °C), similar storage modulus (2.8 MPa versus 2.9 MPa) and lower 5% thermal degradation (321 °C versus 341 °C). Eugenol-based epoxy resins display very comparable performance with respect to bisphenol-A-based one.

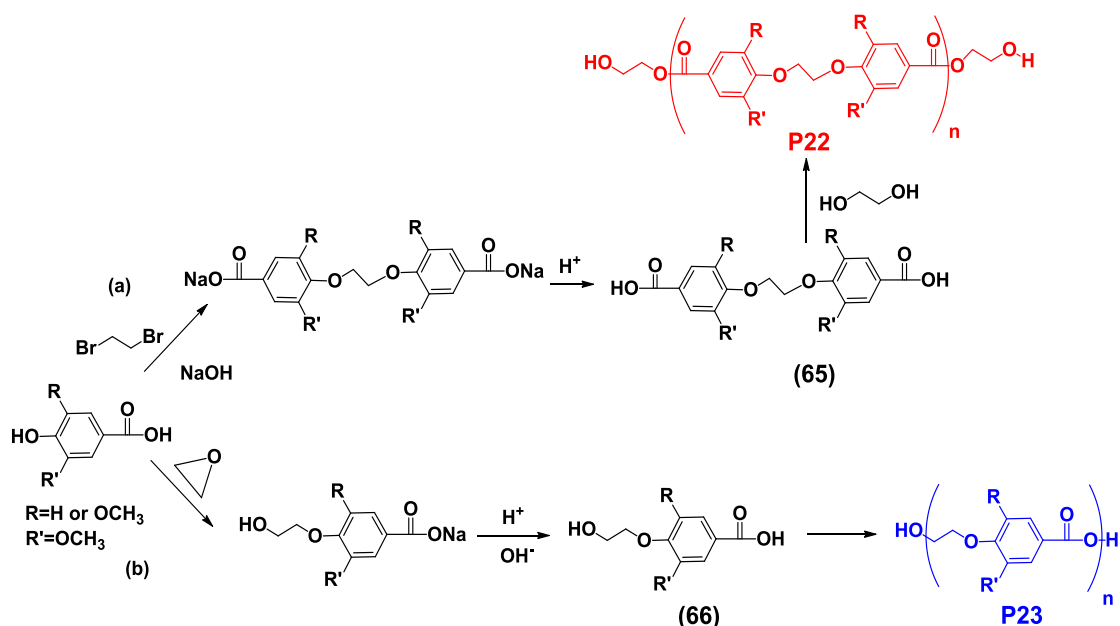


Scheme 39: Synthesis of eugenol bisepoxide.

### 3. Synthesis and properties of thermoplastic polymers from phenols potentially derived from lignin

To the best of our knowledge, the first example of polymerization of vanillic acid was described in 1955. Indeed, vanillic acid was converted to carboxylate by etherifying the phenolic moiety with ethylene dihalides (**65**) (Scheme 40 (a)). Subsequently, the carboxylate was esterified with ethylene glycol and condensed to linear polyester, **P22**, with T<sub>g</sub> of 80 °C and T<sub>m</sub> of 210 °C.<sup>70</sup> This polymer has been studied several times between 1955 and 1974.<sup>71,72</sup> Later, in 1981, the same strategy as well as a new one were adopted by Kordsachia and coll. to synthesize vanillic and syringic acid-based polymers.<sup>73</sup> In the second synthetic pathway,

the phenolic moiety of vanillic acid was reacted with ethylene oxide, yielding **(66)** (Scheme 40 (b)). The self-condensation of **(66)** leads to **P23**.



**Scheme 40: First syntheses of polyester from vanillic acid and syringic acid.**

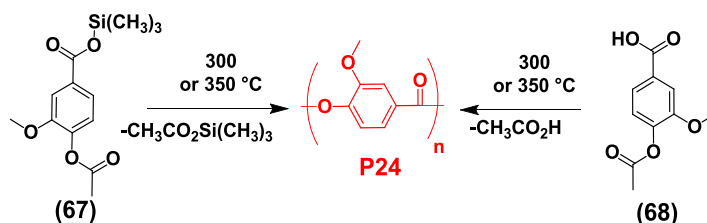
Molar masses of the polymers, measured by viscometry, indicated that the first synthetic pathway (a) provided polyesters exhibiting higher molar mass respectively 44 500 g/mol and 50 000 g/mol for vanillic acid and syringic acid than polyester produced from the second method (b) 30 000 g/mol and 12 000 g/mol. With respect to the first method, the reported polymers showed  $T_g$  of 69 °C and  $T_m$  of 212 °C in the case of vanillic acid and  $T_g$  of 58 °C and  $T_m$  of 172 °C for syringic acid. The polymers synthesized by the second method showed  $T_g$  of 55 °C and  $T_m$  of 254 °C in the case of vanillic acid and  $T_g$  of 45 °C and  $T_m$  of 73 °C for syringic acid. The polymer produced from vanillic acid exhibited thermal properties similar to PET ( $T_m = 265$  °C,  $T_g = 67$  °C).

These first polymerizations were followed about 15 years by a wide number of studies on the conversion of vanillic acid, syringic acid and 4-hydroxybenzoic acid into thermotropic polymers. The next section focuses on the influence of the incorporation of vanillic acid in thermotropic polymers on their properties. Thermotropic polymers are material which exhibit liquid crystal formation in the melt form. Due to their high order and aromatic structure, they possess high mechanical strength at high temperatures, extreme chemical resistance, and inherent flame retardancy.

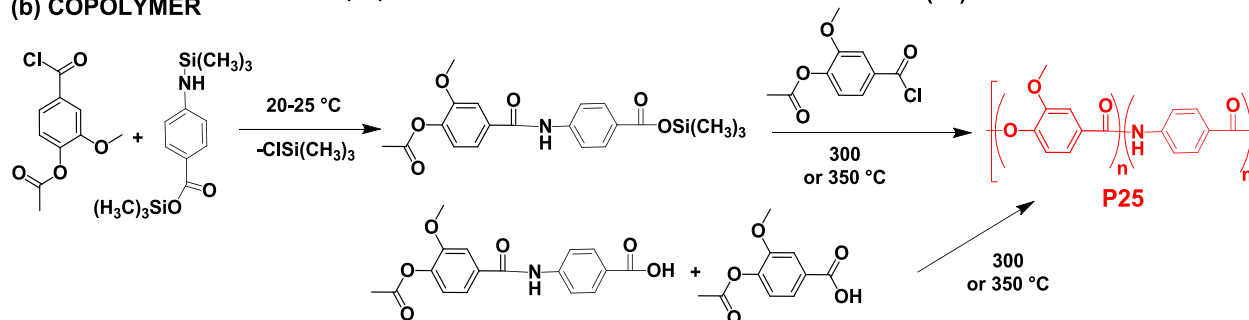
### 1) Synthesis of thermotropic polymers from vanillic acid

The first report on incorporation of vanillic acid (VA) in thermotropic polymers is the study of Kricheldorf and coll. in 1995. They prepared polyesters and poly(ester-amide)s derived from vanillic acid and 4-aminobenzoic acid.<sup>74</sup> The motivation of this work was to synthesize whisker-like crystals with biodegradable properties. Homopolymer of vanillic acid was obtained *via* two synthetic pathways: a silylacetate method and an acetate method (Scheme 41). On one hand, trimethylsilyl-4-acetoxy-3-methoxybenzoate (**67**) was homopolymerized, leading to poly(vanillic acid), **P24**. Trimethylsilylacetate was released during polymerization. The second approach involved the reaction of free carboxylic acid of the 4-acetoxy-3-methoxybenzoic acid (**68**) and generated acetic acid. High reaction temperatures, between 300 °C and 350 °C, were required. The two synthetic methods gave different yields, crystallinities and morphologies. Higher yield was reached with the acetate method, 95% versus 43%. Unfortunately, **P24** did not lead to whisker-like crystals. Copolymers with 4-aminobenzoic acid were synthesized, **P25**, by both silylacetate and acetate methods. In both cases, the composition of the polymer agreed with the feed ratio. The crystallinity of the copolymers increased with higher vanillic acid molar ratio. Free carboxylic acid groups led to globular aggregates regardless the composition, whereas silylated monomers yielded ordered columnar particles.

#### (a) HOMOPOLYMER



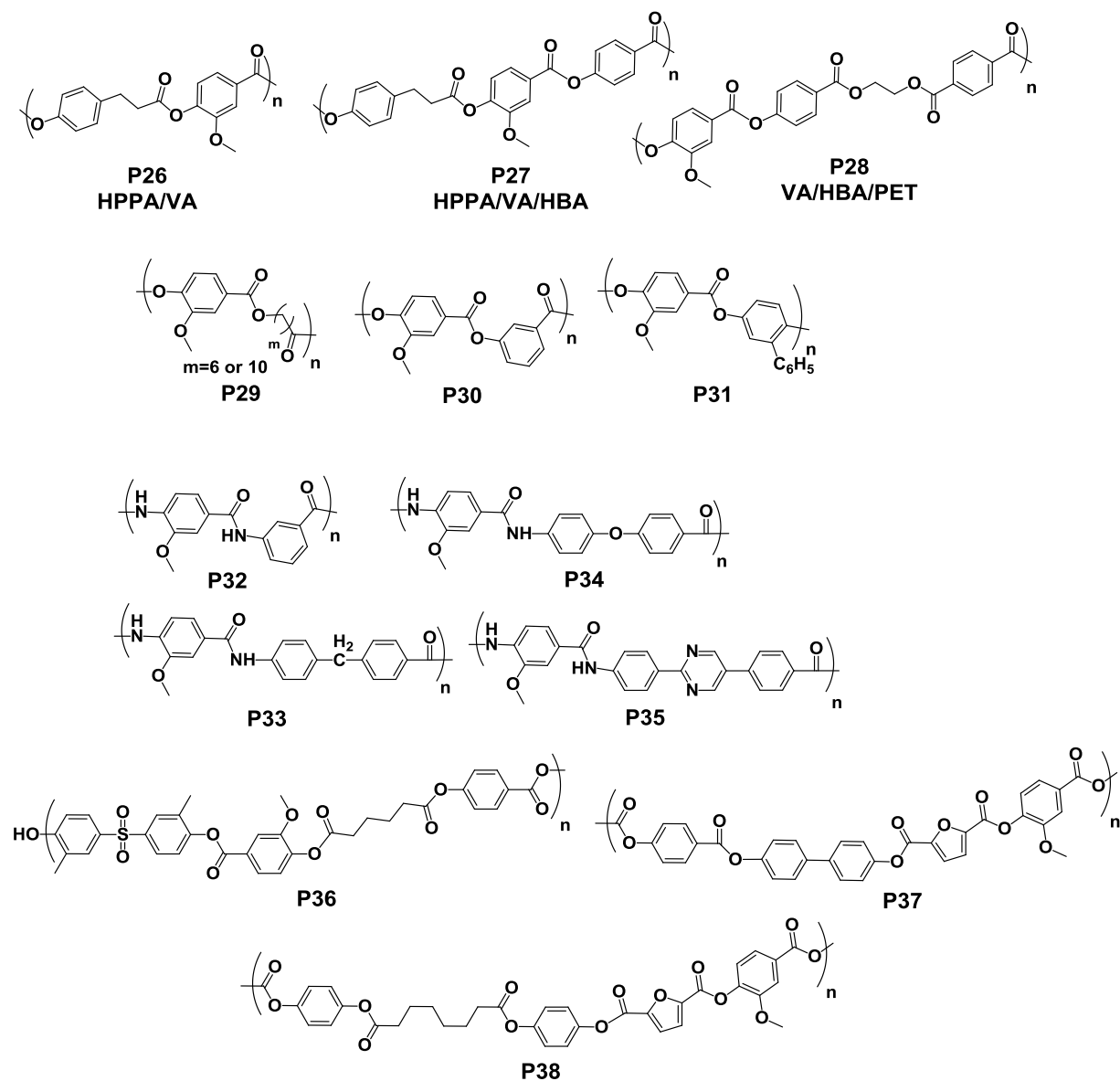
#### (b) COPOLYMER



**Scheme 41: Synthesis of poly(vanillic acid) and its copolymer with 4-aminobenzoic acid by silylacetate and acetate pathways.**

Based on this work several other thermotropic (co)polymers were synthesized from vanillic acid (VA) (Scheme 42). Biodegradable liquid crystal polyesters were investigated in order to

combine the good thermomechanical properties of the liquid crystal and the biodegradability of ester bond.



**Scheme 42: Synthesis of thermotropic polymers from vanillic acid.**

First, copolyester from 4-hydroxyphenyl propanoic acid (HPPA) and vanillic acid, **P26**, were produced by the silylated method using titanium isopropoxide as transesterification catalyst.<sup>75</sup> At 1/1 molar ratio, the incorporation of vanillic acid in the polyester was lower than expected. Probably, the reactivity of the acetoxy group was decreased due to steric and electronic effects of the methoxy group in *ortho* position. The soluble polyester showed a T<sub>g</sub> of 95 °C and an isotropic melt. To solve the problem of reactivity, Nagata and coll., developed another synthetic pathway to synthesize HPPA/VA copolyesters.<sup>76</sup> They prepared copolymers with different compositions, in pyridine using diphenyl phosphoryl chloride and lithium bromide

as condensing agents, thus improving the incorporation of vanillic acid into the polyester. A molar mass of 21 800 g/mol was reached for a composition of 30% of vanillic acid. Higher vanillic acid to 4-hydroxyphenyl propanoic acid ratio led to higher T<sub>g</sub> (108 °C for 70% and 83 °C for 30%) but lower thermal degradation (356 °C for 70% and 403 °C for 30%). These binary copolymers were not thermotropic. Thus, terpolymers with 4-hydroxybenzoic acid (HBA), **P27**, were investigated (Scheme 42) and were proven to be soluble, thermotropic and to form a homogeneous nematic phase above 250 °C.

Sun and coll. also investigated the properties of liquid crystalline polymers.<sup>77-79</sup> They synthesized terpolymers, **P28**, by melt polycondensation of 4-acetoxybenzoic acid, polyethylene terephthalate and 5% of an acetoxy-based third monomer. Vanillic acid was used as co-monomer and was compared to seven other molecules including to bisphenol-A and terephthalic acid. Vanillic acid copolymers exhibited a faster polycondensation rate, better spinnability, lower melting temperature, higher molar mass and thermostability than all the other copolymers (Table 9). It also showed a highly oriented fibrillar structure.

**Table 9: Properties of the terpolymers synthesized from *p*-hydroxybenzoic acid, polyethylene terephthalate and a third monomer.**

Monomer	Polycondensation time (h)	Spinnability	T <sub>g</sub> (°C)	T <sub>m</sub> (°C)	Td5% (°C)	$\bar{M}_n$ (g/mol)	G' (GPa)	$\epsilon$ (%)
<b>Vanillic acid</b>	4.1	Very good	69	183-207	417	7 300	67	9
<b>Bisphenol-A</b>	7.0	Bad	100	/	/	/	/	/
<b>Terephthalic acid</b>	6.0	Medium	64	196-220	/	5 400	/	/

In addition, Kudriavtsev and coll. developed a series of polyesters, **P28-P31** and polyamides **P32-P35** employing vanillic acid (Scheme 42).<sup>80</sup> They first studied the thermostability of these copolymers. The same diols and diamines were used to produce terpolymers from vanillic acid and *p*-hydroxybenzoic acid. The polymers were casted from solution of *N*-methylpyrrolidone on glass supports. Depending on the chemical structure of the co-monomer, elongational break ranged from 234% and 67% for the polyesters and 14.1% and 20.8% for the polyamides. The strength properties were similar.

After these studies, the excellent thermomechanical properties and processability of the vanillic acid-based liquid crystalline polymers attracted attention for the biomedical applications. Indeed, recent studies report the synthesis of aromatic-aliphatic bioresorbable polyester from vanillic and *p*-hydroxybenzoic acid, **P36**.<sup>81-83</sup> More precisely, polyesters

derived from *p*-hydroxybenzoic acid (HBA), vanillic acid (VA), 4,4'-sulfonylbis(2-methylphenol) (dBPS) and various aliphatic diacids (spacer) have been developed by the company *Smith & Nephew*. *In vitro* and *in vivo* biocompatibility has been proven. Selected composition, such as 50/25/12.5/12.5 in HBA/VA/dBPS/Spacer, has been shown to be processable in the nematic melt phase. However, the fibers show comparatively low tensile modulus due to low level of molecular orientation in the nematic phase. Further developments are necessary to address the mechanical requirements for orthopedic applications.

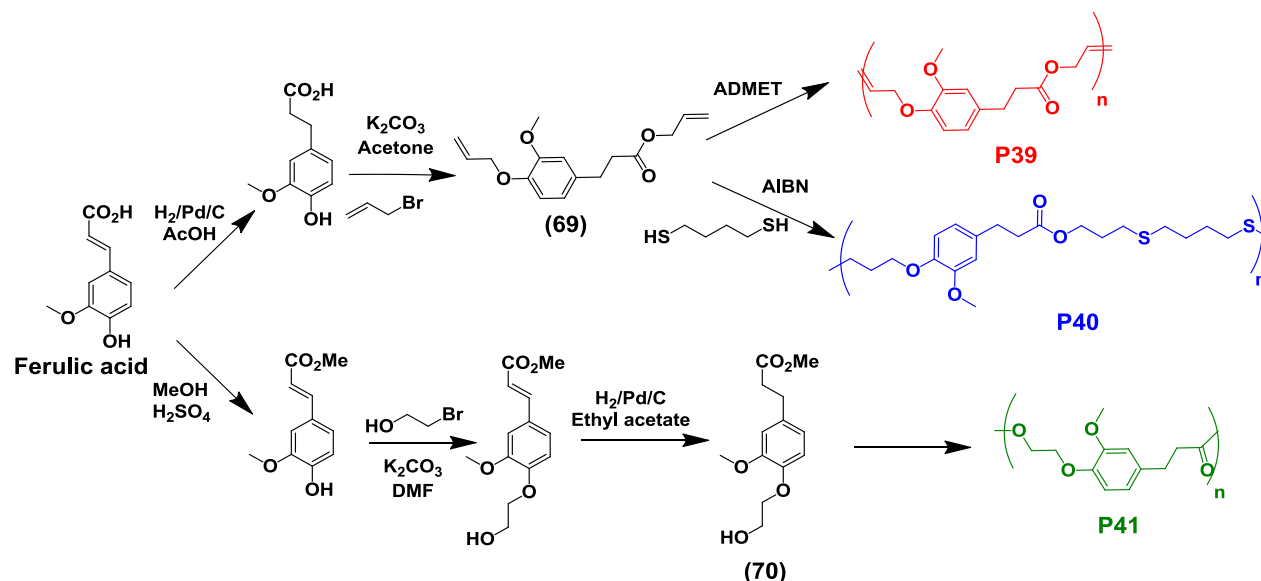
Finally, very recently, a study reported the synthesis of biobased thermotropic polyesters from 2,5-furandicarboxylic acid, 4-hydroxybenzoic acid, 4,4'-bisphenol and vanillic acid, **P37**.<sup>84,85</sup> First, the polymers were formed without vanillic acid but the rapid crystallization of the mixture from the melt did not allow reaching high molar mass. Vanillic acid was introduced as co-monomer to lower the crystallization temperature of the polymer. The polymerizations were performed in bulk in the presence of zinc acetate. The polymer produced with 20% of vanillic acid showed a T<sub>g</sub> of 109 °C, and a melting temperature of 230 °C (versus 96.7 °C and 336 °C without vanillin). The ability of vanillic acid to lower the crystallization temperature of the polymer was also evidenced by a similar study on the synthesis of thermotropic polymer from 4-hydroxybenzoic acid, suberic acid, 1,4-dihydroxybenzene, FDCA and vanillic acid, **P38** (Scheme 42). The molar mass of the composition 30/15/39/15/10 reached 12 000 g/mol.

## 2) Synthesis of fully biobased polyesters from vanillin, syringaldehyde and ferulic acid

### a) Copolyesters of vanillin or ferulic acid and vegetable oil derivatives

In the current context of “green” chemistry, 100% biobased polymers were synthesized from vanillin, ferulic acid and vegetable oil derivatives. Meier and coll. produced polyester from ferulic acid by ADMET polymerization, thiol-ene addition as well as by polycondensation (Scheme 43).<sup>86,87</sup> For ADMET and thiol-ene methodologies, a bis-unsaturated monomer, (**69**) was synthesized. First, hydrogenation of the internal double bond of ferulic acid was performed to avoid side reactions during polymerization. The resulting compound reacted with allyl bromide leading simultaneously to the formation of the allyl ester from the carboxylic acid and allyl ether on the phenol moiety. The resulting (**69**) was obtained with 76% yield. Seven catalysts were tested for ADMET polymerization, **P39**. Among them, only Hoveyda Grubbs 2nd generation, Zhan and M51 (*Umicore* company) catalysts were able to oligomerize the bis-unsaturated (**69**), leading to **P39** with molar masses of 2 400 g/mol,

2 150 g/mol and 3 050 g/mol respectively. On the other hand, the polyaddition of **(69)** was performed with 1,4-butanedithiol and AIBN as radical initiator, yielding **P40**. In comparison to ADMET, slightly higher molar mass was observed (4 150 g/mol). Finally, ferulic acid was transformed in a more reactive monomer to perform polycondensation. The carboxylic acid was first esterified with methanol and the phenol moiety was converted with bromoethanol under basic conditions. This AB compound, was obtained with 64% yield and hydrogenated, yielding **(70)**. **P41** was produced by homopolmerization of **(70)** in the presence of TBD.



**Scheme 43: Synthesis of ferulic acid polyesters by ADMET polymerization, thiol-ene addition and polycondensation.**

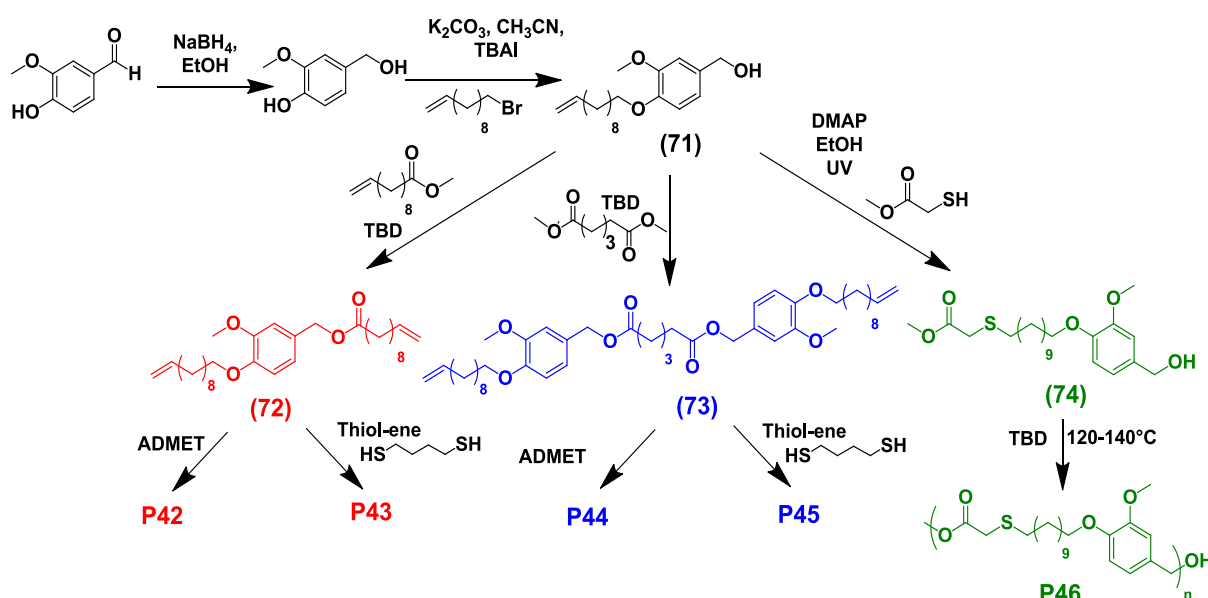
**P41** exhibits higher molar mass (5 450 g/mol) than **P39** and **P40**. The thermal properties also differ with the synthetic pathway (Table 10). Indeed, ADMET and thiol-ene lead to amorphous polymers, whereas semi-crystalline polymers are synthesized *via* polycondensation. The glass transition temperature of **P40** is very low, due to longer alkyl chain. In these studies, Meier and coll. also copolymerized ferulic acid with erucic or oleic acid and show that the glass transition temperature increased with the increasing amount of ferulic acid.

**Table 10: Properties of ferulic polyesters synthesized by ADMET, thiol-ene and polycondensation.**

Name	Polymerization	$\bar{M}_n$ (g/mol)	$\bar{D}$	Tg (°C)	Tm (°C)
<b>P39</b>	ADMET	3 050	1.81	7	/
<b>P40</b>	Thiol-ene	4 150	1.49	-33	/
<b>P41</b>	Polycondensation	5 450	1.50	-27	25



Recently, the same group developed copolymers from vanillin and fatty acid derivatives (Scheme 44).<sup>88</sup> They first provided two bisunsaturated compounds, (72) and (73) from the intermediate compound (70). (70) was prepared by reduction of the aldehyde moiety into alcohol, and etherification of the phenol moiety with an undecenoic acid derivative. In order to get difunctional compounds (72) and (73), respectively, the alcohol was esterified with methyl undecenoate, in a molar ratio 1:1, or with dimethyl adipate, a biobased compound, in a molar ratio 2:1 or. (72) and (73) were polymerized by ADMET or thiol-ene addition to yield P42, P43, P44 and P45. A third compound, (74), was synthesized to perform homopolycondensation. The thiol-ene addition of methylthioglycolate on (70) leads to an AB monomer, (74), which is able to undergo homopolymerization, yielding P46. Polymers obtained by ADMET exhibit the highest molar mass. The difference with the previous study is the length of the alkyl chain between the aromatic moiety and the double bond. This longer chain allows to reach higher molar mass by ADMET.



Scheme 44: Synthesis of vanillin-based polyesters by ADMET polymerization, thiol-ene addition and polycondensation.

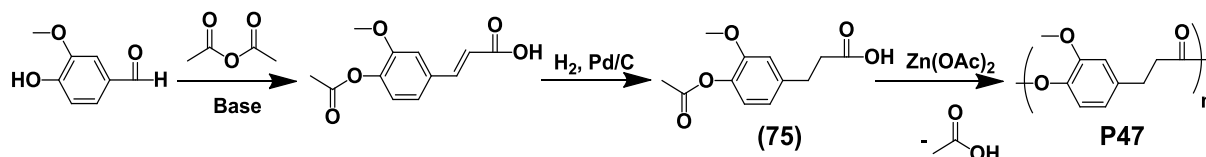
The polymers synthesized via thiol-ene and polycondensation are semi-crystalline whereas the ADMET-ones are amorphous (Table 11).

Table 11: Properties of vanillin polyesters synthesized by ADMET, thiol-ene and polycondensation.

Polymer	Monomer	Polymerization	$\bar{M}_n$ (g/mol)	$\bar{D}$	Tg (°C)	Tm (°C)
P42	(72)	ADMET	49 600	1.96	-31	/
P43	(72)	Thiol-ene	15 400	1.77	-32	57.65
P44	(73)	ADMET	25 600	1.88	-17	/
P45	(73)	Thiol-ene	12 100	1.94	-22	68
P46	(74)	Polycondensation	16 600	1.81	-13	77

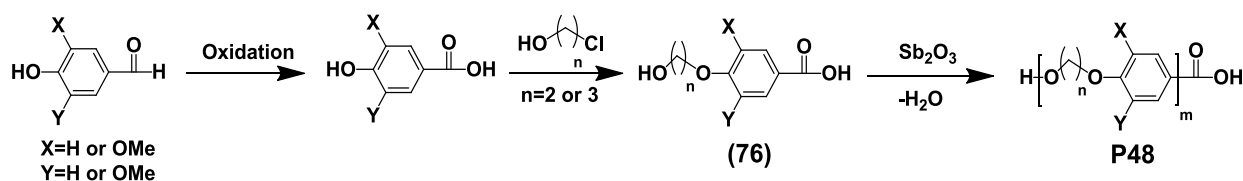
b) Synthesis of PET mimic polymers from vanillin, 4-hydroxybenzoic acid and syringaldehyde

In 2010, Miller and coll. reported the synthesis of biorenewable polyethylene terephthalate mimics, **P47**, derived from lignin and acetic acid.<sup>55</sup> The reaction of vanillin and acetic anhydride leads to both Perkin reaction and acetylation of the phenolic group. The resulting compound was hydrogenated and the resulting acetyldihydroferulic acid, (**75**), was homopolymerized, yielding **P47** (Scheme 45).  $\text{Zn}(\text{OAc})_2$  proved to be the most efficient catalyst. **P47** exhibits a molar mass of 17 800 g/mol (degree of polymerization around 100), a melting temperature of 234 °C, a transition temperature of 73 °C and a 50% thermal decomposition at 462 °C. All these values are similar to the corresponding values of PET ( $T_m = 265$  °C,  $T_g = 67$  °C,  $T_{d50\%} = 470$  °C).



Scheme 45: Synthesis of PET mimic polymers based on vanillin.

The same group synthesized poly(alkylenehydroxybenzoate)s (PAHBs) from three lignin derivatives, vanillin, 4-hydroxybenzoic acid and syringic acid (Scheme 46) in order to target materials with a wide range of thermomechanical properties.<sup>89</sup> These aromatic aldehydes were oxidized into corresponding carboxylic acids and the phenol moiety was derivatized with 2-chloroethanol or 3-chloropropan-1-ol. The resulting hydroxyl acid monomers (**76**), were able to homopolymerize, yielding **P48**, using  $\text{Sb}_2\text{O}_3$  as catalyst. The thermomechanical properties of P48 are varying with respect to the aromatic unit substitution. Indeed, the substitution on the aromatic ring increases the free volume of the polymer chains, which limits their association and thus decreases the glass transition temperature. Additionally, the length of the aliphatic segment between the aromatic units has also an impact on the thermal properties. The thermal stability of all the polymers is high (Table 12). In this series of polymers, the glass transition temperature was tuned between 50 and 70 °C and the melting temperature between 170 and 239 °C.



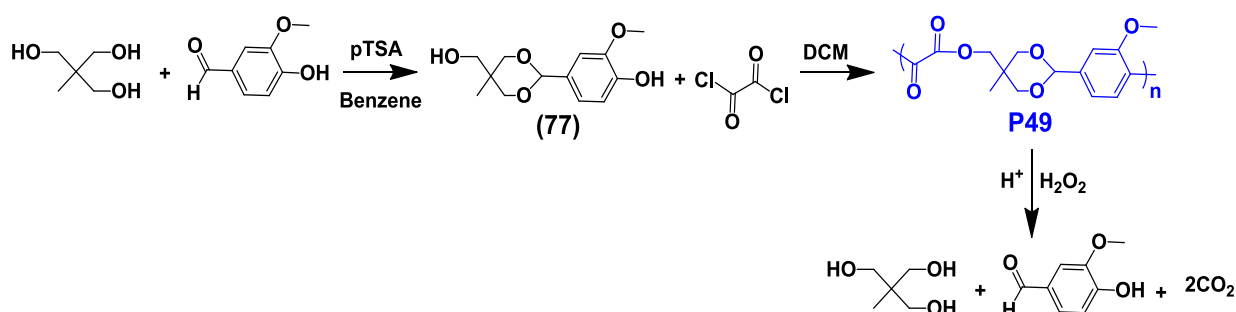
Scheme 46: Synthesis of poly(alkylenehydroxybenzoate)s from lignin derivatives.

Table 12: Properties of the lignin-based poly(alkylenehydroxybenzoate)s.

Number of methoxy	Alkyl chain	$\bar{M}_w$ (g/mol)	$\bar{D}$	Tg (°C)	Tm (°C)	Td50% (°C)
1	2	14 500	2.69	71	239	417
2	2	14 000	2.08	66	/	433
0	3	5 200	3.18	67	179	450
1	3	16 300	3.19	66	191	435
2	3	6 700	2.43	50	170	433

### 3) Synthesis and properties of vanillin-based polyoxalate

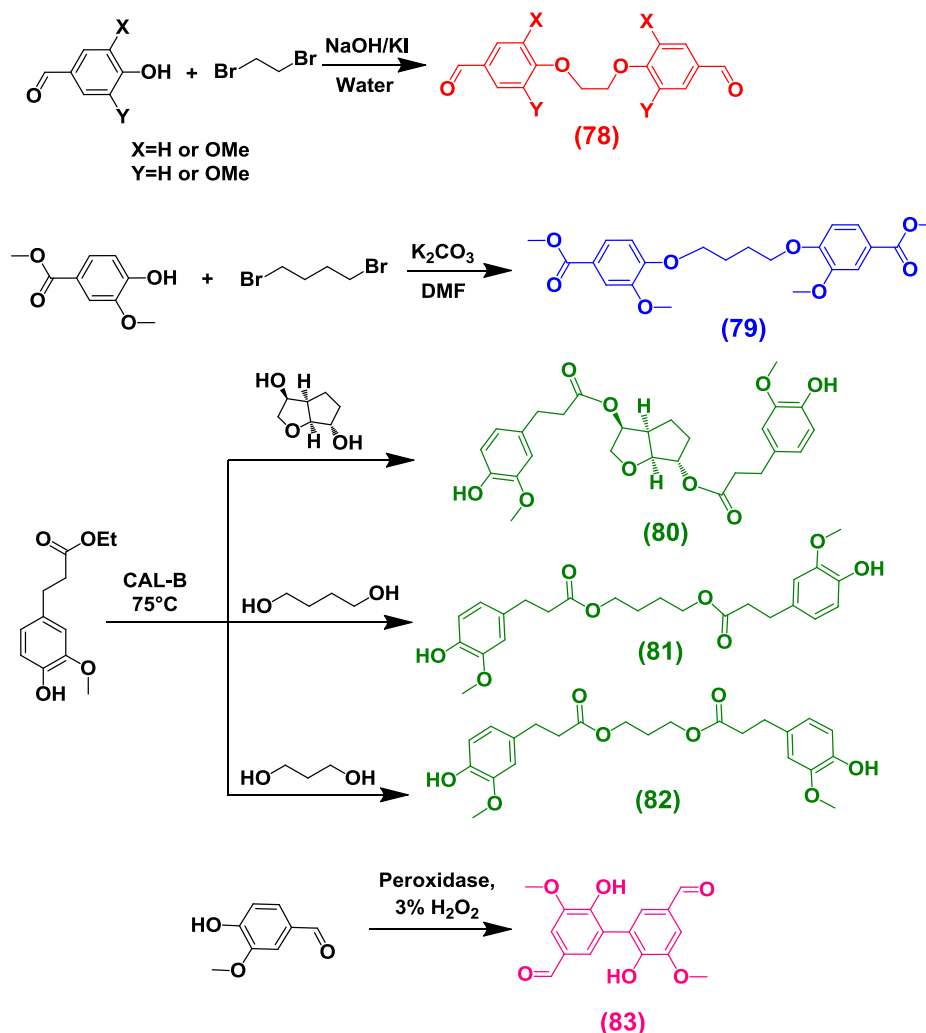
In 2013, Lee and coll. synthesized poly(vanillin oxalate), **P49**, as inflammation-responsive antioxidant polymeric prodrug (Scheme 47).<sup>90</sup> 4-(5-(hydroxymethyl)-5-methyl-1,3-dioxan-2-yl)-2-methoxyphenol, (**77**), was synthesized from vanillin and 2-methylpropane-1,3-diol. The polymer **P49** was produced by step growth polymerization using oxalyl chloride. **P49** exhibits a molar mass of 22 000 g/mol with a dispersity of 1.6 and a glass transition temperature of 120 °C. As poly(vanillin oxalate) has an hydrophobic backbone, it could be formulated into nanoparticles by conventional oil/water method. Poly(vanillin oxalate) releases vanillin during its H<sub>2</sub>O<sub>2</sub> and acid mediated hydrolytic degradation due to the presence of acid cleavable acetal linkage in its backbone. H<sub>2</sub>O<sub>2</sub> was chosen because oxidative stress is induced by accumulation of hydrogen peroxide, and therefore, H<sub>2</sub>O<sub>2</sub> could serve as a potential biomarker of various oxidative stress-associated inflammatory diseases. The nanoparticles showed excellent biocompatibility, antioxidant and anti-inflammatory activity and could potentially be used as therapeutics.

Scheme 47: Synthesis of poly(vanillin oxalate) and vanillin release of under H<sub>2</sub>O<sub>2</sub> stimulus .

### 4) Coupling of lignin derivatives, building blocks for polymer synthesis

## a) Synthesis of symmetric building blocks from lignin derivatives

An interesting way to obtain symmetric difunctional monomer from vanillin or lignin derivatives is based on the coupling of phenolic substrates. According to literature data, this coupling occurred either on the phenol, the aldehyde or the aromatic moieties (Scheme 48).



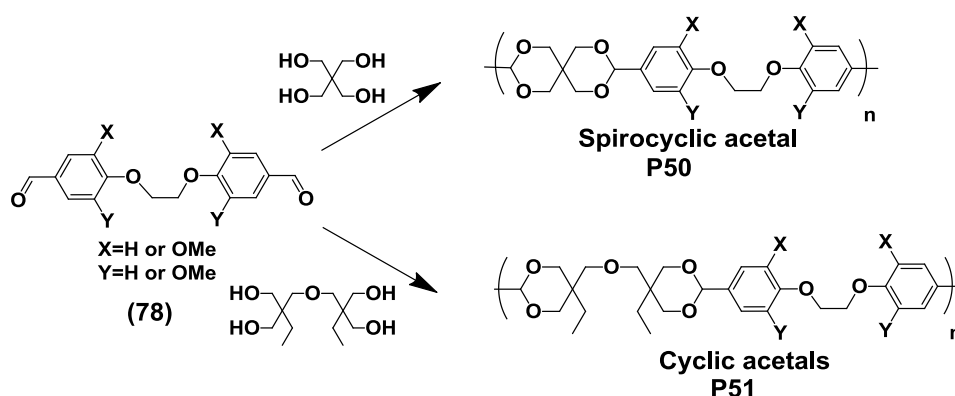
**Scheme 48: Synthesis of building blocks from coupling of lignin derivatives.**

The dialdehyde (**78**) was prepared by the reaction of lignin derivatives (vanillin, syringaldehyde or 4-hydroxybenzaldehyde) with 1,2-dibromoethane. Compounds (**78**) were obtained with a yield of around 50%.<sup>91</sup> The diester (**79**) was also synthesized *via* Williamson ether synthesis with 70% yield. This monomer was produced from the reaction of two equivalents of methylvanillate and one equivalent of 1,4-dibromobutane.<sup>92</sup> The bisphenols (**80**), (**81**), (**82**) were obtained by a chemo-enzymatic pathway. First, ethyl dihydroferulate was synthesized in 72% yield, from vanillin by reaction with malonic acid, piperidine and pyridine followed by hydrogenation. The transesterification of this compound with isosorbide, 1,3-propanediol and 1,4-butanediol was performed in the presence of lipase. One of the main

advantage of using CAL-B lies on its inactivity toward phenol. The reaction was performed either in hexane, with a Dean Stark apparatus or in bulk, at 75 °C. In each case, a yield of about 90% was achieved without the presence of by-product after a reaction time of three days.<sup>54</sup> Finally, **(83)** was obtained by oxidative dimerization of vanillin.<sup>93</sup> More details on this coupling will be given in the following section. These building blocks were used for polymer synthesis.

#### b) Polymerization of the lignin derivatives with symmetric structure

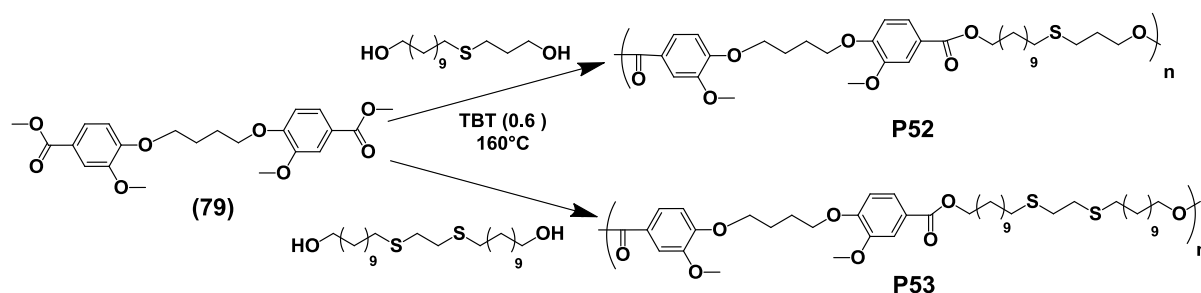
Polyacetal is a class of biodegradable polymers as acetal linkages are sensitive to hydrolysis. For this reason, Miller and coll. synthesized cyclic and polycyclic polyacetal ethers from lignin-based aromatics.<sup>91</sup> 4-Hydroxybenzaldehyde, vanillin and syringaldehyde were investigated in this study. Polycondensation of the dialdehyde **(78)** with tetraol yield cyclic polyacetal ethers **P50**, in the case of di-trimethylolpropane and spirocyclic acetal and to **P51**, in the case of pentaerythritol (Scheme 49). Molar masses between 10 600 and 22 200 g/mol were obtained. Polymers from 4-hydroxybenzaldehyde are semi-crystalline, whereas all the others are amorphous. Spirocyclic polyacetals exhibit higher glass transition temperature than the cyclic equivalent ones (for vanillin: 129 °C versus 80 °C). As already reported, syringaldehyde-based polymers show higher glass transition than vanillin-based ones (152 °C for the spirocyclic one and 98 °C for the cyclic equivalent). All the polymers present high 5% degradation temperature, between 307 and 349 °C.



**Scheme 49:** Synthetic pathway of polyacetals from lignin derivatives.

In 2014, Ma and coll. copolymerized **(79)** with vegetable oil derivatives to synthesize fully biobased semi-aromatic polyesters (Scheme 50).<sup>92</sup> The vegetable oil-based diols were prepared *via* thiol-ene addition on undecenol. The polycondensation was performed in bulk in the presence of titanium butoxide catalyst. The resulting polyesters **P52** and **P53** exhibit

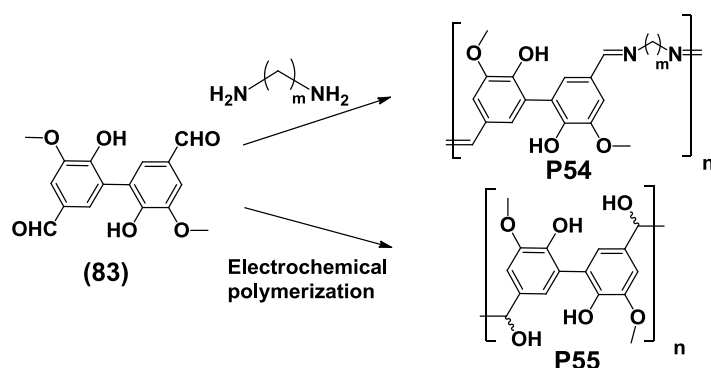
molar masses respectively of 11 800 and 14 700 g/mol and dispersities around 2. The shorter aliphatic chain of **P52** leads to a better thermal stability than **P53** (Td5% of 357 °C versus 339 °C). Moreover, **P52** is amorphous, with a Tg of 13.0 °C whereas **P53** is semi-cristalline, with a Tg of -4.4 °C and a Tm of 70.1 °C. In addition, **P52** possess a higher Young modulus (99.7 MPa) than **P53** (66.2 MPa) and a lower strain at break (22.8% versus 43.7%).



Scheme 50: Synthesis of polyesters from phenol vanillin coupling.

A similar study concerning the influence of aliphatic or cycloaliphatic segments on the thermomechanical properties of polyesters was conducted on **(80)**, **(81)** and **(82)** by Allais and coll. in 2014 (Scheme 48).<sup>94</sup> The bisphenols were copolymerized with diacyl chloride (succinic or azelaic) in *o*-dichlorobenzene or in bulk, yielding low molar mass polymers ( $3\,700\text{ g/mol} < \bar{M}_n < 5\,200\text{ g/mol}$ ). The glass transition temperatures were tuned from 0.4 °C to 75.6 °C by the design of the monomer. All the polymers exhibit good thermal stability with 5% weight loss temperatures over 347 °C.

Finally, Razzaq and coll. reported two polymerizations of the dialdehyde compound **(83)**. They first described the synthesis of *Schiff* base polymers of divanillin, **P54** (Scheme 51).<sup>93</sup> Divanillin, **(83)** and alkyl diamine (1,2-diaminoethane, 1,3-diaminopropane, 1,6-diaminohexane) were heated in ethanol at reflux, leading polymer with a degree of polymerization between 25 and 32. The three polymers were stable up to 250 °C. The polymer synthesized with 1,6-diaminohexane complexed with Cu(II), Fe(II) and Co(II). In addition, the authors synthesized polyvanillin, **P55**, by reductive coupling of the aldehyde group of divanillin using an electrochemical polymerization cell.<sup>95</sup> **P55** was prepared with molar mass of about 10 000 g/mol and dispersities of 1.5. DSC showed no identifiable peak. The polymer exhibits good thermal stability with an onset temperature of 300 °C.



Scheme 51: Synthesis of *Schiff* base polymers and polyvanillin from divanillin.

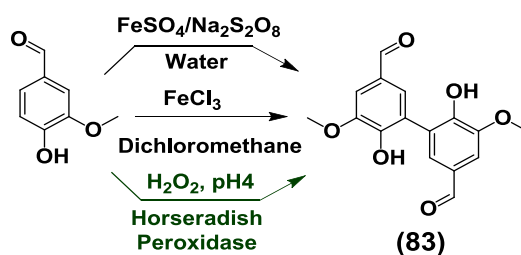
## Conclusion

The majority of the studies described in this section are very recently published, showing the growing interest of researchers in the synthesis of lignin derivative polymers. Only few examples of thermosets were investigated but new bisepoxides from vanillin were developed. In the past decades, lignin derivatives have been widely used in thermotropic polymers. In the current context of sustainability, vanillin-based thermoplastic polymers recently attracted attention again. For instance, this synthon was used for the synthesis of PET mimic polymers or fully biobased copolymers with fatty acids. Through all these examples of polymerization, lignin derivatives were proven to enhance the rigidity and thermostability to the corresponding polymers.

## 4. Vanillin dimer synthesis: promising synthon for polymer synthesis

As shown previously, only few examples of polymerization of divanillin were described in literature. As this synthon appeared to be interesting, its synthesis is described in this section.

Divanillin, also called dehydrodivanillin, is important as flavoring<sup>96</sup> and antioxidant agent in food, cosmetic and pharmaceutical industry. It is also used in microlithography<sup>97</sup> and in polymer synthesis as reported previously. Over the years, it has been synthesized by different methods, either chemical or enzymatic (Scheme 51).



Scheme 52: Synthetic pathways for vanillin dimerization.

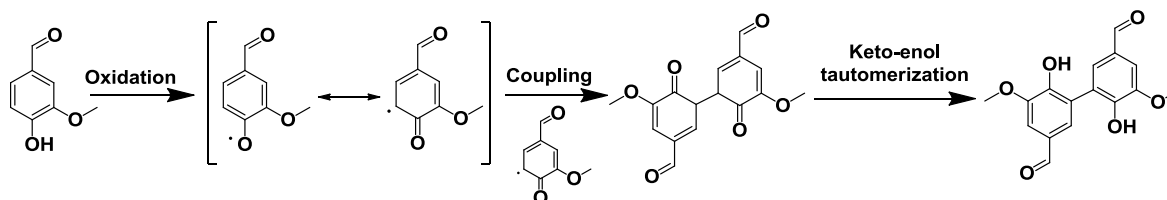
### 1) Synthesis of divanillin *via* chemical methods

Divanillin is commonly produced by different chemical methods. It has been synthesized by oxidative phenol coupling using iron(II) chloride ( $\text{FeCl}_3$ ) or iron(II) sulfate ( $\text{FeSO}_4$ ). The first synthesis of divanillin using  $\text{FeCl}_3$  was reported in 1885 and was followed by several works later.<sup>98-100</sup> A stoichiometric amount of  $\text{FeCl}_3$  was used for the oxidation of the *ortho* position of the phenol group. The resulting divanillin precipitated and was filtered out of the solution and washed. A yield of 57% was achieved.

The first synthesis of divanillin using potassium/sodium persulfate was described in 1918.<sup>100-103</sup> In this study, vanillin was converted to divanillin by oxidation with an iron(II) sulfate heptahydrate and sodium peroxodisulfate in hot water. Recently, this synthetic pathway was enhanced, whereby an increased yield of 95% was obtained, which is 20% higher than in the previous study. More precisely, vanillin and  $\text{FeSO}_4$  were mixed into water, stirred for 10 min at 50 °C, before adding  $\text{Na}_2\text{S}_2\text{O}_8$ . After a reaction time of 5 days, the brown precipitate was filtered off, dissolved in NaOH (2 M). HCl (2 M) was then added and the resulting precipitate was isolated by filtration. These two methods employ not sustainable metal catalysts and need long reaction time to reach high yield. To avoid the use of inorganic salts and toxic agents (sodium persulfate), an enzymatic pathway was developed.

### 2) Synthesis of divanillin *via* enzymatic coupling

In 1972, divanillin was detected for the first time after oxidation of vanillin in aqueous solution with peroxidase in the presence of hydrogen peroxide.<sup>104</sup> Other works reported the presence of divanillin while oxidating vanillin with peroxidase in dairy products. In 2004, Dordick and coll., studied the structural diversity of peroxidase-catalyzed oxidation products of *o*-methoxyphenols (Scheme 53).<sup>105</sup>



**Scheme 53: Phenoxyl radical coupling and keto-enol tautomerization in the synthesis of divanillin.**

Commercially available and highly active, soybean peroxidase enzyme was used. 1.0  $\mu\text{g}/\text{mL}$  of enzyme was dissolved in 0.5 L of aqueous buffer containing 12 mM of vanillin and 1% (v/v) of DMF to solubilize the substrate. The reaction was initiated by slow feed of  $\text{H}_2\text{O}_2$ . This procedure leads to the formation of oligomers. The quantity of DMF influenced the number of units of the resulting oligomers. 1% of DMF was enough to synthesize oligomers



with 2 to 5 units. After 12 h, an overall yield of 80% was obtained. The reaction is also pH-dependent. Indeed, slightly acidic conditions favored the formation of dimers, as well as several trimers and small fractions of tetramers, pentamers and quinone. Further improvements of the conditions were needed to reach a good selectivity in dimer formation. For instance, in 2010 Vosburg and coll. reported that the use of 1000 units of enzyme, on 1 g of product lowering the pH to 4 using acetic acid and adding 3% of hydrogen peroxide leads to 80% yield of dimers after 5 min.<sup>106</sup>

## 5. Laccase-catalyzed oxidative phenolic coupling

Phenolic compounds can be dimerized by oxidative enzymatic coupling catalyzed by laccase. This coupling will be studied in the third chapter of this thesis, so the state of the art concerning laccase phenolic coupling is described in the next section.

### 1) Biochemical, structural characteristics and reaction mechanism of laccases

Laccase is a very well-known class of oxidative enzyme studied since 1883.<sup>107</sup> They were identified in several plants, insects, bacteria and fungus, where they have different biological functions.<sup>108-110</sup> Indeed, in plants, they play a role in the cell wall and in the lignin formation (associated with peroxidase), but they are also involved in the depolymerization of lignin with the participation of several oxydo-reductase.<sup>111</sup> Most of the laccase described in literature are isolated from fungi. Most common laccase producers are the wood rotting fungi *Trametes versicolor*, *Trametes hirsute*, *Trametes ochracea*, *Trametes villosa*, *Trametes gallica*, *Cerrena maxima*, *Coriolopsis polyzona*, *Lentinus tigrinus*, *Pleurotus eryngii*, etc.<sup>112</sup> Depending on its source, the molecular structure of the laccase is different and as a consequence, its catalytic activity is different too.

Laccases are glycoproteins which belong to the blue copper family of oxidase (Figure 3 (a)). The reactions catalyzed by laccase consist in the monoelectronic reaction of substrate to form the corresponding reactive radical. The initiation process is catalyzed by the metal center. Copper, which is in its highest state of oxidation in the laccase native form ( $\text{Cu}^{2+}$ ), is reduced during the substrate oxidation and re-oxidated by air oxygen in the process. The overall catalytic cycle involves the reduction of one molecule of oxygen to two molecules of water which allows reduced copper atoms of the laccase ( $\text{Cu}^{1+}$ ) to be back to its oxidized native state ( $\text{Cu}^{2+}$ ) (Figure 3 (b)).

Laccase possess 2 to 4 copper atoms located inside the protein active site, represented by the orange spheres in Figure 3 (a).<sup>113</sup> For instance, laccase from *Trametes Versicolor* represented on Figure 3 contains four copper atoms. A mononuclear copper atom, T1 site, imparts the blue color and is the site of the primary oxidation. Electrons are transferred from this atom to a three nuclear copper cluster, T2/T3 sites where the oxygen reduction occurs. T2 is mononuclear and T3 binuclear.<sup>114</sup>

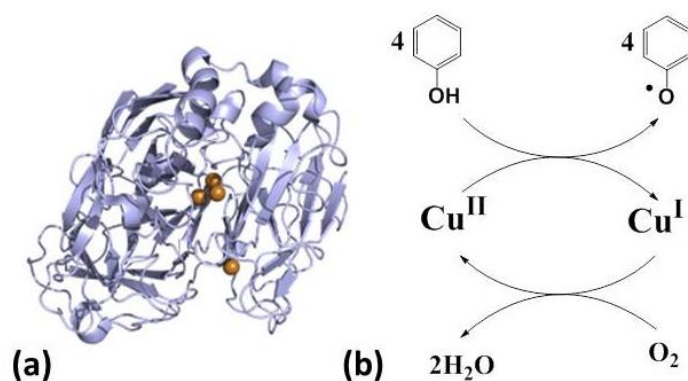


**Figure 3: X-ray-determined crystal structure of laccase from *Trametes versicolor* (a), Schematic representation of Laccase catalytic cycle (b).**

Laccase are characterized by their oxidation-reduction potential which is comprised between 400 and 800 mV depending on the source.<sup>115</sup> For instance, the oxidation-reduction potential of the laccase employed in the studies described in the next section are reported in table 13. Laccase optimal utilization is reached at pH between 3 and 6 and temperature between 50 and 60 °C.<sup>116</sup>

**Table 13: Redox potential ( $E^\circ$ ) of laccase at optimal pH compared to normal hydrogen electrode (NHE).<sup>117-120</sup>**

Laccase source	$E^\circ$ (V vs NHE)
<i>Melanocarpus albomyces</i>	0.46
<i>Mytheliophthora thermophila</i>	0.48
<i>Pycnoporus coccineus</i>	0.72
<i>Trametes pubescens</i>	0.74
<i>Trametes hirsuta</i>	0,78
<i>Trametes versicolor</i>	0.79
<i>Trametes villosa</i>	0.79

Currently, a lot of studies report the use of laccase as biocatalyst for chemical reaction.<sup>121-129</sup> They have been intensively used for oxidation of functional groups or for oxidative coupling

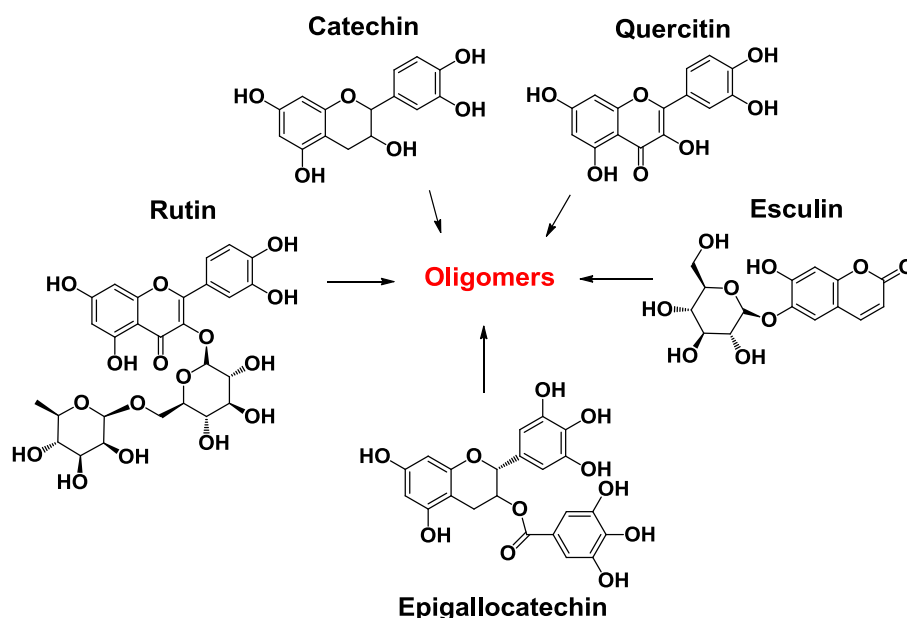
of phenolic substrates. Indeed, laccase generates radical intermediates on phenolic compounds which can undergo self-coupling reactions yielding dimers, oligomers or polymers. The selectivity of the coupling and size of the oligomers depends on a wide range of parameters such as source of laccase, pH, temperature, phenol substitution, co-solvent, etc.

## 2) Laccase-catalyzed oxidative coupling phenolic compounds

### a) Synthesis of ill-defined oligomers from polyphenols

Laccase was used to synthesize oligomers from phenolic substrates. Due to the delocalization of the radical, the selectivity of laccase catalysis is generally poor. The presence of several phenol moieties in a compound multiplies the possibility of coupling and so leads to ill-defined oligomers.

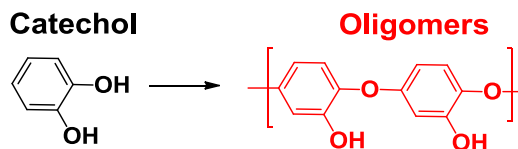
In order to amplify the beneficial physiological properties of antioxidant flavonoid, their oxidative polymerization by laccase was studied (Scheme 54). Rutin and catechin were polymerized using laccase from *Myceliophthora*. The molar masses of the obtained oligomers were about 3 000 g/mol with a large dispersity of 5 for poly(catechin) and 7 000 g/mol with a dispersity of 1.5 for poly(rutin). The oligomers were proven to possess radical species by ESR analysis.<sup>130,131</sup> Similar studies have been conducted on other flavonoid such as quercetin, esculin and epigallocatechin<sup>132-135</sup>



**Scheme 54: Laccase-catalyzed synthesis of ill-defined oligomers from flavonoids.**

Simpler polyphenols, such as catechol, lead to oligomers with a more defined structure (Scheme 55). Indeed, the reaction of catechol with laccase from *Trametes versicolor* leads to

oligomers of 800 g/mol with a relatively narrow dispersity of 1.7 showing the improved selectivity of the synthesis. FTIR analyses revealed oxyphenylene units and free hydroxyl groups in the structure. This polymer exhibits a melting temperature of 125°C and thermal stability up to 180°C.<sup>136,137</sup>

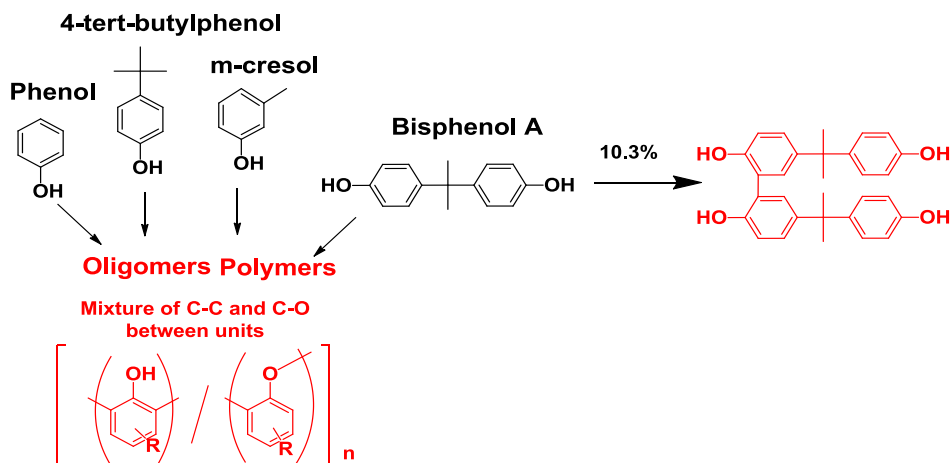


Scheme 55: Laccase-catalyzed catechol oligomerization.

b) Synthesis of ill-defined oligomers from *ortho* unsubstituted phenolic compounds

Employing a monophenol as substrate simplifies the coupling reactions. However, if there is no substituent in the *ortho* position of the phenol, the oxidative coupling can occur on these positions *via* a C-C or C-O linkage and leads to polymers. For instance, in the presence of laccases, coupling reactions of bisphenol-A, phenol, 4-*tert*-butylphenol, *m*-cresol yield oligomers or polymers, most of the time with a non-controlled structure.

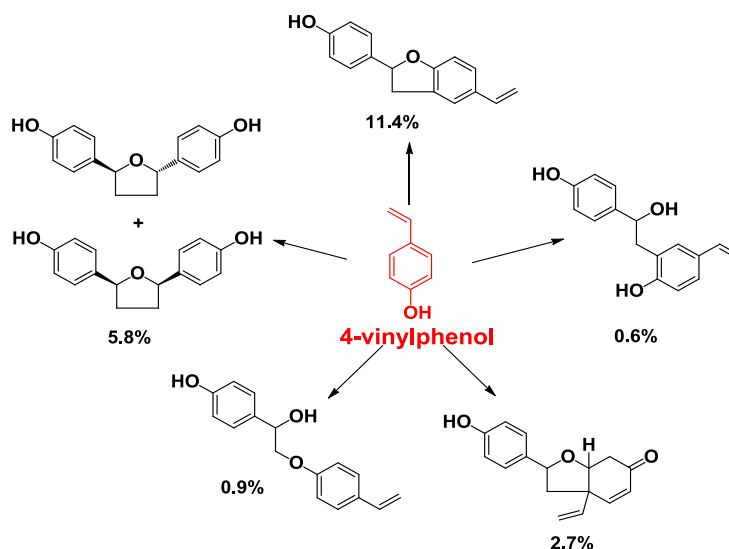
The reaction of bisphenol-A with laccase from *Trametes villosa* yields oligomers mainly with molar mass of 1 500 g/mol and a dimer which represents 10.3% of the mixture (Scheme 56).<sup>138</sup> In another study, bisphenol-A, as well as phenol, *m*-cresol and 4-*tert*-butylphenol were reacted with laccase from *Pycnoporus Coccineus* (Scheme 55). Polymers were obtained in high yield (over 95%). The molar masses were around 2 000 g/mol for phenol and 4-*tert*-butylphenol and 15 000 and 21 000 g/mol for *m*-cresol and bisphenol-A. The structure of the polymers revealed to be a mixture of phenylene and oxyphenylene units (around 50/50). The molar mass, as well as the phenylene/oxyphenylene ratio can be tuned by varying the co-solvent and its concentration.<sup>127</sup>



Scheme 56: Laccase-catalyzed non-controlled oligomerization of *ortho* unsubstituted phenols.

c) Synthesis of dimers from *ortho* unsubstituted phenols

The oxidative coupling of *ortho* unsubstituted phenols do not systematically lead to oligomers. The experimental conditions and structure of the substrate are very important parameters to tune the selectivity and oligomerization. For instance, the reaction of 4-vinylphenol with laccase from *Trametes versicolor*, in ethylacetate/water (1:1) biphasic system yields dimers only. Indeed, five dimers are obtained with yields below 10%. The coupling can occur at several positions, including the double bond which is conjugated to the aromatic system. The five dimers have very different structures (Scheme 57).<sup>139,140</sup>

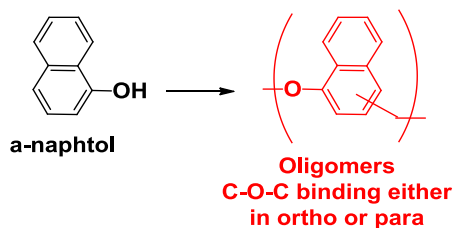


Scheme 57: Laccase-catalyzed dimerization of 4-vinylphenol.

d) Synthesis of ill-defined oligomers from *ortho,para*-unsubstituted phenols

The radical can also be delocalized to the phenol *para* position. For instance,  $\alpha$ -naphthol coupling can lead to bonds in *ortho, para* or phenolic positions.

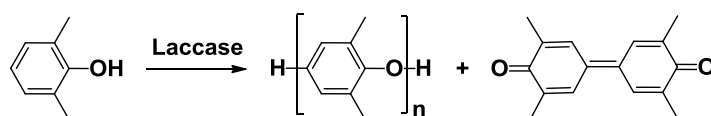
The effect of reaction conditions of polymerization of  $\alpha$ -naphthol catalyzed by laccase from *Trametes versicolor* were studied (Scheme 58).<sup>141</sup> After optimization of the conditions, a polymer with a molar mass of 5 000 g/mol was obtained. The units were linked by C-O-C binding, either on the carbon in *ortho* or *para* position of the hydroxyl group.

Scheme 58: Laccase-catalyzed oligomerization of  $\alpha$ -naphthol.

e) Laccase-catalyzed synthesis of well-defined polymers and dimers from *ortho*-disubstituted phenols

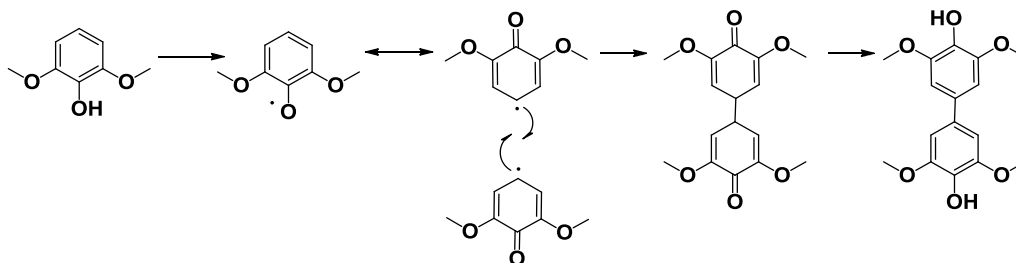
Laccase also catalyzes the synthesis of polymers with a precise structure, employing appropriate substrates. If the phenol possesses two substituents in the *ortho* position, a free *para* position, the coupling preferentially occurs on the phenol and on *para* position yielding either dimers or oligomers with a precise structure.

Indeed, the oxidative polymerization of 2,6-dimethylphenol catalyzed by laccase from *Pycnoporus Coccineous* yields a poly(phenylene oxide), poly(2,6-dimethyl-1,4-oxyphenylene) (Scheme 59). Oligomers with a molar mass of 3 000 g/mol and a dispersity of around 2 were prepared. The yield of oligomers was not above 50% because of the formation of a dimer, 3,5,3',5'-tetramethyl-4,4'-diphenoquinone, produced by oxidative coupling of two molecules at the position 4 of the monomer. The polymer exhibits a Tg of 136 °C and the 10% weight loss occurs at 360 °C. These values are lower than the ones of poly(phenylene oxide)s reported in literature because of the lower molar mass of the polymer.<sup>123,142</sup>



**Scheme 59:** Laccase-catalyzed synthesis of poly(2,6-dimethyl-1,4-oxyphenylene) and 3,5,3',5'-tetramethyl-4,4'-diphenoquinone from 2,6-dimethylphenol.

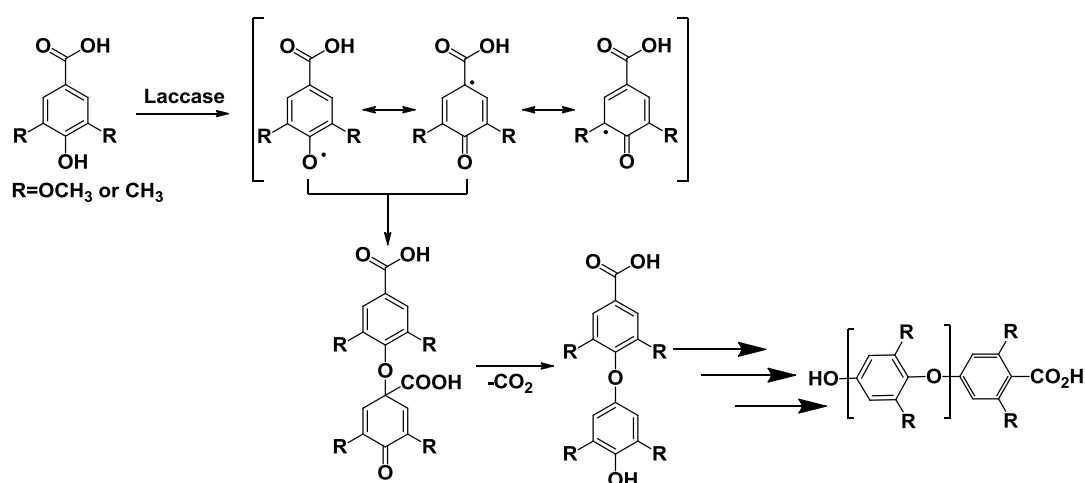
Interestingly, the reaction of 2,6-dimethoxyphenol with laccase from *Trametes pubescens* does not lead to the formation of polymers but to 5 dimers. 2,6-dimethoxyphenol dimer is obtained with 20% yield (Scheme 60). The other dimers, produced with lower yields correspond to demethylated dimers. Demethylation of methoxy-substituted compounds is a well-known reaction in the modification of similar lignin molecules.



**Scheme 60:** Laccase-catalyzed dimerization of 2,6-dimethoxyphenol.

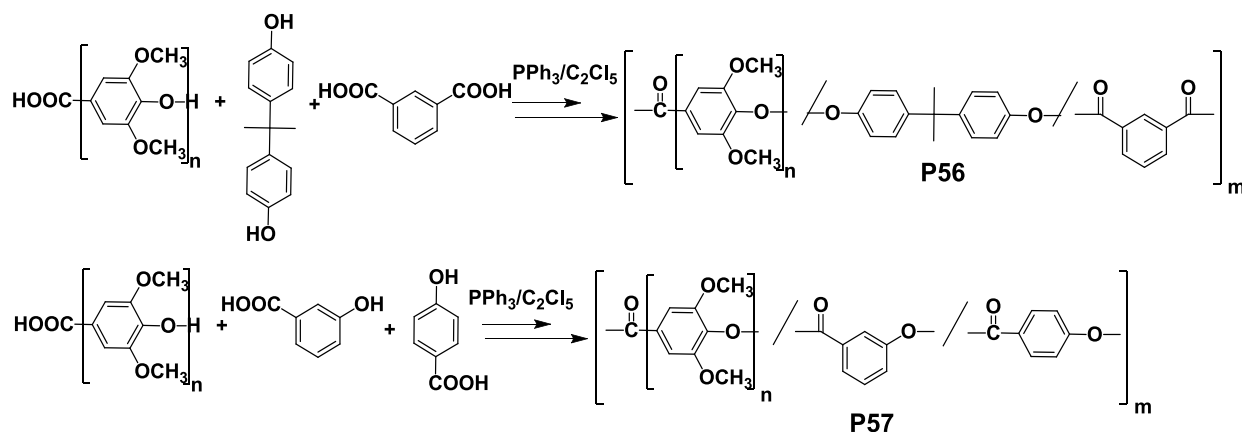
Poly(phenylene oxide)s can also be synthesized from *ortho*-substituted 4-hydroxybenzoic acid derivatives.<sup>143</sup> These derivatives are very difficult to polymerize oxidatively by metal complex catalysts. However, oxidase and peroxidase induce their polymerization. Syringic

acid and 3,5-dimethyl-4-benzoic acid were polymerized by Laccase from *Pycnoporus Coccineus* and *Myceliophthora*, whereas the polymerization did not take place with Laccase from *Pyricularia Oryzae*. Optimization of the reaction conditions led to polymers with molar mass of 7 700 g/mol. The postulated reaction mechanism is explained by the formation of phenoxy radicals which can couple each other to give the quinoide-type intermediates. The dimer is formed by liberation of carbon dioxide from the intermediate. Further couplings lead to the formation of poly(phenylene oxide)s (Scheme 61). The glass transition temperatures of the polymers are respectively 169 °C and 178 °C for polymers with methoxy and methyl moieties. 5% weight loss occurs at 358 °C.



**Scheme 61:** Synthetic pathway proposed for decarboxylation of *ortho*-substituted 4-hydroxybenzoic acid derivatives catalyzed by Laccase.

The polymers exhibit phenolic group at one end and benzoic acid group at the other end. These chain ends make them attractive as prepolymers for the synthesis of new polymeric material. One example of block copolymer was already described by Kobayashi and coll.<sup>144</sup> Poly(phenylene oxide) with a degree of polymerization of 13 (around 1 700 g/mol) was copolymerized using a mixture of triphenylphosphine and hexachloroethane. **P56**, prepared by copolymerization with bisphenol-A and isophthalic, shows a molar mass of 7 800 g/mol and a dispersity of 1.3. **P57**, produced by copolymerization with *m*- and *p*-hydroxybenzoic acid, exhibits a molar mass of 7 400 g/mol (Scheme 62). **P56** and **P57** exhibit glass transition temperature of around 150 °C and 5% weight loss temperature at around 370 °C. These two values are higher than the corresponding poly(phenylene oxide) ones.

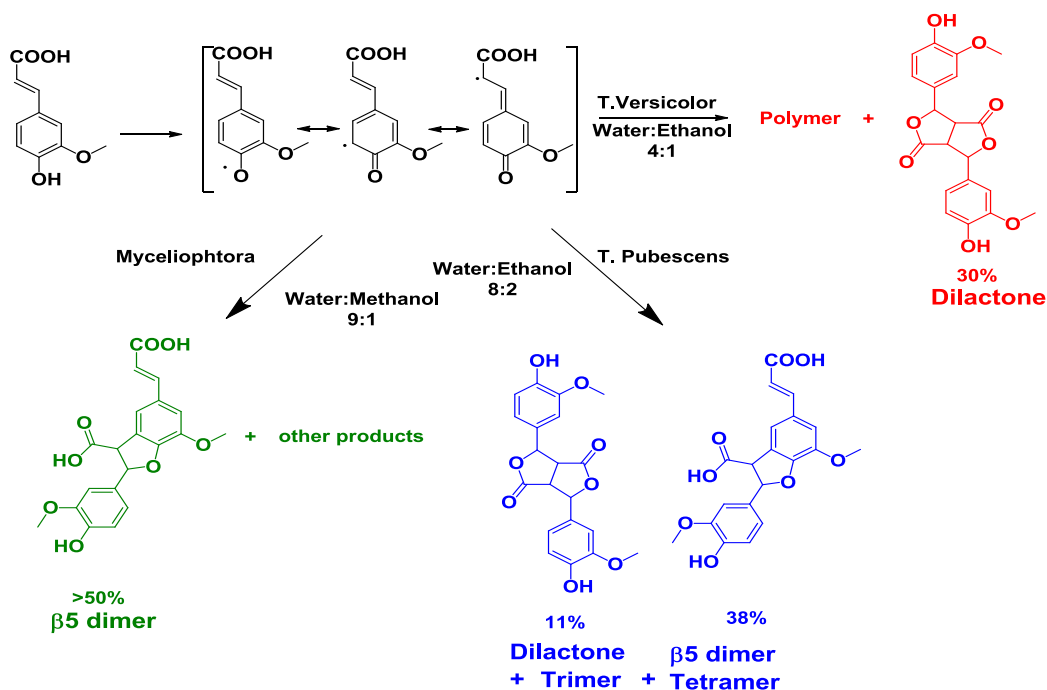


Scheme 62: Synthesis of block copolymers from poly(phenylene oxide) synthesized by laccase.

f) Laccase-catalyzed oxidative coupling of *ortho* methoxy *para* substituted phenols

The coupling of *ortho* methoxy *para* substituted phenol yield dimers mainly. In most cases a mixture of several dimers and traces of oligomeric structures are obtained. Varying experimental conditions and substrates enables to tune the production of dimers in terms of structures and yield. The best example to illustrate this statement is ferulic acid (Scheme 63).

The reaction of ferulic acid with laccase from *Trametes versicolor* in a water/ethanol mixture (4/1) yields a 2 700 g/mol polymer and 30% of dilactone.<sup>145</sup> The use of laccase from *Trametes pubescens* in water/ethanol (20/80) results in the formation of a tetramer, a trimer and two dimers. The dilactone and the  $\beta$ -5 dimer represent 11% and 38% of the mixture.

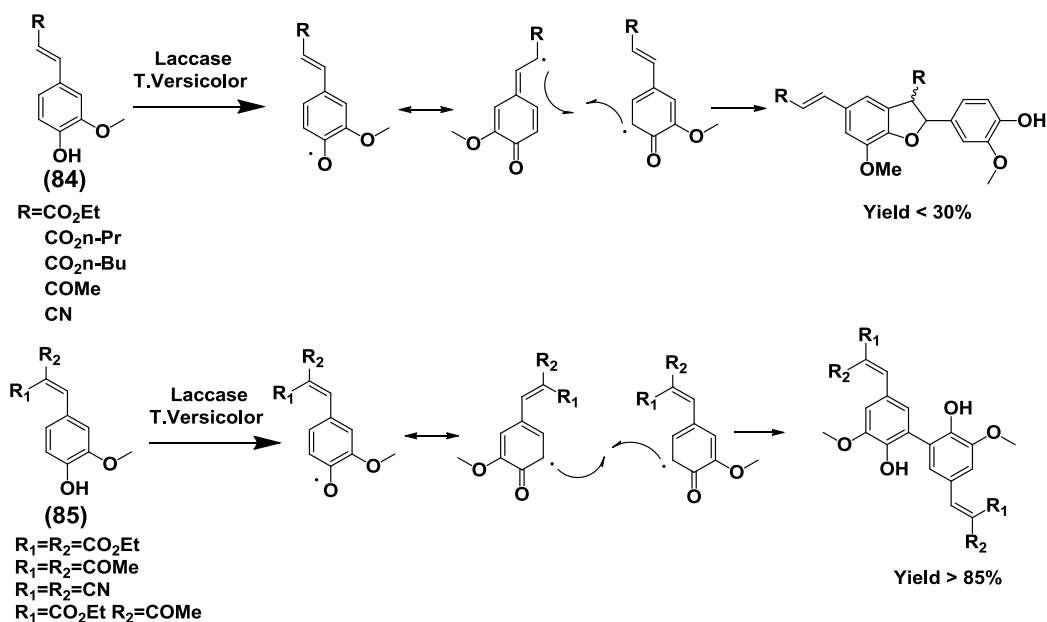


Scheme 63: Laccase-catalyzed ferulic acid oxidative coupling.



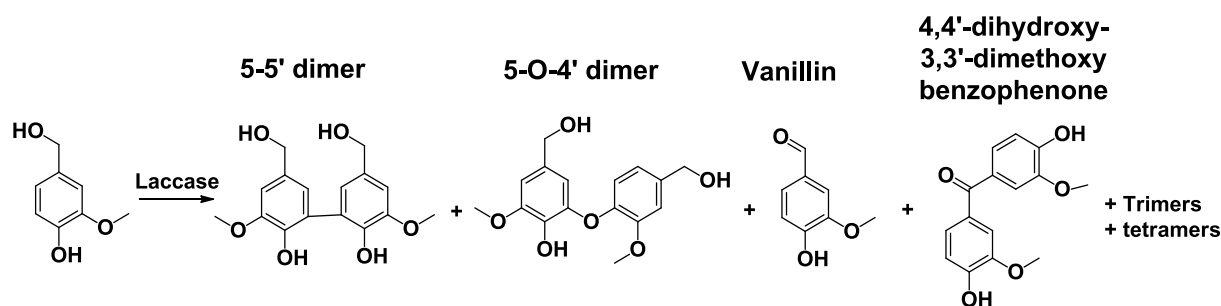
The use of dioxane instead of ethanol increases the amount of  $\beta$ -5 dimer.<sup>146</sup> The reaction of ferulic acid with laccase from *Myceliophthora* in water/methanol (10/90) produced mainly the  $\beta$ -5 dimer, associated with several other products which were not identified.<sup>147</sup>

Recently, Beifuss and coll. reported a study on the coupling of vanillidene derivatives, **(84)**, **(85)** catalyzed by Laccase from *Trametes versicolor* (Scheme 64). Similarly to ferulic acid, the coupling of compounds **(84)** produce mainly dihydrobenzofurans ( $\beta$ -5 dimer) with a yield which did not exceed 40%, due to the presence of other structures. However, molecules with trisubstituted double bonds **(85)** lead to the formation of biphenyl compounds with a yield over 80%.<sup>148</sup> This result constitutes the best result, in terms of yield/selectivity, of synthesis of dimer employing laccase.



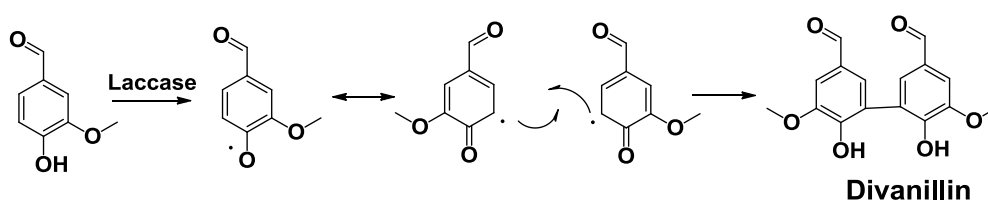
Scheme 64: Laccase-catalyzed oxidative coupling of vanillidene derivatives.

The dimerization of vanillyl alcohol leads to a complex mixture too.<sup>149,150</sup> In the study of Sipilä and coll., the reaction catalyzed by Laccase from *Trametes hirsute* and *Melanocarpus albomyces* was stopped after 2 h leading to low conversion of vanillyl alcohol (below 35%). After this time, three products were detected: 5-5' dimer, 5-O-4' dimer and vanillin. Previous studies revealed also the formation of 4,4'-dihydroxy-3,3'-dimethoxybenzophenone and some trimers or tetramers (Scheme 65). The main dimer is the 5-5' dimer with 30% yield.



Scheme 65: Laccase-catalyzed oxidative coupling of vanillyl alcohol.

In the concern of this study, the same group dimerized vanillin using Laccase from *Trametes hirsuta* ( $1 \text{ kat} \cdot \text{mL}^{-1}$ ). Only one dimer was formed with a conversion of 45% in 24 h (Scheme 66).



Scheme 66: Laccase-catalyzed vanillin dimerization.

### Conclusion:

Oxidative coupling of phenolic compounds catalyzed by laccase leads to the formation of dimers or oligomers. The type of substrate, source of laccase and experimental conditions control the regio-selectivity and yield of the coupling. In most cases a mixture of several compounds is obtained. The synthesis of polymers requires compounds with a well-defined structure and high purity. Oligomers and dimers synthesized from 2,6-dimethylphenol and 2,6-dimethoxyphenol and vanillyl alcohol dimer are suitable for polymer synthesis after development of a separation procedure. Finally, vanillin and vanillidene derivatives (85) dimers could be directly polymerized.

## III REFERENCES

1. [http://www.sust-forest.eu/sites/www.sust-forest.eu/files/Taller%20Industria%20LURE%202011\\_1.pdf](http://www.sust-forest.eu/sites/www.sust-forest.eu/files/Taller%20Industria%20LURE%202011_1.pdf).
2. D. E. Zinkel and J. Russel, eds., *Naval Stores, Production, Chemistry, Utilization*, New York, 1989.
3. S. Maiti, S. S. Ray and A. K. Kundu, *Progress in Polymer Science*, **1989**, 14, 297-338.
4. R. Auvergne, S. Caillol, G. David, B. Boutevin and J.-P. Pascault, *Chemical Reviews*, **2013**, 114, 1082-1115.
5. N. J. Halbrook and R. V. Lawrence, *Product R&D*, **1972**, 11, 200-202.
6. A. M. Atta, S. M. El-Saeed and R. K. Farag, *Reactive and Functional Polymers*, **2006**, 66, 1596-1608.
7. Q. Ma, X. Liu, R. Zhang, J. Zhu and Y. Jiang, *Green Chemistry*, **2013**, 15, 1300-1310.
8. X. Liu, W. Xin and J. Zhang, *Green Chemistry*, **2009**, 11, 1018-1025.
9. J. Qin, H. Liu, P. Zhang, M. Wolcott and J. Zhang, *Polymer International*, **2014**, 63, 760-765.
10. H. Wang, X. Liu, B. Liu, J. Zhang and M. Xian, *Polymer International*, **2009**, 58, 1435-1441.
11. A. M. Atta, R. Mansour, M. I. Abdou and A. M. Sayed, *Polymers for Advanced Technologies*, **2004**, 15, 514-522.
12. A. M. Atta, I. F. Nassar and H. M. Bedawy, *Reactive and Functional Polymers*, **2007**, 67, 617-626.
13. X. Liu and J. Zhang, *Polymer International*, **2010**, 59, 607-609.
14. I. Bicu and F. Mustață, *Die Angewandte Makromolekulare Chemie*, **1994**, 222, 165-174.
15. I. Bicu and F. Mustață, *Die Angewandte Makromolekulare Chemie*, **1999**, 264, 21-29.
16. A. Atta, R. Mansour, M. Abdou and A. El-Sayed, *J Polym Res*, **2005**, 12, 127-138.
17. A. L. Brocas, A. Llevot, C. Mantzaridis, G. Cendejas, R. Auvergne, S. Caillol, S. Carlotti and H. Cramail, *Designed Monomers and Polymers*, **2014**, 17, 301-310.
18. C. Mantzaridis, A.-L. Brocas, A. Llevot, G. Cendejas, R. Auvergne, S. Caillol, S. Carlotti and H. Cramail, *Green Chemistry*, **2013**, 15, 3091-3098.
19. L. J. Bai, X. Zhang and H. Y. Lan, *Chemical & Engineering* **2007**, 24, 24-26.
20. J. F. wang, M. T. Lin, F. Chu, C. P. Wang and M. H. Liu, *Biomass Chem. Eng.*, **2008**, 42, 1-4.
21. J. S. Lee and S. I. Hong, *European Polymer Journal*, **2002**, 38, 387-392.
22. J.-F. Wang, M.-T. Lin, C.-P. Wang and F.-X. Chu, *Journal of Applied Polymer Science*, **2009**, 113, 3757-3765.
23. Y. Zheng, K. Yao, J. Lee, D. Chandler, J. Wang, C. Wang, F. Chu and C. Tang, *Macromolecules*, **2010**, 43, 5922-5924.
24. J. Wang, K. Yao, P. Wilbon, P. Wang, F. Chu and C. Tang, eds., *Rosin-based chemicals and Polymers*, Shawbury, UK, 2012.
25. P. A. Wilbon, Y. Zheng, K. Yao and C. Tang, *Macromolecules*, **2010**, 43, 8747-8754.
26. Z. Yu, G. R. Stewart and W. W. Mohn, *Applied and Environmental Microbiology*, **2000**, 66, 5148-5154.
27. S. N. Liss, P. A. Bicho and J. N. Saddler, *Canadian Journal of Microbiology*, **1997**, 43, 599-611.
28. J. Wang, K. Yao, A. L. Korich, S. Li, S. Ma, H. J. Ploehn, P. M. Iovine, C. Wang, F. Chu and C. Tang, *Journal of Polymer Science, Part A: Polymer Chemistry*, **2011**, 49, 3728-3738.
29. J. Yu, Y. Liu, X. Liu, C. Wang, J. Wang, F. Chu and C. Tang, *Green Chemistry*, **2014**, 16, 1854-1864.
30. Y. Liu, K. Yao, X. Chen, J. Wang, Z. Wang, H. J. Ploehn, C. Wang, F. Chu and C. Tang, *Polymer Chemistry*, **2014**, 5, 3170-3181.
31. J. Wang, K. Yao, C. Wang, C. Tang and X. Jiang, *Journal of Materials Chemistry B*, **2013**, 1, 2324-2332.
32. S. J. Kim, B. J. Kim, D. W. Jang, S. H. Kim, S. Y. Park, J.-H. Lee, S.-D. Lee and D. H. Choi, *Journal of Applied Polymer Science*, **2001**, 79, 687-695.

33. B. J. Kim, S. J. Kim and S. Y. Park, *Journal of Industrial and Engineering Chemistry*, **1998**, 4, 238-244.
34. L. Zhang, Y. Jiang, Z. Xiong, X. Liu, H. Na, R. Zhang and J. Zhu, *Journal of Materials Chemistry A*, **2013**, 1, 3263-3267.
35. F. Mustață and I. Bicu, *Polimery/Polymers*, **2005**, 50, 176-181.
36. I. Bicu and F. Mustata, *Macromol. Mater. Eng*, **2000**, 47, 280-281.
37. A. M. Atta, A. M. Elsaheed, R. K. Farag and S. M. El-Saeed, *Reactive and Functional Polymers*, **2007**, 67, 549-563.
38. F. Mustata and I. Bicu, *European Polymer Journal*, **2010**, 46, 1316-1327.
39. P. A. Wilbon, A. L. Gullledge, B. C. Benicewicz and C. Tang, *Green materials*, **2013**, 1, 96-104.
40. I. Bicu and F. Mustata, *Journal of Applied Polymer Science*, **2004**, 92, 2240-2252.
41. Prashant M. Satturwar, Suniket V. Fulzele and A. K. Dorle, *AAPS Pharm. Sci. Tech*, **2005**, 6, E649-E654.
42. G. Brus, V. Thoi and H. Francis, *Peintures, Pigments, Vernis*, **1953**, 8, 29-36.
43. Y. Morillon, *Double liaison*, **1964**, 106, 91-100.
44. I. I. Bardyshev and O. D. Strizhakov, *Dokl. Akad. Nauk*, **1968**, 181, 343-349.
45. R. Fujii, K. Arimoto and D. F. Zinkel, *J Am Oil Chem Soc*, **1987**, 64, 1144-1149.
46. B. Gigante, R. Jones, A. M. Lobo, M. J. Marcelo-Curto, S. Prabhakar, H. S. Rzepa, D. J. Williams and D. F. Zinkel, *Journal of the Chemical Society, Chemical Communications*, **1986**, 1, 1038-1039.
47. A. Grün and R. Winkler, *Chemische Umschau auf dem Gebiet der Fette, Oele, Wachse und Harze*, **1919**, 26, 77-79.
48. R. H. Leonard, K. A. Kubitz and J. N. Rockwell, *J Am Oil Chem Soc*, **1965**, 42, 111-113.
49. R. G. Sinclair, D. A. Berry, W. H. Schuller and R. V. Lawrence, *Product R&D*, **1970**, 9, 60-65.
50. D. Stewart, *Industrial Crops and Products*, **2008**, 27, 202-207.
51. M. P. Pandey and C. S. Kim, *Chemical Engineering and Technology*, **2011**, 34, 29-41.
52. C. O. Tuck, E. Pérez, I. T. Horváth, R. A. Sheldon and M. Poliakoff, *Science*, **2012**, 337, 695-699.
53. I. A. Pearl, *Journal of the American Chemical Society*, **1942**, 64, 1429-1431.
54. F. Pion, A. F. Reano, P.-H. Ducrot and F. Allais, *RSC Advances*, **2013**, 3, 8988-8997.
55. L. Mialon, A. G. Pemba and S. A. Miller, *Green Chemistry*, **2010**, 12, 1704-1706.
56. M. B. Hocking, *Journal of Chemical Education*, **1997**, 74, 1055-1059.
57. Z. Wong, K. Chen and J. Li, *BioResources*, **2010**, 5, 1509-1516.
58. E. A. B. d. Silva, M. Zabkova, J. D. Araújo, C. A. Cateto, M. F. Barreiro, M. N. Belgacem and A. E. Rodrigues, *Chemical Engineering Research and Design*, **2009**, 87, 1276-1292.
59. J. D. P. Araújo, C. A. Grande and A. E. Rodrigues, *Chemical Engineering Research and Design*, **2010**, 88, 1024-1032.
60. J. F. Stanzione Iii, J. M. Sadler, J. J. La Scala, K. H. Reno and R. P. Wool, *Green Chemistry*, **2012**, 14, 2346-2352.
61. H. A. Meylemans, B. G. Harvey, J. T. Reams, A. J. Guenther, L. R. Cambrea, T. J. Groshens, L. C. Baldwin, M. D. Garrison and J. M. Mabry, *Biomacromolecules*, **2013**, 14, 771-780.
62. B. G. Harvey, M. E. Wright, S. Compel, A. J. Guenther, K. Lamison, L. R. Cambrea, H. A. Meylemans and S. McCormick, *polymer preprint*, **2011**, 52, 282-283.
63. H. A. Meylemans, T. J. Groshens and B. G. Harvey, *ChemSusChem*, **2012**, 5, 206-210.
64. M. Fache, E. Darroman, V. Besse, R. Auvergne, S. Caillol and B. Boutevin, *Green Chemistry*, **2014**, 16, 1987-1998.
65. C. Aouf, C. Le Guernevé, S. Caillol and H. Fulcrand, *Tetrahedron*, **2013**, 69, 1345-1353.
66. J. K. Cho, J.-S. Lee, J. Jeong, B. Kim, B. Kim, S. Kim, S. Shin, H.-J. Kim and S.-H. Lee, *Journal of Adhesion Science and Technology*, **2012**, 27, 2127-2138.
67. C. Aouf, J. Lecomte, P. Villeneuve, E. Dubreucq and H. Fulcrand, *Green Chemistry*, **2012**, 14, 2328-2336.
68. T. Koike, *Polymer Engineering and Science*, **2012**, 52, 701-717.

69. İ. Kaya, F. Doğan and M. Gül, *Journal of Applied Polymer Science*, **2011**, 121, 3211-3222.
70. L. H. Bock and J. K. Anderson, *Journal of Polymer Science*, **1955**, 17, 553-558.
71. M. Korematsu and S. Kuriyama, *Nippon Kagaku Zasshi*, **1960**, 81, 852-855.
72. V. Era and J. Hannula, *Paperi ja Puu*, **1974**, 56, 489-496.
73. W. Lange and O. Kordsachia, *Holz als Roh-und Werkstoff*, **1981**, 39, 107-112.
74. H. R. Kricheldorf and G. Löhden, *Polymer*, **1995**, 36, 1697-1705.
75. H. R. Kricheldorf and T. Stukenbrock, *Macromolecular Chemistry and Physics*, **1997**, 198, 3753-3767.
76. M. Nagata, *Journal of Applied Polymer Science*, **2000**, 78, 2474-2481.
77. X.-G. Li, M.-R. Huang, G.-H. Guan and T. Sun, *Journal of Applied Polymer Science*, **1996**, 59, 1-8.
78. X.-G. Li, M.-R. Huang, G.-H. Guan and T. Sun, *Journal of Applied Polymer Science*, **1997**, 66, 2129-2138.
79. X.-G. Li, M.-R. Huang, G.-H. Guan and T. Sun, *Die Angewandte Makromolekulare Chemie*, **1995**, 227, 69-85.
80. Y. N. Sazanov, M. Y. Goykhman, I. V. Podeshvo, G. N. Fedorova, G. M. Mikhailov and V. V. Kudriavtsev, *Journal of Thermal Analysis and Calorimetry*, **1999**, 55, 721-726.
81. H. Montes de Oca, J. E. Wilson, A. Penrose, D. M. Langton, A. C. Dagger, M. Anderson, D. F. Farrar, C. S. Lovell, M. E. Ries, I. M. Ward, A. D. Wilson, S. J. Cowling, I. M. Saez and J. W. Goodby, *Biomaterials*, **2010**, 31, 7599-7605.
82. C. S. Lovell, M. E. Ries, I. M. Ward, H. Montes de Oca and D. Farrar, *Macromolecules*, **2013**, 46, 1201-1211.
83. C. S. Lovell, H. Montes de Oca, D. Farrar, M. E. Ries and I. M. Ward, *Polymer*, **2010**, 51, 2013-2020.
84. C. H. R. M. Wilsens, B. A. J. Noordover and S. Rastogi, *Polymer (United Kingdom)*, **2014**, 55, 2432-2439.
85. C. H. R. M. Wilsens, J. M. G. A. Verhoeven, B. A. J. Noordover, M. R. Hansen, D. Auhl and S. Rastogi, *Macromolecules*, **2014**, 47, 3306-3316.
86. O. Kreye, S. Oelmann and M. A. R. Meier, *Macromolecular Chemistry and Physics*, **2013**, 214, 1452-1464.
87. O. Kreye, T. Tóth and M. A. R. Meier, *European Polymer Journal*, **2011**, 47, 1804-1816.
88. M. Firdaus and M. A. R. Meier, *European Polymer Journal*, **2013**, 49, 156-166.
89. L. Mialon, R. Vanderhenst, A. G. Pemba and S. A. Miller, *Macromolecular Rapid Communications*, **2011**, 32, 1386-1392.
90. J. Kwon, J. Kim, S. Park, G. Khang, P. M. Kang and D. Lee, *Biomacromolecules*, **2013**, 14, 1618-1626.
91. A. G. Pemba, M. Rostagno, T. A. Lee and S. A. Miller, *Polymer Chemistry*, **2014**, 5, 3214-3221.
92. C. Pang, J. Zhang, G. Wu, Y. Wang, H. Gao and J. Ma, *Polymer Chemistry*, **2014**, 5, 2843-2853.
93. A. S. Amarasekara and A. Razzaq, *ISRN Polymer Science*, **2012**, vol 2012, 1-5.
94. F. Pion, P. H. Ducrot and F. Allais, *Macromolecular Chemistry and Physics*, **2014**, 215, 431-439.
95. A. S. Amarasekara, B. Wiredu and A. Razzaq, *Green Chemistry*, **2012**, 14, 2395-2397.
96. I. Reiss, I. L. Gatfield, G. Krammer, A. Clerc and G. Kindel, Google Patents, 2006.
97. M. J. Gaur, J. Lohani, V. R. Balakrishnan, P. Raghunathan and S. V. Eswaran, *Bull. Korean Chem. Soc.*, **2009**, 30, 2895-2898.
98. H. Yamamoto, T. Hoshino and T. Uchiyama, *Bioscience, Biotechnology, and Biochemistry*, **1999**, 63, 390-394.
99. F. Tiemann, *Berichte der deutschen chemischen Gesellschaft*, **1885**, 18, 3493-3496.
100. D. R. Kelly, S. C. Baker, D. S. King, D. S. de Silva, G. Lord and J. P. Taylor, *Organic & Biomolecular Chemistry*, **2008**, 6, 787-796.
101. K. Elbs and H. J. Lerch, *J. Prakt. Chem*, **1916**, 93, 1-6.

102. M. Delomenède, F. Bedos-Belval, H. Duran, C. Vindis, M. Baltas and A. Nègre-Salvayre, *Journal of Medicinal Chemistry*, **2008**, 51, 3171-3181.
103. E. Anklam, S. Gaglione and A. Müller, *Food Chemistry*, **1997**, 60, 43-51.
104. J. Baumgartner and H. Neukom, *Chimia (Aarau)*, **1972**, 26, 366-368.
105. S. Antoniotti, L. Santhanam, D. Ahuja, M. G. Hogg and J. S. Dordick, *Organic Letters*, **2004**, 6, 1975-1978.
106. R. T. Nishimura, C. H. Giammanco and D. A. Vosburg, *Journal of Chemical Education*, **2010**, 87, 526-527.
107. H. Yoshida, *J. Chem. Soc.*, **1883**, 43, 472-486.
108. G. Benfield, S. M. Bocks, K. Bromley and B. R. Brown, *Phytochemistry*, **1964**, 3, 79-88.
109. G. Diamantidis, A. Effosse, P. Potier and R. Bally, *Soil Biology and Biochemistry*, **2000**, 32, 919-927.
110. L. Gianfreda, F. Xu and J. M. Bollag, *Bioremediation Journal*, **1999**, 3, 1-25.
111. A. C. Mot and R. Silaghi-Dumitrescu, *Biochemistry Moscow*, **2012**, 77, 1395-1407.
112. O. V. Morozova, G. P. Shumakovich, M. A. Gorbacheva, S. V. Shleev and A. I. Yaropolov, *Biochemistry Moscow*, **2007**, 72, 1136-1150.
113. P. M. Coll, C. Taberner, R. Santamaria and P. Perez, *Applied and Environmental Microbiology*, **1993**, 59, 4129-4135.
114. S. Witayakran and A. J. Ragauskas, *Advanced Synthesis & Catalysis*, **2009**, 351, 1187-1209.
115. K. Li, F. Xu and K. E. L. Eriksson, *Applied and Environmental Microbiology*, **1999**, 65, 2654-2660.
116. J. M. Bollag and A. Leonowicz, *Applied and Environmental Microbiology*, **1984**, 48, 849-854.
117. F. Xu, W. Shin, S. H. Brown, J. A. Wahleithner, U. M. Sundaram and E. I. Solomon, *Biochimica et Biophysica Acta (BBA) - Protein Structure and Molecular Enzymology*, **1996**, 1292, 303-311.
118. E. Uzan, P. Nousiainen, V. Balland, J. Sipila, F. Piumi, D. Navarro, M. Asther, E. Record and A. Lomascolo, *Journal of Applied Microbiology*, **2010**, 108, 2199-2213.
119. S. Shleev, O. Nikitina, A. Christenson, C. T. Reimann, A. I. Yaropolov, T. Ruzgas and L. Gorton, *Bioorganic Chemistry*, **2007**, 35, 35-49.
120. S. Shleev, A. Christenson, V. Serezhenkov, D. Burbaev, A. Yaropolov, L. Gorton and T. Ruzgas, *Biochem.J.*, **2005**, 385, 745-754.
121. M. Mogharabi and M. A. Faramarzi, *Advanced Synthesis & Catalysis*, **2014**, 356, 897-927.
122. J.-R. Jeon and Y.-S. Chang, *Trends in Biotechnology*, **2013**, 31, 335-341.
123. S. Kobayashi and H. Higashimura, *Progress in Polymer Science*, **2003**, 28, 1015-1048.
124. S. Kobayashi and A. Makino, *Chemical Reviews*, **2009**, 109, 5288-5353.
125. S. Kobayashi, S.-i. Shoda and H. Uyama, in *Polymer Synthesis/Polymer Engineering*, Springer Berlin Heidelberg, 1995, vol. 121, ch. 1, pp. 1-30.
126. S. Kobayashi, H. Uyama and S. Kimura, *Chemical Reviews*, **2001**, 101, 3793-3818.
127. N. Mita, S.-i. Tawaki, H. Uyama and S. Kobayashi, *Macromolecular Bioscience*, **2003**, 3, 253-257.
128. S. Riva, *Trends in Biotechnology*, **2006**, 24, 219-226.
129. E. I. Solomon, U. M. Sundaram and T. E. Machonkin, *Chemical Reviews*, **1996**, 96, 2563-2606.
130. M. Kurisawa, J. E. Chung, H. Uyama and S. Kobayashi, *Macromolecular Bioscience*, **2003**, 3, 758-764.
131. M. Kurisawa, J. E. Chung, H. Uyama and S. Kobayashi, *Biomacromolecules*, **2003**, 4, 1394-1399.
132. R. M. Desentis-Mendoza, H. Hernández-Sánchez, A. Moreno, E. Rojas del C, L. Chel-Guerrero, J. Tamariz and M. E. Jaramillo-Flores, *Biomacromolecules*, **2006**, 7, 1845-1854.
133. J. Anthoni, L. Chebil, F. Lionneton, J. Magdalou, C. Humeau and M. Ghoul, *Canadian Journal of Chemistry*, **2011**, 89, 964-970.
134. J. Anthoni, C. Humeau, E. R. Maia, L. Chebil, J. M. Engasser and M. Ghoul, *European Food Research and Technology*, **2010**, 231, 571-579.



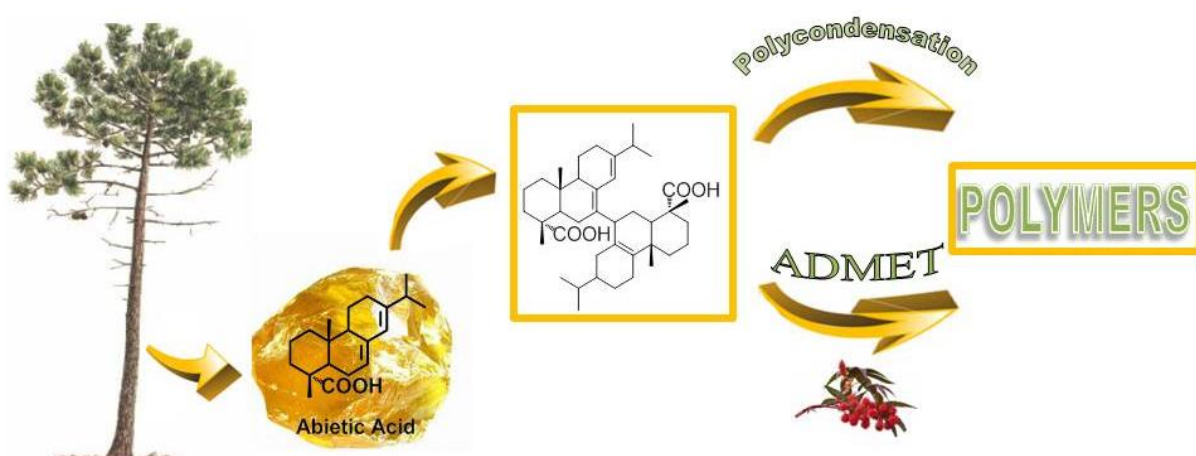
135. M. Kurisawa, J. E. Chung, H. Uyama and S. Kobayashi, *Chemical Communications*, **2004**, 10, 294-295.
136. N. Aktaş, N. Şahiner, Ö. Kantoğlu, B. Salih and A. Tanyolaç, *Journal of Polymers and the Environment*, **2003**, 11, 123-128.
137. N. Aktaş and A. Tanyolaç, *Journal of Molecular Catalysis B: Enzymatic*, **2003**, 22, 61-69.
138. H. Uchida, T. Fukuda, H. Miyamoto, T. Kawabata, M. Suzuki and T. Uwajima, *Biochemical and Biophysical Research Communications*, **2001**, 287, 355-358.
139. C. Navarra, P. Gavezzotti, D. Monti, W. Panzeri and S. Riva, *Journal of Molecular Catalysis B: Enzymatic*, **2012**, 84, 115-120.
140. C. Ponzoni, E. Beneventi, M. R. Cramarossa, S. Raimondi, G. Trevisi, U. M. Pagnoni, S. Riva and L. Forti, *Advanced Synthesis & Catalysis*, **2007**, 349, 1497-1506.
141. N. Aktaş, G. Kibarer and A. Tanyolaç, *Journal of Chemical Technology and Biotechnology*, **2000**, 75, 840-846.
142. R. Ikeda, J. Sugihara, H. Uyama and S. Kobayashi, *Macromolecules*, **1996**, 29, 8702-8705.
143. R. Ikeda, J. Sugihara, H. Uyama and S. Kobayashi, *Polymer International*, **1998**, 47, 295-301.
144. R. Ikeda, J. Sugihara, H. Uyama and S. Kobayashi, *Polymer Bulletin*, **1998**, 40, 367-371.
145. Y. N. Kupriyanovich, S. A. Medvedeva, A. V. Rokhin and L. V. Kanitskaya, *Russ J Bioorg Chem*, **2007**, 33, 516-522.
146. O. E. Adelakun, T. Kudanga, A. Parker, I. R. Green, M. le Roes-Hill and S. G. Burton, *Journal of Molecular Catalysis B: Enzymatic*, **2012**, 74, 29-35.
147. A. Aljawish, I. Chevalot, J. Jasniewski, C. Paris, J. Scher and L. Muniglia, *Food Chemistry*, **2014**, 145, 1046-1054.
148. M.-A. Constantin, J. Conrad and U. Beifuss, *Green Chemistry*, **2012**, 14, 2375-2379.
149. M. Lahtinen, K. Kruus, P. Heinonen and J. Sipilä, *Journal of Agricultural and Food Chemistry*, **2009**, 57, 8357-8365.
150. H. P. Lahtinen M, Oivanen M, Karhunen P, Kruus K, Sipilä J., *Org Biomol Chem*, **2013**, 11, 5454-5464.





# CHAPTER 2:

## Abietic acid dimer synthesis and purification towards new biobased polymers



**Key words:** abietic acid, abietic acid dimers, dimerization, vegetable oil, polycondensation, acyclic diene metathesis, thermoplastic polymers.

**Mots clés:** acide abiétique, dimères de l'acide abiétique, dimérisation, huiles végétales, polycondensation, polymérisation par métathèse de diènes acycliques, polymères thermoplastiques

## TABLE OF CONTENTS

<b>I</b>	<b>Introduction.....</b>	<b>95</b>
<b>II</b>	<b>Abietic acid dimer synthesis .....</b>	<b>95</b>
	<b>1. Abietic acid dimerization, purification and characterization .....</b>	<b>96</b>
	1) Dimerization of abietic acid.....	96
	2) Isolation of abietic acid dimers.....	97
	3) Characterization of the abietic acid dimers .....	101
	<b>2. Investigation of the dimerization mechanism of abietic acid .....</b>	<b>102</b>
	<b>3. Optimization of the dimerization of abietic acid .....</b>	<b>105</b>
	1) Influence of the monomer purity on the dimerization of abietic acid .....	105
	2) Experimental condition screening of abietic acid dimerization .....	107
<b>III</b>	<b>Synthesis of polyesters from abietic acid dimers <i>via</i> direct polycondensation. 109</b>	<b>109</b>
	<b>1. Polycondensation of abietic acid dimers .....</b>	<b>109</b>
	<b>2. Thermomechanical properties of abietic acid dimer copolymers.....</b>	<b>112</b>
<b>IV</b>	<b>Synthesis of unsaturated polyester <i>via</i> ADMET polymerization.....</b>	<b>113</b>
	<b>1. Bis-unsaturated abietic ester dimer synthesis and characterization .....</b>	<b>113</b>
	<b>2. ADMET polymerization of bis-unsaturated abietic ester dimers.....</b>	<b>115</b>
	1) Chemical structure and molar mass of the unsaturated polyesters .....	115
	2) Thermomechanical properties of the unsaturated polyesters.....	118
<b>V</b>	<b>Conclusion and perspectives.....</b>	<b>120</b>
<b>VI</b>	<b>References .....</b>	<b>121</b>
<b>VII</b>	<b>Experimental .....</b>	<b>122</b>

## I Introduction

As described in the previous chapter, polymers with abietic acid moiety either as pendant group or in the main chain have already been described.<sup>1,2</sup> Polymers with pendant abietic acid moiety have been mainly synthesized by controlled radical polymerization. The latter possess well-defined structures, high molar masses and could potentially be used as negative photoresist, drug carrier, hydrophobic materials, UV absorption coating, etc. However, these polymers do not exhibit high glass transition temperatures because the cyclo-aliphatic structure of abietic acid is not incorporated in the polymer backbone. Polymers with main chain rosin moiety were synthesized from maleopimarate or acrylopimarate adducts. High thermal properties could be achieved but the polymers generally exhibit low molar masses. In order to investigate another way to polymerize abietic acid, the synthesis and polymerization of symmetrical abietic acid dimer were performed, and is thus described in the following section.

In a first part, abietic acid dimers were synthesized, isolated from the crude mixture and characterized. The polycondensation of these dimers with aliphatic diols resulted in low molar mass polyesters. In order to increase the reactivity of these dimers, the latter were esterified with undecenol leading to bis-unsaturated dimers, which were then homopolymerized and copolymerized with undecenyl undecenoate through acyclic diene metathesis (ADMET) methodology.

## II Abietic acid dimer synthesis

This section describes the dimerization of abietic acid. It is important to mention that commercial abietic acid is purchased either as rosin which contains several isomers or as abietic acid but with a purity which never exceed 85% due to a complex purification process. The structure of these isomers, as well as their reactivity towards dimerization, is discussed in this section. Figure 1 displays the structures and names of isomers.

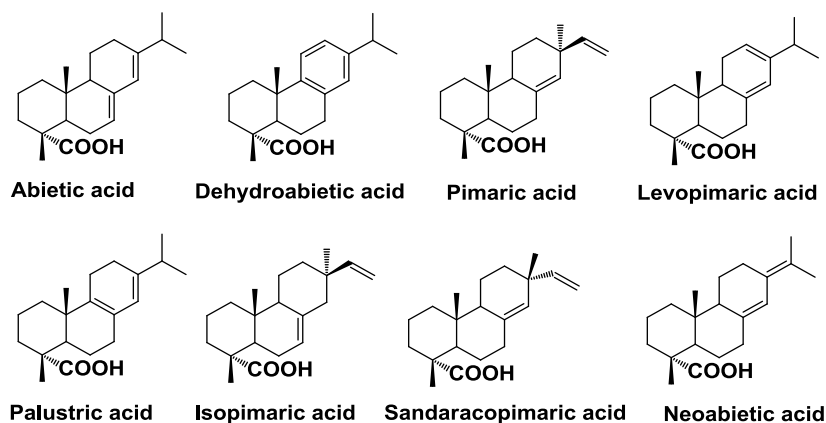
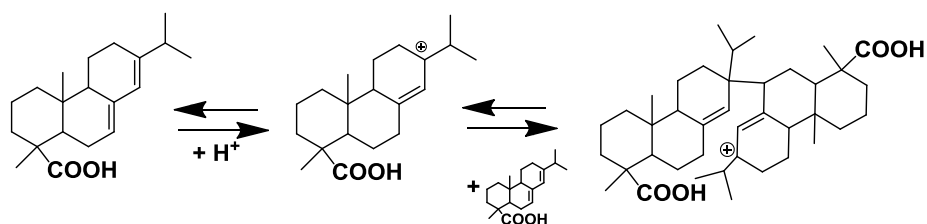


Figure 1: Structure of abietic acid and its isomers.

## 1. Abietic acid dimerization, purification and characterization

### 1) Dimerization of abietic acid

Dimerization of abietic acid is a long known reaction which occurs through a cationic mechanism (Scheme 1). This mechanism was proposed by Sinclair and coll. and will be discussed in this section. Usually, a mixture of compounds containing unreacted abietic acid, dimers and oligomers is obtained.



Scheme 1: Proposed mechanism for abietic acid dimerization.<sup>3</sup>

Abietic acid (purchased from Sigma, 85% pure) has been dimerized, employing sulfuric acid as a catalyst in chloroform, at 45 °C, for 5 h using the method developed by the Sinclair and coll.<sup>4</sup> The composition of the crude mixture, before any purification, was determined by SEC measurements in THF (Figure 2). Three peaks were detected and assigned to abietic acid ( $M = 302$  g/mol), abietic acid dimers ( $M = 604$  g/mol) and trimers ( $M = 906$  g/mol) which represent 31%, 57% and 12% of the mixture, respectively, assuming that the three compounds possess similar  $dn/dc$ . A method of dimer isolation was then developed.

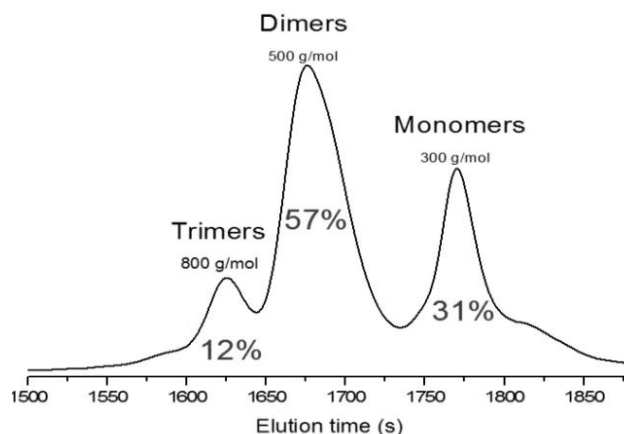


Figure 2: SEC in THF of the crude mixture after dimerization of abietic acid, RI detection.

## 2) Isolation of abietic acid dimers

In order to get diunctional compounds for the synthesis of thermoplastic polymers, several methods to isolate the dimers have been scrutinized. Among them, recrystallizations in several solvents, selective precipitation and dialysis using a 500 Da cellulose ester membrane did not give good result. Thin Layer Chrommatography (TLC) was carried out on different phases: cellulose, alumina, silica and C18 grafted silica. Only the TLC with C18 grafted silica support, using methanol/water as eluent, presents two clear spots (Retardation Factor (Rf) around 0.10 and 0.40), indicating the separation of the products. Hence, high performance liquid chromatography (HPLC) (Figure 3), using a C18 grafted silica column, was performed in order to find the best solvent conditions for the isolation of the dimers.

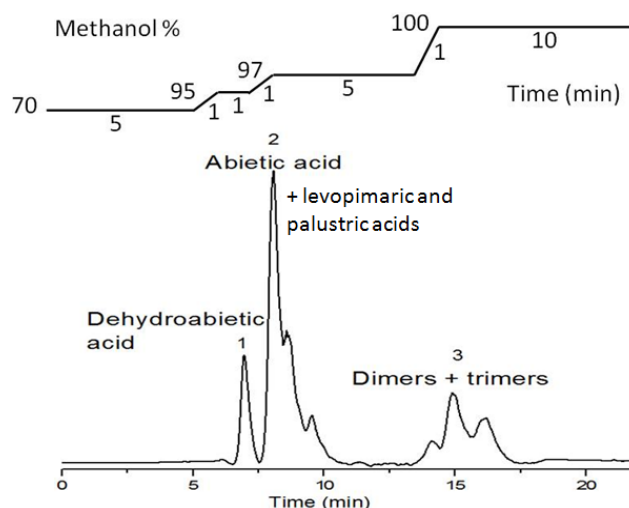


Figure 3: HPLC profile of crude mixture after dimerization of abietic acid, using a C18 grafted silica column.

Starting from a 70% methanol/water solution and gradually increasing the methanol concentration, three separated peaks were observed. The two first peaks were attributed to

dehydroabietic acid and abietic acid by comparison with pure standard products. The third peak was supposed to correspond to dimers and trimers.

The separation conditions developed by HPLC were adapted to a preparative apparatus (flash chromatography). A similar profile was observed (Figure 4). Three fractions were collected and analyzed by  $^1\text{H}$  NMR spectroscopy and SEC.

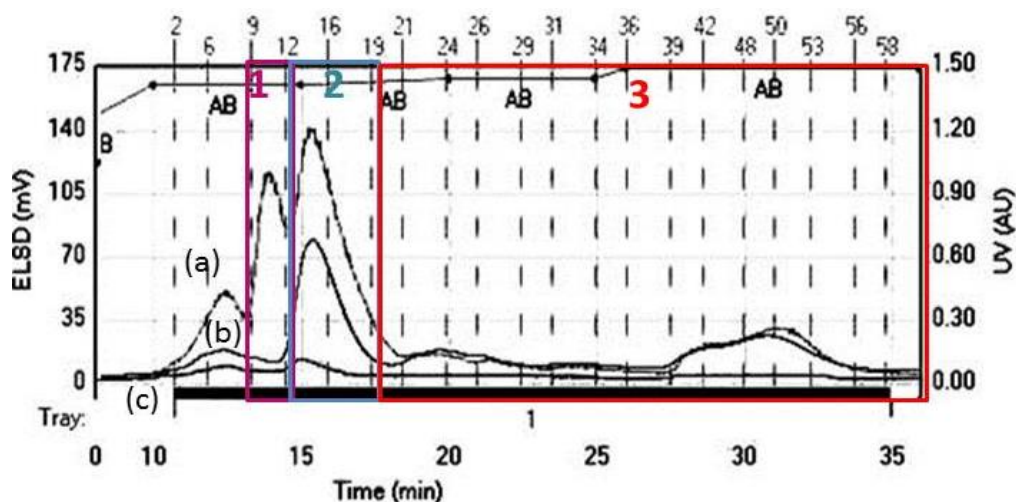


Figure 4: Flash chromatography profile of crude mixture after dimerization of abietic acid: (a) ELSD detector, (b) UV 254 nm, (c) UV 280 nm, using a water methanol gradient and a C18 grafted silica column.

The yield of fraction 1, isolated from the crude mixture, represents 10 wt%. The peaks of the  $^1\text{H}$  NMR spectrum of the first fraction were assigned to the dehydroabietic acid (Figure 5). Especially the signals at 6.90, 7.00 and 7.19 ppm attributed to an aromatic structure are characteristic of this isomer.

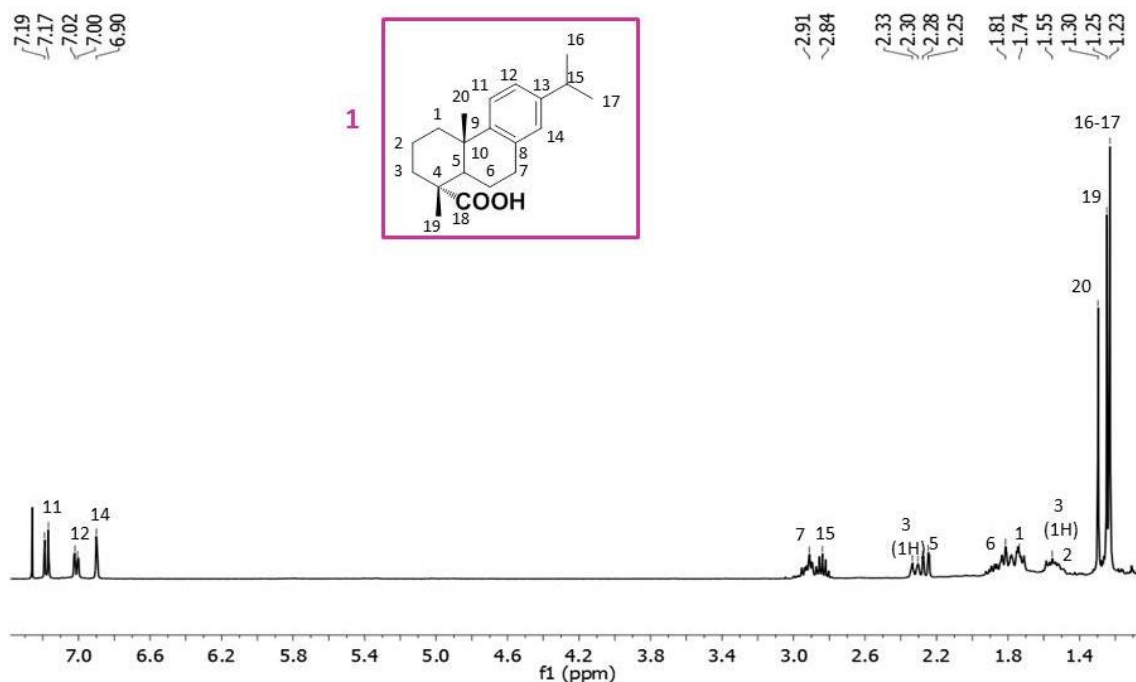


Figure 5:  $^1\text{H}$  NMR spectrum of fraction 1 (dehydroabietic acid) in  $\text{CDCl}_3$ , at room temperature.

The yield of fraction 2, isolated from the crude mixture, represents 20 wt%. This fraction contains several compounds. The four signals between 5.3 and 5.7 ppm on the  $^1\text{H}$  NMR spectrum of the fraction 2 are characteristic of abietic acid, levopimaric acid and palustric acid (Figure 6).<sup>5</sup>

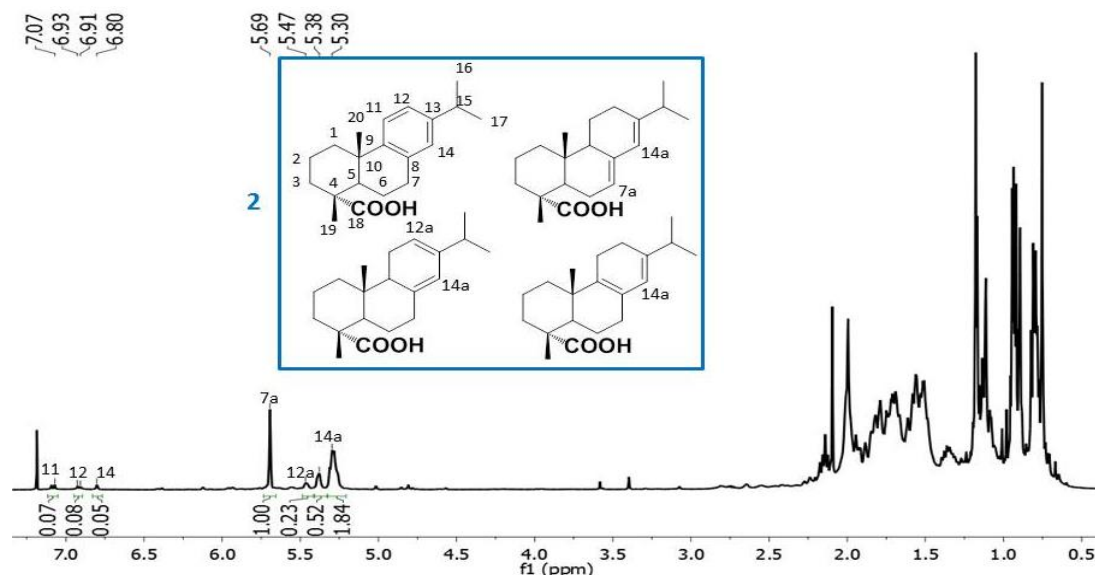


Figure 6:  $^1\text{H}$  NMR spectrum of fraction 2 (pre-isomerized abietic acid) in  $\text{CDCl}_3$ , at room temperature.

$^1\text{H}$  NMR spectrum of this mixture also presents peaks in the aromatic region, between 6.8 and 7.1 ppm, indicating some traces of dehydroabietic acid (around 3%). The ratio of the integration of the double bond protons shows that abietic acid represents 54% of the fraction. The structure of the last fraction 3 could not be completely determined through NMR spectroscopy (Figure 7).

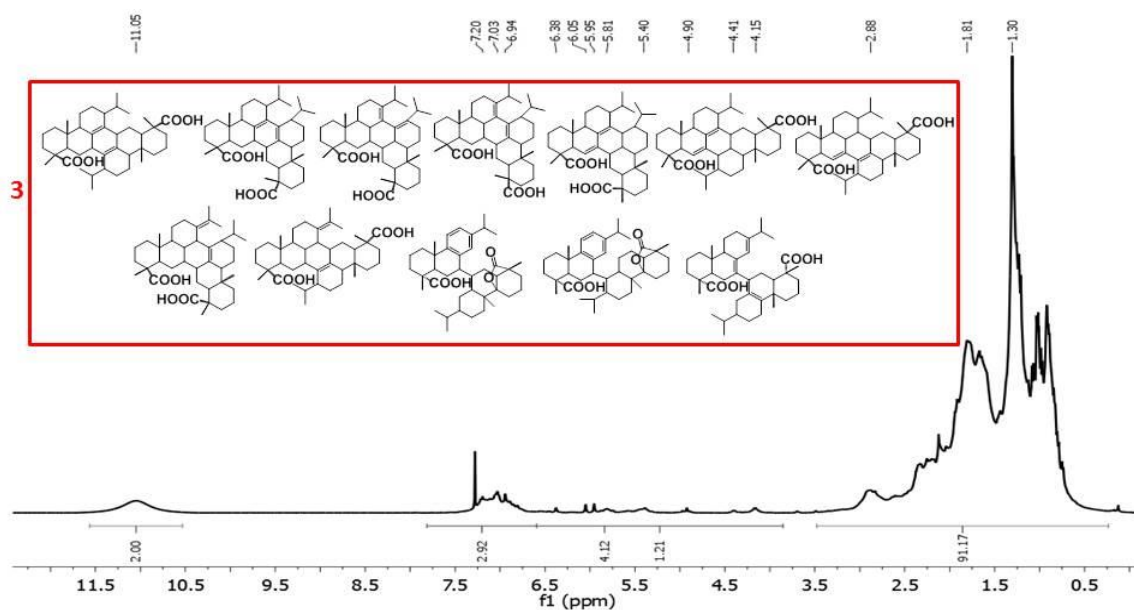
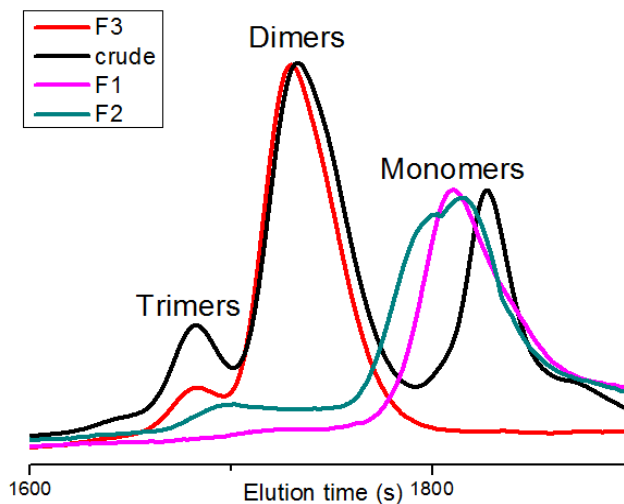


Figure 7:  $^1\text{H}$  NMR spectrum of fraction 3 (dimers + trimers of abietic acid) in  $\text{CDCl}_3$ , at room temperature.

However, the SEC analysis of this fraction shows the disappearance of the monomer peak and the presence of dimers and trimers (red curve Figure 8). An acid-base titration with a KOH solution coupled with SEC data allowed us to estimate the functionality in acidic functions, which is close to 2.0 for this fraction. The yield of dimers and trimers (fraction 3), isolated from the crude mixture represents 35 wt%.



**Figure 8:** SEC in THF analyses of (a) the fraction 1 (pink), (b) the fraction 2 (blue), (c) the fraction 3 (red) and (d) the crude mixture after dimerization (black), RI detection.

Finally, gas chromatography (GC), was performed in order to confirm the dimer purification efficiency (Figure 9). The appearance of peaks above 15 min enables the determination of the dimer region, which represents 98% of the total chromatogram area after purification by flash chromatography (Figure 9 (c)). Interestingly, this analysis reveals several peaks in the dimer region, indicating the formation of various isomers (see dimerization mechanism p 98 and discussion section I.2 p 105). In addition, it is noteworthy that trimers are not detected because of their high molar mass. The characteristics of the three fractions are summarized in Table 1.

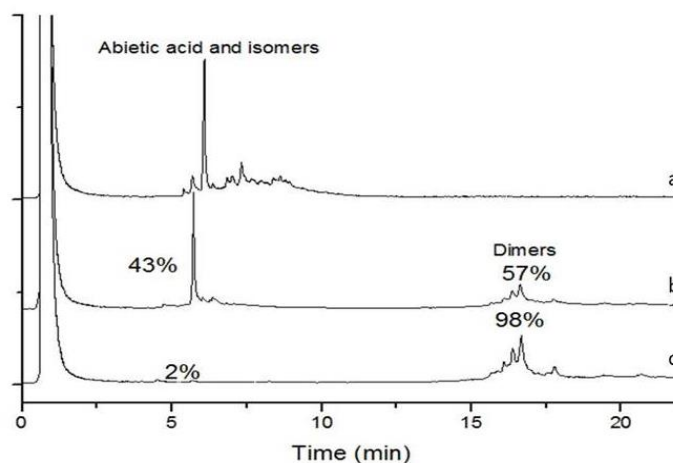


**Figure 9:** GC analyses of abietic acid (a), abietic acid dimer before and after purification (b and c).



**Table 1: Chemical properties of the initial abietic acid (a), the mixture obtained after dimerization (b) and the fractions obtained after Flash Chromatography (c).**

	Sample	%mol Monomer <sup>a</sup>	%mol Dimer <sup>a</sup>	%mol Trimer <sup>a</sup>	Acid functions (mmol/g) <sup>b</sup>	M (g/mol) <sup>a</sup>	F <sup>c</sup>
(a)	Abietic acid	74	26	0	3.1	380	1.2
(b)	Abietic acid after dimerisation	31	57	12	3.3	550	1.8
(c)	<b>Fraction 1</b> Dehydroabietic acid	100	0	0	3.3	300	1.0
	<b>Fraction 2</b> Pre-isomerized abietic acid	100	0	0	3.7	300	1.1
	<b>Fraction 3</b> Dimers + trimers	0	91	9	3.2	630	2.0

<sup>a</sup>Determined by SEC measurements with a RI detector, <sup>b</sup>Determined by KOH titration, <sup>c</sup>F, functionality, number of acid functions which can participate in the polymerization

In conclusion, the isolation of abietic acid dimers (still containing a small quantity of trimers) was manufactured from the crude mixture. An average functionality, F, in acidic functions close to 2, was achieved. Thus, fraction 3 was directly used in polycondensation.

However, before studying the polymerization of fraction 3, further investigation on the dimers structure is required.

### 3) Characterization of the abietic acid dimers

Several structures of the dimers have already been proposed in literature but none of them have been fully characterized (Figure 10) and the mechanism of the cationic dimer formation is not completely elucidated.

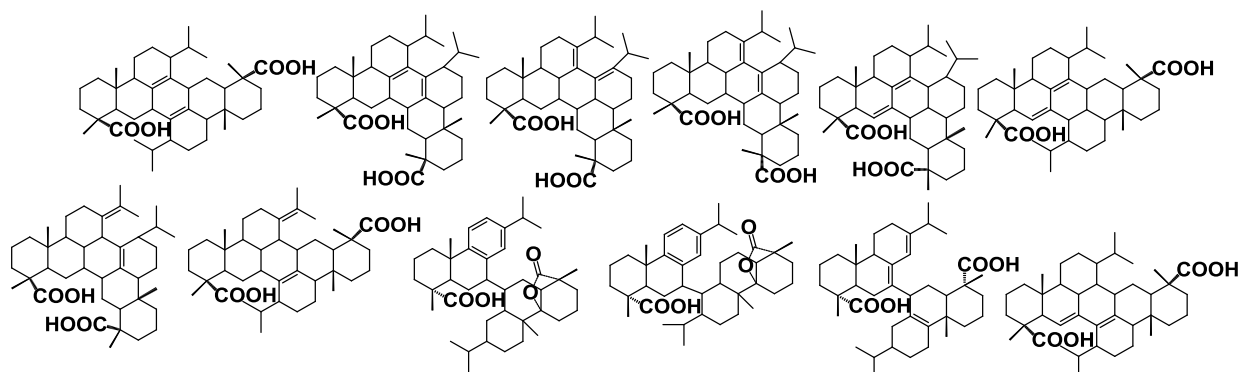


Figure 10: Abietic dimer structures suggested in literature by Brus<sup>6</sup>, Morillon<sup>7</sup>, Bardyshev<sup>8</sup> and Zinkel<sup>9</sup>.

The  $^1\text{H}$  NMR spectrum of fraction 3 (Figure 7) reveals some characteristics of the dimer structures. Indeed, some molecules present aromatic signals (6.7 - 7.3 ppm signals) and thus dehydroabietic moieties. The ratio of vinylic protons decreases compared to abietic acid (from 7.4 to around 5%) indicating that tetrasubstituted double bonds are present.

FTIR spectrum of the dimers shows a band at  $1772\text{ cm}^{-1}$  attributed to lactone and a band at  $1693\text{ cm}^{-1}$  characteristic of carboxylic acids (Figure 11). 30% of dimers bear a carbonyl group in the form of lactone whereas 70% are carboxylic acid.

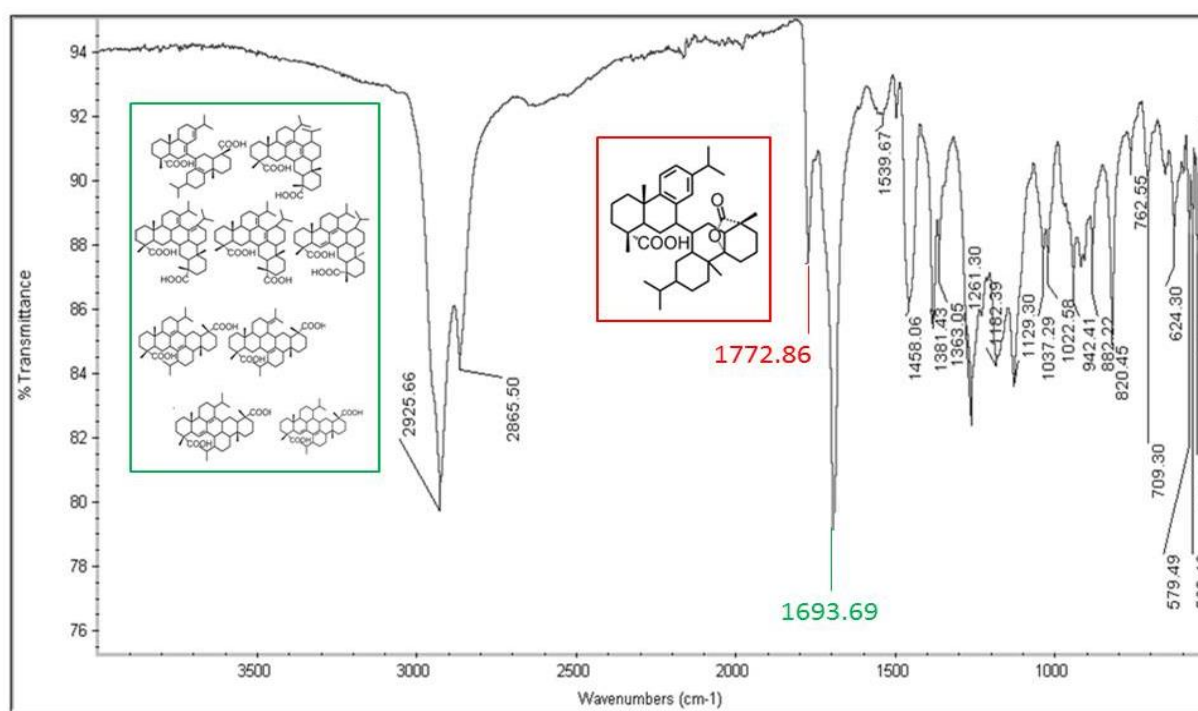


Figure 11: IR spectrum of fraction 3 (dimers + trimers of abietic acid).

## 2. Investigation of the dimerization mechanism of abietic acid

The presence of the three fractions provides information regarding to the mechanism of dimerization. For a better understanding, calculations of potential energies of the reaction intermediates were carried out by DFT calculations using Gaussian2009 with the B3LYP hybrid functional and a high quality 6-311++G(d) basis set taking into account  $\text{CHCl}_3$  as a continuous field. All possible intermediates and their energies, are presented on Figure 12.

The addition of a proton on the abietic acid double bond leads to two molecules A and B. The potential energy of B is 50 kJ/mol lower than the one of A. Hence, molecule B should be mainly considered formed in the reaction mechanism.

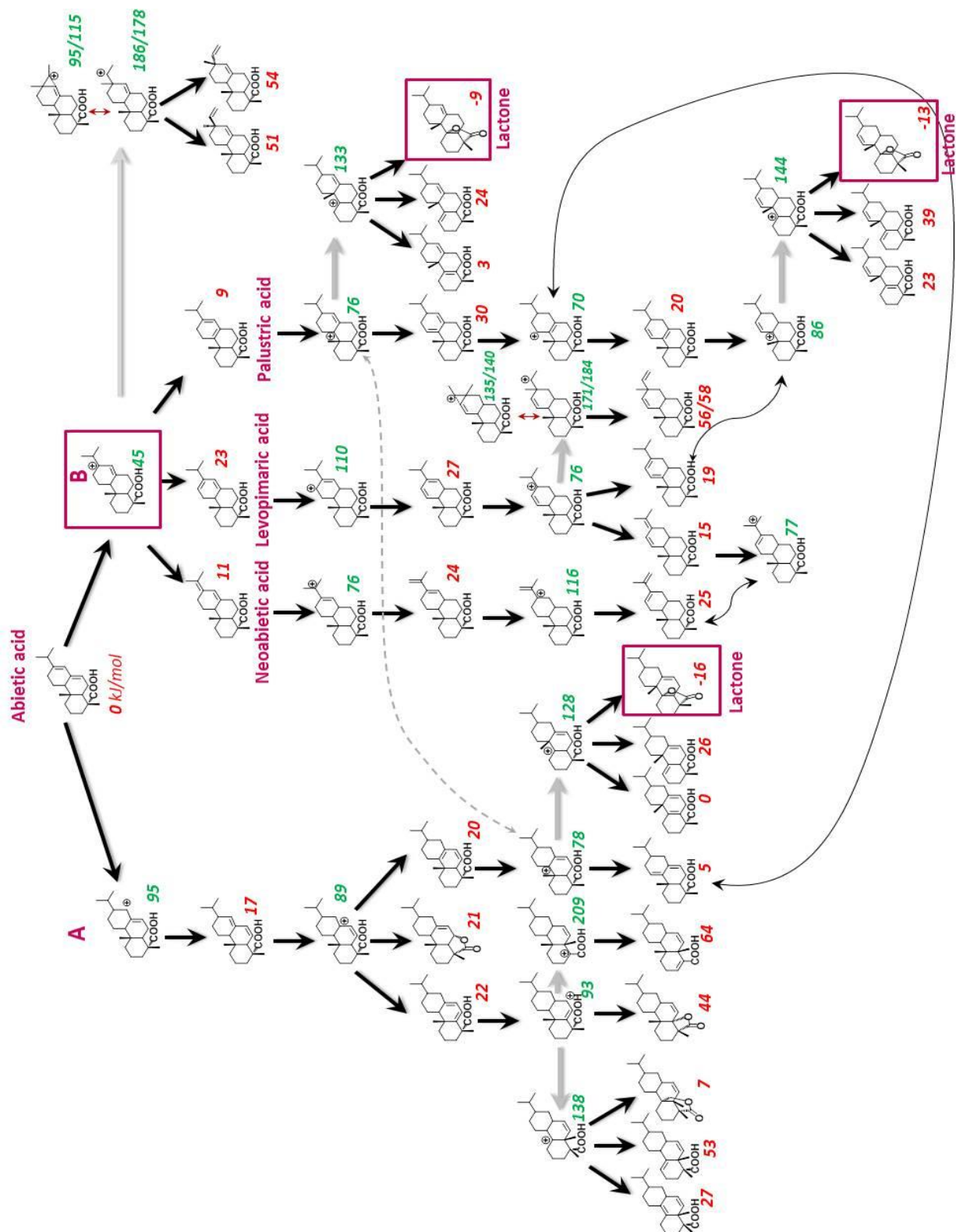


Figure 12: Reaction intermediates of abietic acid dimerization by proton addition/elimination reactions and their potential energy.

As previously described, during dimerization, some isomers of abietic acid, levopimaric and palustric acid, are produced and collected in fraction 2. Their formation is due to an elimination reaction on the molecule B. Surprisingly, potential energies predict the formation

of neoabietic acid too, which was not observed. This could be due to high energy transition state. Further proton addition and elimination reactions on these molecules yield a large number of possible intermediates. The multitude of the structures can explain the formation of several dimeric compounds. It is also worth to mention that lactones can be produced after sigmatropic rearrangement. With energies of -9 and -13 kJ/mol, the lactones correspond to potential energy minima of depth. These low values allow us to understand the non-negligible formation of dimers with lactone moieties.

However, these successive reactions of proton addition/elimination do not highlight the formation of dehydroabietic unit. The only way to obtain an aromatic product is to consider proton transfer reactions. This new step yields even other triunsaturated intermediates (Figure 13). Dehydroabietic acid, with a relative energy of -96 kJ/mol is very stable. Thus, during the reaction of sulfuric acid with abietic acid, three distinctive processes seem to take place: isomerization, dehydrogenation and the dimerization of abietic acid resulting in a complex mixture.

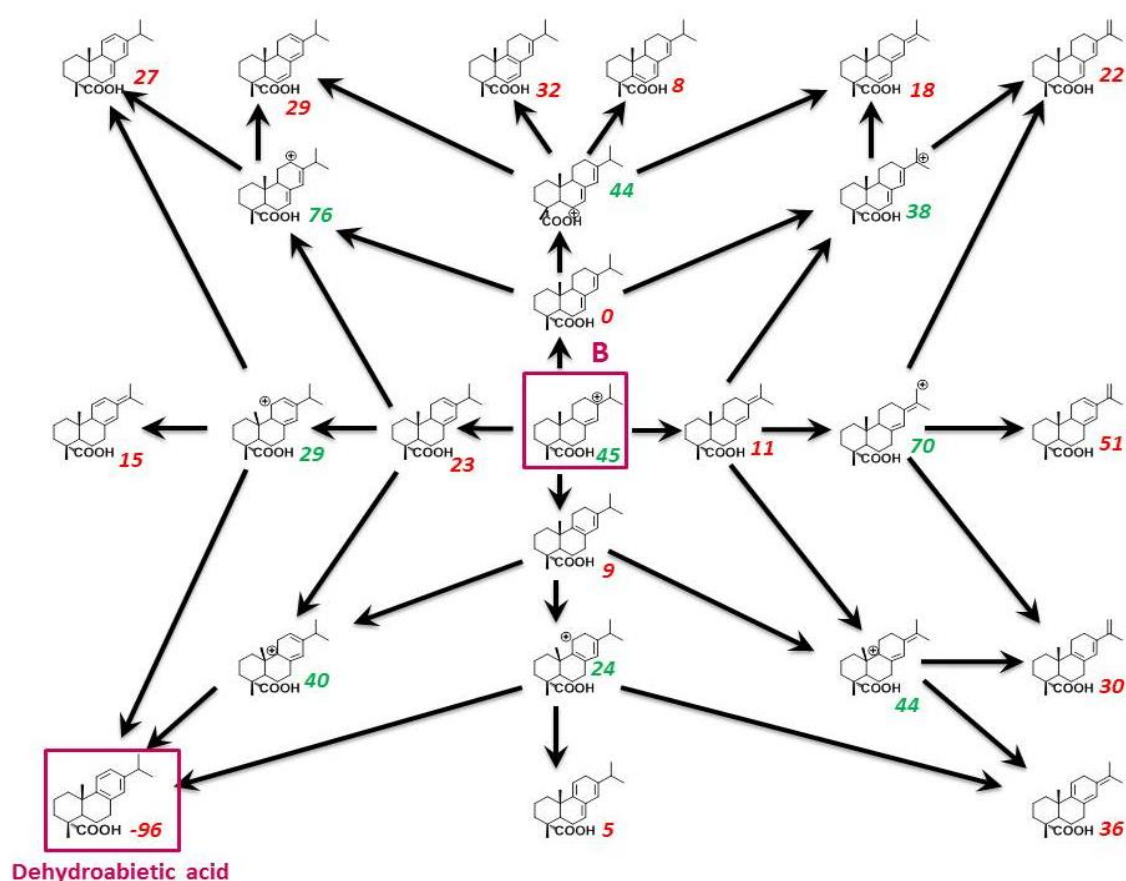


Figure 13: Reaction intermediates of abietic acid dimerization by proton transfer reactions/elimination and their potential energies.

The mechanisms described above can be applied to the dimer formation and may explain the multiplicity of the structures, including the trend to aromatization and lactonization in agreement with the IR and NMR analyses.

### 3. Optimization of the dimerization of abietic acid

This section is dedicated to the optimization of the reaction conditions in order to improve the dimerization selectivity while conserving a good yield. Several parameters such as monomer purity, time, temperature and catalysts are studied.

#### 1) Influence of the monomer purity on the dimerization of abietic acid

In their study, Sinclair and coll. highlighted the fact that the dimerization yield depends on the composition of the starting material.<sup>3</sup> We carried out the same study and also investigated the influence of starting material on the dimer selectivity. Three commercial abietic acids: abietic acid purchased at Sigma Aldrich with an indicated purity over 85% (a), pre-isomerized abietic acid (fraction 2) (b), and abietic acid extracted from gum (c) and tall oil (d) rosin were analyzed. The composition in isomers of the different materials was determined by integration of the vinylic protons on the <sup>1</sup>H NMR spectrum (Figure 14)) and is described in Table 2. Abietic acid commercially available at Sigma Aldrich (a) is composed at 95% of abietic acid and 5% of dehydroabietic acid. As previously explained, pre-isomerized abietic acid (b) contains 54% of abietic acid and 43% of levopimaric and palustric acids. Abietic acid extracted from gum rosin includes 19% of neoabietic acid while the one extracted from tall oil rosin is composed of 45% of dehydroabietic acid.<sup>5</sup>

**Table 2 : Isomer composition of the starting mixtures containing abietic acids determined by integration of the vinylic protons on the <sup>1</sup>H NMR spectra: (a) abietic acid purchased at Sigma Aldrich, (b) pre-isomerized abietic acid, (c) raw abietic acid from pine resin distillation, (d) raw abietic acid from tall oil.**

Isomers	%			
	a	b	c	d
Abietic acid	95	54	78	55
Dehydroabietic acid	5	3	3	45
Levopimaric/palustric acid	0	43	0	0
Neoabietic	0	0	19	0

These four abietic acid mixtures were dimerized using the conditions previously described. The compositions of the resulting mixtures were analyzed by SEC (Figure 14). Raw abietic acids, from the distillation of pine resin (c) or tall oil (d), respectively lead to 35% and 37% of





representing 43%), leads to higher dimer conversion (75%) than 85% pure commercial abietic acid (a). Furthermore, only 5% of trimers are formed, compared to 12% from 85% pure abietic acid. Thus, in this case, a better selectivity toward dimerization vs oligomerization is observed also.

The dimers synthesized from the four different starting materials were analyzed by GC in the expectation that some abietic acids will show better selectivity. Raw abietic acids from pine resin and tall oil distillation (c) and (d) show the lowest selectivity with the presence of 8 main peaks on the GC chromatogram. 85% pure abietic acid with 2 main peaks and 3 with lowest intensities presents the best selectivity (Figure 15). Thus, the abietic acid purity has an important impact on the dimer yield and a lower influence on the selectivity of dimerization.

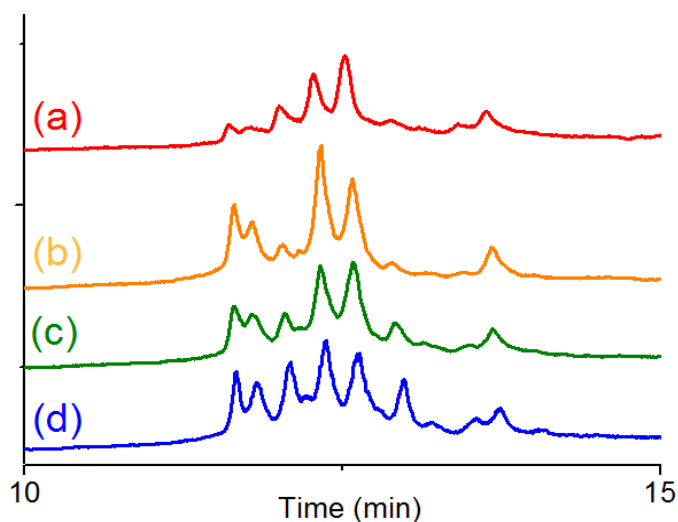


**Figure 15: GC analyses of the dimers synthesized from different starting abietic acids: 85% pure abietic acid (a), pre-isomerized abietic acid (b), raw abietic acid from pine resin distillation (c), raw abietic acid from tall oil distillation (d).**

## 2) Experimental condition screening of abietic acid dimerization

Further, the dimerization process was studied using different conditions, such as temperature and acid catalysts with the aim to reach higher selectivity. The dimerization conversion and number of dimer structures was determined by GC (Table 3). The dimerization was performed in the presence of sulfuric acid, phosphoric acid and para-toluenesulfonic acids. The highest yields of dimers (35-60%) were reached using sulfuric acid, between 8 to 13 structures are observed. Employing this catalyst, varying time and temperature of the reaction, did not improve the selectivity (Figure 16 (a)). However, a

modification in the relative dimer peak intensities was observed indicating that a kinetic product is formed followed by a thermodynamic compound.

Since Gigante and coll. observed the crystallization of one of the dimer when the dimerization was catalyzed by PTSA, samples with different amounts of PTSA were prepared and analyzed (Figure 16 (b)).<sup>10</sup> The dimer yield, around 3%, was very low, but with the formation of 3 structures under specific conditions; the selectivity being improved compared to sulfuric acid. The best amount of PTSA/abietic acid is 1/1 molar ratio. The dimerization selectivity depends on reaction time. Indeed, after 5 h reaction time, the dimer with a retention time of 16.5 min is majority but after one week of reaction, the one with a retention time at 17.8 min becomes majority.

Finally, for both sulfuric acid and PTSA, increasing the temperature to 45 °C improves the selectivity. In conclusion, neither the Lewis acid catalyst nor the temperature enable the high yield/high selectivity dimerization of abietic acid. The best results in terms of high yield/high selectivity were obtained employing the Sinclair method, sulfuric acid catalyst, at 45 °C for 5 h. This method will be used for the rest of our study.

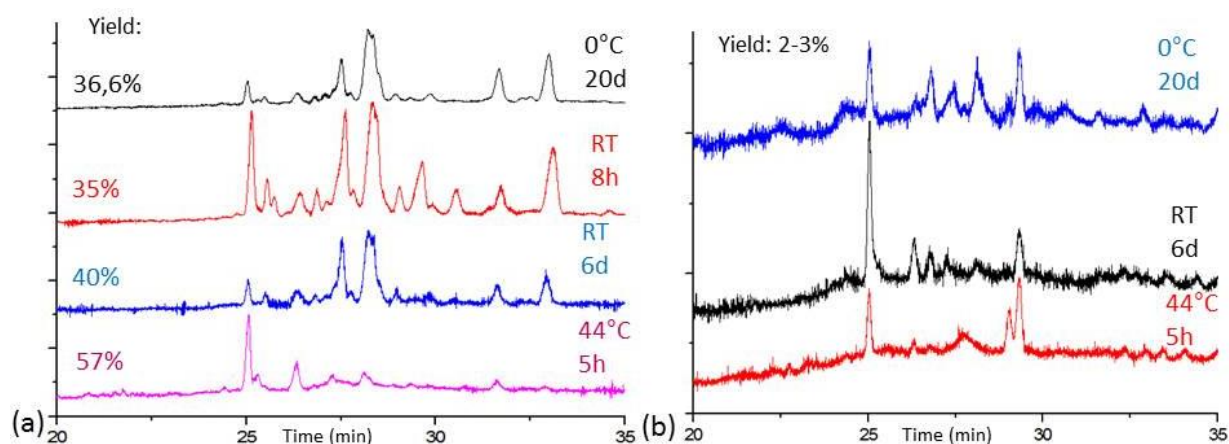


Figure 16: GC analyses after dimerization catalyzed by H<sub>2</sub>SO<sub>4</sub> (a) and PTSA (b).

### Conclusion:

Abietic acid was dimerized employing sulfuric acid as catalyst, at 45 °C for 5 h. The resulting crude mixture was separated in three fractions. The first fraction contained dehydroabietic acid, with a good purity. For instance, this compound could be used for synthesis of polymers with abietic acid moiety as pendant group. The second fraction which represents 20 wt% of the mixture contains abietic acid, levopimaric and palustric acids. Further dimerization of this fraction, under the aforementioned conditions, reached higher yield than commercial abietic acid. This fraction can thus be used for dimer synthesis. However, the main focus of this part



is assigned to the isolation of abietic acid dimers (and small amount of trimers) from the crude mixture. This final mixture, namely fraction 3, with a functionality in acidic function of 2, is prone for polymerization. The investigation of the dimer structures revealed the presence of several compounds, including lactones. The screening of reaction conditions did not lead to the selective formation of one dimer in high yield. Thus, in the next section, fraction 3 produced employing the Sinclair method was directly polymerized.

**Table 3: Results of the dimerization of abietic acid: number of dimers and yield depending on experimental conditions**

Catalyst (molar equivalent vs carboxylic acid function)	Time	Temperature	Number of dimers	Yield
H <sub>2</sub> SO <sub>4</sub> (100%)	5 h	45 °C	8*	57%
H <sub>2</sub> SO <sub>4</sub> (100%)	8 h	RT	13	35%
H <sub>2</sub> SO <sub>4</sub> (100%)	6 d	RT	10 <sup>+</sup>	40%
H <sub>2</sub> SO <sub>4</sub> (100%)	20 d	0 °C	10	37%
H <sub>3</sub> PO <sub>4</sub> (100%)	5 h	45 °C	5*	10%
PTSA (100%)	20 d	0 °C	7	<5%
PTSA (100%)	5 h	45 °C	5 <sup>+</sup>	<5%
PTSA (100%)	3 h	RT	3*	<5%
PTSA (100%)	1 d	RT	4*	<5%
PTSA (100%)	6 d	RT	5*	<5%
PTSA (100%)	13 d	RT	13	<5%
PTSA (200%)	5 h	RT	8	<5%
PTSA (200%)	6 d	RT	9	<5%
PTSA (200%)	24 d	RT	11 <sup>+</sup>	<5%
PTSA (20%)	5 h	RT	8*	<5%
PTSA (20%)	6 d	RT	8*	<5%
PTSA (20%)	24 d	RT	14	<5%
PTSA (1%)	5 h	RT	nothing	<5%
PTSA (1%)	6 d	RT	7	<5%
PTSA (1%)	24 d	RT	15	<5%

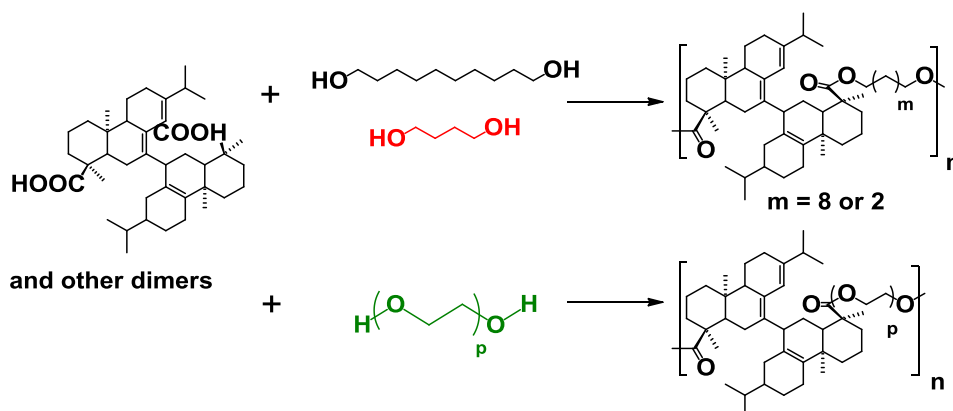
\*) 1 main compound, +) 2 or 3 main compounds

### III Synthesis of polyesters from abietic acid dimers *via* direct polycondensation

#### 1. Polycondensation of abietic acid dimers

With a functionality of 2 in acidic functions, the fraction mainly composed of abietic acid dimers, has been polymerized. Abietic acid dimers, or their methyl esters, were polycondensated with different aliphatic diols (Scheme 2). A screening for the best catalyst was carried out. The objective was to synthesize copolyesters of abietic acid dimers and

several vegetable oil derivatives. First polymerization tests were performed using commercial 1,10-decanediol, 1,4-butanediol and PEG 600 as co-monomers.



**Scheme 2: Synthesis of polyesters from abietic acid dimers and decanediol, butanediol, PEG 600.**

All the syntheses were performed under nitrogen flow or under vacuum in order to remove the water or methanol released during the reaction (Table 4).

None of the polymerizations yielded high molar mass polymers. Only oligomers with low dispersity were formed (Table 4). The best results were obtained with titanium (IV) butoxide catalyst. Indeed, molar mass of 8 800 g/mol was achieved for the polymers synthesized by copolymerization of abietic acid dimers with 1,10-decanediol (**P1**) and 5 400 g/mol for the one with PEG600 (**P2**). Such molar masses correspond to degrees of polymerization of 13 and 11, respectively. The synthesis of abietic dimethyl ester dimers and their polymerization by transesterification with the same diols were carried out but did not improve the molar mass of the obtained polymers. The low concentration of abietic acid isomers (2% determined by GC determination) cannot explain the low reactivity towards polycondensation. Some other explanations linked to the dimer structure itself, could be proposed and are discussed below.

**Table 4: SEC data of polycondensation reactions of abietic acid diacid dimer or diester dimer with decanediol, butanediol or PEG600 using different catalysts.**

Polymer	Diol	Catalyst (%mol)	$\bar{M}_n^a$ (kg/mol)	$\bar{M}_w^a$ (kg/mol)	$\bar{D}$	$\bar{DP}_n$
<b>P1</b>	<b>Decanediol</b>	<b>TiOBu<sub>4</sub> (1%)</b>	<b>8.8</b>	<b>10.3</b>	<b>1.2</b>	<b>13</b>
<b>P2</b>	<b>PEG600</b>	<b>TiOBu<sub>4</sub> (1%)</b>	<b>5.4</b>	<b>13.0</b>	<b>2.4</b>	<b>11</b>
P3	Butanediol	TiOBu <sub>4</sub> (1%)	2.4	2.5	1.1	4
P4	PEG600	Zn(OAc) <sub>2</sub> (1%)	2.3	2.3	1.0	2
P5	PEG600	SbO <sub>3</sub> (1%)	1.1	1.2	1.1	1
P6	PEG600	PTSA	1.4	1.5	1.1	1

<sup>a</sup>Determined by SEC in THF, RI DETECTOR

First, the lactone moiety may have a negative impact on the polymerization process. During polycondensation, the opening of the lactone by the diol results in the formation of an ester and a hydroxyl groups (Figure 17). The latter hydroxyl group can react with the acidic functions thus modifying the stoichiometry, which is crucial in polycondensation reactions. This scenario may explain the formation of oligomers instead of high molar mass polymers.

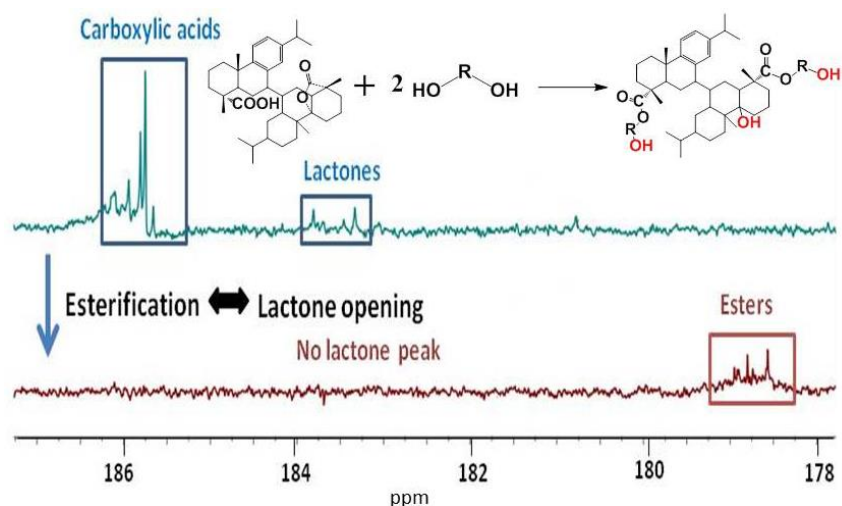


Figure 17: Carbonyl region  $^{13}\text{C}$  NMR spectra of abietic acid dimers before (blue) and after esterification (red) in  $\text{CDCl}_3$ , at room temperature.

In addition, the steric hindrance of some abietic acid dimer structures might reduce their reactivity. For instance, the isomers displayed in Figure 18 (a) might be more reactive for polymerization than the ones shown in Figure 18 (b) due to the steric hindrance around the carboxylic acid moieties.

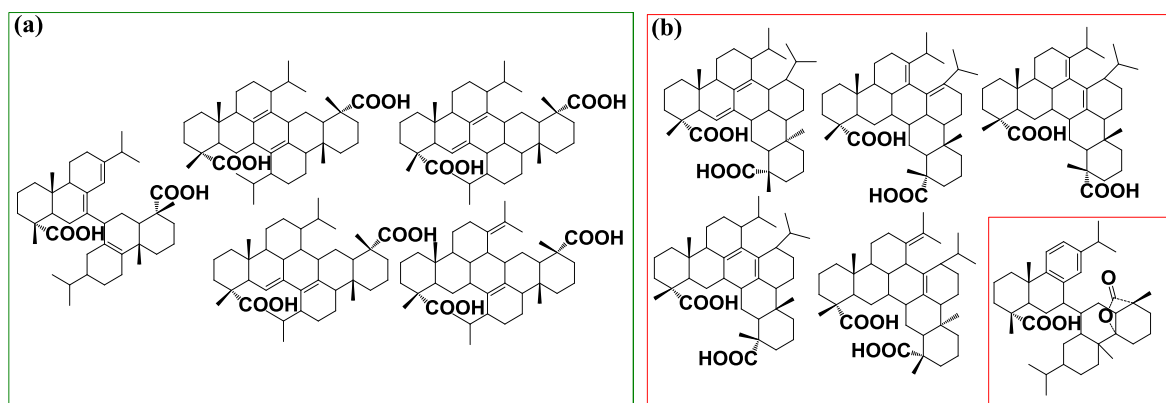
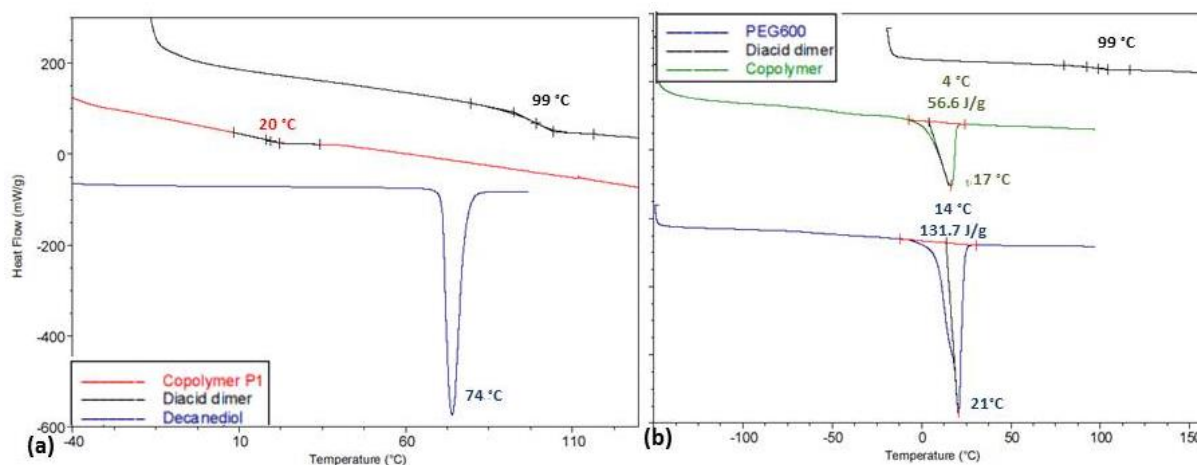


Figure 18: Structure of abietic acid dimers: less steric hindered structures (a), very steric hindered molecules (b).

## 2. Thermomechanical properties of abietic acid dimer copolymers

Despite the low molar masses of the abietic acid-based polyesters, the thermomechanical properties of the two highest molar mass polymers, **P1** and **P2** (Table 4), synthesized using 1,10-decanediol and PEG600 as co-monomers, respectively, were investigated by DSC and TGA. **P1** is an amorphous polyester with a glass transition temperature of 19.5 °C. **P2** is a semi-crystalline polyester with a melting temperature of 16.5 °C (Figure 19). The semi-crystallinity is attributed to the longest aliphatic chain of PEG 600 than 1,10-decanediol.



**Figure 19: DSC analyses of copolyesters from abietic acid dimers and 1,10-decanediol (a), from abietic acid dimers and PEG600 (b).**

The melting temperature of **P2** is lower than the melting temperature of PEG 600 (16.5 °C versus 20.7 °C) due to the cycloaliphatic structure of abietic acid dimers. The incorporation of this structure also leads to the decrease of the melting enthalpy from 131.7 for PEG 600 to 56.6 J/g for **P2**.

The 5% weight losses of **P1** and **P2** occur respectively at 227 °C and 197 °C (Figure 20). **P2** decomposition temperature is lower due to the longer aliphatic chains of PEG 600 than 1,10-decanediol. The thermal stability of these polymers remains low, probably because of the low molar mass of the polymers.

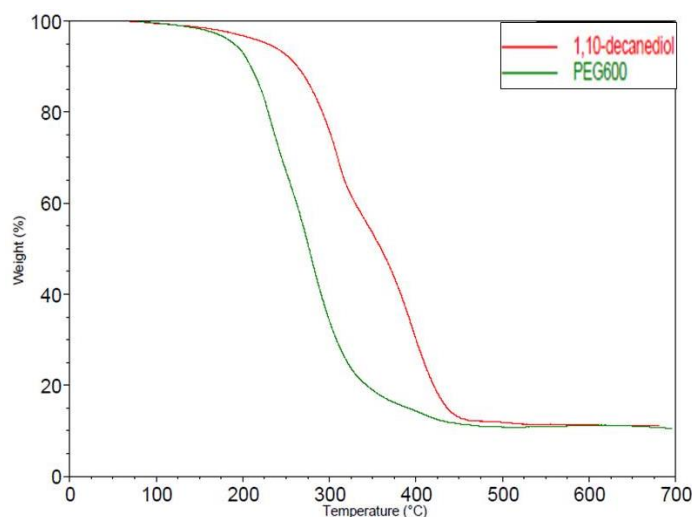


Figure 20: TGA analyses of copolyesters from abietic acid dimers and 1,10-decanediol and PEG600.

### Conclusion:

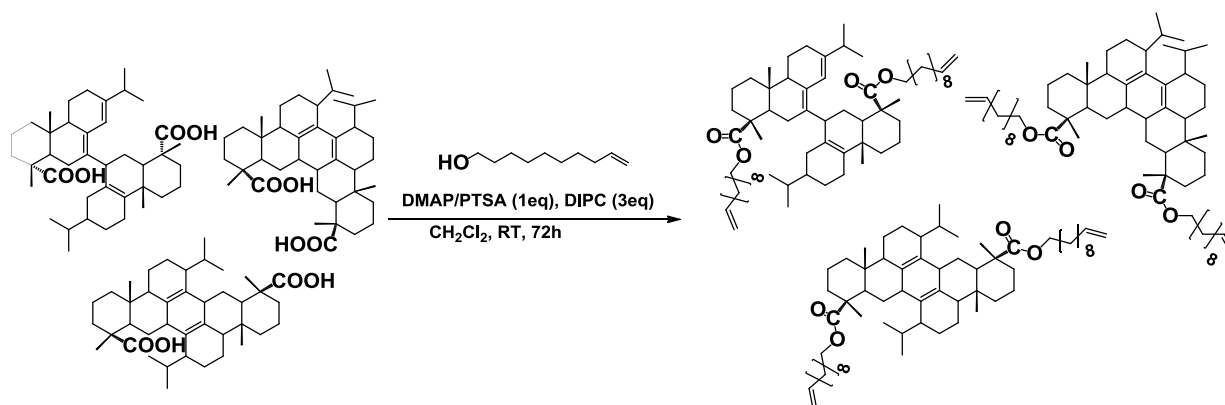
The molar masses of the copolyesters synthesized *via* direct polycondensation of abietic acid dimers and aliphatic diols is low, probably due to the presence of lactone moieties and steric hindered dimers. However, the thermal properties of the polymers from rigid and biobased abietic acid dimers are promising. Therefore, further efforts on an alternative polymerization method were carried out.

## IV Synthesis of unsaturated polyester *via* ADMET polymerization

In order to decrease the steric hindrance next to the reactive acidic functions and to get around the problem of the hydroxyl group from the lactone opening, abietic acid dimers (fraction 3) was esterified with undecenol, a vegetable oil derivative. The resulting bis-unsaturated dimers were then (co)polymerized with undecenyl undecenoate by ADMET polymerization which revealed to be an efficient polymerization method.<sup>11,12</sup>

### 1. Bis-unsaturated abietic ester dimer synthesis and characterization

The esterification of the dimers was performed under mild conditions using PTSA/DMAP catalyst (Scheme 3). These conditions have already been used for the esterification of Polygral (a mixture of abietic acid, dimers and trimers of abietic acid).<sup>13</sup>



**Scheme 3: Esterification of abietic acid dimers with undecenol yielding bis-unsaturated abietic ester dimers (example on few structures).**

The esterification reaction between the diacid and the unsaturated alcohol is confirmed by  $^{13}\text{C}$  NMR (Figure 21). The disappearance of signals assigned to the carboxylic acid function at 185 ppm and to the lactone between 183 and 184 ppm as well as the emergence of new peaks at 178.6 ppm and 65 ppm, respectively assigned to the ester bond and its  $\alpha$ -carbon, demonstrate the completion of the esterification. First, undecenol was introduced in excess to ensure the complete conversion into the diesters. After the reaction, the unreacted undecenol was removed *via* silica column chromatography using cyclohexane/ethyl acetate as eluent. The efficiency of the purification is revealed on the  $^{13}\text{C}$  NMR spectrum of **(2)** by the absence of peak at 63 ppm attributed to methylene group close to the hydroxyl moiety of undecenol. Furthermore, the spectrum of the final product presents also the peak characteristic of the terminal double bonds at 139 ppm and 114 ppm.

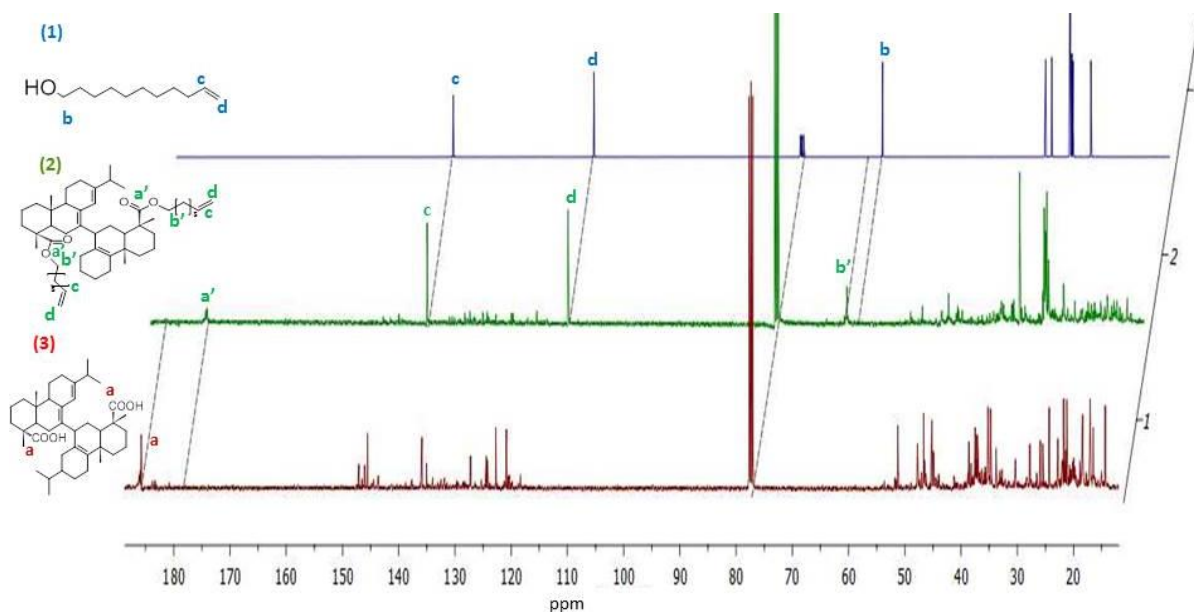


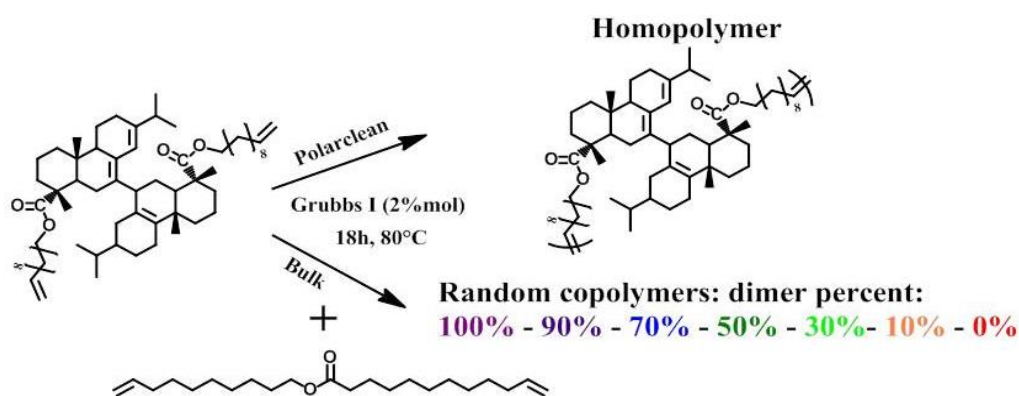
**Figure 21:  $^{13}\text{C}$  NMR spectra of undecenol (1), bis-unsaturated abietic ester dimers (2) and abietic acid dimers (3) in  $\text{CDCl}_3$ .**

The main advantage of this modification is that all the dimers, regardless of their structure, bear terminal pendant double bonds which should possess the same reactivity towards ADMET polymerization.

## 2. ADMET polymerization of bis-unsaturated abietic ester dimers

### 1) Chemical structure and molar mass of the unsaturated polyesters

The bis-unsaturated dimers synthesized previously were polymerized by ADMET polymerization. ADMET polymerization is a step-growth polymerisation driven by the release of a condensate, usually ethylene. ADMET is typically performed on  $\alpha,\omega$ -dienes to produce well-defined polymers with unsaturated backbones. Grubbs 1st generation metathesis catalyst was chosen to prevent any double bond isomerization. ADMET polymerization was performed either in bulk or in solvent, depending on the starting material. On the one hand, homopolymerization of the bis-unsaturated abietic ester dimers was performed for 18 h at 80 °C, under vacuum, in *Polarclean* solvent because abietic acid dimers possess a too high viscosity to perform the homopolymerization in bulk. *Polarclean* solvent was selected in this study because it shows a high boiling point and is known to be compatible with ADMET methodology.<sup>11</sup> On the other hand, the copolymerizations were performed under the same conditions in bulk, because the undecenyl undecenoate enables a reduction of the medium viscosity and allows stirring (Scheme 4). Undecenyl undecenoate was added in different proportions, gradually from 10 mol% to 90 mol%.



Scheme 4: Polymerization of bis-unsaturated abietic ester dimers (only one dimer form has been represented).

The <sup>1</sup>H NMR analyses of the copolymers were performed to follow the completion of the reaction and to analyze the composition of the copolymers (Figure 22). For each polymerization, the completion of the reaction was checked by the disappearance of the



terminal double bond signals at 4.9 and 5.7 ppm and the appearance of a peak characteristic to internal double bonds at 5.3 ppm. The copolymer composition was determined by following the modification of the integration of the signal at 0.9 ppm, assigned to abietic acid dimer methylene protons. The experimental copolymer composition is slightly different than the theoretical one with respect to the abietic acid dimer incorporation. The small gap between feed and incorporation ratio may be explained by a difference of reactivity of the two comonomers probably due to the steric hindrance of the abietic acid dimer.

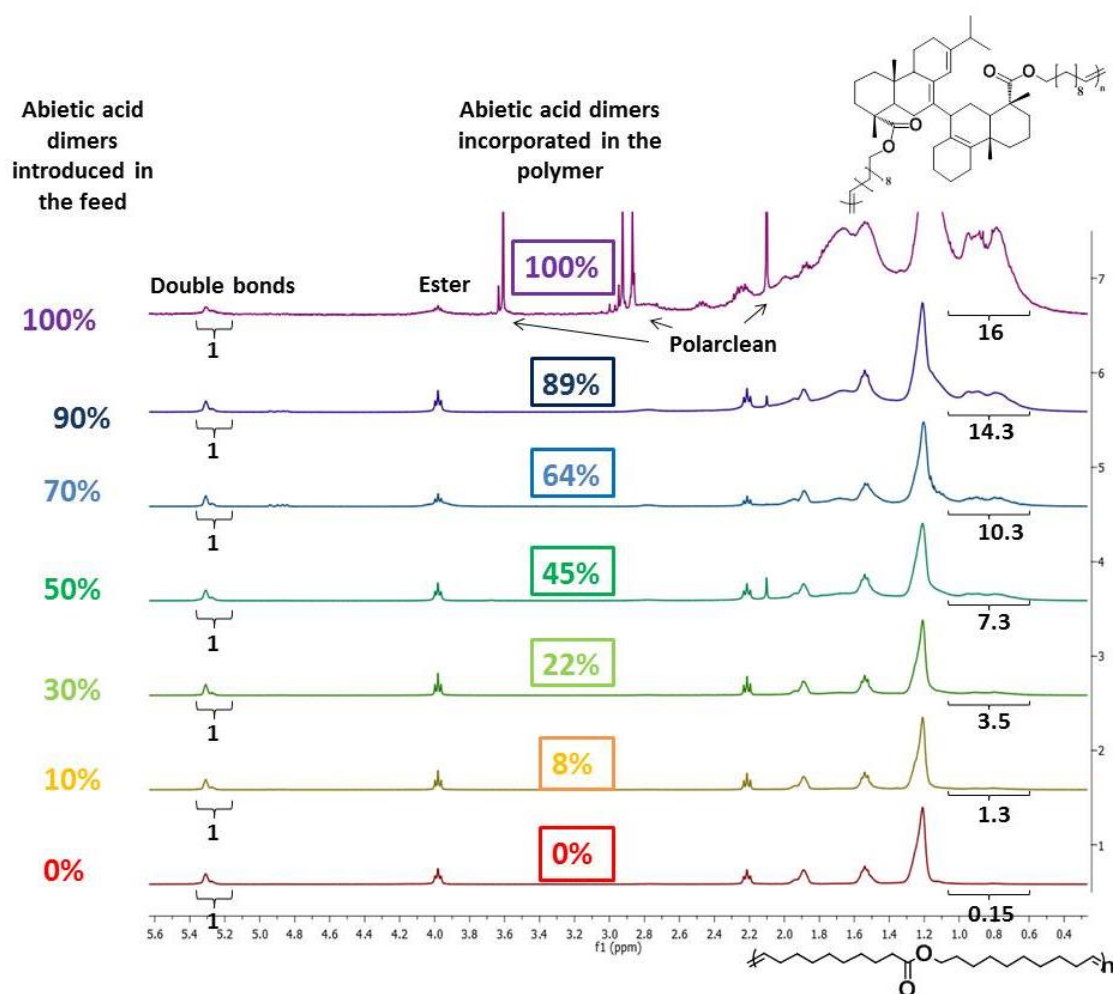


**Figure 22:**  $^1\text{H}$  NMR spectra of the ADMET polymers, calculation of bis-unsaturated abietic ester dimer/Undecenyl undecenoate incorporation in  $\text{CDCl}_3$  at room temperature (100% abietic acid dimer derivative, 0% = 100% undecenylundecenoate).

The molar masses of the (co)polymers prepared by ADMET were determined by SEC in THF. Data are summarized in Table 5.



**Table 5: SEC, DSC and TGA results of bis-unsaturated abietic ester dimers/undecenyl undecenoate copolymers after ADMET polymerization (percentages of bis-unsaturated abietic ester dimer are indicated).**

Entry	Abietic acid dimer Feed (mol%)	Abietic acid dimer incorporated (mol%) <sup>a</sup>	$\bar{M}_n$ <sup>b</sup> (kg/mol)	$\mathcal{D}$	Tm <sup>c</sup> (°C)	$\Delta H$ <sup>c</sup> (J/g)	Td5% <sup>e</sup> (°C)
1	100	100	3.5	3.7	No Tm, Tg = 102°C <sup>d</sup>		310
2	90	89	3.4	3.2	51	27	308
3	70	64	4.1	2.8	50	25	325
4	50	45	4.8	4	51	47	339
5	30	22	19	1.7	43	51	342
6	10	8	29	1.6	45	52	337
7	0	0	42	2.0	55	86	382

<sup>a</sup>Determined by <sup>1</sup>H NMR, <sup>b</sup>determined from SEC in THF, <sup>c</sup>determined by DSC, <sup>d</sup>determined by DMA, <sup>e</sup>determined by TGA

The polymer molar masses decrease with increasing abietic acid dimer content can be explained by steric hindrance. Below 50 mol% of bis-unsaturated abietic ester dimer in the monomer feed, the polymer molar mass ranged from 19 to 29 kg/mol with a dispersity of around 2 (Figure 23, Table 5 entries 5, 6). For an equal feed ratio of the two comonomers, the SEC trace shows the formation of a second population eluted at a higher elution time. For higher content of bis-unsaturated ester dimer, this second population with a molar mass ranging from 3.5 to 4.8 kg/mol and a dispersity around 3, becomes the majority. The dispersity increase may be attributed to the incorporation of more trimers, representing 10% of the starting mixture yielding branching on the polymer backbone. This increase may also be explained by a demixtion due to two non-miscible types of chains.

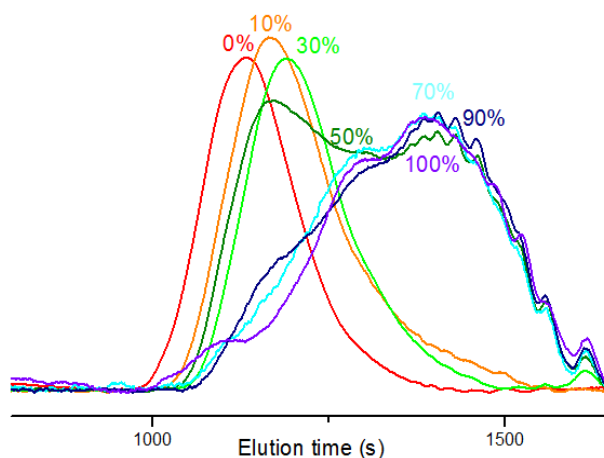


**Figure 23: SEC traces of bis-unsaturated abietic ester dimer/undecenyl undecenoate copolymers after ADMET polymerization (percentages of bis-unsaturated abietic ester dimer are indicated), RI detection.**

## 2) Thermomechanical properties of the unsaturated polyesters

DSC analyses of the copolymers were performed (Figure 24). The 100% vegetable oil-based polymer displays a melting temperature ( $T_m$ ) at 55 °C. In agreement with SEC results, DSC analyses reveal a different feature above 50 mol% of abietic acid dimers incorporated. Indeed, below this threshold, the melting temperature of the copolymers decreases progressively from 55 °C to 43 °C (entries 5-7 Table 5) in agreement with an increasing incorporation of bis-unsaturated abietic ester dimers into the copolymer, as proved by the continuous decrease of the  $\Delta H$  values. Above this ratio, the melting temperatures of the copolymers remain identical to the one of the homopolymer obtained from 100% vegetable oil (entries 1-4 Table 5). This feature may be explained by the presence of two non-miscible types of chains, either containing low amount or high amount of bis-unsaturated abietic ester dimer, in accordance with the SEC trace.

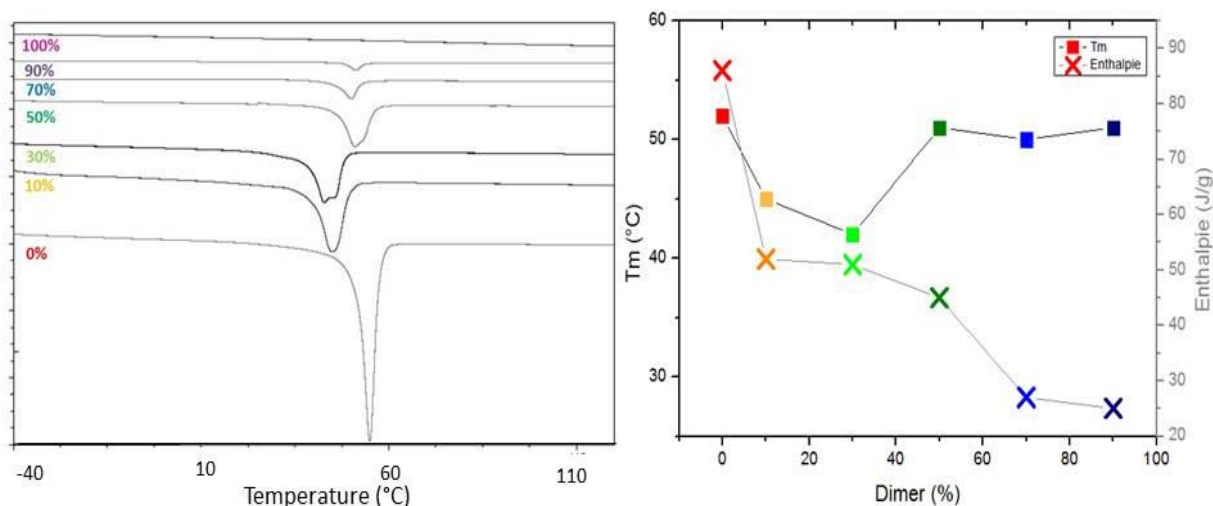


Figure 24 : DSC thermograms (second heating cycle) (percentage of bis-unsaturated abietic acid dimer).

The crystalline structure of copolymers with 90 and 30% of abietic acid dimers was observed with a polarized microscope (Figure 25) and showed the presence of spherulites in both cases.

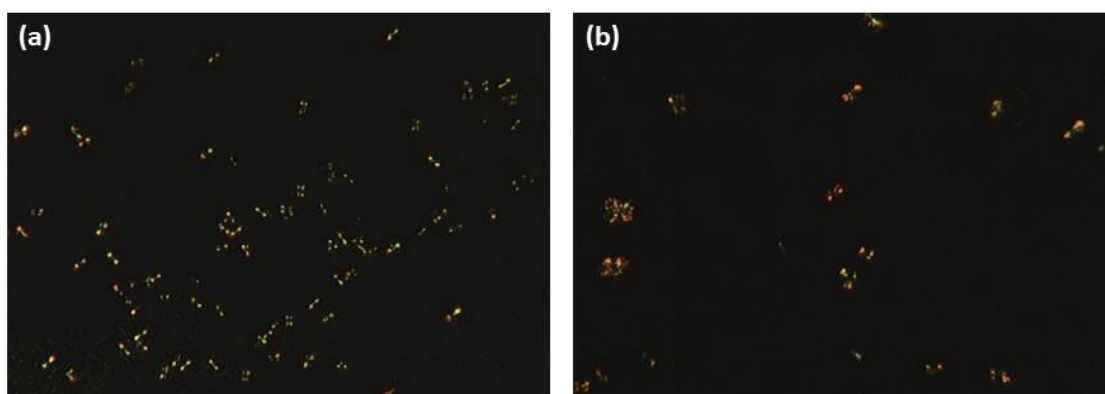
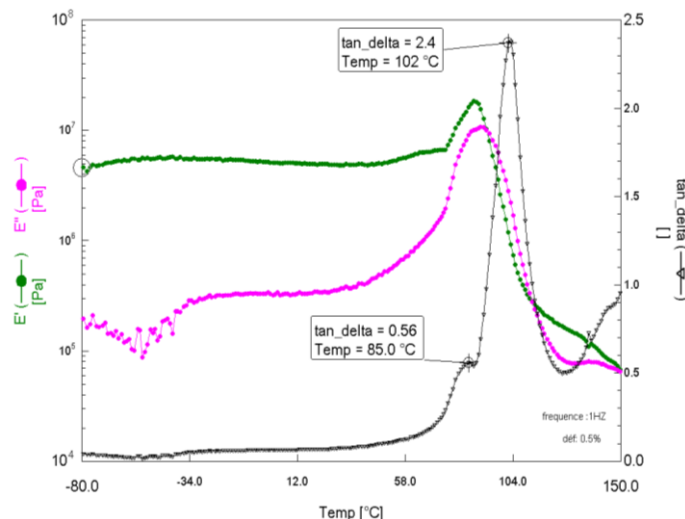


Figure 25: Crystalline structure of copolymers containing (a) 30% and 90% (b) of abietic acid dimers. Photo taken by polarized microscope

The homopolymer of abietic acid dimer neither shows any melting nor glass transition temperature on DSC analyses. Thus, DMA analysis was carried out in order to investigate the thermomechanical properties of the homopolymer. One Tg could be observed at 102 °C (Figure 26).



**Figure 26: DMA analysis of the homopolymer bis-unsaturated abietic ester dimer. Using compression test at 1 Hz from -80°C to 150°C at 10 K/min.**

Finally, TGA shows that all the polymers degrade over 300°C. The first weight loss of the homopolymer of abietic acid is attributed to the evaporation of *Polarclean* solvent, which has a boiling point of 270 °C. Higher temperatures are assigned to higher molar mass polymers (Figure 27 and Table 5).

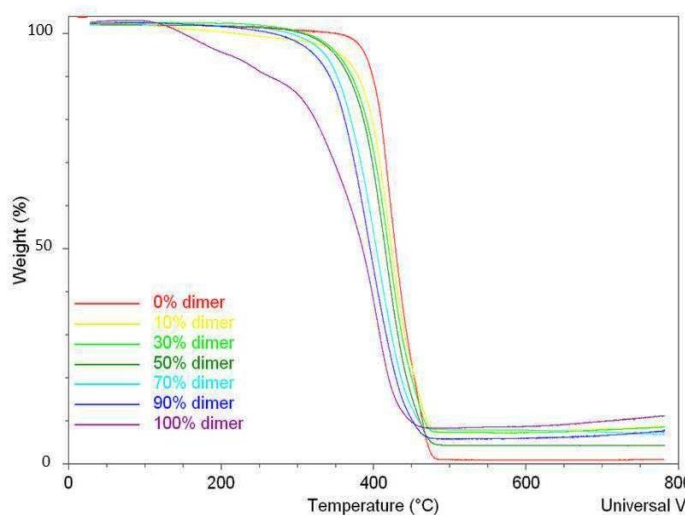


**Figure 27: TGA curves of bis-unsaturated abietic ester dimer/undecenyl undecenoate copolymers after ADMET polymerization (percentages of bis-unsaturated abietic ester dimer are indicated).**

## V Conclusion and perspectives

In conclusion, abietic acid dimer was successfully synthesized from abietic acid and purified (98% purity) in reasonable yield (35%). An extensive study of the dimerization proved that dimerization is a complex mechanism of proton addition, transfer and proton elimination. It results in the formation of not only one dimer but several different structures. Among them, sterically hindered compounds and molecules bearing a carbonyl as form of lactone were identified. These two points prevented the synthesis of high molar mass polymers by direct polycondensation. However, the resulting polymer exhibits promising thermal properties. To avoid reactivity issues, abietic acid dimers were successfully esterified with undecenol to obtain bis-unsaturated dimers prone to ADMET polymerization. This derivatisation allowed the production of dimers with reactive terminal double bonds, even in the case of lactones and sterically hindered compounds. The homopolymer of bis-unsaturated abietic ester dimers exhibits a high glass transition temperature equal to 102 °C while random copolymers with undecenyl undecenoate revealed semi-crystalline structures with melting temperatures between 40 °C and 50 °C. The demixtion phenomenon was observed for incorporation of abietic acid dimers over 50 mol%. Finally, all the polymers exhibit excellent thermal stability, over 300 °C.

In future works, the dimerization mechanisms would need to be further investigated in order to improve the selectivity of coupling reaction. However, the bis-unsaturated abietic ester dimers developed in this part can be used for the synthesis of other polymers, by varying the polymerization method itself. For instance, the epoxidation of the double bond could be interesting for the preparation of epoxy resins, polyhydroxyesters or polyurethanes.

Finally, the esterification of sterically hindered molecules with undecenol (or other aliphatic molecules) is a method that enables the polymerization of low reactive compounds and could be adapted to other biobased synthons.

## VI References

1. P. A. Wilbon, F. Chu and C. Tang, *Macromolecular Rapid Communications*, **2012**, 34, 8-37.
2. K. Yao and C. Tang, *Macromolecules*, **2013**, 46, 1689-1712.
3. R. G. Sinclair, W. H. Berry, W. H. Schuller and R. V. Lawrence, *Ind. Eng. Chem. Prod. Res. Develop.*, **1969**, 9, 60-65.
4. R. G. Sinclair, D. A. Berry, W. H. Schuller and R. V. Lawrence, *Product R&D*, **1970**, 9, 60-65.
5. A. Enoki, *Wood research*, **1976**, 59/60, 57-59.
6. G. Brus, V. Thoi and H. Francis, *Peintures, Pigments, Vernis*, **1953**, 8, 29-36.
7. Y. Morillon, *Double liaison*, **1964**, 106, 91-100.
8. I. I. Bardyshev and O. D. Strizhakov, *Dokl. Akad. Nauk*, **1968**, 181, 343-349.
9. R. Fujii, K. Arimoto and D. F. Zinkel, *J Am Oil Chem Soc*, **1987**, 64, 1144-1149.
10. B. Gigante, R. Jones, A. M. Lobo, M. J. Marcelo-Curto, S. Prabhakar, H. S. Rzepa, D. J. Williams and D. F. Zinkel, *Journal of the Chemical Society, Chemical Communications*, **1986**, 1, 1038-1039.
11. T. Lebarbé, A. S. More, P. S. Sane, E. Grau, C. Alfos and H. Cramail, *Macromolecular Rapid Communications*, **2014**, 35, 479-483.
12. T. Lebarbe, M. Neqal, E. Grau, C. Alfos and H. Cramail, *Green Chemistry*, **2014**, 16, 1755-1758.
13. C. Mantzaridis, A.-L. Brocas, A. Llevot, G. Cendejas, R. Auvergne, S. Caillol, S. Carlotti and H. Cramail, *Green Chemistry*, **2013**, 15, 3091-3098.

## VII Experimental

### *Abietic acid dimer synthesis*

A solution of 3 g (0,01mol) of abietic acid in 40 ml of chloroform was mixed with 1.05 ml (1 eq) of concentrated sulfuric acid (98%). The reaction flask was warmed and stirred at 45°C in oil bath, under nitrogen flow for 5 hours, after which time the reaction was quenched with 60 ml of water. Activated carbon was added and filtered in order to eliminate oxidized products. 2.8-3 g of pale yellow solid was obtained after evaporation of the solvent and dried overnight under vacuum at 70°C.

### *Abietic acid dimer isolation*

The product was dissolved in a minimum of methanol and injected in a Flash chromatography apparatus from Grace. The constituents were separated on a C18 grafted silica column, using a methanol-water gradient (*vide infra*) and detected by two UV detectors (wavelengths: 254 and 280 nm) and an Evaporating Light Scattering Detector (ELSD). Three fractions corresponding to dehydroabietic acid, isomerized abietic acid and dimers plus trimers were collected.

### *Abietic acid dimer esterification with undecenol*

Abietic acid dimer (3 g, 0.01 mol of acid functional groups) was dissolved in 50 ml of CH<sub>2</sub>Cl<sub>2</sub> under stirring. Subsequently p-toluene sulfonic acid/4-dimethylaminopyridine catalyst in a molar ratio 1/1.2 was added (2.92g, 0,01mol). The flask was placed in an ice bath and subsequently an excess of undecenol (3 ml, 0.015 mol) was added to the solution. Finally, N,N'-diisopropyl carbodiimide (DIPC, 4.5 ml 0.03 mol) was added dropwise under stirring. The reaction was left under stirring for 72 hours at room temperature. Afterwards the solution was washed three times with water, dried and the solvent was removed under reduced pressure. The product was a yellow brown viscous liquid. The acylurea formed was eliminated by filtration after dissolution of the product in toluene. The remaining reactants were eliminated by silica column purification using dichloromethane/methanol 98/2 eluant. The total removal of undecenol during the purification over column is checked by the disappearance of the peak at 62 ppm in <sup>13</sup>C NMR. Yield: 46%. The purity was confirmed by <sup>13</sup>C NMR analysis (-COOCH<sub>2</sub>- 178 ppm, -COOCH<sub>2</sub>- 65 ppm, CH<sub>2</sub>=CH- 139 ppm; CH<sub>2</sub>=CH- 114 ppm).

*Synthesis of undecenyl undecenoate*

Undecenol (12.8 g, 0.08 mol) was blended with 10-methylundecenoate (15 g, 0.08 mol). TBD (5% mol) was added as a catalyst. The reaction was performed under a nitrogen flow at 120°C for 2h then the temperature was increased to 160°C for 2h more and vacuum was applied for the 2 last hours. Purification over silica was performed using cyclohexane/ethylacetate 94/6 eluant. Yield: 76%. <sup>1</sup>H NMR (400MHz, CDCl<sub>3</sub>, δ (ppm)): 5.8 (m, 1H, -CH=CH<sub>2</sub>), 4.9 (m, 2H, CH<sub>2</sub>=CH-), 4.0 (t, 2H, -CH<sub>2</sub>COO-), 2.2 (t, 2H, -COOCH<sub>2</sub>-).

*General procedure for polycondensation reaction of abietic acid dimer*

Diol (1 equivalent) and diester/diacid (1 equivalent via acid base titration) were stirred at 160°C for 2 h under nitrogen flow and at 200°C under vacuum for 6h in the presence of 1 mol% of catalyst relative to acid or ester functions for all catalysts excepted for TBD. In this case, the reaction is performed at 120°C under vacuum for 24h.

*ADMET polymerization of the esterified abietic acid dimer and undecenyl undecenoate*

Homopolymerization of esterified abietic acid dimer. Esterified abietic acid dimer (0.2 g, 0.22 mmol) was dissolved in 1 mL of Polarclean. Grubbs 1<sup>st</sup> generation (2% mol) was added to the flask. The flask was heated at 80°C under vacuum for 18h. Then 3 ml of ethyl vinyl ether was introduced to the flask to quench the reaction. The final polymer was obtained by reprecipitation in cold methanol.

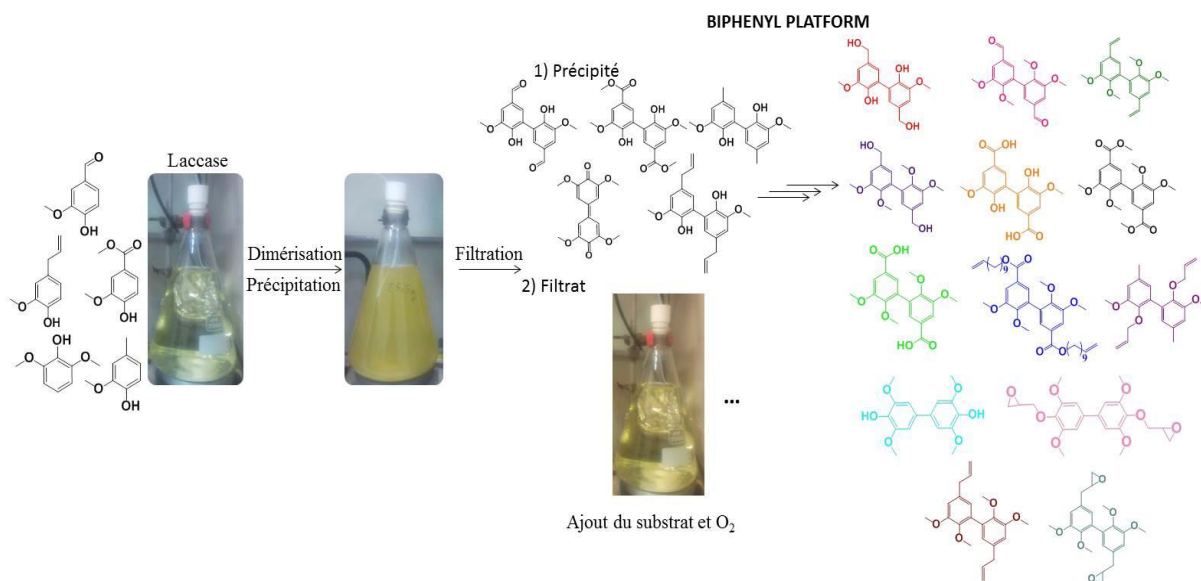
Copolymerization. Esterified abietic acid dimer (0.2 g, 0.22 mmol) and the corresponding amount of undecenyl undecenoate (10-90%) were mixed and dried overnight under vacuum. Grubbs 1<sup>st</sup> generation catalyst (2% mol) was added and the flask was heated at 80°C under vacuum for 8h. 3 ml of ethyl vinyl ether and 4 mL of THF were introduced to the flask. The final polymer was obtained by precipitating in cold methanol.





# Chapter 3:

## Laccase-catalyzed coupling of potentially biobased phenyl compounds



**Key words:** Laccase, oxidative coupling, oligomers, dimers, vanillin, selectivity, bisphenyl

**Mots clés:** Laccase, couplage oxydatif, oligomères, dimères, vanilline, sélectivité, biphényles

## TABLE OF CONTENTS

<b>I</b>	<b>Introduction .....</b>	<b>127</b>
<b>II</b>	<b>Laccase-catalyzed vanillin dimerization .....</b>	<b>127</b>
1.	<b>Dimerization procedure and dimer characterization .....</b>	<b>127</b>
2.	<b>Optimization of the experimental conditions.....</b>	<b>130</b>
1)	Enzyme quantity .....	131
2)	Kinetic study: time, co-solvent and gas solution saturation influence.....	131
3)	Refill procedure: re-use of the filtrate.....	134
<b>III</b>	<b>Laccase-catalyzed oxidative coupling: substrate screening .....</b>	<b>135</b>
1.	<b>Synthesis of oligomer mixtures catalyzed by laccase .....</b>	<b>135</b>
1)	Laccase-catalyzed coupling of <i>ortho</i> unsubstituted phenols .....	136
2)	Laccase-catalyzed coupling of <i>ortho</i> disubstituted phenols .....	139
3)	Laccase-catalyzed coupling of <i>ortho</i> monosubstituted phenols .....	143
4)	Laccase-catalyzed coupling of aniline derivatives.....	153
2.	<b>Laccase-catalyzed selective coupling leading to single dimer formation .....</b>	<b>156</b>
1)	An aniline derivative: 2,6-dimethoxyaniline .....	156
2)	Laccase-catalyzed synthesis of bisphenols in high yield.....	157
<b>IV</b>	<b>Chemical modifications of the biphenyl compounds .....</b>	<b>165</b>
1.	<b>Chemical modifications of divanillin (1) .....</b>	<b>165</b>
2.	<b>Chemical modifications of methyl vanillate dimer (4) .....</b>	<b>167</b>
3.	<b>Chemical modifications of 2-methoxy-4-methylphenol dimer (5) .....</b>	<b>169</b>
4.	<b>Chemical modifications of 2,6-dimethoxyphenol dimer (6) .....</b>	<b>170</b>
5.	<b>Chemical modifications of dieugenol (7) .....</b>	<b>171</b>
<b>V</b>	<b>Conclusion and perspectives .....</b>	<b>172</b>
<b>VI</b>	<b>References .....</b>	<b>174</b>
<b>VII</b>	<b>Experimental.....</b>	<b>175</b>
<b>VIII</b>	<b>Supporting information .....</b>	<b>179</b>

## I Introduction

As described in the first chapter, laccase(s) is(are) widely employed as biocatalyst(s) for the oxidation of functional moieties or the oxidative coupling of phenolic substrates.<sup>1-9</sup> Laccase generates radical intermediates on phenolic compounds, which can undergo self-coupling reactions resulting in the formation of dimers and oligomers. The selectivity of the coupling and size of the oligomers depend on a wide range of parameters such as laccase source, pH value, temperature, aromatic substituents of the phenolic compound, co-solvent, etc. The use of laccase is limited due to its lack of selectivity, which generally leads to product mixtures.

Recently, Beifuss and coll., described a study on the coupling of vanillidene derivatives catalyzed by laccase from *Trametes versicolor*. Their method provided the best result, in terms of yield/selectivity, of dimer synthesis by laccase catalysis.<sup>10</sup> Some of the substrates led to one dimer in over 80% yield but the authors did not investigate the coupling of vanillin.

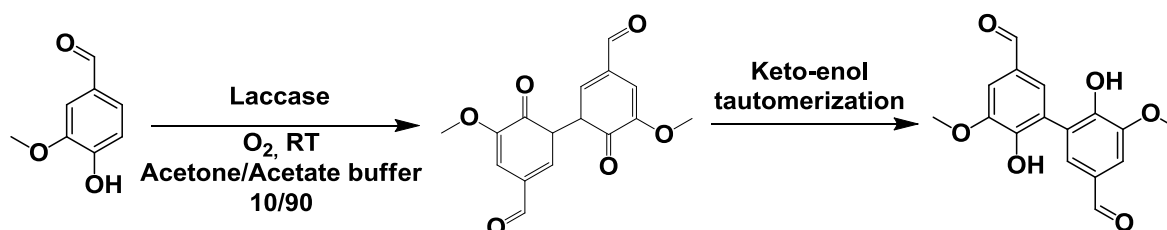
This chapter is dedicated to the development of a new biobased biphenyl platform, obtained from enzymatic coupling. First, the experimental conditions investigated by Beifuss and coll. were applied on vanillin and parameters such as reaction time, laccase and solvent quantities were optimized. A refill procedure was developed in order to re-use the solution containing the laccase. Afterwards, coupling reactions of several substrates were investigated employing the same reaction conditions. In several reactions, oligomers or dimer mixtures were obtained. However, some aromatic compounds potentially obtained from lignin lead to pure dimers, in good yields, and constitute interesting building blocks for the synthesis of semi-aromatic and aromatic polymers. Indeed, the dimers were modified in order to produce a biphenyl platform with a broad range of chemical functions and to broaden the types of polymeric materials obtained thereof.

## II Laccase-catalyzed vanillin dimerization

### 1. Dimerization procedure and dimer characterization

Vanillin dimerization, catalyzed by laccase from *Trametes Versicolor*, was performed at room temperature, in a solution saturated in oxygen (Scheme 1). To ensure the solubility of vanillin, the compound was dissolved completely into acetone (10 vol%) before adding the acetate buffer (90 vol%) to set the pH at 5.0. These solvent conditions allowed the reactant to stay

soluble while the resulting product precipitated. After addition of the laccase, the colorless solution turned yellow, which might indicate the formation of radicals or quinone structures. After few minutes, a brown solid precipitated. The precipitate was filtered off, washed with water and analyzed by mass spectrometry, NMR and HPLC. The first reactions were performed on 1.5 g scale of vanillin, without any optimization, employing 100 U of laccase, in 200 mL of solvent, for 24 h.



**Scheme 1: Laccase-catalyzed vanillin dimerization, in acetone/acetate buffer 10/90, under oxygen, at room temperature.**

The HPLC profile of the resulting product shows the appearance of one new peak at 3.2 min and the disappearance of the peak attributed to vanillin at 6 min (Figure 1 (a)). This main peak indicates the formation of a product with a good purity. Its mass, investigated by mass spectroscopy revealed a value of 302 g/mol, in agreement with a structure of vanillin dimer (Figure 1 (b)).

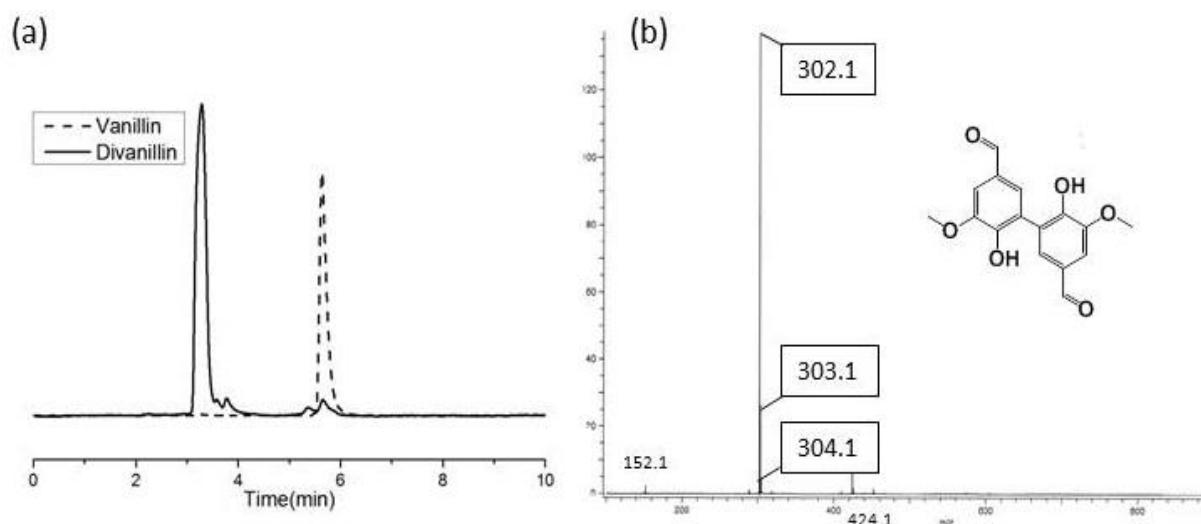


**Figure 1: HPLC profile of vanillin (dashed line) and divanillin (straight line), using a C18 grafted silica column in acetonitrile with a UV detector (a), Mass spectrum of divanillin ionized by electronic impact positive mode, direct introduction (b).**

The molecular structure of the product so-formed was investigated by NMR. The  $^1\text{H}$  NMR and  $^{13}\text{C}$  NMR spectra were consistent with the symmetric dimer displayed in Scheme 1. Indeed, the main difference between the  $^1\text{H}$  NMR spectra of vanillin and of divanillin is the

disappearance of the phenol  $\beta$ -carbon proton (4) (Figure 2). The simplicity of the  $^1\text{H}$  NMR spectrum indicates a high degree of symmetry provided by the *ortho* coupling. The  $^1\text{H}$  NMR spectrum displays a singlet at 9.81 ppm, characteristic of aldehydes, a signal at 7.43 ppm assigned to the two remaining aromatic protons and a singlet at 3.93 ppm attributed to the  $\text{CH}_3$  of the methoxy moiety. The integration of the  $^1\text{H}$  NMR peak at 6.95 ppm shows remaining traces of vanillin (about 5%) that can be reduced by washing the crude product with dichloromethane.

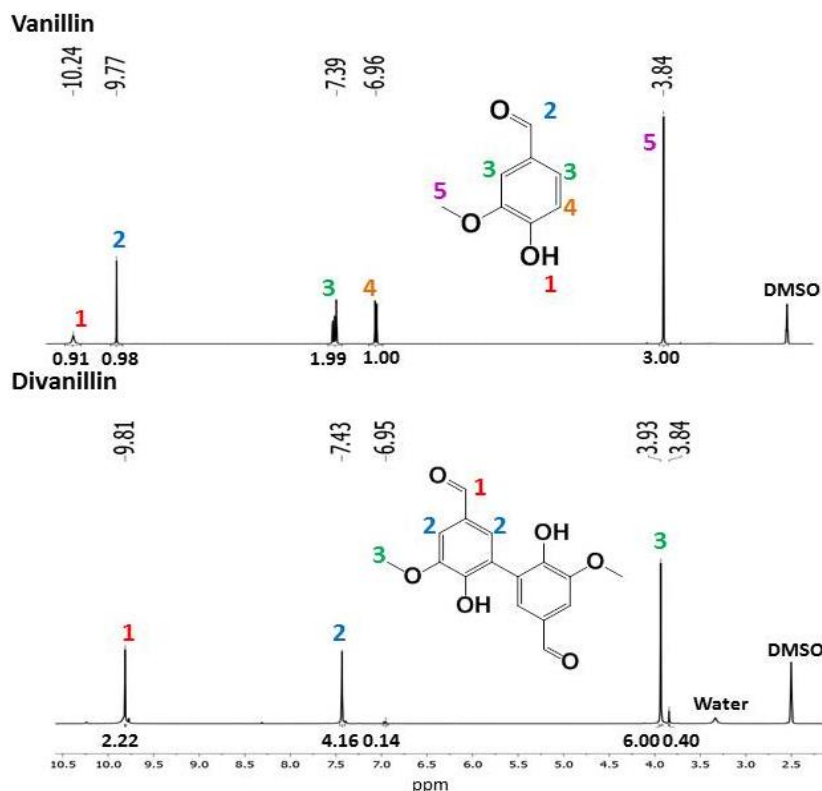


Figure 2:  $^1\text{H}$  NMR spectra of vanillin (top) and divanillin (bottom) in DMSO at room temperature.

The  $^{13}\text{C}$  NMR peaks were assigned using HMBC and HSQC NMR experiments (Figure 3 and Figure 4) and were in agreement with the study of Eswaran and coll.<sup>11</sup> The signals at 191 and 55.9 ppm are attributed respectively to the aldehyde (C1) and the methoxy (C8) moieties. The six other signals correspond to the aromatic carbons. HSQC spectroscopy showed that the carbons at 109.02 and 128.23 ppm bear hydrogen. C7 which  $\alpha$ -carbons bear methoxy and aldehyde groups is the most downfield shifted to 109.1 ppm; as a result, the signal at 128.3 ppm is attributed to C4. HMBC reveals a 3-bond correlation between the methoxy protons and the signal at 147.9 ppm, which is assigned to C3. Thus, the peak at 150.7 ppm is attributed to the carbon bearing the hydroxyl group, C2. Finally, HMBC spectrum shows a correlation between the aldehyde and the peak 127.6 ppm, which is attributed to C5. The last signal at 124.5 ppm displays only correlation to aromatic protons and is thus attributed to C6.

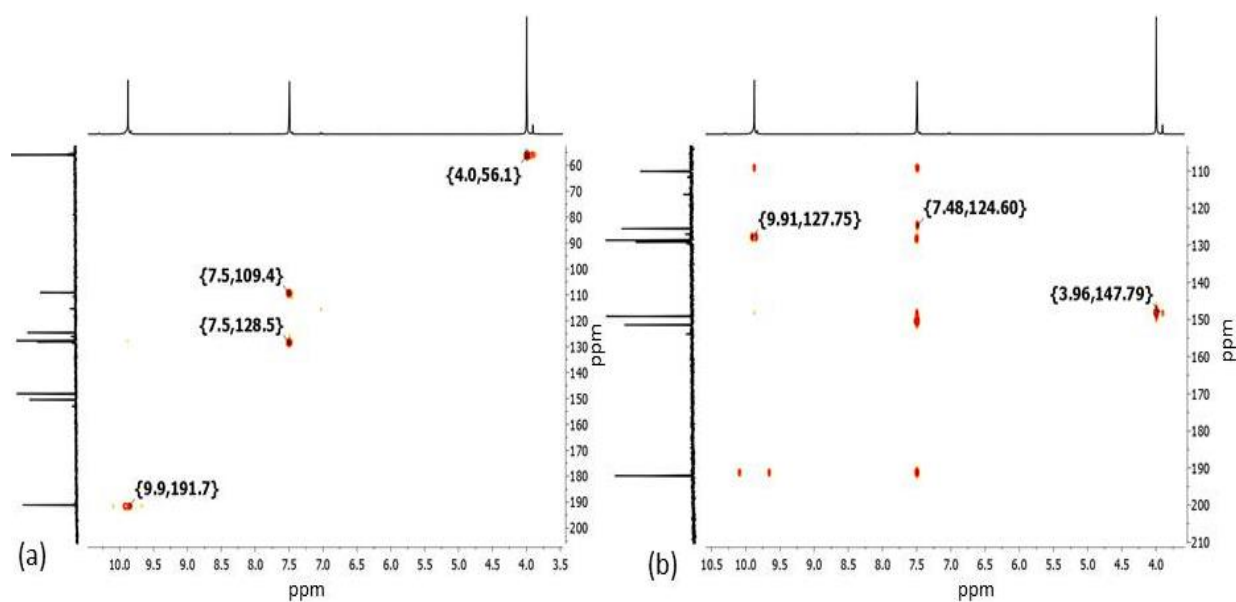


Figure 3: HSQC (a) and HMBC (b) spectra of divanillin in DMSO, at room temperature.

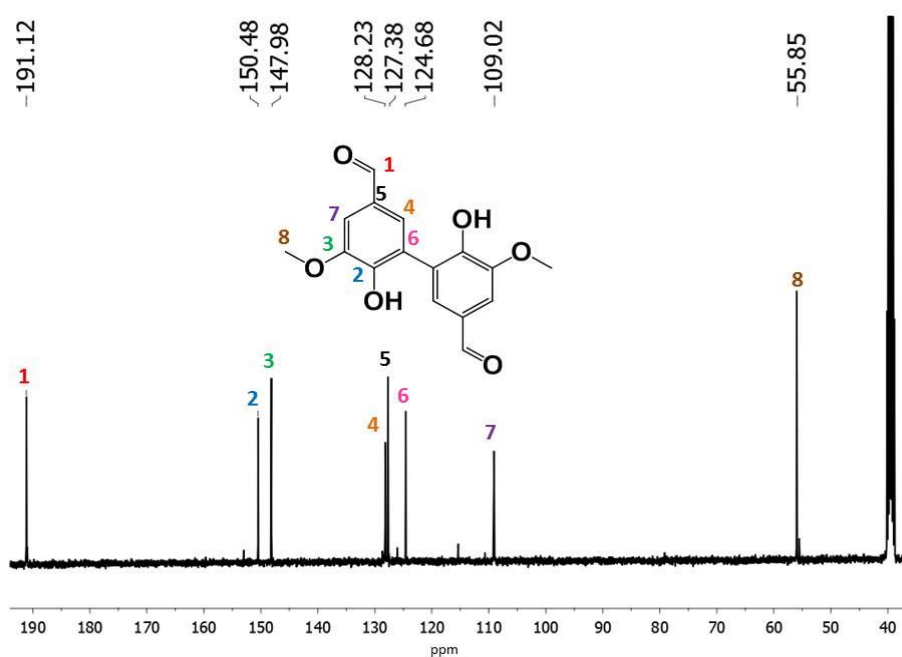


Figure 4:  $^{13}\text{C}$  NMR spectrum of divanillin in DMSO, at room temperature.

## 2. Optimization of the experimental conditions

In order to reduce the consumption of enzyme, solvent, oxygen and time, the influence of these parameters on the reaction yield and selectivity was investigated.

### 1) Enzyme quantity

The activity of commercial laccase from *Trametes versicolor* was determined spectrophotometrically by monitoring the oxidation of 2,2'-azino-bis-(3-ethylbenzthiazoline-6-sulfonic acid) (ABTS,  $\epsilon = 36\,000\text{ mol}^{-1}\cdot\text{cm}^{-2}$ ). The reaction mixture contained 0.04 mM of ABTS, 50 mM of acetate buffer (pH 5.0) and laccase. The absorbance change was monitored at 414 nm for 5 min at room temperature.<sup>12</sup> The amount of laccase that generated 1  $\mu\text{mol}$  of ABTS radical cation per minute was defined as one unit, U. The activity of laccase batch used in this study was evaluated at 1.6 U/mg.

The first reactions were performed on 1.5 g of vanillin, employing 100 U of laccase, in 200 mL of solvent, for 24 h. In order to optimize the process, the quantity of enzyme in the solution was gradually decreased to 5 U (Figure 5).

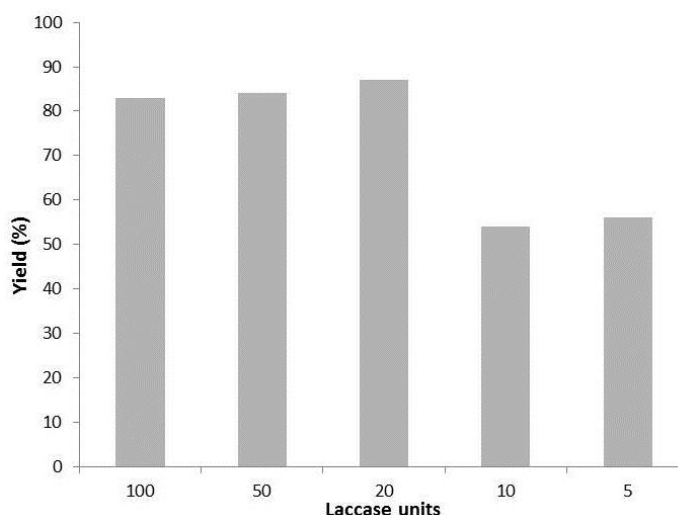


**Figure 5: Divanillin yields depending on laccase quantity for 1.5 g of vanillin, in 200 mL of solvent saturated in O<sub>2</sub>, after 24 h.**

The precipitate was filtered and dried. The yield of divanillin, after 24 h remained high, around 90% down to 20 U. Below this value, the yield drastically decreased to 50% after 24 h. The quantity of laccase for the following reactions was set at 20 U.

### 2) Kinetic study: time, co-solvent and gas solution saturation influence

In order to optimize the reaction time, vanillin conversion was followed by <sup>1</sup>H NMR spectroscopy. Dioxane was chosen as an internal reference for its compatibility with laccase and its characteristic signal at 3.63 ppm on <sup>1</sup>H NMR spectrum. To the 200 mL reaction medium already containing 1.5 g of vanillin and 20 U of laccase, 0.1 mL of dioxane was

added. 0.4 mL of solution was regularly sampled, filtered to remove the dimer, diluted in acetone d6 and analyzed by  $^1\text{H}$  NMR. The percentage of conversion was determined by quantification of unreacted vanillin within the reaction solution. During the reaction, the integration of the signals characteristic of vanillin, at 9.70, and 3.85 ppm, decreased in comparison to the dioxane reference signal (Figure 6). The reaction was completed when full consumption of vanillin was observed. However, the  $^1\text{H}$  NMR spectroscopy was not sensitive enough to determine conversions over 85% due to a large amount of solvent in the sample.

Vanillin conversion was calculated by the ratio of the aldehyde integrations at 9,81 ppm and the dioxane signal integration at 3.63 ppm. The conversion of vanillin versus time, under different reaction conditions, is plotted on Figure 7.

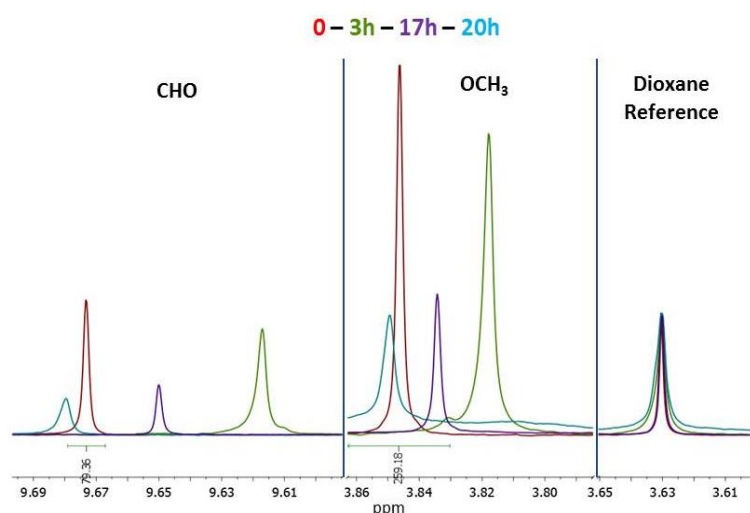


**Figure 6:**  $^1\text{H}$  NMR spectra of remaining vanillin in solution during dimerization initial (red), after 3 h (green), after 17 h (purple), after 20 h (blue).

The conversion of the reaction performed under the optimized conditions that we previously described corresponds to the pink graph. After 8 h reaction time, 85% conversion of vanillin into divanillin was achieved. In the following samples, the concentration of vanillin in the solution was too low to be detected.

The influence of the co-solvent/buffer ratio was studied with acetone. Similar studies have already been performed by Kobayashi and coll. in order to investigate the co-solvent/buffer ratio on the yield and molar mass of oligomers so-formed.<sup>13</sup> The pink graph, corresponding to 10% of acetone, was compared to the green graph, 40% of acetone and to the purple one, 70% of acetone. Increasing the acetone/buffer ratio to 40% dramatically decreased the reaction kinetic. Even after 24 h, the conversion was still below 20%. With 70% of acetone, no conversion of the starting compound was observed. It is thus important to minimize the



quantity of organic co-solvent in order to achieve high yields. The minimal amount of solvent required to solubilize the organic compound should be used. 10% of DMSO was tested as alternative co-solvent and led to a yield around 90%, after 8 h. Acetone can be substituted by other organic solvents as long as the latter are compatible with laccase; however, depending on the solvent and quantity, the reaction yield can decrease.

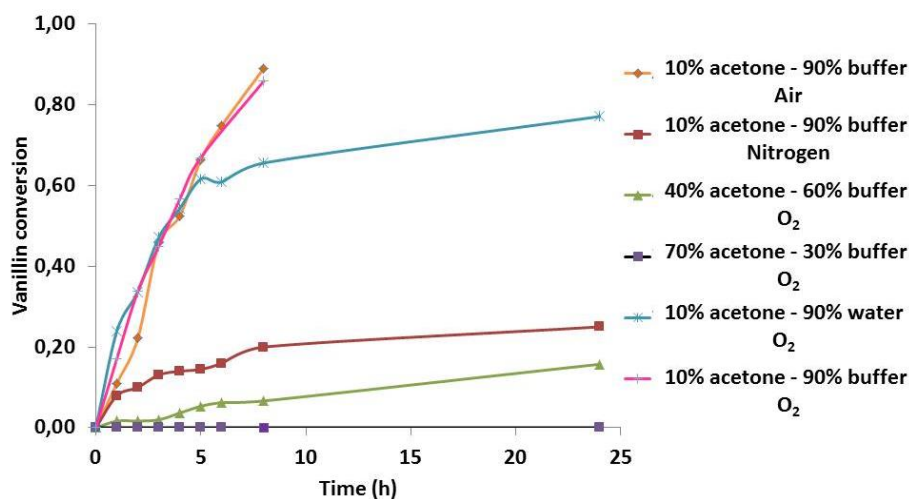


**Figure 7: Vanillin conversion versus time using data extracted from  $^1\text{H}$  NMR spectra (aldehyde peak).**

The influence of oxygen source within the reaction solution was also investigated (Figure 7). The pink curve, which displays the vanillin conversion in oxygen-saturated solution by bubbling, was chosen as reference. The same experiment was performed without bubbling oxygen. Instead, the reaction was carried out in a beaker with a large surface in contact with air, under vigorous stirring. The conversion, plotted in orange, is similar to the conversion obtained in a solution saturated in oxygen. The reaction was also performed in a solution saturated with nitrogen. After 25 h reaction time, the conversion, plotted in red, reached only 25%. This value indicates that the solution was not fully saturated to 100% with nitrogen. Otherwise, no reaction should occur, because laccase needs oxygen for its regeneration.

Finally, the acetate buffer was substituted by water. The conversion is plotted in blue. Until a reaction time of 5 h, the conversion profile follows the pink reference curve and reaches 61%. Beyond this time, the kinetic decreased and, after 24 h, only 75% conversion was achieved. An increase of the pH from 5 to 7 was observed after the reaction was stopped, that can explain the low conversion observed in the last hours. Indeed, the optimal pH zone for laccase is ranging from 4 to 6; outside this zone, the laccase activity decreases.

### 3) Refill procedure: re-use of the filtrate

The recovery of divanillin presents three main advantages: (i) as vanillin is soluble into the solution, the purity of the obtained dimer is very good (95%), (ii) the precipitation shifts the reaction equilibrium to divanillin formation, (iii) after filtration, the filtrate can be reused for a new reaction. Indeed, after 24 h reaction time, the precipitate was filtered off. The filtrate, which still contains the laccase, was saturated again with oxygen and the same amount of vanillin was added (Figure 8). After few seconds, vanillin was solubilized and after few minutes, a brown precipitate appeared. After 24 h reaction time, the precipitate was filtered off and weighted.

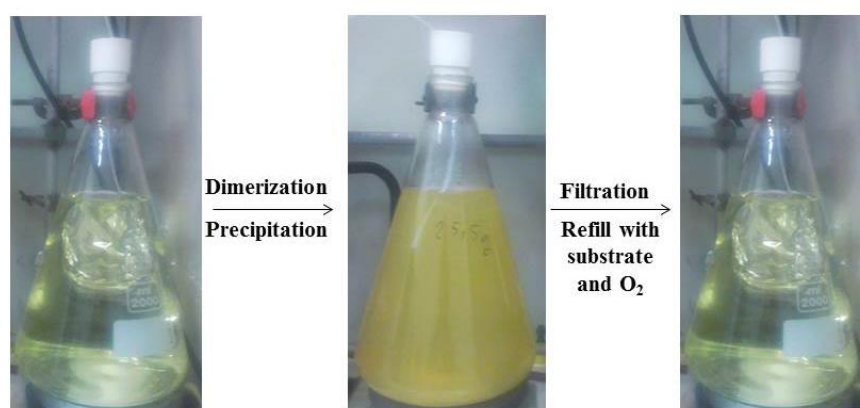


**Figure 8: Process of vanillin dimerization: precipitation, filtration, refill.**

Even after 8 runs of recharging the catalyst material with the substrates, more than 80% of product was isolated (Figure 9). The combination of the easy recovery method without a marginal loss of activity makes the entire process economically very promising.

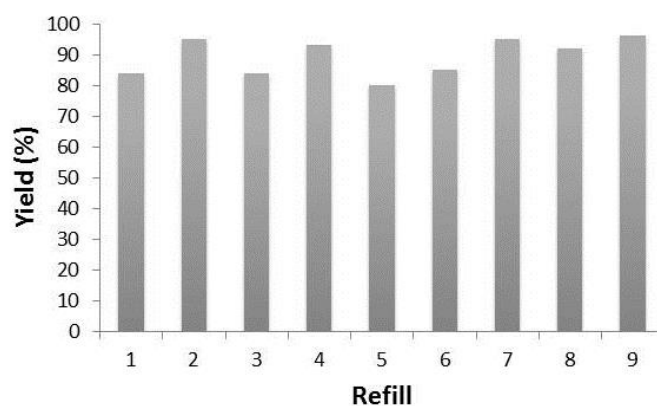


**Figure 9: Divanillin yield, after 24 h of reaction under optimized conditions for 8 refills.**

### Conclusion:

A green and easy process to synthesize high purity divanillin in good yield and large amount was developed. All the experiments were performed on 1.5 g of vanillin employing 20 U of laccase. A good conversion, 85%, was reached after 8 h and the resulting product was recovered with a yield of 95% after 24h. After filtration of the product, the filtrate can be recharged with substrate and oxygen and re-used again. The product extraction is easy and the purity is high (95%) because the solvent conditions allow the reactant solubility while the so-formed product precipitates. Kinetic studies allowed us to determine some important parameters to reach high vanillin conversion. Organic solvent compatible with laccase is required to solubilize the substrate but its amount should be minimized and the solution should contain enough oxygen to allow laccase catalysis activity to be at a maximum. The use of a buffer maintains the optimal pH ensuring the completion of the reaction. The temperature parameter was not investigated but should remain between 20 °C and 60 °C not to denature the enzyme. Around 150 g of divanillin were thus produced in our laboratory.

### III Laccase-catalyzed oxidative coupling: substrate screening

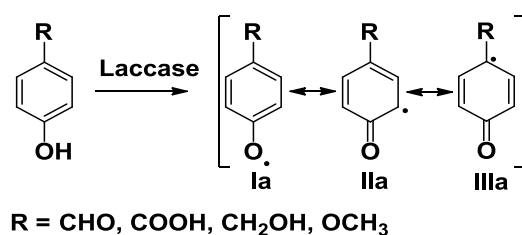
In literature, different reaction conditions, substrates, as well as sources of laccase are employed. This heterogeneity of experimental data makes the prediction of substrate coupling difficult. In this section, we extended the procedure developed previously to several substrates. The aim was both to investigate the structures of the resulting products and to produce pure dimers or oligomers, which could be used as building blocks in order to design novel aromatic bio-based polymers. The influence of the aromatic substituents on the coupling selectivity was investigated. The obtained products were analyzed by HPLC, <sup>1</sup>H NMR spectroscopy and SEC.

#### 1. Synthesis of oligomer mixtures catalyzed by laccase

The nomenclature *ortho* and *para* employed in this section corresponds for all the compounds to the *ortho* and *para* phenolic positions.

### 1) Laccase-catalyzed coupling of *ortho* unsubstituted phenols

The first class studied includes *ortho* unsubstituted phenols with a substituent in *para* position, namely alcohol, carboxylic acid, methoxy and aldehyde. The phenoxy radical produced by laccase oxidation forms *ortho* and *para* radical species through resonance stabilization (Scheme 2). Recombination of the radicals produces dimers or oligomers. The *para* radical **IIIa** is sterically more hindered and should have lower probability to be involved in coupling reaction.



**Scheme 2: Resonance forms of *ortho* unsubstituted phenol obtained by laccase-catalyzed oxidation.**

The reaction was carried out on four *para* substituted phenols. Two electron-donating groups,  $\text{CH}_2\text{OH}$  and  $\text{CH}_3\text{O}$  and two electron-withdrawing groups,  $\text{COOH}$  and  $\text{CHO}$ , were selected as *para* substituents. The obtained results enable to investigate the influence of electronic effects on the coupling. After 24 h reaction time, both electron-donating groups yielded a precipitate with 95% yield. SEC analysis revealed that the oxidative coupling of 4-methoxyphenol and 4-hydroxybenzyl alcohol respectively leads to oligomers constituted of 2 to 5 units and polymers of 5 800 g/mol (Figure 10 (b), Figure 11 (b)). The multitude of peaks, observed on the HPLC profile of the oligomers produced from 4-methoxyphenol, Figure 10 (c) indicates that several structures are formed by different radical recombinations. The homocoupling of structures **IIa** leads to a C-C bond formation whereas the hetero coupling of structures **Ia** and **IIa** produces a C-O linkage. C-O and C-C couplings can occur randomly within an oligomer leading to a multitude of structures.  $^1\text{H}$  NMR spectrum of the product did not allow us proposing any oligomer structure, Figure 10 (a).

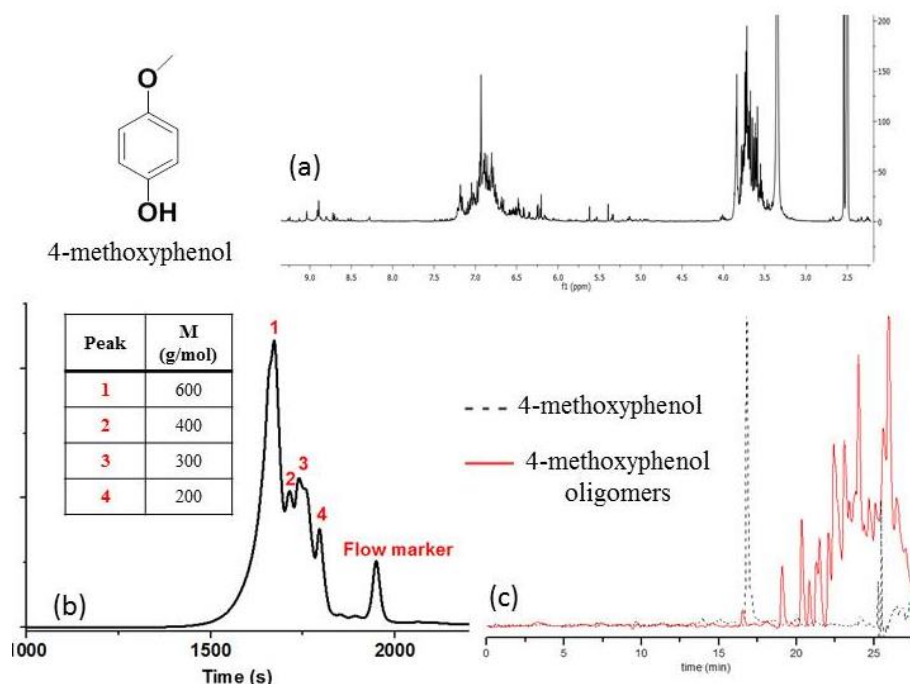


**Figure 10:**  $^1\text{H}$  NMR spectrum in DMSO at room temperature (a), SEC trace in THF, RI detection (b), HPLC profile using a C18 grafted silica column and acetonitrile as eluent (c) of products formed by coupling of 4-methoxyphenol catalyzed by laccase.

The polymer produced by oxidative coupling of 4-hydroxybenzyl alcohol is characterized by broad peaks on the  $^1\text{H}$  NMR spectrum, attributed to an oligomeric structure (Figure 11 (a)). This structure was confirmed by SEC analysis which revealed the formation of oligomers of 5 700 g/mol, Figure 11 (b).

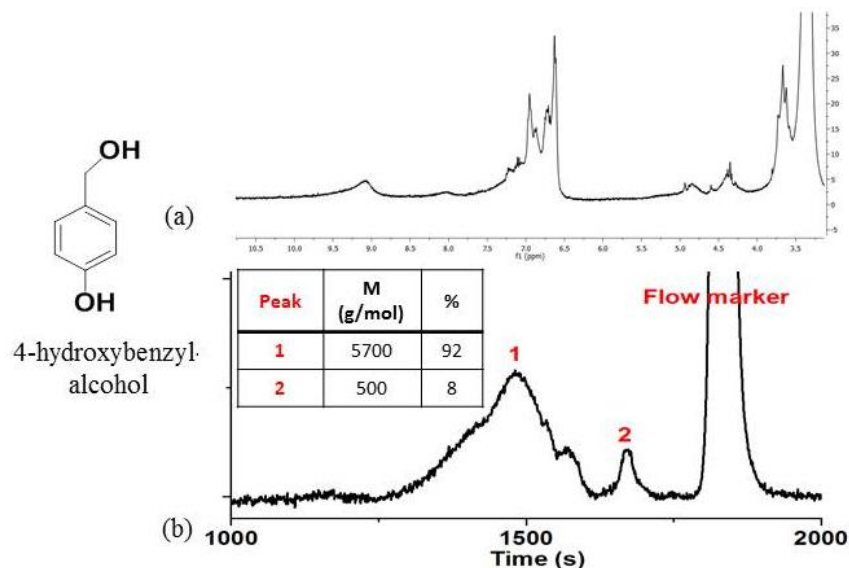


**Figure 11:**  $^1\text{H}$  NMR spectrum in DMSO at room temperature (a), SEC trace in DMF, RI detector (b) of products formed by coupling of 4-hydroxybenzyl alcohol catalyzed by laccase.

On the contrary, no precipitate appeared after 24 h reaction time of phenol bearing *para* electron-withdrawing group. The HPLC profile and the  $^1\text{H}$  NMR spectrum of the solution

present peaks only assigned to the reactant, hydroxybenzoic acid (Figure 12) and hydroxybenzaldehyde, respectively (Figure 13).

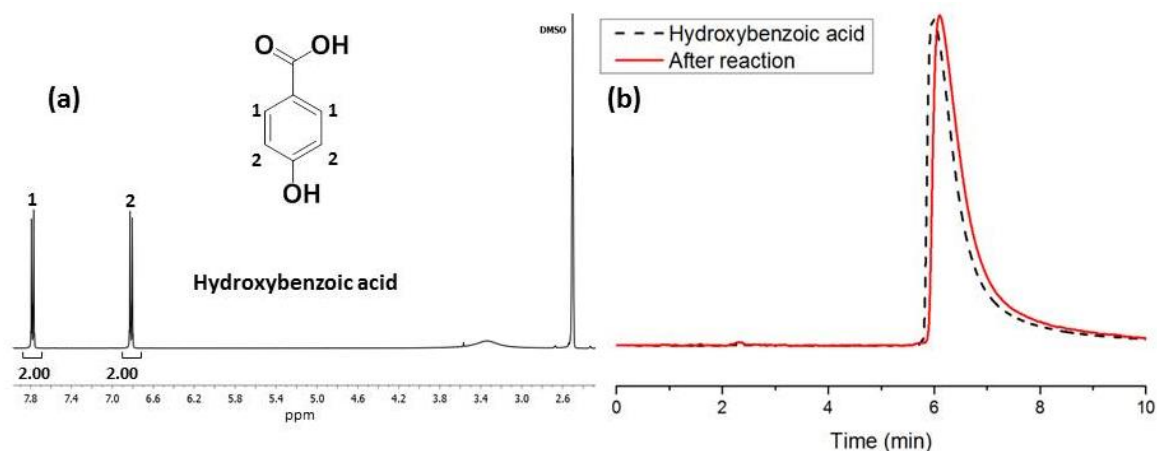


**Figure 12:** <sup>1</sup>H NMR spectrum in DMSO at room temperature (a), HPLC profile using a C18 grafted silica column and acetonitrile as eluent (b) of product formed by coupling of hydroxybenzoic acid catalyzed by laccase.

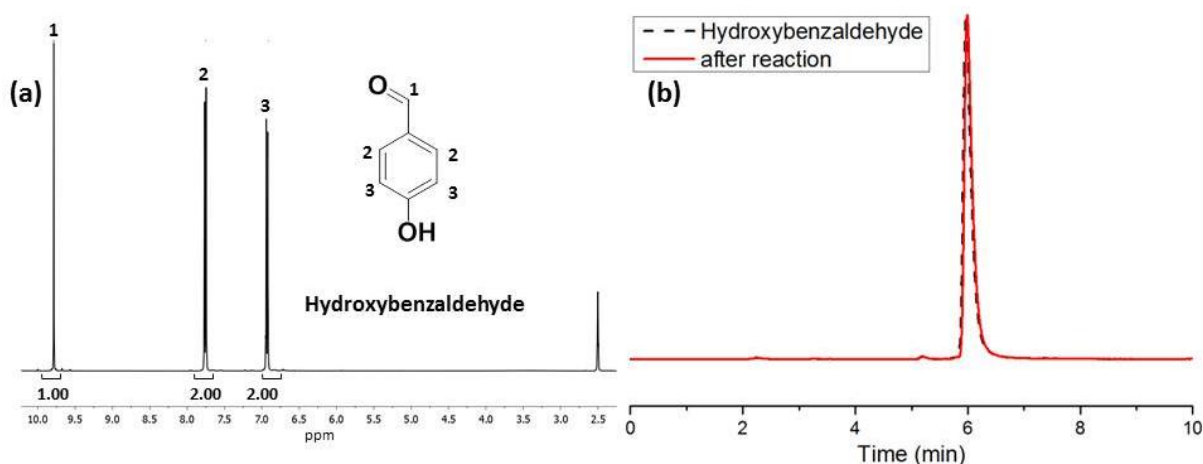


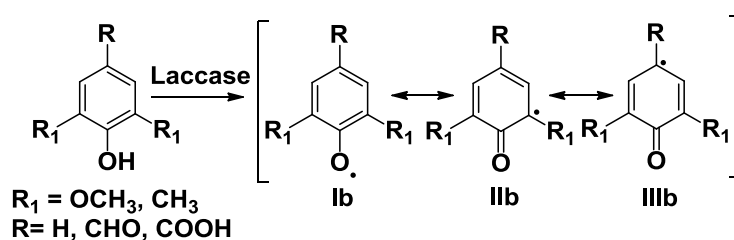
**Figure 13:** <sup>1</sup>H NMR spectrum in DMSO at room temperature (a), HPLC profile using a C18 grafted silica column and acetonitrile as eluent (b) of product formed by coupling hydroxybenzaldehyde catalyzed by laccase.

These results highlight the influence of the *para* substituent electronic effect on the coupling reaction. Data concerning the formation and stability of radical on phenolic compounds were extracted from structure/activity relationship studies for laccase mediator systems.<sup>14</sup> Several parameters, such as redox potential, ionization energy, pKa, enthalpy of formation of the radical and O-H bond dissociation energy influence the reaction between laccase and substrates. The ionization energy, which is the energy required to abstract one electron to a molecule, best reflects the laccase capacity to oxidize phenolic substrates. Phenolic derivatives with electron withdrawing substituents show high ionization energies (8.83 eV and 8.89 eV for 4-hydroxybenzoic acid and 4-hydroxybenzaldehyde) whereas phenolic

derivatives with electron-donating groups show lower ionization energies (8.11 eV for 4-hydroxybenzyl alcohol). Oligomerization of 4-hydroxybenzyl alcohol and 4-methoxyphenol could be explained by the low ionization energy of these molecules. However, under the aforementioned experimental conditions, a change of the solution color is observed during the reaction of 4-hydroxybenzoic acid and 4-hydroxybenzaldehyde with laccase, respectively. This color change might be due to the formation of free radicals or quinone compounds. Electron paramagnetic resonance (EPR) studies would be needed for a better investigation of this phenomenon.

## 2) Laccase-catalyzed coupling of *ortho* disubstituted phenols

The presence of methoxy groups in *ortho* position significantly decreases the ionization energies of the phenolic compounds. *Ortho* disubstituted *para* substituted phenols with, either hydrogen, carboxylic acid or aldehyde in *para* position and methoxy or methyl groups in *ortho* positions, were studied. The phenoxy radical produced by laccase oxidation is delocalized on three resonance forms (Scheme 3). Coupling of structure **IIb** has not been observed in literature. Coupling at this position likely occurs but the process does not lead to a stable product because there is no good way for the aromatic ring to be regenerated with methoxy or methyl group present at this position. Consequently, the coupling likely reverses back to the individual radical species, which find other ways to couple.



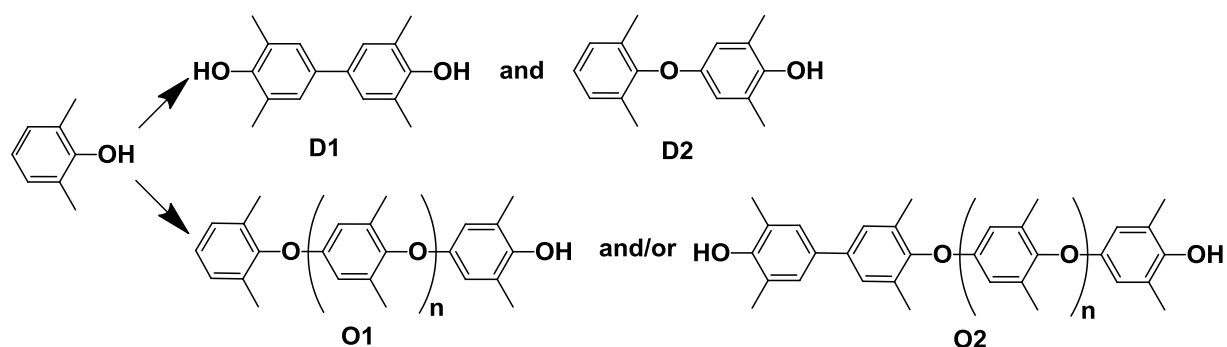
**Scheme 3: Resonance forms of *ortho* disubstituted phenol obtained by laccase-catalyzed oxidation.**

### a) 2,6-Dimethylphenol coupling

The oxidative coupling of 2,6-dimethylphenol catalyzed by laccase, under the aforementioned conditions, led to a precipitate in 60% yield. SEC analysis indicated that the formed solid contained 12% of dimers and several oligomers with up to 11 units. Peaks 8 and 9 correspond to a molar mass of around 300 g/mol and can be assigned to two dimers with different structures, Figure 14 (b). They can be produced either by homo-coupling of structure **IIIb**



leading to C-C bonds (**D1**) or hetero-coupling of structures **Ib** and **IIIb** leading to ether linkage (**D2**) (Scheme 4).



HPLC analysis monitored the presence of only 3 new peaks, indicating that some of the nine oligomers possess structures with the similar polarity and have the same affinity for the HPLC column, Figure 14 (c). The broad intense peak at 6.5 ppm in the  $^1\text{H}$  NMR spectrum is characteristic of the aromatic protons of poly(phenylene oxide). The smaller peaks observed in the aromatic region are attributed to dimers and oligomer terminal units, Figure 14 (a). Indeed, oligomers can be terminated by one or two OH moieties, respectively **O1** and **O2**, and thus show different structures (Scheme 4).

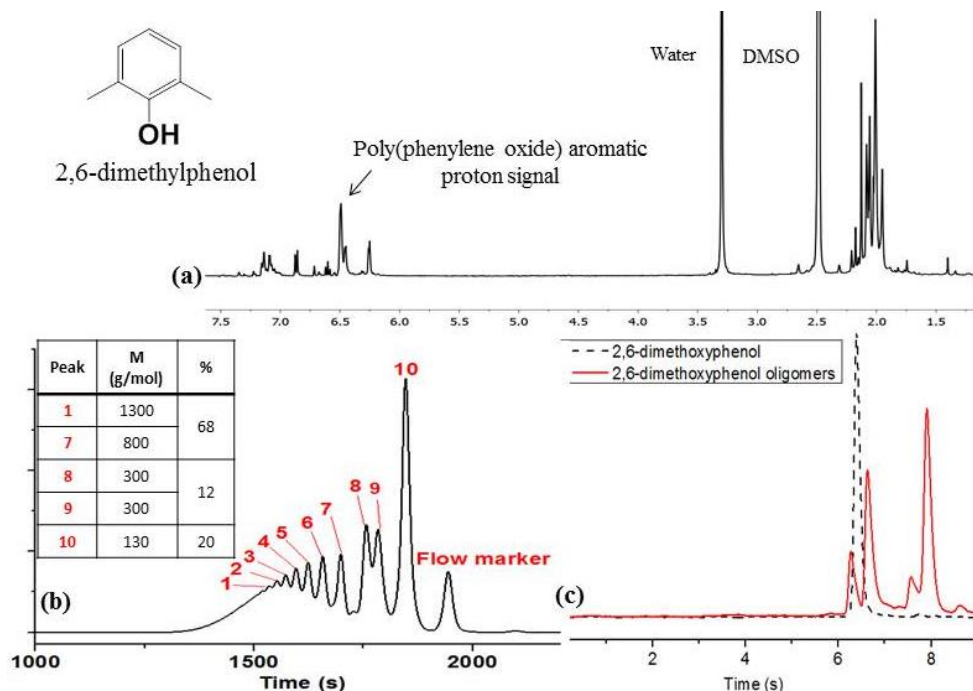


**Figure 14:**  $^1\text{H}$  NMR spectrum in DMSO at room temperature (a), SEC trace in THF, RI detection (b), HPLC profile using a C18 grafted silica column and acetonitrile as eluent (c) of product obtained by 2,6-dimethylphenol coupling catalyzed by laccase.

Kobayashi and coll. have already reported about the enzymatic oxidative polymerization of 2,6-dimethylphenol employing laccase from *Pycnoporus coccineus*.<sup>15</sup> The authors studied



the influence of the buffer/acetone ratio on the polymer yield and molar mass. The yield never exceeded 60% due to the formation of a dimer. The author obtained polymers with a molar mass of 3 000 g/mol in an acetone/acetate buffer solvent 10/90. This molar mass is around 3 times higher than the molar mass of the polymer synthesized under our experimental conditions. This difference can be attributed to different laccase sources and quantities.

### b) Syringic acid

Syringic acid oxidative coupling under the aforementioned conditions, led to a precipitate with 70% yield. The HPLC analysis of the resulting solid shows the appearance of two new peaks at 4 and 6 min and the disappearance of the syringic acid peak at 8 min, Figure 15 (c). Considering the  $^1\text{H}$  NMR spectrum, the singlets at 5.97 and 6.18 ppm are attributed to two aromatic protons. The two singlets at 3.75 and 3.63 ppm are assigned to methoxy moieties, Figure 15 (a). These observations might be attributed to the formation of two poly(phenylene oxide)s with different molar masses. The SEC analysis reveals the presence of an oligomer with 10 units, 1 500 g/mol which represents 74% of the mixture and of some dimers or trimers, Figure 15 (b).

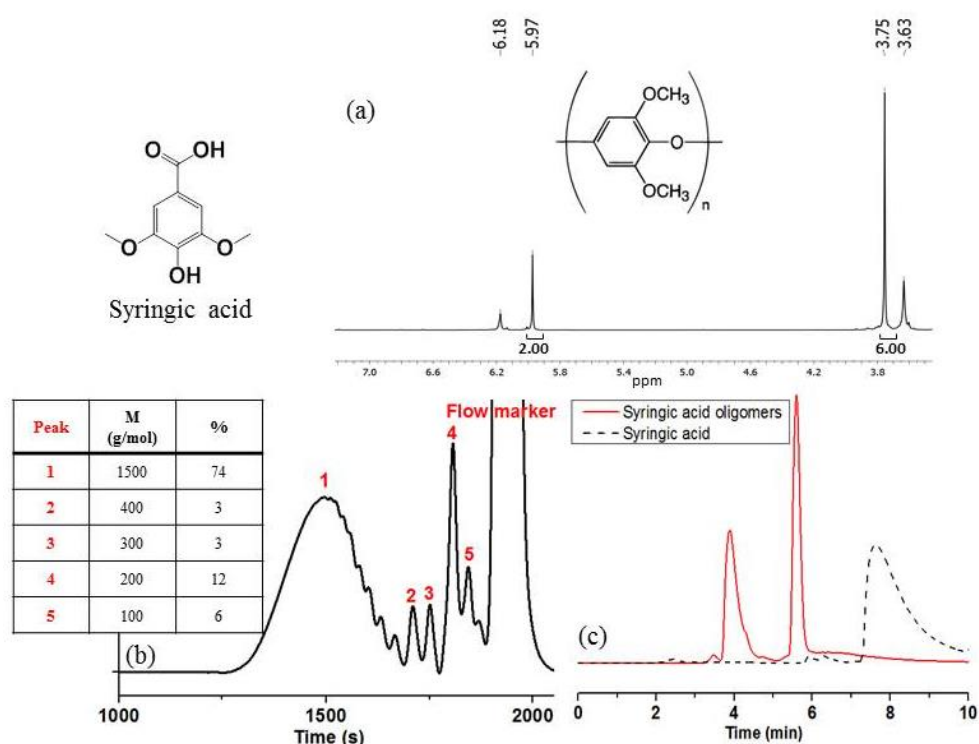
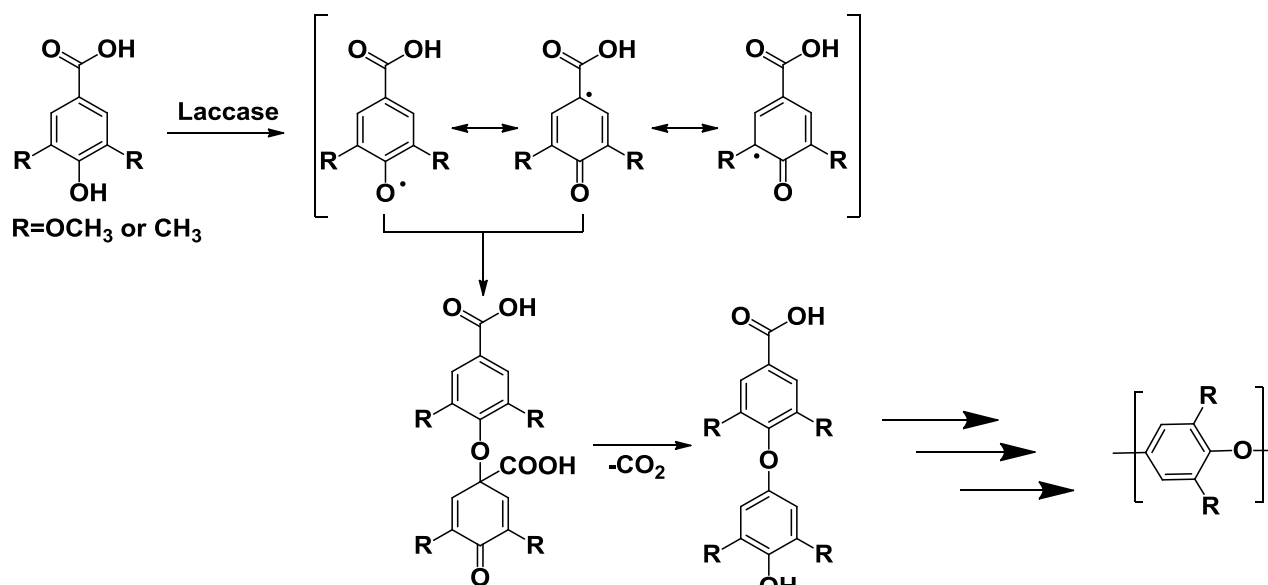


Figure 15:  $^1\text{H}$  NMR spectrum in DMSO at room temperature (a), SEC trace in THF, RI detection (b), HPLC profile using a C18 grafted silica column and acetonitrile as eluent (c) of product obtained by coupling of syringic acid catalyzed by laccase.

Kobayashi and coll. have already described the enzymatic oxidative polymerization of syringic acid employing laccase from *Pycnoporus Coccineus* and *Myceliophthore*.<sup>13</sup> The reaction was performed in the presence of 20% acetone and produced oligomers with a molar mass of 4 900 g/mol in 26% yield. Optimization of the reaction conditions led to polymers with molar mass up to 7 700 g/mol. The postulated reaction pathway displays the formation of phenoxy radicals, which can recombine to give the quinoid-type intermediates. The dimer is formed by release of carbon dioxide. Further coupling leads to the formation of poly(phenylene oxide), (Scheme 5).



Scheme 5: Proposed mechanism for decarboxylation of *ortho*-substituted 4-hydroxybenzoic acid derivatives catalyzed by laccase.

### c) Syringaldehyde

A fine powder was obtained in 10% yield by coupling of syringaldehyde catalyzed by laccase. The HPLC profile of this product shows the presence of unreacted syringaldehyde eluted at 6 min and the appearance of a new peak eluted at 3.5 min, Figure 16 (c). Signals observed at 9.9, 7.4 and 3.9 ppm on the <sup>1</sup>H NMR spectrum are characteristic of syringaldehyde, Figure 16 (a). Additionally, new signals appeared at 5.9 ppm and 3.8 ppm and could be attributed to phenylene oxide moieties. SEC analysis shows the presence of syringaldehyde, dimers and trimers, Figure 16 (b). This oligomerization may occur because syringaldehyde can be oxidized to syringic acid. The latter can undergo the decarboxylation previously described. The yield and oligomer molar mass are limited by the completion of the first step. The molar mass could be increased by increasing the reaction time or the acetone/buffer ratio.

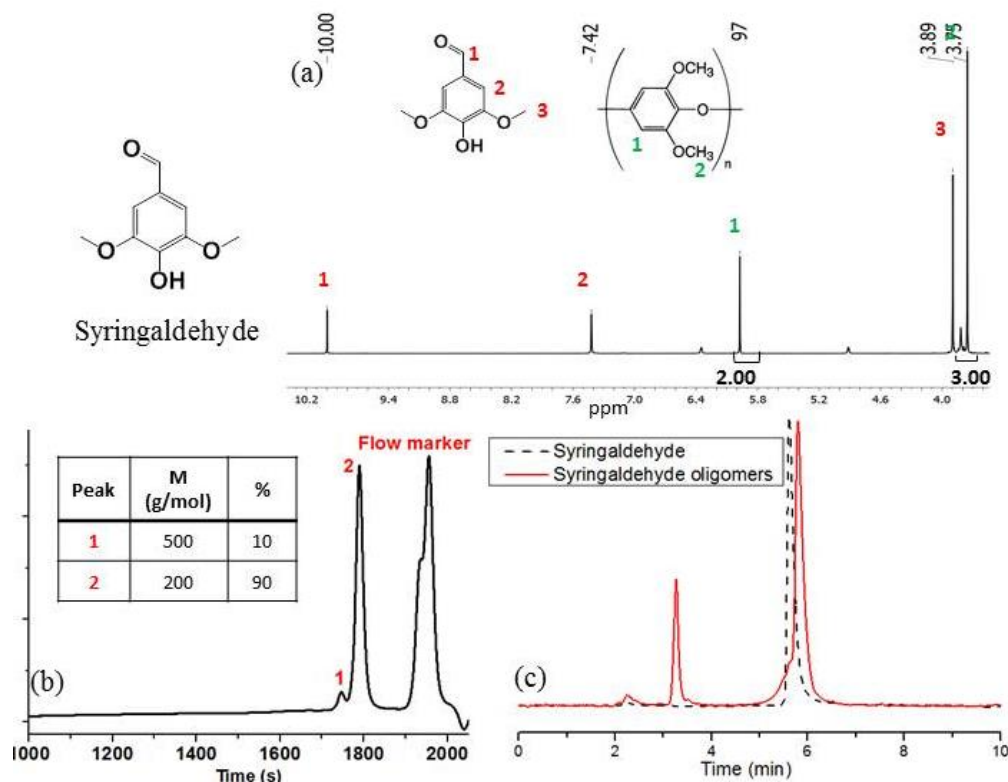
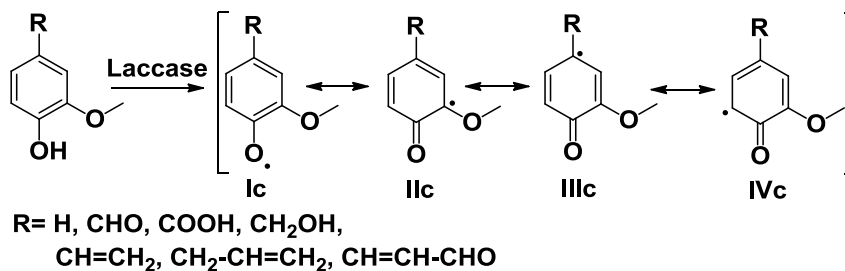


Figure 16: <sup>1</sup>H NMR spectrum in DMSO at room temperature (a), SEC trace in THF, RI detection (b), HPLC profile, using a C18 grafted silica column and acetonitrile as eluent (c) of products obtained by coupling of syringaldehyde catalyzed by laccase.

### 3) Laccase-catalyzed coupling of *ortho* monosubstituted phenols

*Ortho* methoxy phenols with different *para* substituents were studied. The phenoxy radical produced by laccase oxidation is delocalized on three resonance forms (Scheme 6). The radical of structure **IIc** is more sterically hindered and should have lower probability to be involved in coupling reactions. Structure **IIIc** is reactive toward coupling if the hydrogen is in *para* position. In all the other cases, homocoupling of structure **IVc** leads to a C-C bond, and coupling of structures **Ic** with **IVc** leads to C-O bond. The *para* substituent can also be involved in the coupling.



Scheme 6: Resonance forms of *ortho* monosubstituted phenol obtained by laccase catalyzed oxidation.

## a) Gaiacol

Reaction of gaiacol with laccase led to a precipitate in 90% yield. SEC analysis indicates the presence of oligomers with around 9 units, which represents 87% of the mixture, Figure 17 (b). The broad signals at 3.8 ppm, 7 ppm and 8.9 ppm, on the  $^1\text{H}$  NMR spectrum are respectively assigned to methoxy, aromatic and phenolic protons, Figure 17(a). The integration of these signals reveals the formation of 50% C-O and 50% C-C linkages either in *ortho* or *para* positions. The resulting oligomers can be produced by coupling of structure **Ic**, **IIIc** and **IVc**.

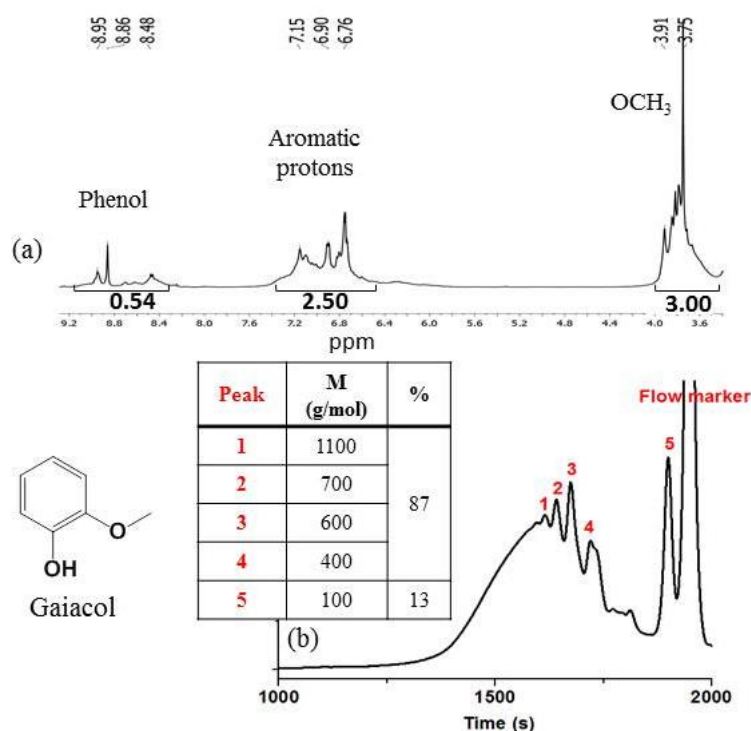
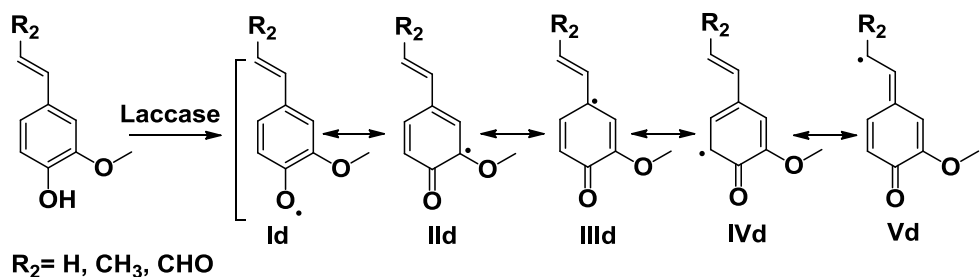


Figure 17:  $^1\text{H}$  NMR spectrum in DMSO at room temperature (a), SEC trace in THF, RI detection (b) of products obtained by coupling of gaiacol catalyzed by laccase.

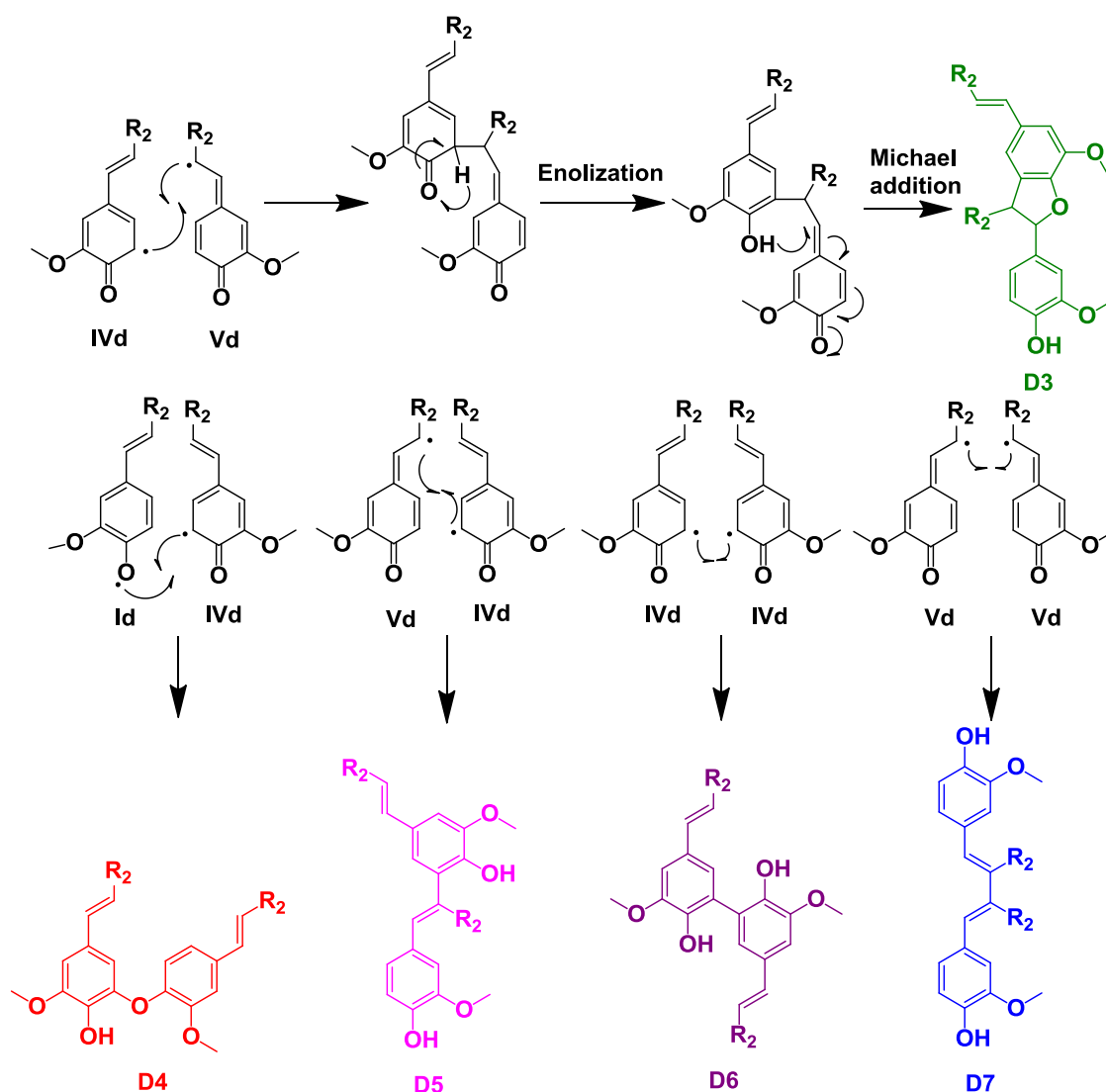
## b) Compounds with conjugated double bonds

Coniferaldehyde, 2-methoxy-4-vinyl phenol and isoeugenol bear a *para* substituent containing a double bond conjugated to the aromatic ring. The radical formed by laccase oxidation is also delocalized to the double bond. This conjugation leads to the formation of an additional structure **Vd** (Scheme 7). In such cases, coupling most probably involves structures **Id**, **IVd** and **Vd**, due to the steric hindrance of the other forms.



**Scheme 7: Resonance forms of *ortho* monosubstituted phenol containing a conjugated double bond obtained by laccase-catalyzed oxidation.**

As already described in literature, the phenyl coumaran **D3** is obtained by coupling structures **Vd** and **Id** and further enolization and Michael addition.<sup>16,17</sup> In addition to this structure, the ether biaryl, **D4**, can be formed by coupling of **Id** and **IVd**. Coupling **IVd** and **Vd**, and homocoupling of **IVd** and **Vd** lead C-C bonds and the formation of **D5**, **D6**, and **D7**, respectively. The possible structures of dimers are presented in Scheme 8.



**Scheme 8: Dimer structures possibly obtained by coupling of vanillidene derivatives.**

Radical species can be produced from these dimers and further recombine with other radical species, resulting in complex oligomeric structures. The same reaction pathway is proposed for the first step of lignin biosynthesis ( $R_2 = \text{CH}_2\text{OH}$ ).

### 2-methoxy-4-vinylphenol

The oxidative coupling of 2-methoxy-4-vinylphenol catalyzed by laccase led to a precipitate in 85% yield. SEC analysis of the product reveals the formation of oligomers with a molar mass of 900 g/mol and a dispersity of 3.6. This peak shows a shoulder at 6 000 g/mol indicating that oligomers with higher molar masses are also produced, Figure 18 (b). The broad peak eluted at 6 min on the HPLC chromatogram can be attributed to oligomers and the multiplicity of this signal to the presence of several structures, Figure 18 (c).

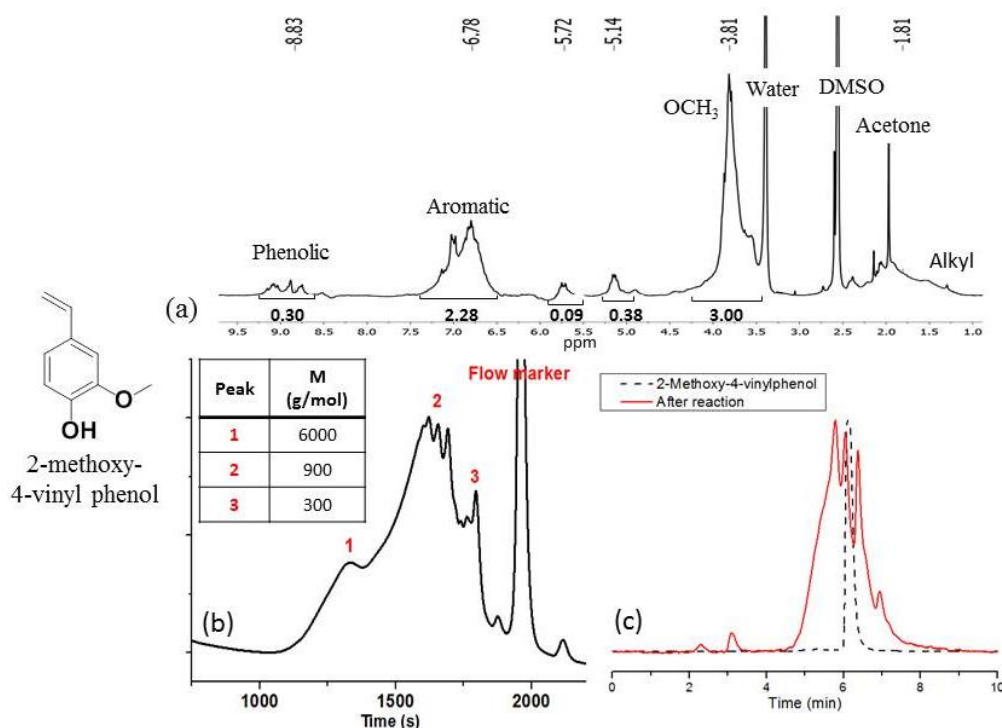


**Figure 18:** <sup>1</sup>H NMR spectrum in DMSO at room temperature (a), SEC trace in THF, RI detection (b), HPLC profile using a C18 grafted silica column and acetonitrile as eluent (c) of products resulting from 2-methoxy-4-vinylphenol coupling catalyzed by laccase.

The <sup>1</sup>H NMR spectrum displays broad signals at around 8.8, 6.8, 5.7 and 5.14 ppm, and 3.9 ppm, which can be assigned to phenolic, aromatic, alkene and methoxy protons, Figure 18 (a). Their integrations show a decrease of the alkene/methoxy protons, phenolic/methoxy protons and aromatic/methoxy protons ratio. This decrease indicates that the coupling might occur *via* C-O and C-C linkages involving structures **Id**, **IVd** and **Vd** (Scheme 7).

### Isoeugenol

The oxidative coupling of isoeugenol catalyzed by laccase led to a precipitate in 83% yield. SEC analyses of the resulting solid show the formation of 86% dimers and 7% of tetramers or pentamers, Figure 19 (b). In this case, the production of dimers was favored in comparison with 2-methoxy-4-vinylphenol, probably due to the steric hindrance of the double bond. Two main peaks and several small shoulders are observed on the HPLC profile, Figure 19 (c).

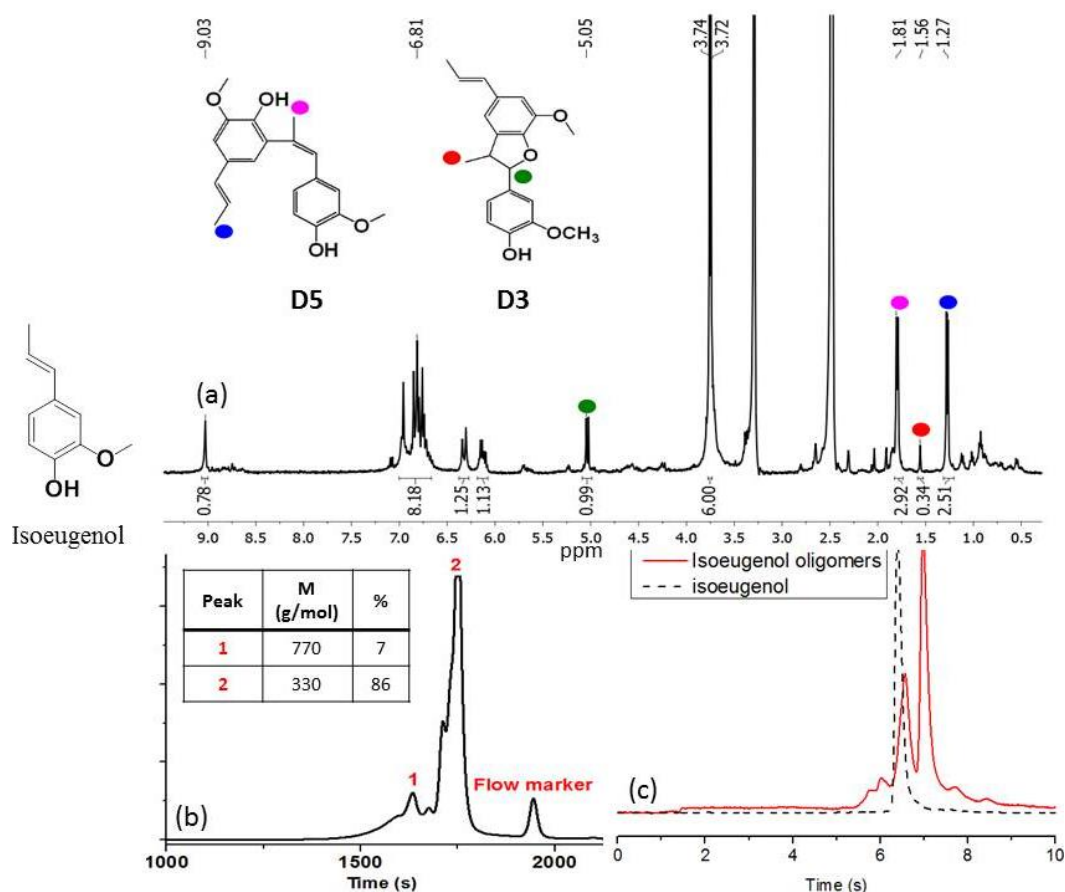


Figure 19:  $^1\text{H}$  NMR spectrum in DMSO at room temperature (a), SEC trace in THF, RI detection (b), HPLC profile using a C18 grafted silica column and acetonitrile as eluent (c) of the product obtained by coupling of isoeugenol catalyzed by laccase.

$^1\text{H}$  NMR predictors allowed us suggesting some structures of dimers or part of the oligomers. Signals at 1.81 and 1.27 ppm, with an integration of 3 can be assigned to the methyl groups of structure **D5**. Signals at 1.5 ppm and 5.1 ppm with an integration of 3 and 1 can be assigned to the methyl and to the coumaran protons of **D3**, respectively, Figure 19 (a). The integration of **D5** methyl protons is three times higher than the integration of the **D3** methyl protons indicating that the formation of **D5** is favored during the coupling reactions.



### Coniferaldehyde

The oxidative coupling of coniferaldehyde catalyzed by laccase led to a precipitate in 92% yield. SEC analysis shows the formation of 43% dimers and 15% trimers and 30% tetramers, Figure 20 (b). The multitude of peaks in the  $^1\text{H}$  NMR spectrum impeded suggesting any structure, Figure 20 (a). Ten peaks are observed on the HPLC chromatogram, meaning that oligomers with different structures are produced, Figure 20 (c). As previously shown for syringaldehyde, the aldehyde moiety can be oxidized, yielding ferulic acid. The laccase oxidation of this compound has been widely studied.<sup>10,18,19</sup> Besides, the structures **D3-D7** displayed on Scheme 8, other structures such as the dilactone **D8**, were also described in literature.

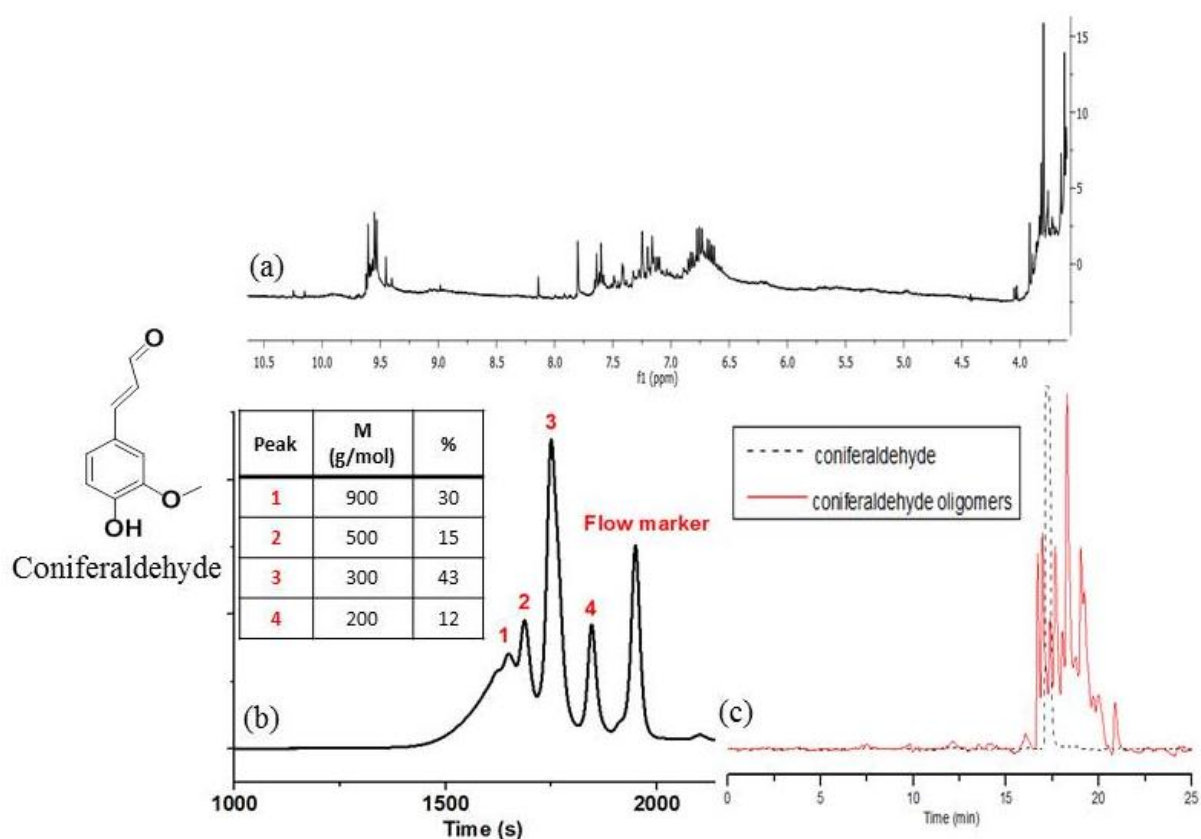
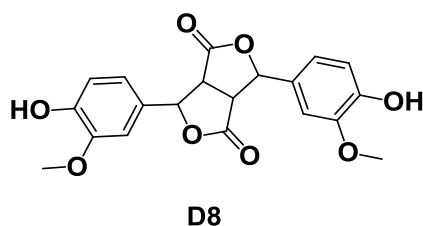


Figure 20: (a)  $^1\text{H}$  NMR spectrum in DMSO at room temperature, (b) SEC trace in THF, RI detection, (c) HPLC profile using a C18 grafted silica column and acetonitrile as eluent of product obtained by coniferaldehyde coupling catalyzed by laccase

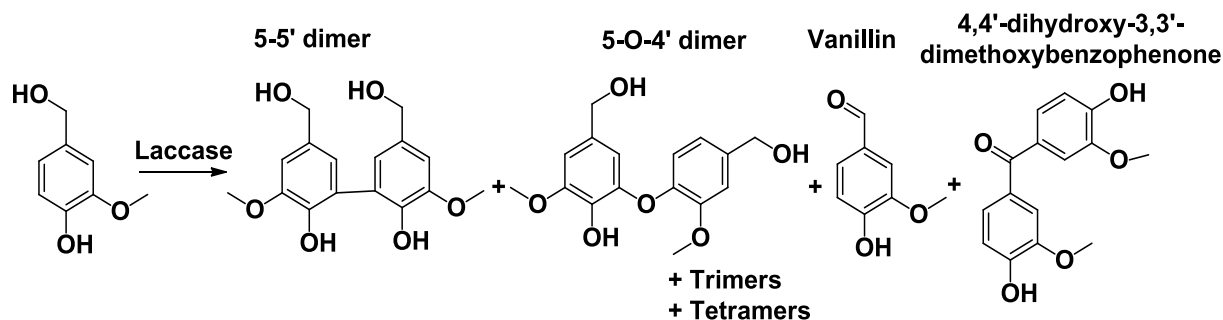


Scheme 9: Dilactone usually synthesized by laccase-catalyzed oxidative coupling of ferulic acid.



## c) Vanillyl alcohol

The coupling of vanillyl alcohol catalyzed by laccase has already been studied in literature.<sup>20,21</sup> The reported oligomer structures are displayed on Scheme 10. The 5-5' dimer was mainly produced in 30% yield.



Under the aforementioned conditions, SEC analysis shows that the mixture obtained from coupling of vanillyl alcohol catalyzed by laccase contains 70% tetramers and 30% dimers, Figure 21 (b).

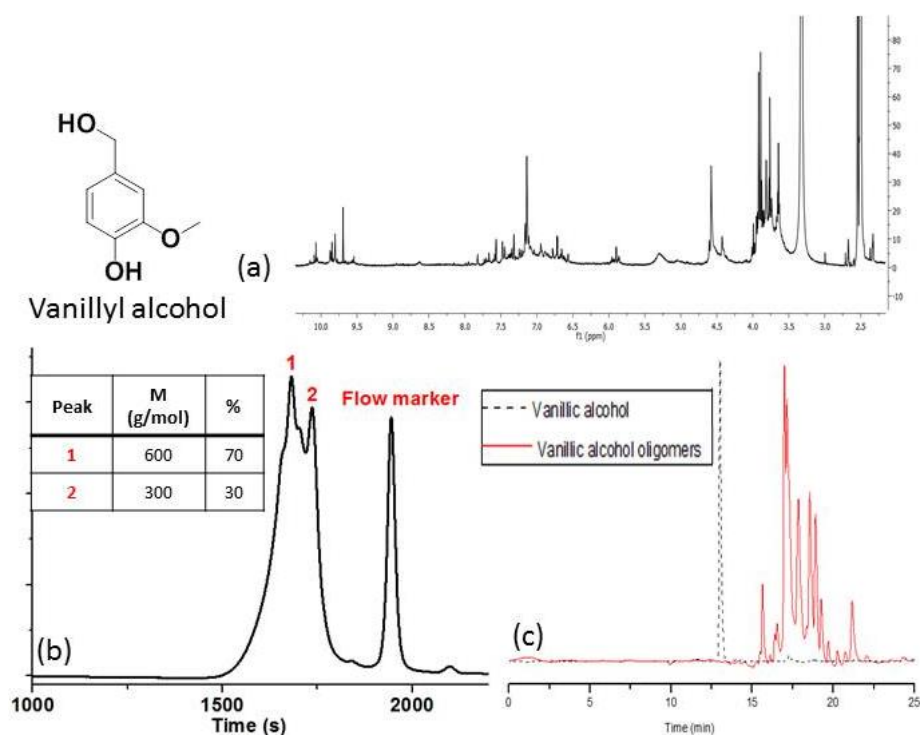
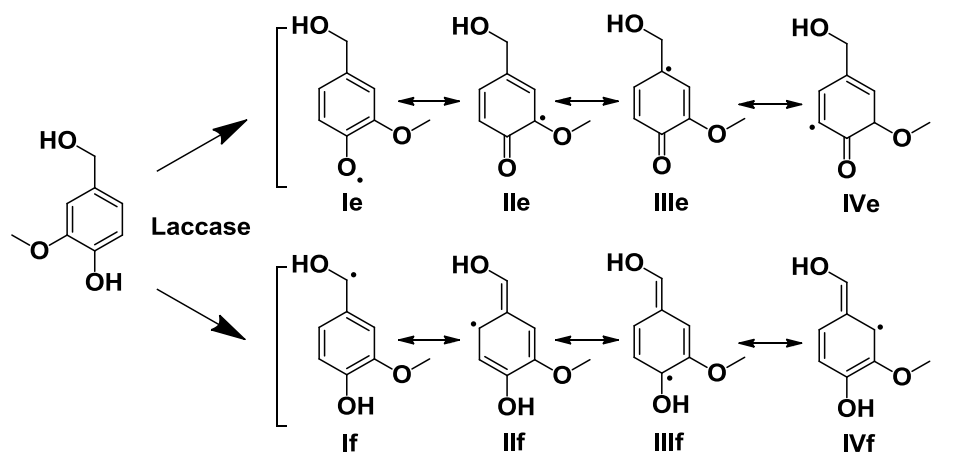


**Figure 21:** <sup>1</sup>H NMR spectrum in DMSO at room temperature (a), SEC trace in THF, RI detection (b), HPLC profile using a C18 grafted silica column and acetonitrile as eluent (c) of the product obtained by vanillyl alcohol coupling catalyzed by laccase.

A multitude of peaks are observed on the HPLC profile and <sup>1</sup>H NMR spectrum, which did not allow us to identify the structures, Figure 21 (c), (a).

In order to better understand the complexity of this mixture, the coupling of vanillyl alcohol with a protected phenol catalyzed by laccase was investigated. This experiment would show the ability of laccase to produce a radical on the alcohol  $\alpha$ -carbon (Scheme 11).



Scheme 11: Laccase-catalyzed coupling of vanillyl alcohol.

After reaction of methylated vanillyl alcohol, a precipitate was obtained in 20% yield. The HPLC profile indicates the formation of a new compound, Figure 22 (b).  $^1\text{H}$  NMR analysis allowed us to propose the structure of a dimer, Figure 22 (a). The signal at 4.4 ppm is assigned to one proton of the alcohol  $\alpha$ -carbon. The decrease of the integration from 2 to 1 after reaction indicates that a coupling may occur on this position. The peak at 5.0 ppm characteristic of the alcohol moiety is shifted downfield and splitted in three new peaks at 4.88, 4.81 and 4.76 ppm. These modifications suggest a symmetric C-C coupling on this position and the presence of three stereoisomers of **D9**. The  $^{13}\text{C}$  NMR of this compound was in agreement with a reported spectrum of this structure, Figure 22 (c).<sup>22</sup> It can be noticed that after reaction, the signal characteristic of alcohol  $\alpha$ -carbon is shifted to higher field, from 62.41 to 71.02 ppm. This shift can be attributed to the transformation of a  $\text{CH}_2$  into a CH.

This coupling illustrates that new radical species are formed and delocalized on four new resonance forms during the oxidative coupling of vanillyl alcohol, in addition to the four mesomeric forms previously described (Scheme 11). This large number of mesomeric forms can explain the complexity of the HPLC and  $^1\text{H}$  NMR profiles.

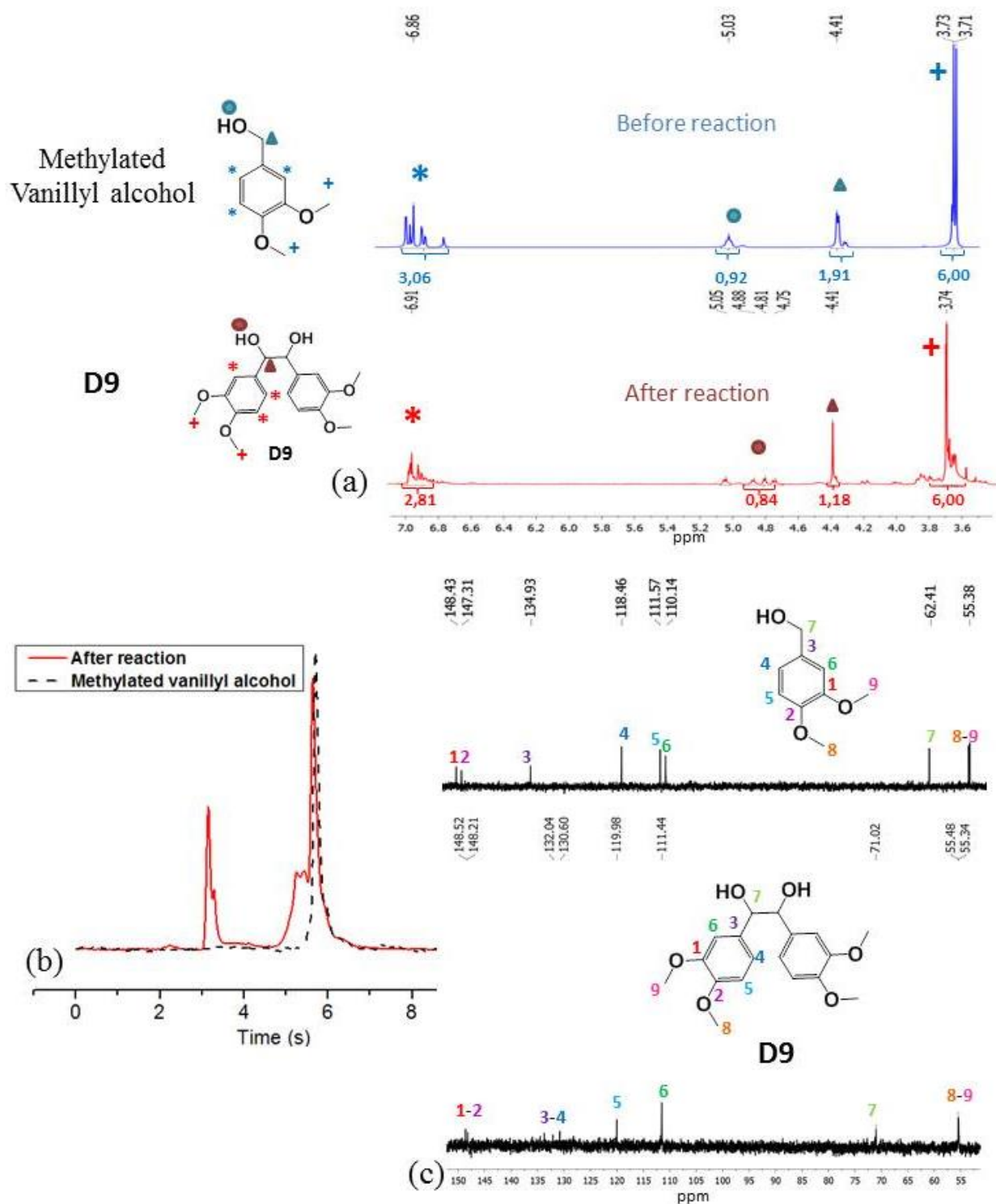
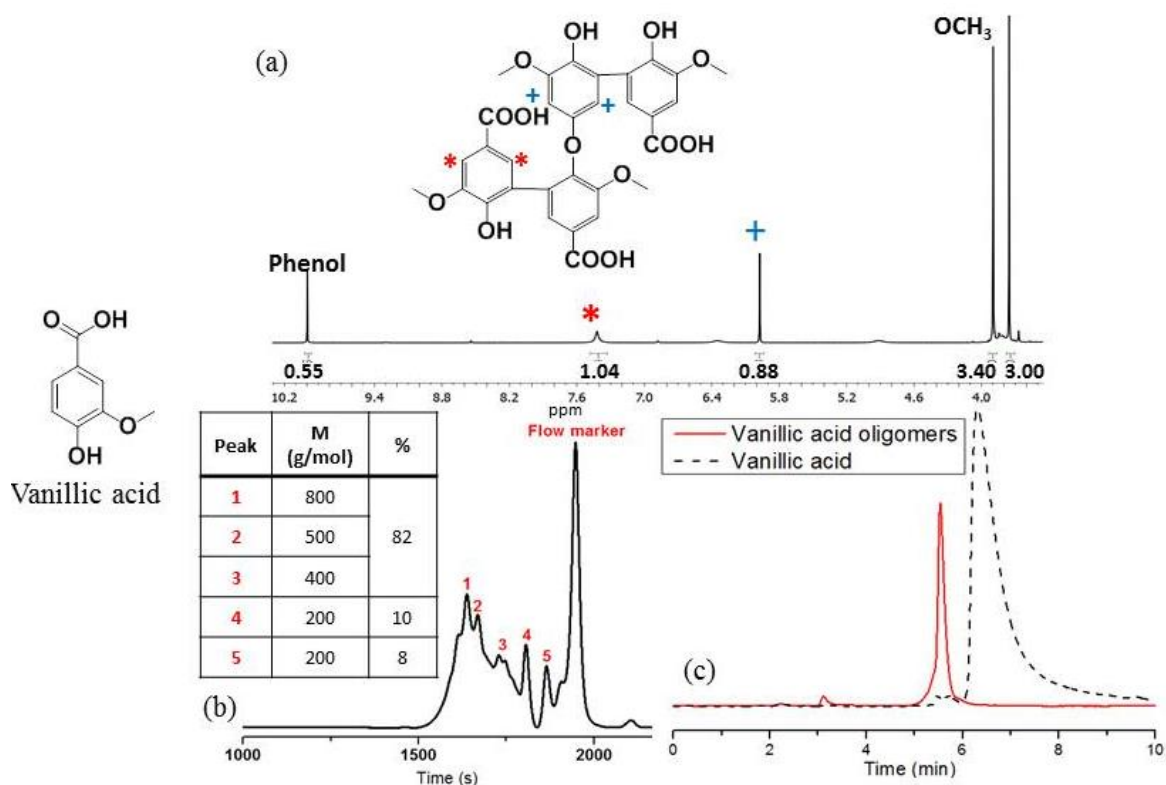


Figure 22:  $^1\text{H}$  NMR spectrum in DMSO at room temperature (a), HPLC profile using a C18 grafted silica and acetonitrile as eluent (b),  $^{13}\text{C}$  NMR in DMSO at room temperature (c) of product obtained by coupling of methylated vanillyl alcohol catalyzed by laccase.

## d) Vanillic acid

The reaction of vanillic acid with laccase produced a precipitate with a yield of 40%. Unfortunately, the sample was not completely soluble in acetonitrile; as a result, the HPLC analysis provided partial characterization of the mixture. The disappearance of the peak at 7 min indicated the consumption of vanillic acid. Only a single new peak appeared at 5.5 min, Figure 23 (c) but, due to solubility issues, other compounds may also be formed.



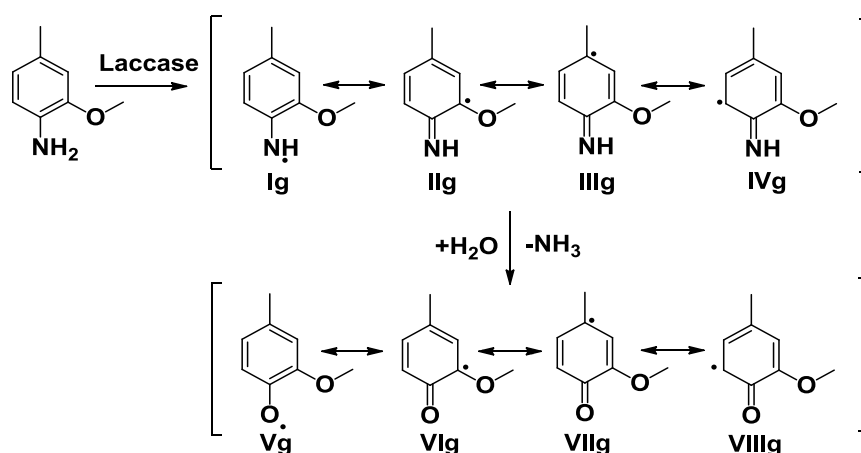
**Figure 23:** <sup>1</sup>H NMR spectrum in DMSO at room temperature (a), SEC trace in THF (b), HPLC profile using a C18 grafted silica column and acetonitrile as eluent (c) of product obtained by coupling of vanillic acid catalyzed by laccase.

As explained previously, phenolic compounds bearing carboxylic acid functions in *para* position can undergo decarboxylation reaction and thus can form poly(phenylene oxide)s. The structure of the vanillic acid oligomer was determined by <sup>1</sup>H NMR, Figure 23 (a). The spectrum showed only three signals probably due to the symmetry of this dimer. The singlet at 5.8 ppm is characteristic for aromatic protons near the oxygen of poly(phenylene oxide)s (+) and the singlet at 7.4 ppm is assigned to the aromatic protons near the carboxylic acid moieties (\*). SEC analysis showed the formation of oligomers constituted of two to five units, Figure 23 (b). Additional analyses are required in order to determine the exact structure of the oligomer, including the number of incorporated monomers and a possible cyclization.

#### 4) Laccase-catalyzed coupling of aniline derivatives

Laccase catalyzed oxidative coupling of aniline derivatives has already been described in literature.<sup>23</sup> The radical formed during the initial step of the oxidative polymerization reaction, produced on the nitrogen atom, can be delocalized either on the *ortho* or *para*-carbons (Scheme 12). However, the imine group is not stable and can easily be transformed into a quinone releasing ammoniac, yielding structures **Vg**, **VIg**, **VIIg**, **VIIIg**.

In order to synthesize diamines, which could be useful for the synthesis of polyamides, epoxy resins and polyurethanes, the coupling of aniline derivatives, in our experimental conditions, was investigated.



**Scheme 12:** Resonance forms of 4-methyl-2-methoxy aniline obtained by laccase-catalyzed oxidative coupling.

The oxidation of 4-methyl-2-methoxy aniline by laccase produced a precipitate in 84% yield. SEC analysis revealed that dimers with a molar mass of around 300 g/mol represent 83% of the mixture, Figure 24 (b). Three components were detected on HPLC analysis, Figure 24 (c). However, the <sup>1</sup>H NMR spectrum of this sample is complex, probably due to the formation of several compounds including some with an asymmetric structure, Figure 24 (a).

We propose mechanical pathways to form six dimers (Scheme 13). Two dimers, **D9** and **D11** can respectively be formed by N-C linkage, from coupling of structures **Ig** and **IVg** and by C-C linkage, from homo-coupling of structure **IIg**. As the dimers were not isolated, the aromatization of the molecules was not proven and the obtained compounds might be imines **I9** and **I11**. Moreover, the modification of imines into quinones can occur before or after coupling. Dimer **D12** can be obtained by coupling of **Ig** and **VIIIg** or by transformation of the imine **I11** into the quinone imine **QI12**. Similarly, **D10** can be produced by homo-coupling of

**VIIIg** or by transformation of the imine **I9** into the quinone **Q10**. The obtained compounds might also be the quinone imine **QI12** and the quinone **Q10**. **D13** can be obtained by recombination of radical species **IVg** and **Vg** and **D14** by coupling of structures **Vg** and **VIIIg** or transformation of the imine **I13** into the quinone **Q14**. The obtained compounds might also be the imines **I13** and the quinone **Q14**.

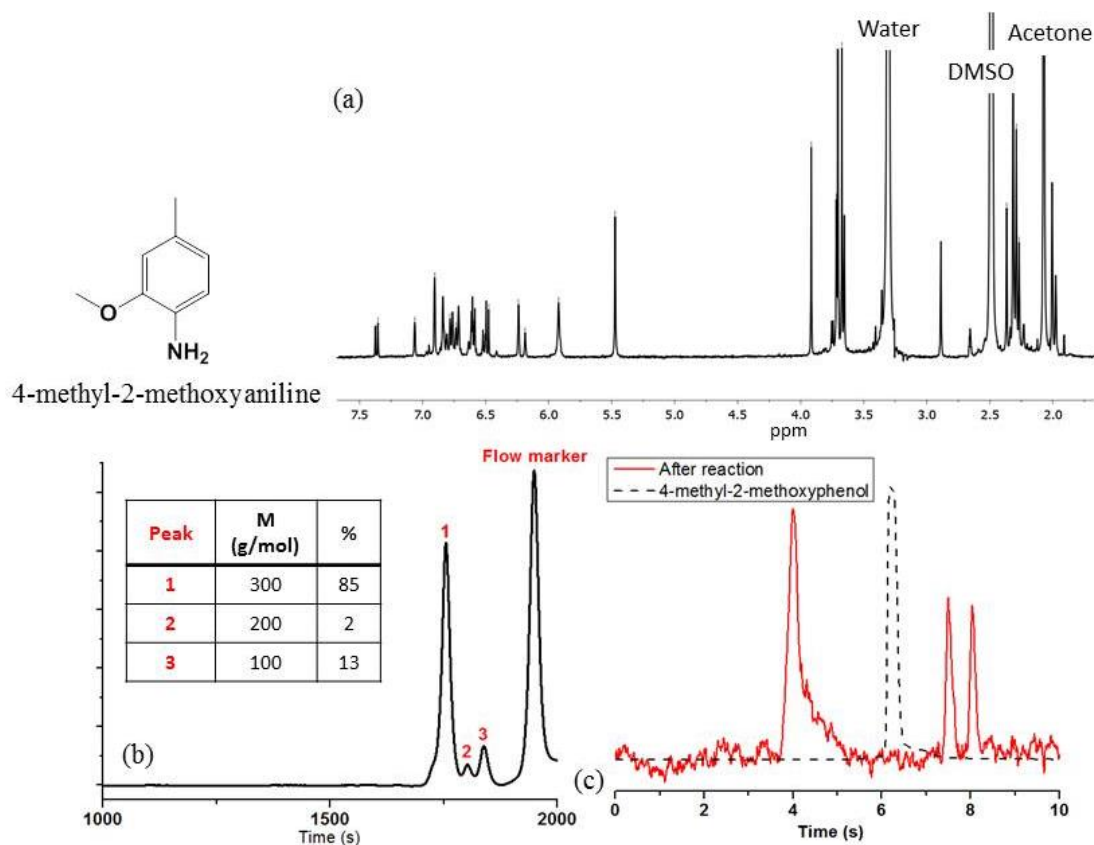
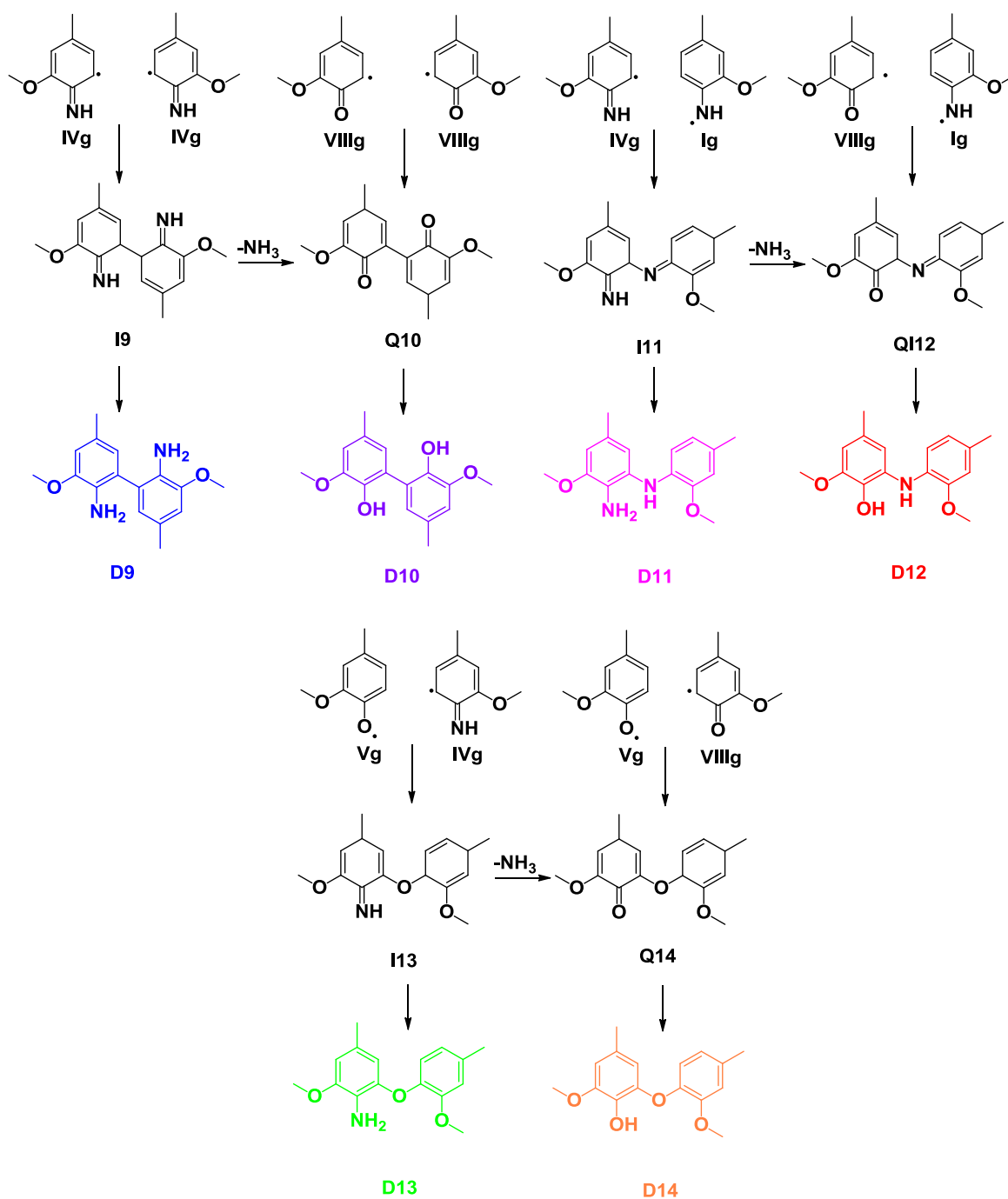


**Figure 24:** <sup>1</sup>H NMR spectrum in DMSO at room temperature (a), SEC trace in THF (b), HPLC profile using a C18 grafted silica column and acetonitrile as eluent (c) of product obtained by oxidative coupling of 4-methyl-2-methoxyaniline catalyzed by laccase.

It would be interesting to separate the dimers using Flash Chromatography, for instance. Especially, the isolation of **D9**, would provide a diamine which could be employed for polymer synthesis.



**Scheme 13:** Possible structures of dimers resulting from oxidative coupling of 4-methyl-2-methoxy aniline catalyzed by laccase.

### Conclusion:

The substrates implemented in this section under our experimental conditions, did not lead to the selective synthesis of dimers due to the large number of mesomeric forms yielding various coupling possibilities. All the results are summarized in Table 1-3 p 38-40. Random oligomers were produced by coupling of 4-methoxy phenol, 4-hydroxybenzyl alcohol, gaiacol and dimethyl phenol. Mixtures of dimers and trimers were obtained by coupling of vanillyl

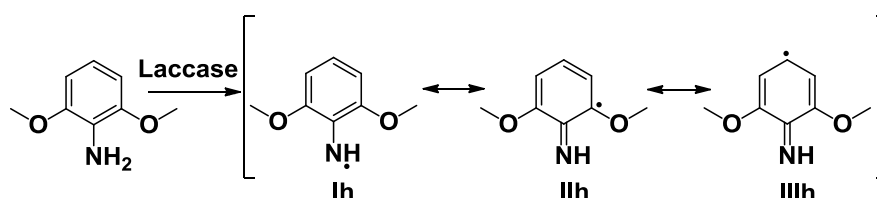
alcohol and 4-methyl-2-methoxyanillin; none of them seem to be majority and could be isolated in modest yield. However, the coupling of syringic acid and syringaldehyde leads to oligomers with a well-defined structure, which can be used as prepolymers. The coupling of vanillic acid seems to lead to tetramers or pentamers with a well-defined structure, which requires further investigations. The homo-coupling of isoeugenol and of 4-methyl-2-methoxy aniline result in the formation of dimers. Some of them could be interesting polymer building blocks after isolation.

## 2. Laccase-catalyzed selective coupling leading to single dimer formation

This section is dedicated to the substrates which oxidative coupling catalyzed by laccase leads to the formation of a single dimer.

### 1) An aniline derivative: 2,6-dimethoxyaniline

After 24 h reaction time, a precipitate is formed from the reaction of 4-methyl-2-methoxy aniline with laccase in only 30% yield. Surprisingly, both HPLC and SEC profiles showed a single peak, Figure 25 (b), (c). Exhibiting a molar mass of around 200 g/mol by SEC analysis, this compound was attributed to a dimer, **D15**. The aromatic triplet, **1**, with an integration of 1 and the aromatic doublet, **2**, with an integration of 2 revealed the presence of an aromatic ring with free *meta* and *para* positions, Figure 25 (a). The methoxy protons of this unit are represented by the singlet at 3.68 ppm, which integrates for 6 protons. Thus, the coupling should occur on the amine moiety. The second unit of the molecule displays two peaks for the methoxy protons at 3.80 and 3.50 ppm with an integration of 3 and two signals for the aromatic protons at 6.52 and 5.70 ppm with an integration of 1, respectively. **D15** is produced by coupling of structures **Ih** and **IIIh** (Scheme 14). A molar mass of 302 g/mol was determined by mass spectroscopy (see supporting information). This value corresponds to the molar mass of **D13** bearing a quinone moiety.



Scheme 14: Resonance forms 2,6-dimethoxyaniline obtained by laccase-catalyzed oxidative coupling.



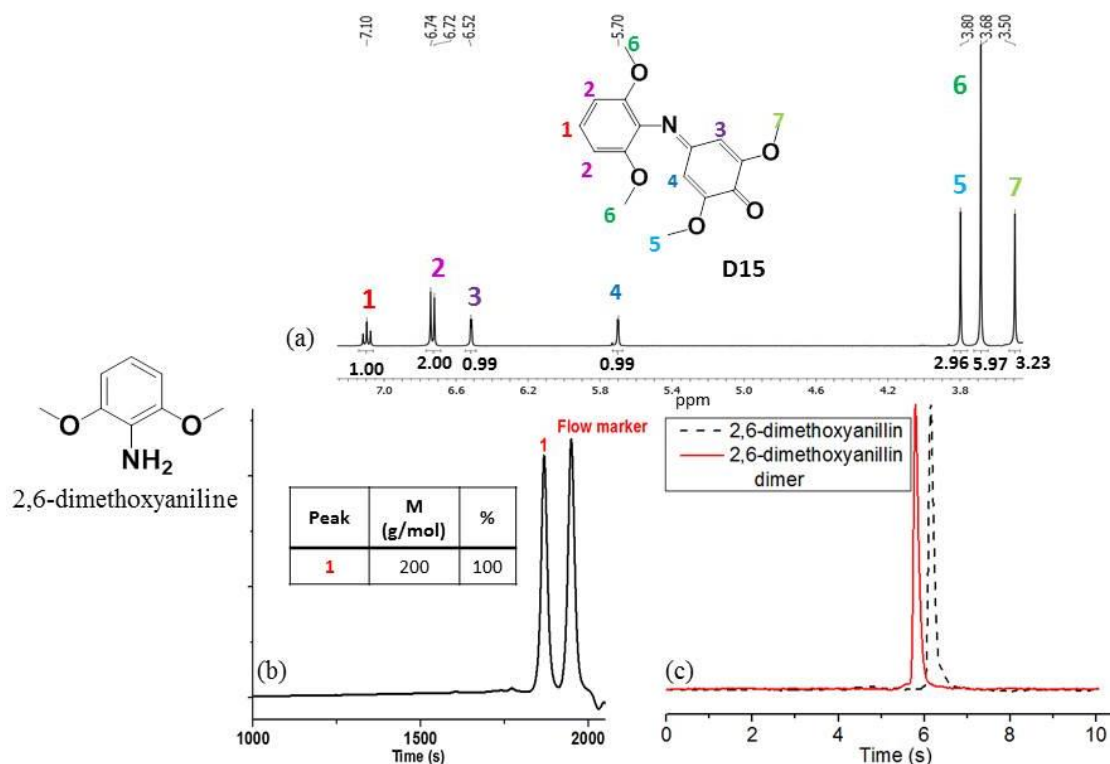
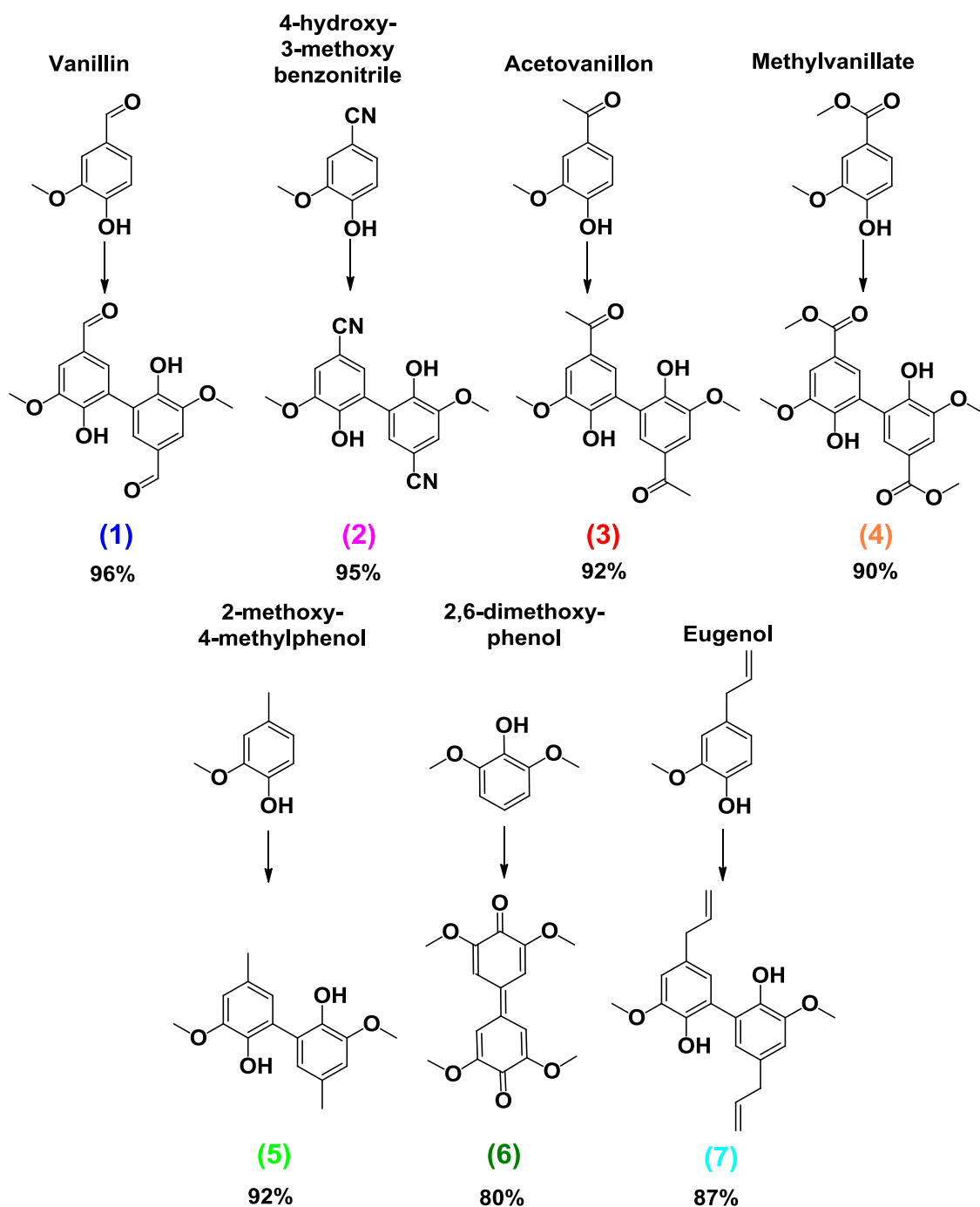


Figure 25: <sup>1</sup>H NMR spectrum in DMSO at room temperature (a), SEC traces in THF (b), HPLC profile using a C18 grafted silica and acetonitrile as eluent (c) of the product obtained by oxidative coupling of 2,6-dimethoxyaniline catalyzed by laccase.

## 2) Laccase-catalyzed synthesis of bisphenols in high yield

Laccase catalyzed selective oxidative coupling of seven compounds, **1-7**, including six *ortho*-monosubstituted-*para*-substituted phenols and one *ortho*-disubstituted phenol, leading to pure dimers in over 80% yield. These products are obtained by filtration and subsequent washing and drying and do not afford any further purification. The *ortho*-monosubstituted-*para*-substituted phenols possess aldehyde, nitrile, ketone, ester, methyl and alkylene as *para* substituents (Scheme 15), leading to divanillin (**1**), 4-hydroxy-3-methoxybenzoxynitrile dimer (**2**), diacetovanillon (**3**), methyl vanillate dimer (**4**), 2-methoxy-4-methylphenol dimer (**5**), and dieugenol (**7**), respectively. 2,6-dimethoxyphenol dimer (**6**) was produced by reaction of 2,6-dimethoxyphenol with laccase.



**Scheme 15: Laccase-catalyzed selective dimerization of vanillin, 4-hydroxy-3-methoxybenzonitrile, acetovanillon, methylvanillate, 2-methoxy-4-methyl phenol, 2,6-dimethoxyphenol and eugenol.**

The HPLC profiles of each reaction product show a single peak and the mass spectrum reveals the formation of the corresponding dimer. These analyses were not performed on acetovanillon dimer, which exhibited a poor solubility in solvents suitable for mass spectroscopy and HPLC. The figures belonging to these results are displayed in the supporting information. The symmetry of the molecule was instrumental in the easy interpretation of the  $^1\text{H}$  NMR. The main difference between substrate and dimer is the

disappearance of an aromatic proton (Figure 26). As explained for divanillin in the first section, the  $^{13}\text{C}$  NMR signals (Figure 27) are assigned by investigation of the 2D NMR, HMBC and HSQC spectroscopies, displayed in the supporting information.

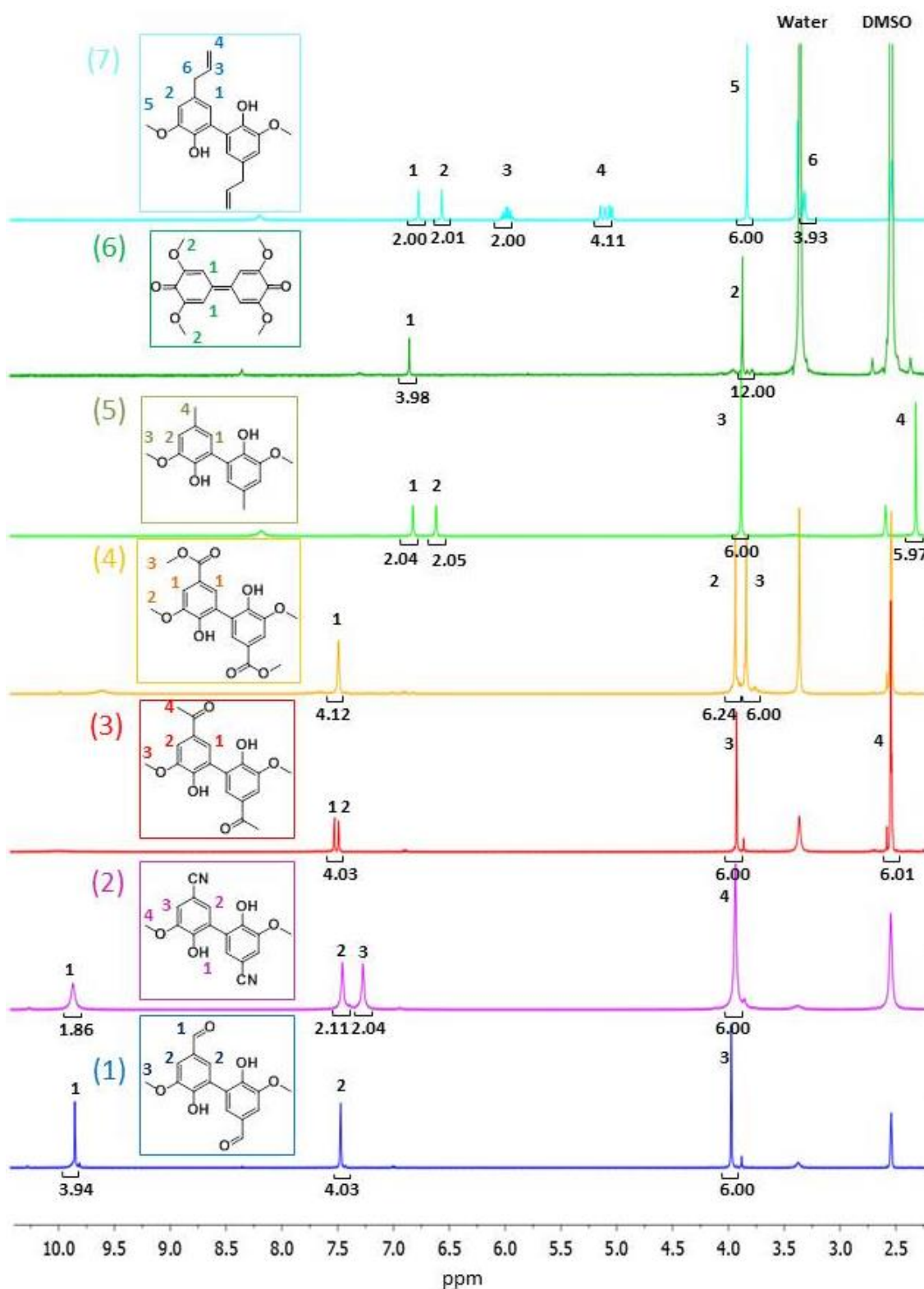
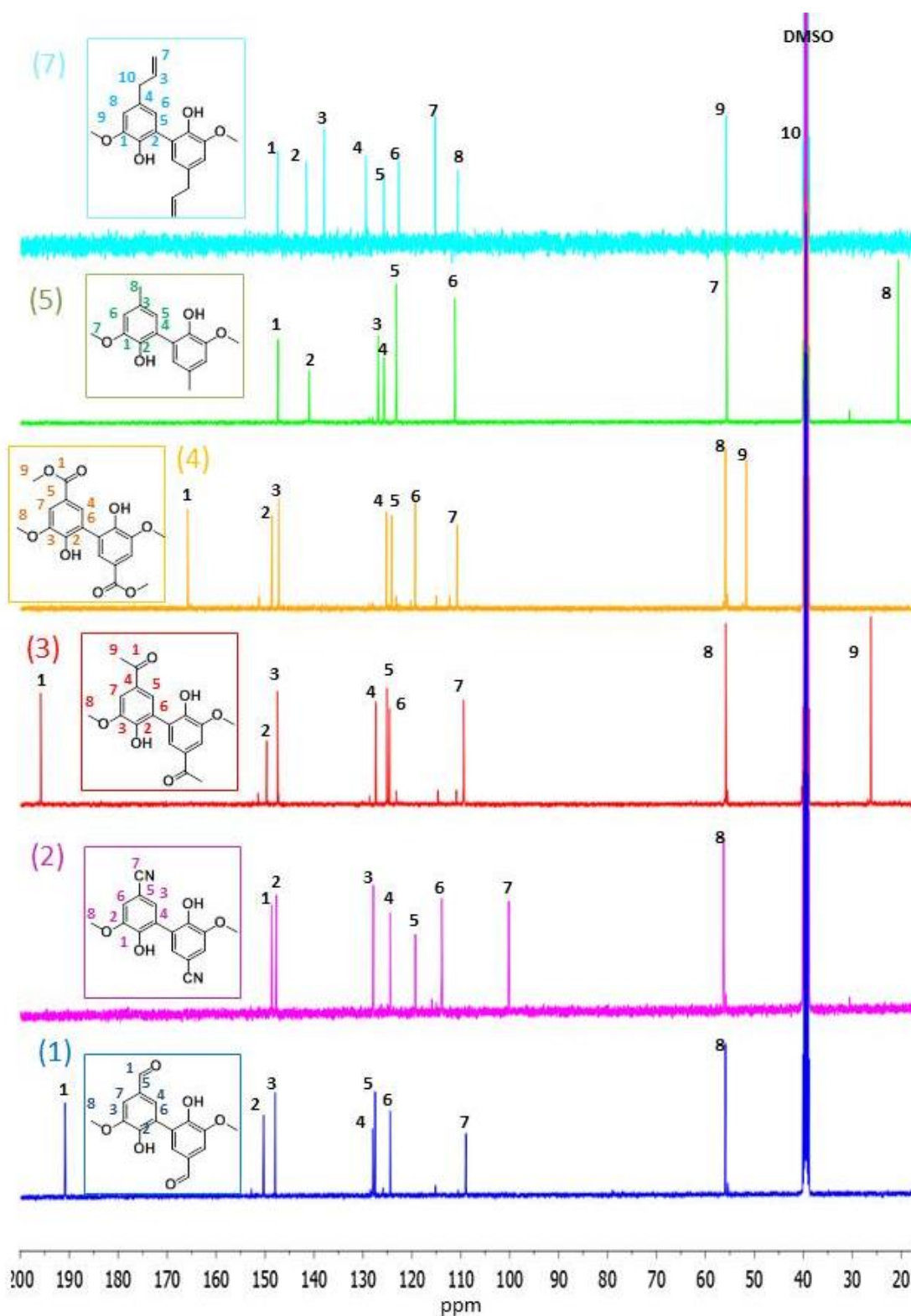


Figure 26:  $^1\text{H}$  NMR spectra in DMSO of the dimers obtained by selective oxidative coupling catalyzed by laccase.

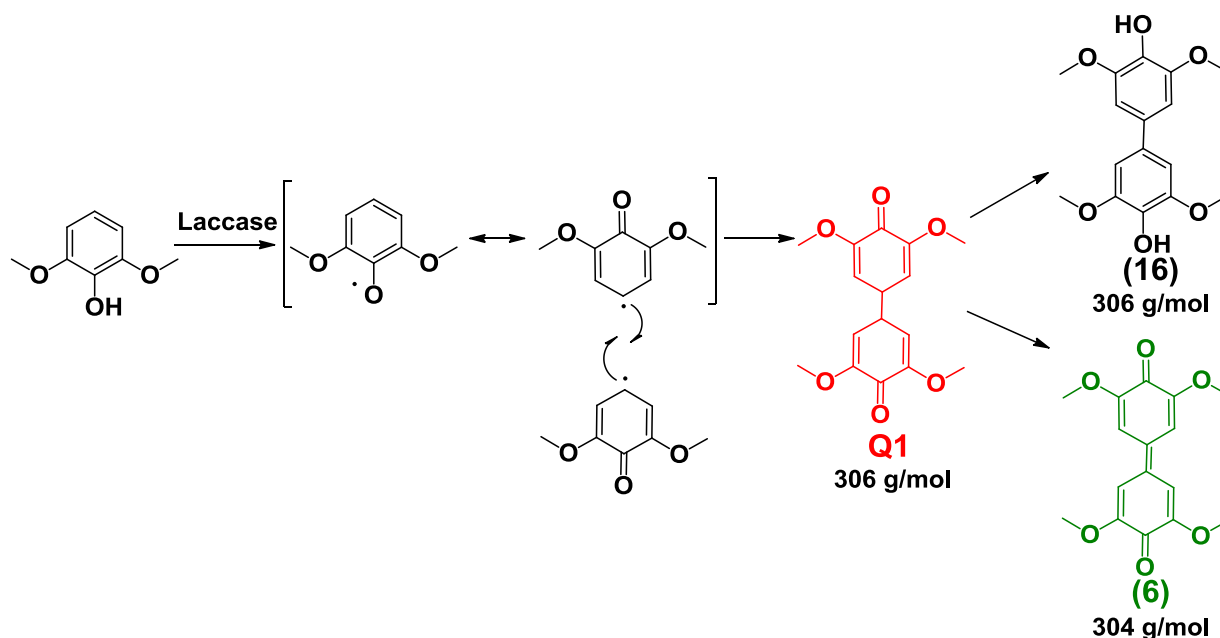


**Figure 27:**  $^{13}\text{C}$  NMR spectra in DMSO of the dimers obtained by selective oxidative coupling catalyzed by laccase.

Some interesting features have to be mentioned. The coupling of 2-methoxy-4-methylphenol is selective while the coupling of 2-methoxy-4-methylaniline leads to a complex mixture of

oligomers. In this case, the phenol moiety favors the C-C coupling, whereas the anillin moiety leads to both C-C and C-N coupling.

Under the aforementioned conditions, the coupling of 2,6-dimethoxyphenol led to a single dimer contrary to a previous study, where four demethylated products were also observed employing laccase from *Trametes pubescens*.<sup>24</sup> Mass spectroscopy resulted in a molar mass of 304 g/mol attributed to the quinone (**6**). During the oxidative coupling of 2,6-dimethoxyphenol, **Q1** is produced by recombination of two *para* radical species. Further reaction of this compound with laccase can lead either to its re-aromatization into compound (**16**) or to the formation of the very stable quinone (**6**) (Scheme 16). Compound (**6**) differs from (**16**) by its molar mass. Depending on the study the formation of **Q1**, (**16**) or (**6**) were reported.<sup>14,24,25</sup>



Scheme 16 : Laccase-catalyzed dimerization of 2,6-dimethoxyphenol.

It also worth to notice that the methoxy groups play an important role in the selectivity, as 2,6-dimethylphenol leads to oligomers whereas 2,6-dimethoxyphenol produces a single dimer, (**6**). This difference may be attributed to different inductive effects.

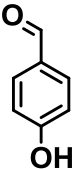
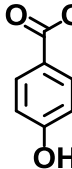
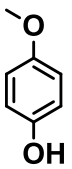
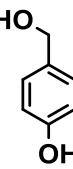
Finally, the 2,6-dimethoxyphenol dimer, (**6**), is formed *via* a C-C coupling although the formation of 2,6-dimethoxyaniline dimer, **D15**, involves a C-N bond. In this case, aniline derivatives favor the C-N coupling compared to the C-C coupling, whereas phenol derivatives favor the C-C linkage compared to the ether bond.

### Summary of phenolic coupling catalyzed by laccase:

The motivation of the substrate screening was to produce selectively dimers or oligomers prone for polymerization. All the substrates were potentially biobased excepted the 2,6-dimethyl phenol which was study to investigate the influence of the *ortho* substituent. The results are summarized in Table 1-3.

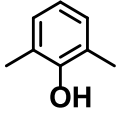
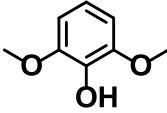
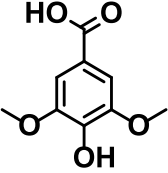
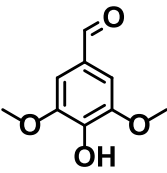
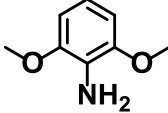
The *ortho* unsubstituted phenols bearing an electron withdrawing groups in para position did not couple, while the one bearing electron donating produced oligomers (Table 1).

**Table 1: Laccase-catalyzed oxidative coupling of *ortho* unsubstituted phenol.**

Name	<i>Ortho</i> unsubstituted phenol			
	Hydroxy-benzaldehyde	Hydroxy-benzoic acid	4-methoxy-phenol	4-hydroxy-benzyl alcohol
Structure				
Substituent in para position	Electron withdrawing	Electron withdrawing	Electron donating	Electron donating
Coupling	No	No	Oligomers up to 5 units C-O and C-C linkages	Polymer 50 units

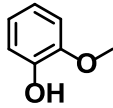
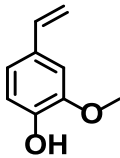
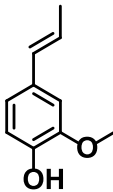
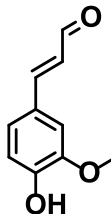
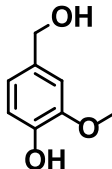
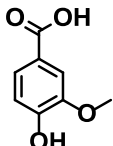
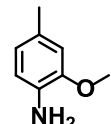
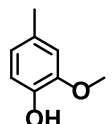
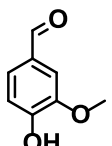
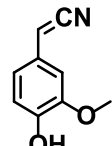
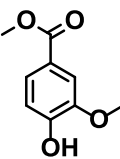
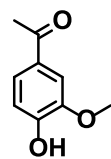
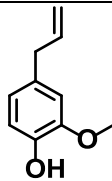
The coupling of *ortho* dimethoxy phenol/aniline led to pure dimers with C-C linkage in para position for the 2,6-dimethoxy phenol and C-N linkage for the 2,6-dimethoxy aniline. Dimethoxy phenol bearing a carboxylic acid moiety or an aldehyde moiety which can be oxidized into carboxylic acid underwent a decarboxylation mechanism producing poly(phenylene oxides) (Table 2).

Table 2: Laccase-catalyzed oxidative coupling of *ortho* disubstituted phenol/aniline.

	<i>Ortho</i> disubstituted phenol/aniline				
Name	2,6-dimethyl phenol	2,6-dimethoxy phenol	Syringic acid	Syringaldehyde	2,6-dimethoxy aniline
Structure					
Product	Oligomers between 2 and 11 units	Pure dimer	Well-defined oligomers 10 units	Well-defined oligomers 4 units	Pure dimer
Coupling position/mechanism	Phenolic and <i>para</i> positions	<i>para</i> position	Decarboxylation Poly(phenylene oxide)	Oxydation decarboxylation Poly(phenylene oxide)	<i>para</i> position/imide

The selectivity *ortho* monosubstituted phenol/aniline coupling depends on the *para* substituent (Table 3). The coupling of phenol with a hydrogen or a conjugated double bond in *para* position produced several oligomers. A carboxylic acid or an alcohol moiety in *para* position led to a mixture of dimers and oligomers due to a decarboxylation mechanism and the presence of benzylic hydrogens, respectively. Finally some *para* substituents such as aldehyde, ketone, methyl, nitrile, ester and non-conjugated double bond enabled the synthesis of pure dimers. These pure dimers will be chemically modified and polymerized.

Table 3: Laccase-catalyzed oxidative coupling of *ortho* mono substituted phenol/aniline.

Ortho monosubstituted phenol/aniline					
Name	Gaiacol	2-methoxy-4-vinyl phenol	Isoeugenol	Coniferaldehyde	Vanillyl alcohol
Structure					
Product	Oligomers up to 9 units	Oligomers up to 40 units	Dimers mainly + oligomers	Several dimers trimers tetramers	Mixture of dimers and tetramers
Coupling position	Phenolic, <i>para</i> , <i>ortho</i> positions C-O and C-C linkages	Phenolic, <i>para</i> , <i>ortho</i> positions C-O and C-C linkages	Phenyl coumaran and <i>ortho</i> - $\beta$ linkage	ND	ND
Ortho monosubstituted phenol/aniline					
Name	Vanillic acid	2-methoxy-4-methylaniline	2-methoxy-4-methylphenol	Vanillin	4-hydroxy-3-methoxy benzonitrile
Structure					
Product	Oligomers up to 5 units	3 Dimers + oligomers	Pure dimer	Pure dimer	Pure dimer
Coupling position / mechanism	Phenolic, <i>ortho</i> positions decarboxylation	ND	<i>ortho</i> positions	<i>ortho</i> positions	<i>ortho</i> positions
Ortho monosubstituted phenol/aniline					
Name	Methylvanillate	Acetovanillon	Eugenol		
Structure					
Product	Pure dimer	Pure dimer	Pure dimer		
Coupling position	<i>ortho</i> positions	<i>ortho</i> positions	<i>ortho</i> positions		

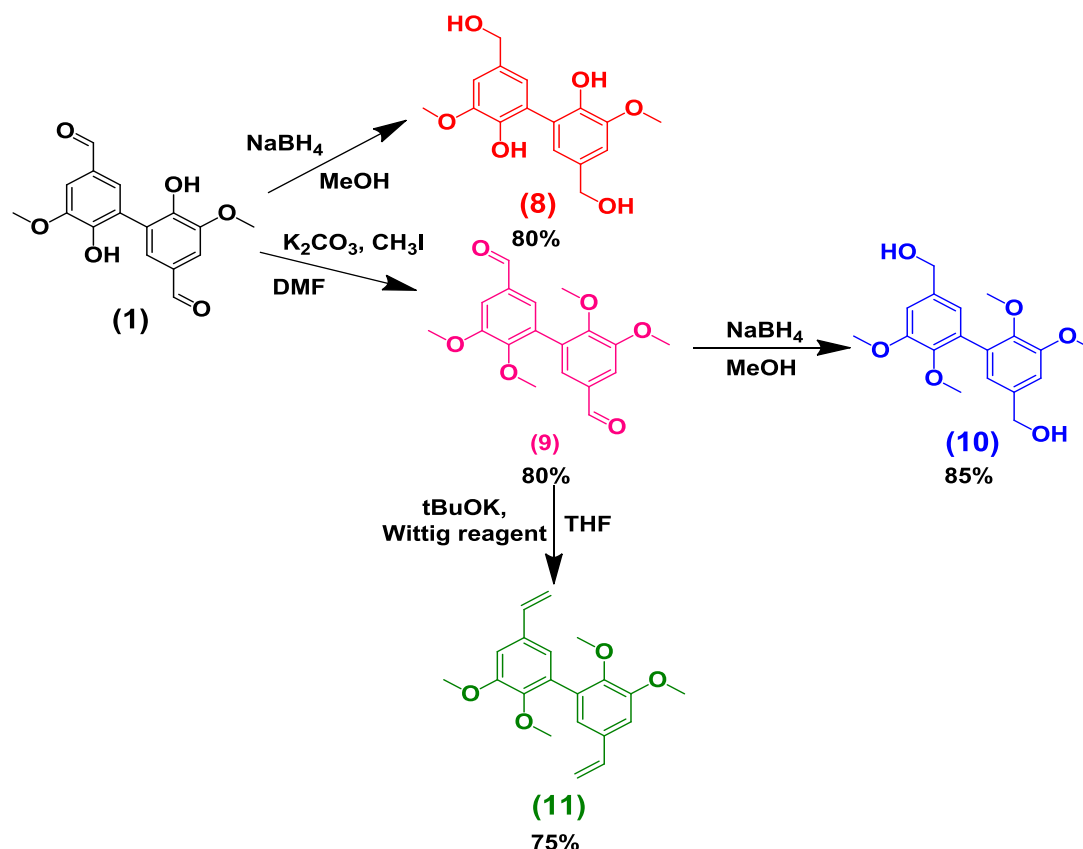


#### IV Chemical modifications of the biphenyl compounds

Dimers (1) to (7) were chemically modified to have a palette of monomers potentially ready to be polymerized. Diols, diacids, divinyl, (bis)epoxides, diesters and bisunsaturated compounds were synthesized and characterized by NMR spectroscopy. The  $^{13}\text{C}$  NMR spectra of the molecules are displayed in supporting information. When needed, 2D NMR, HMBC and HSQC were run to assign the  $^{13}\text{C}$  NMR signal. These spectra are also included in the supporting information.

##### 1. Chemical modifications of divanillin (1)

Divanillin produced by laccase-catalyzed oxidative coupling of vanillin was modified into several compounds (Scheme 17).



**Scheme 17: Chemical modifications of divanillin (1), synthesis of diol, divinyl compound and methylated compounds.**

In the previous section, we observed that the coupling of vanillyl alcohol did not lead to a pure dimer. So, divanillyl diol (8) was synthesized by reduction of divanillin employing  $\text{NaBH}_4$  as reduction agent. In order to have a difunctional monomer and to further synthesize thermoplastic polymers, phenol moieties must be protected. Phenols were methylated with

iodomethane, in a basic medium, in DMF, yielding methylated divanillin (**9**). Divanillyl diol (**10**) was then prepared by reduction of (**9**). A Wittig reaction was performed on (**9**), in dry THF, employing methyltriphosponiumiodide as Wittig reagent, and potassium tert-butoxide as a base. The resulting divinyl compound (**11**) could be a bio-based substitute to divinyl benzene. All compounds, excepted (**11**) were obtained without any further purification. In case of (**11**), the crude product was purified by column chromatography.

The completion of the reaction and purity of the resulting products were determined by  $^1\text{H}$  NMR spectroscopy (Figure 28).

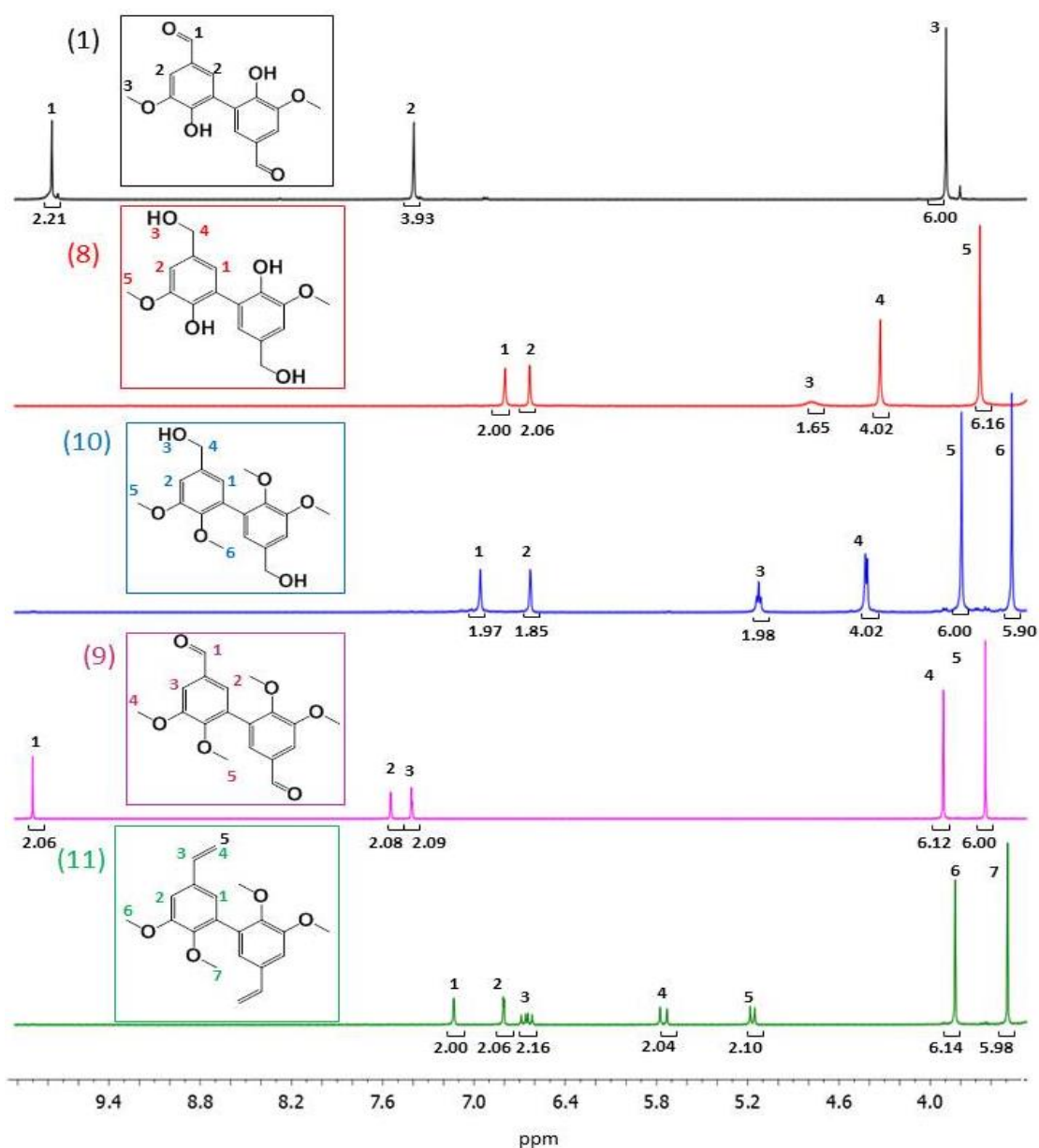


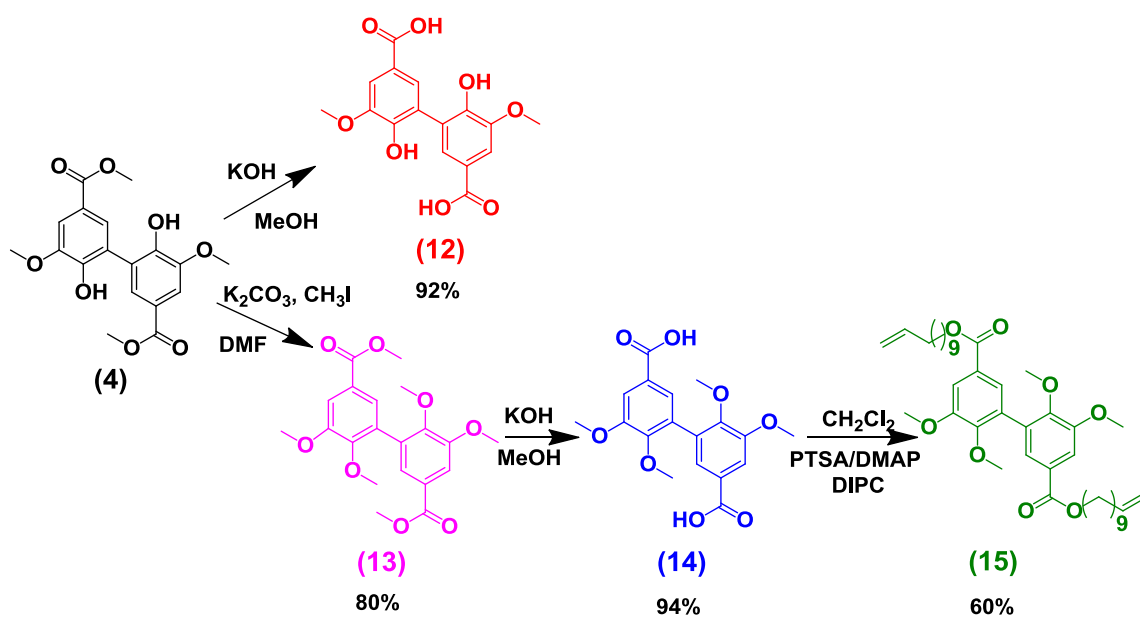
Figure 28:  $^1\text{H}$  NMR spectra in DMSO, at room temperature of molecules (**8**), (**9**), (**10**), (**11**) synthesized from divanillin (**1**).

The  $^1\text{H}$  NMR spectrum of the diol (**8**) shows the disappearance of the aldehyde signal at 9.84 ppm and the appearance of signals assigned to the alcohol  $\alpha$ -carbon at 4.37 ppm and to the hydroxyl proton at 4.81 ppm. The success of the methylation reaction is confirmed by the appearance of a second methoxy singlet at 3.69 ppm on the spectrum of (**9**). The reduction of the dialdehyde (**9**) in diol (**10**) is proven by the absence of the aldehyde signal at 9.94 ppm and the formation of two new peaks at 5.17 and 4.47 ppm, assigned to hydroxyl moiety and the protons of the alcohol  $\alpha$ -carbon, respectively. Finally, the  $^1\text{H}$  NMR spectrum of the divinyl compound (**11**) displays the absence of the aldehyde signal at 9.94 ppm and the appearance of three peaks at 6.68, 5.81 and 5.77 ppm assigned to the vinyl moiety.

## 2. Chemical modifications of methyl vanillate dimer (**4**)

Methyl vanillate dimer produced by laccase-catalyzed oxidative coupling of methyl vanillate was also modified into several compounds (Scheme 18).

As the coupling of vanillic acid did not lead to a pure dimer, divanillic diacid (**12**) was synthesized by hydrolysis of methyl vanillate dimer with potassium hydroxide. In order to synthesize a difunctional monomer, the phenol moieties of (**4**) were methylated with iodomethane, under basic conditions resulting in methylated diester (**13**). Afterwards, methylated diacid (**14**) was prepared by hydrolysis of (**13**) with potassium hydroxide. Bisunsaturated diester (**15**) was synthesized by esterification of (**14**) with undecenol, using PTSA/DMAP and DIPC. All the compounds, excepted (**15**) were obtained without any further purification step. In case of (**15**), the crude product was purified by column chromatography.



Scheme 18: Chemical modifications of the diester (**4**) leading to diacids and bisunsaturated diester.

The completion of the reaction and purity of the so-formed products were monitored by  $^1\text{H}$  NMR spectroscopy (Figure 29). The hydrolysis of diesters (**12**) and (**14**) was confirmed by the disappearance of the methyl ester peak at 3.84 ppm. The appearance of the second methoxy singlet at 3.67 ppm on the spectrum of (**13**) shows the completion of the methylation of (**4**).

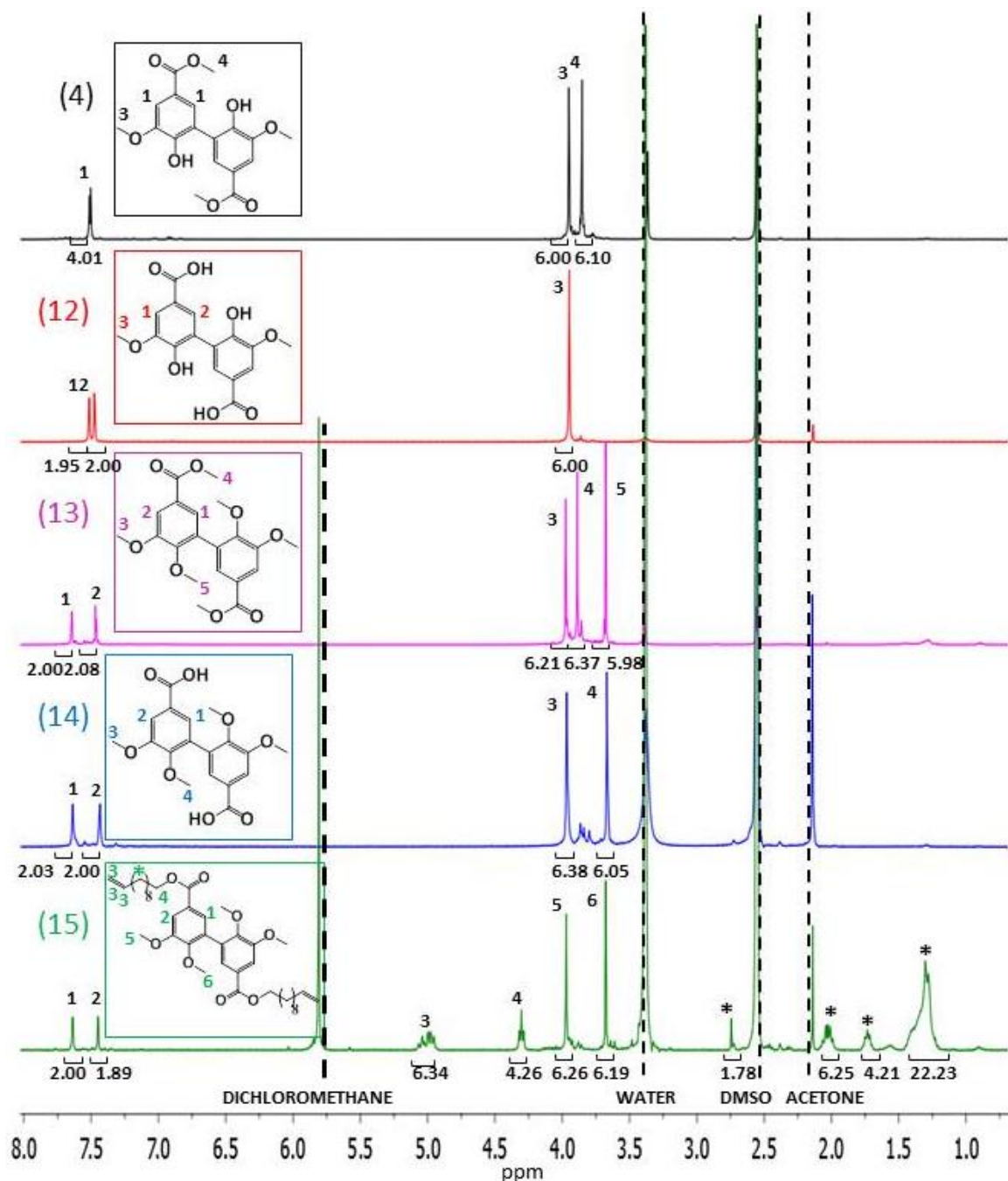
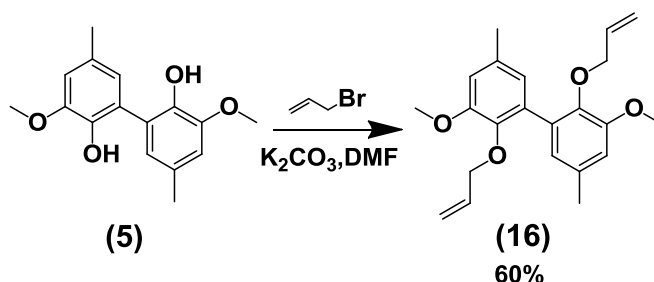


Figure 29:  $^1\text{H}$  NMR spectra in DMSO, at room temperature of (**12**), (**13**), (**14**), (**15**) synthesized from methyl vanillate dimer (**4**).

Finally, the disappearance of the methyl ester peak at 3.84 ppm and the appearance of all the peaks assigned to undecenoate moiety, with a 1:1 integration to the aromatic peaks are observed on the  $^1\text{H}$  NMR spectrum of **(15)**.

### 3. Chemical modifications of 2-methoxy-4-methylphenol dimer **(5)**

In addition, a new bis-unsaturated compound **(16)** was synthesized by etherification of **(5)** with allyl bromide, under basic conditions (Scheme 29).



Scheme 19: Chemical modification of 2-methyl-4-methoxyphenol dimer **(5)**.

The completion of the reaction was monitored by  $^1\text{H}$  NMR. The appearance of the peak at 4.23 ppm is assigned to the  $\alpha$ -carbon of the ether moiety. The peaks at 5.70 and 4.99 ppm are attributed to the terminal double bonds (Figure 30).

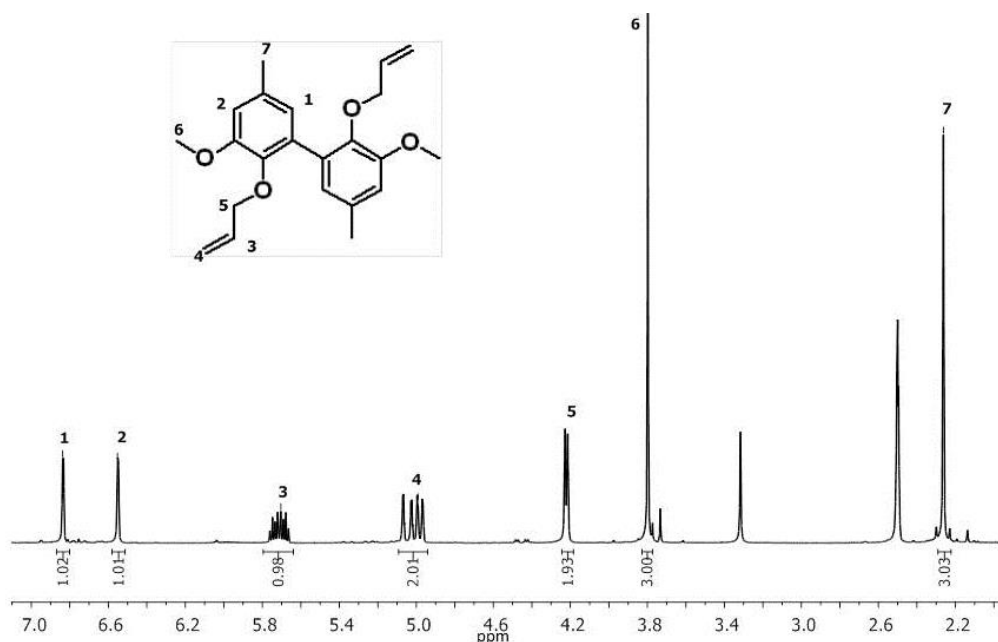
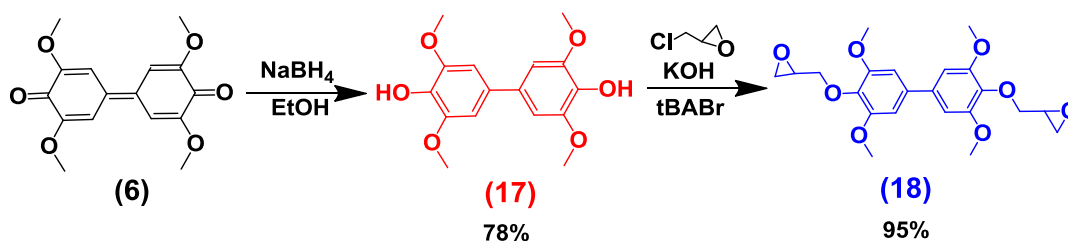


Figure 30:  $^1\text{H}$  NMR of allylated 2-methoxy-4-methylphenol dimer **(16)** in DMSO, at room temperature.

The epoxidation of **(16)** employing mCPBA was not a success. Other epoxidation methods should be investigated in order to synthesize epoxy resins.

#### 4. Chemical modifications of 2,6-dimethoxyphenol dimer (6)

The dimerization of 2,6-dimethoxyphenol led to a purple product which was identified as a quinone (6) with a molar mass of 304 g/mol. Subsequent reduction of (6) with NaBH<sub>4</sub> produced a white solid with a molar mass of 306 g/mol, attributed to the bisphenol (17) (Scheme 20). The appearance of the phenol signal was observed at 8.4 ppm on the <sup>1</sup>H NMR spectrum.



Scheme 20: Chemical modifications of 2,6-dimethoxyphenol dimer (6).

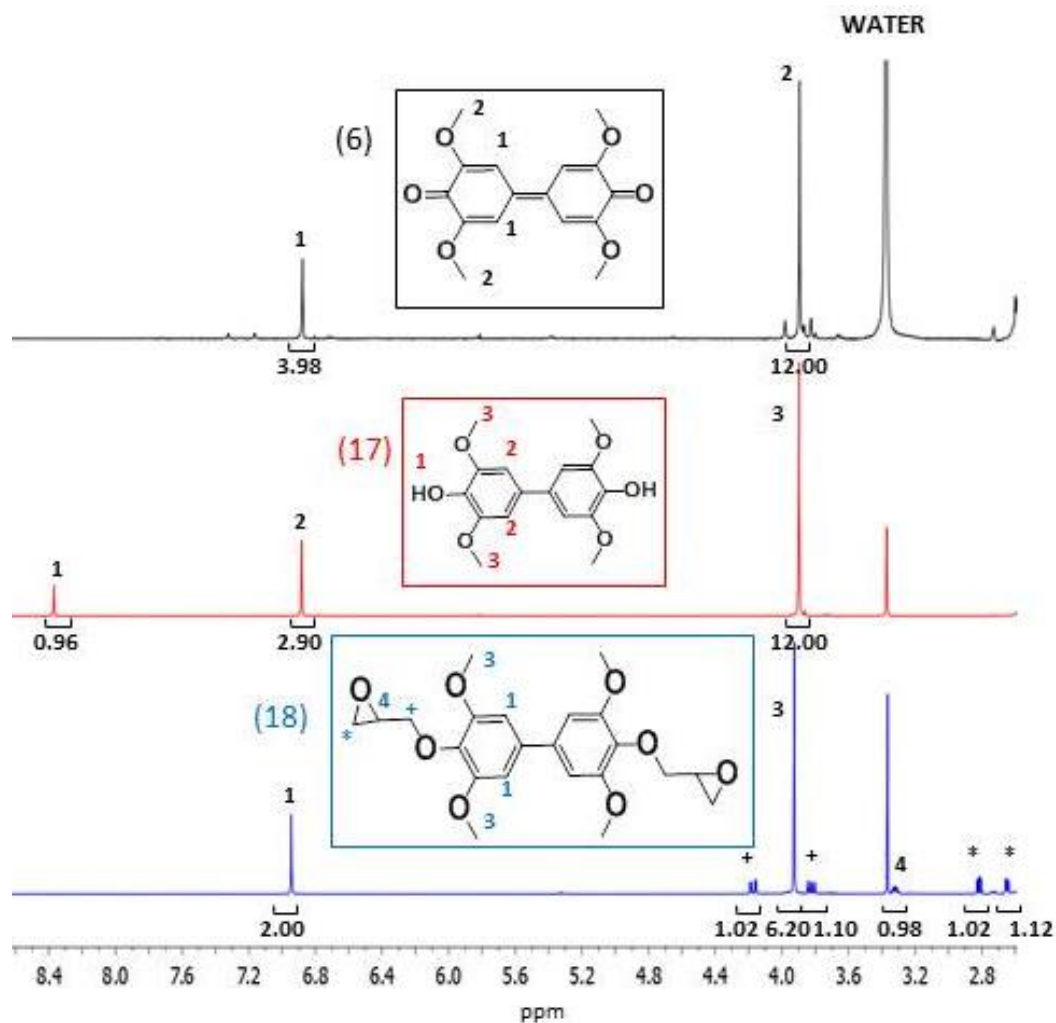


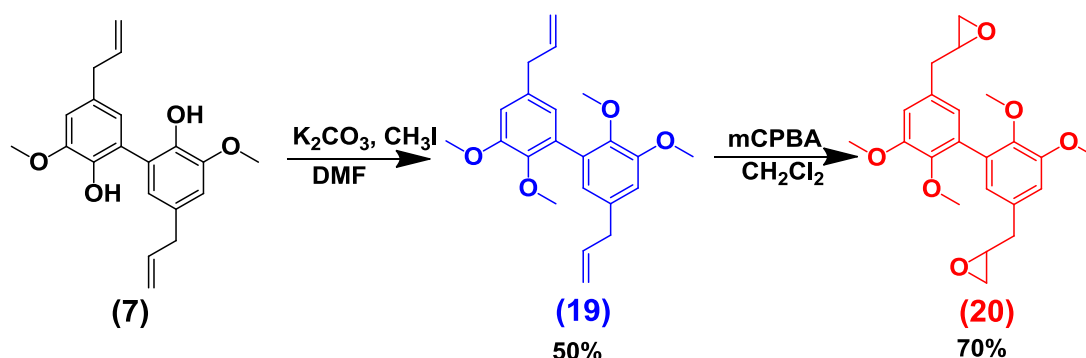
Figure 31: <sup>1</sup>H NMR spectra, in DMSO, at room temperature, of (17) and (18) synthesized from 2,6-dimethoxyphenol dimer (6).

The reaction between the bisphenol (**17**) and epichlorohydrin, employing TBABr as transfer agent, under basic conditions resulted in the bisepoxide (**18**) in 95% yield. The  $^1\text{H}$  NMR spectrum of (**18**) displays aromatic and methoxy singlets at 6.94 and 3.93 ppm, characteristic of the biphenyl and signals at 3.26, 2.82 and 2.64 ppm assigned to the epoxy group. The peaks at 4.18 and 3.80 ppm correspond to the protons of the  $\alpha$ -carbon of the ether moiety (Figure 31).

### 5. Chemical modifications of dieugenol (**7**)

Dieugenol produced by laccase-catalyzed oxidative coupling of eugenol was modified into several compounds (Scheme 21).

Some catalysts may be sensitive to phenol moieties. In order to modify dieugenol, the phenol moieties of (**7**) were methylated with iodomethane, under basic conditions, resulting in methylated dieugenol (**19**). Mild Oxidation of (**19**) in presence of *m*CPBA led to the bisepoxide (**20**).



Scheme 21: Chemical modifications of dieugenol (**7**).

The completion of the reaction and purity of the so-formed products were monitored by  $^1\text{H}$  NMR spectrum (Figure 32). The appearance of the second methoxy singlet at 3.67 ppm on the  $^1\text{H}$  spectrum of (**19**) shows the completion of the methylation of (**7**). The  $^1\text{H}$  NMR spectrum of (**20**) shows that the complete disappearance of the signals of the double bond signals at 5.11 and 6.02 ppm and the appearance of new signals attributed to oxirane at 2.62, 2.80 and 3.19 ppm.



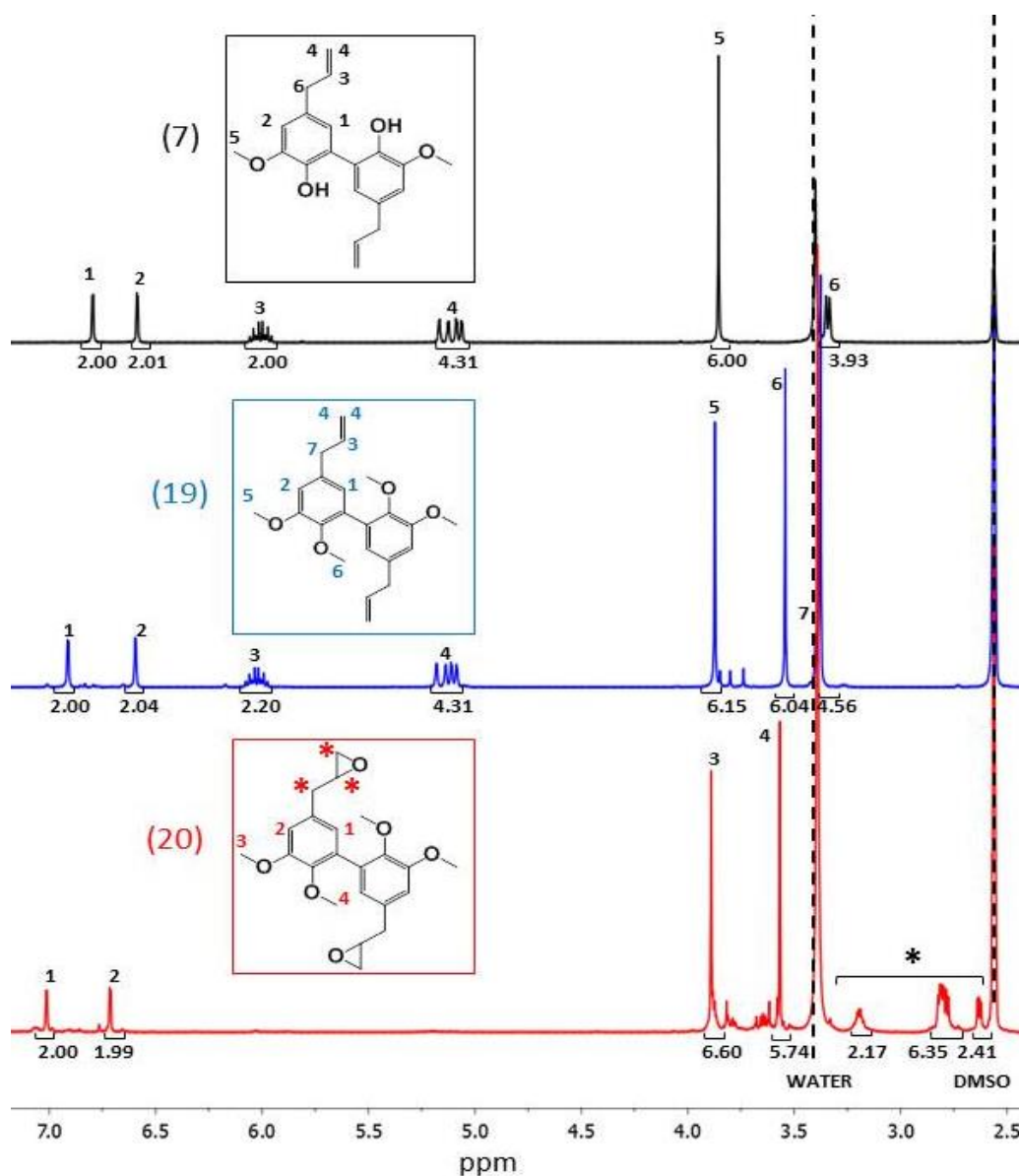


Figure 32:  $^1\text{H}$  NMR spectra, in DMSO, at room temperature, of (19) and (20) synthesized from dieugenol (7).

## V Conclusion and perspectives

In this chapter, a green and easy way to synthesize high purity divanillin in high yield and large quantity was developed. This process presents several advantages: (i) the divanillin formation occurs at room temperature, under oxygen which could be replaced by air, (ii) the employed solvent, 10% of acetone, shows a low toxicity, (iii) the product extraction is easy and the purity is high (95%) because the solvent conditions enabled the reactant solubility while the so-formed product precipitated, (iv) a low quantity of enzyme is needed, 20 U of laccase for 1.5 g of vanillin and can be reused. Kinetic studies allowed us to determine some



parameters important to reach high vanillin conversion. Organic solvent compatible with laccase is required to solubilize the organic compound but its amount should be minimized in order to reach high yield. The solution should contain enough oxygen allowing laccase catalysis activity to be a maximum. The use of a buffer allows the pH to stay optimal, requirement for the completion of the reaction. Temperature parameter was not investigated but should be between 20 °C and 60 °C to avoid the enzyme denaturation.

This procedure was applied to several substrates in order to synthesize other dimers or oligomers suitable for polymer synthesis and to understand better the oxidative coupling mechanism of laccase. Depending on the aromatic substituents, this procedure leads to a oligomeric mixture or selective dimers.

The coupling of some compounds results in the formation of single dimer. Indeed, vanillin, 4-hydroxy-3-methoxybenzonitrile, methyl vanillate, 4-methyl-2-methoxyphenol, 2,6-dimethoxyphenol and eugenol produced dimers with yield over 80%. These compounds were obtained with high purity and do not need further purification.

These dimers were chemically modified into diols, diacids, bis-unsaturated diesters, divinyl compound and bisepoxides. Phenols were protected by methylation in several cases. The synthesis of polymers from this palette of phenolic compounds is discussed in the next chapter.

## VI References

1. M. Mogharabi and M. A. Faramarzi, *Advanced Synthesis & Catalysis*, **2014**, 356, 897-927.
2. J.-R. Jeon and Y.-S. Chang, *Trends in Biotechnology*, **2013**, 31, 335-341.
3. S. Kobayashi and H. Higashimura, *Progress in Polymer Science*, **2003**, 28, 1015-1048.
4. S. Kobayashi and A. Makino, *Chemical Reviews*, **2009**, 109, 5288-5353.
5. S. Kobayashi, S.-i. Shoda and H. Uyama, in *Polymer Synthesis/Polymer Engineering*, Springer Berlin Heidelberg, 1995, vol. 121, ch. 1, pp. 1-30.
6. S. Kobayashi, H. Uyama and S. Kimura, *Chemical Reviews*, **2001**, 101, 3793-3818.
7. N. Mita, S.-i. Tawaki, H. Uyama and S. Kobayashi, *Macromolecular Bioscience*, **2003**, 3, 253-257.
8. S. Riva, *Trends in Biotechnology*, **2006**, 24, 219-226.
9. E. I. Solomon, U. M. Sundaram and T. E. Machonkin, *Chemical Reviews*, **1996**, 96, 2563-2606.
10. M.-A. Constantin, J. Conrad and U. Beifuss, *Green Chemistry*, **2012**, 14, 2375-2379.
11. J. L. Manoj Gaur, V. R. Balakrishnan, P. Raghunathan and a. S. V. Eswaran, *Bull. Korean Chem. Soc.*, **2009**, 30, 2895-2898.
12. C. Bohlin, K. Lundquist and L. J. Jönsson, *Bioorganic Chemistry*, **2009**, 37, 143-148.
13. R. Ikeda, J. Sugihara, H. Uyama and S. Kobayashi, *Polymer International*, **1998**, 47, 295-301.
14. F. Medina, S. Aguila, M. C. Baratto, A. Martorana, R. Basosi, J. B. Alderete and R. Vazquez-Duhalt, *Enzyme and Microbial Technology*, **2013**, 52, 68-76.
15. R. Ikeda, J. Sugihara, H. Uyama and S. Kobayashi, *Macromolecules*, **1996**, 29, 8702-8705.
16. C. Navarra, P. Gavezzotti, D. Monti, W. Panzeri and S. Riva, *Journal of Molecular Catalysis B: Enzymatic*, **2012**, 84, 115-120.
17. C. Ponzoni, E. Beneventi, M. R. Cramarossa, S. Raimondi, G. Trevisi, U. M. Pagnoni, S. Riva and L. Forti, *Advanced Synthesis & Catalysis*, **2007**, 349, 1497-1506.
18. O. E. Adelakun, T. Kudanga, A. Parker, I. R. Green, M. le Roes-Hill and S. G. Burton, *Journal of Molecular Catalysis B: Enzymatic*, **2012**, 74, 29-35.
19. Y. N. Kupriyanovich, S. A. Medvedeva, A. V. Rokhin and L. V. Kanitskaya, *Russ J Bioorg Chem*, **2007**, 33, 516-522.
20. M. Lahtinen, K. Kruus, P. Heinonen and J. Sipilä, *Journal of Agricultural and Food Chemistry*, **2009**, 57, 8357-8365.
21. H. P. Lahtinen M, Oivanen M, Karhunen P, Kruus K, Sipilä J., *Org Biomol Chem*, **2013**, 11, 5454-5464.
22. A. S. Amarasekara, B. Wiredu and A. Razzaq, *Green Chemistry*, **2012**, 14, 2395-2397.
23. G. Shumakovich, A. Streltsov, E. Gorshina, T. Rusinova, V. Kurova, I. Vasil'eva, G. Otrokhov, O. Morozova and A. Yaropolov, *Journal of Molecular Catalysis B: Enzymatic*, **2011**, 69, 83-88.
24. O. E. Adelakun, T. Kudanga, I. R. Green, M. le Roes-Hill and S. G. Burton, *Process Biochemistry*, **2012**, 47, 1926-1932.
25. C. Aouf, C. Le Guernevé, S. Caillol and H. Fulcrand, *Tetrahedron*, **2013**, 69, 1345-1353.

## VII Experimental

### *Enzymatic dimerization general procedure*

A solution of 1.5 g of phenol in 20 mL of acetone was added to 180 mL of NaOAc buffer (0.1 M, pH 5.0). The solution was saturated in O<sub>2</sub> for 5 min. Laccase from *Trametes versicolor* (20 U, 12.4 mg) was added and the reaction was stirred at room temperature for 24 h. The precipitate was filtered, or if no precipitate was formed, the product was extracted with dichloromethane.

This procedure was adapted on 15 g in the case of vanillin. Yield: 96%.

### *Refill procedure*

After filtration of the dimer, the solution was kept, refilled with 1.5 g of vanillin O<sub>2</sub> again. After 24 h, the precipitate was filtered and the refill procedure followed again up to 10 times.

### *4-Hydroxy-3-methoxybenzotrile synthesis*

750 mg (5 mmol) of vanillin were dissolved in 15 mL of acetic acid. 520 mg of NH<sub>2</sub>OH.HCl (7.5 mmol) were added and the mixture was stirred and warmed at 110°C for 2 h. The reaction was stopped by adding H<sub>2</sub>O, the organic product extracted using CH<sub>2</sub>Cl<sub>2</sub>, dried and purified by flash chromatography (Ethyl acetate/cyclohexane 3/7). Yield: 95%

### *Methylvanillate synthesis*

15 g of vanillic acid (0.09 mol) were dissolved in 75 mL of methanol. 2.1 mL of sulfuric acid were added and the mixture was stirred and warm to reflux for 8 h. After evaporation of Methanol, the solid was dissolved in 60 mL of ethylacetate, washed with 30 mL of NaHCO<sub>3</sub> solution, water (2 times) and brine (1 time). The organic phase was evaporated under reduced pressure. Yield: 90%

### *General procedure of phenol methylation (9), (13), (19)*

26 mmol of bisphenol compound (divanillin, dimethyl divanillate or dieugenol) (≈ 8 g) were dissolved in 120 mL of DMF. 15.2 g of potassium carbonate (110 mmol) were added before a slow addition of 9.6 mL of iodomethane (158 mmol). After 15 h of stirring at 80°C, the

mixture was filtered and the resulting solution poured into cold water. The methylated compound, which precipitated was filtered off and dried under vacuum. Yield: 75-80%

*General procedure for aldehyde reduction (8), (10)*

20 mmol of dialdehyde (divanillin or methylated divanillin) ( $\approx 6$  g) were dissolved in 100 mL of ethanol. The flask was put in an ice bath and 3.6 g of sodium borohydride (100 mmol) were added slowly. Then the mixture was stirred at room temperature for 30 min. 45 mL of water were added to stop the reaction and the solution is acidified with HCl to pH 7 and warmed for 5 min at 50°C. The solvent was evaporated; the resulting solid was solubilized in dichloromethane and washed 3 times with water. Yield: 80-85%

*Divinyl synthesis: Wittig reaction (11)*

3 g of triphenylphosphine (11.4 mmol) were dissolved in 30 mL of toluene. 0.7 mL of iodomethane (11.4 mmol) was added drop-wise. The mixture is stirred to reflux at 120°C under nitrogen flow. Methyltriposponiumiodide precipitated and was filtered off and dried under vacuum.

To a solution of methyltriposponiumiodide (8.8 g, 22 mmol) in dry THF (36 mL), 2.7 g of potassium tert-butoxide were added at 0°C. After 1h of stirring at room temperature under nitrogen, 3.2 g of divanillin (10 mmol) was added. The mixture is stirred at 35°C for 24h. The solution was diluted with 75 mL of dichloromethane, washed with water and 2 times with brine. The solvent of the organic phase is evaporated. The remaining reactants were eliminated by silica column purification using dichloromethane/cyclohexane 50/50. Yield: 75%

*General procedure for diester saponification (12), (14)*

7 mmol of diester (dimethyl divanillate or methylated dimethyl divanillate) ( $\approx 2.5$  g) were dissolved in 10 mL of methanol. 2.5 g of KOH (45 mmol) were added and the solution was warmed to reflux for 9h. The reaction was stopped with 2.5 mL of water. The remaining diester was extracted with diethylether. The aqueous phase was acidified with HCl and the diacid precipitated. Yield: 93%

*Bisunsaturated diester synthesis (15)*

3 g of dimethyldivanillate (16 mmol of acid functional groups) was dissolved in 80 ml of CH<sub>2</sub>Cl<sub>2</sub> under stirring. Subsequently p-toluene sulfonic acid/4-dimethylaminopyridine catalyst

in a molar ratio 1/1.2 was added (4.42 g, 16 mmol). The flask was placed in an ice bath and subsequently an excess of undecenol (4.8 mL, 24 mmol) was added to the solution. Finally, N,N'-diisopropyl carbodiimide (DIPC, 7.2 ml 46 mol) was added dropwise under stirring. The reaction was left under stirring for 72 hours at room temperature. Afterwards the solution was washed three times with water, dried and the solvent was removed under reduced pressure. The product was a yellow brown viscous liquid. The acylurea formed was eliminated by filtration after dissolution of the product in toluene. The remaining reactants were eliminated by silica column purification using dichloromethane. Yield: 60%

#### *Synthesis of allyl compounds (16)*

26 mmol of bisphenol compound (**7**) (8 g) were dissolved in 120 mL of acetone. 15.2 g of potassium carbonate (110 mmol) were added before a slow addition of 13.5 mL of allyl bromide (158 mmol). After 15 h of stirring at 80°C, the mixture was filtered, the solvent evaporated and the resulting solid dried under vacuum. Yield: 60%

#### *Reduction of 2,6-dimethoxy phenol dimer (17)*

6 g of 2,6-dimethoxy phenol dimer (20 mmol) were dissolved in 180 mL of Ethanol. The flask was put in an ice bath and 6.75 g of sodium borohydride (178 mmol) were added slowly. Then the mixture was stirred at room temperature for 30 min. 80 mL of water were added to stop the reaction and the solution was acidified with HCl to pH 7 and warmed for 5 min at 50°C. The solvent was evaporated; the resulting solid was solubilized in dichloromethane and washed 3 times with water. Yield: 78%

#### *Synthesis of bisepoxide (18)*

5 g of reduced 2,6-dimethoxy phenol dimer (16 mmol) were dissolved in 16 mL of epichlorohydrin. 7.9 g of potassium hydroxide (141 mmol) and 1 g of tetrabutylammonium bromide (3.1 mmol) were added and the solution is stirred at room temperature for 4 h. The product is extracted with dichloromethane and washed with water. Dichloromethane and epichlorohydrin are removed from the organic phases under vacuum. Yield: 95%

#### *Synthesis of epoxidized dieugenol (20)*

To a solution containing 5 mmol of methylated dieugenol (**19**) 50 mL of chloroforme was added drop-wise a solution containing 10 mmol of mCPBA in 2 mL of chloroforme. The

solution was stirred under static nitrogen at room temperature for 20 h. The resulting solution was washed 3 times with a saturated solution of  $\text{NaHCO}_3$  and 3 times with water. The organic phase was dried with anhydrous  $\text{MgSO}_4$  and filtrated. The filtrate solvent was evaporated. Yield: 70%.

### VIII Supporting information

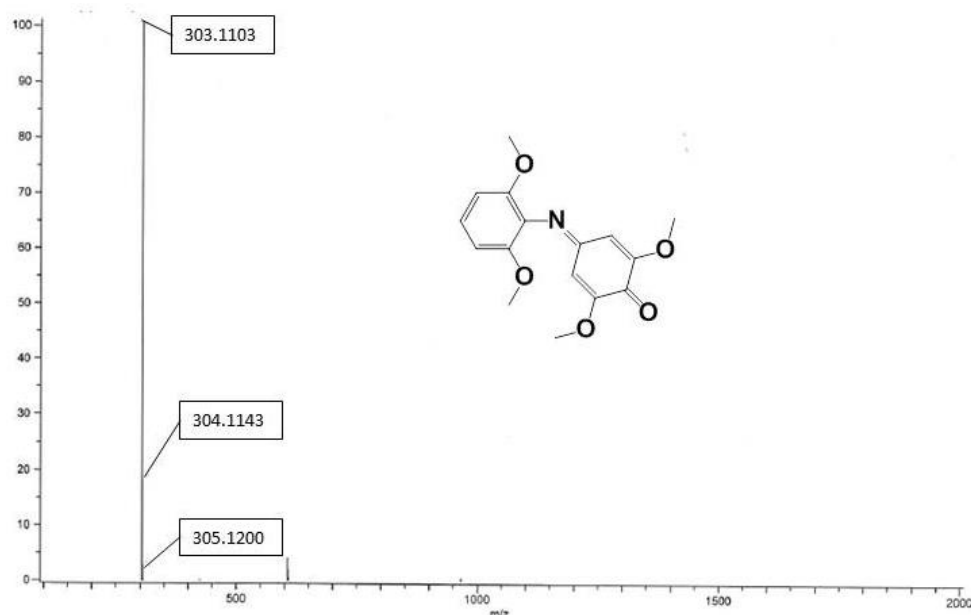


Figure 33: Mass spectrum of 2,6-dimethoxy aniline dimer (D13) ionized by electronic impact, positive mode, direct introduction.

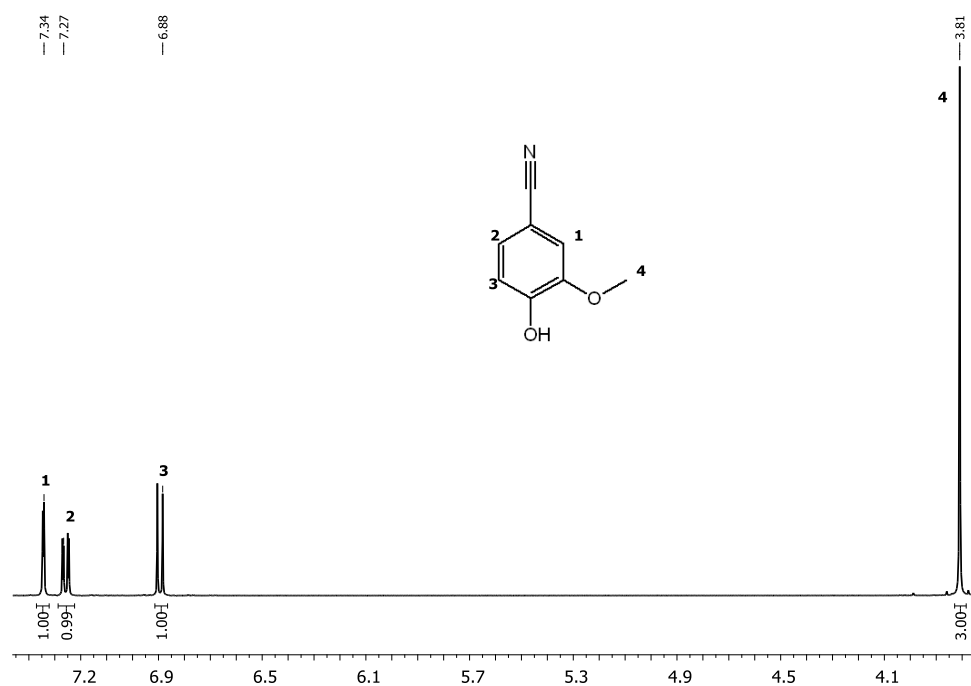


Figure 34: <sup>1</sup>H NMR spectrum of 4-hydroxy3-methoxybenzonitrile in DMSO, at room temperature.

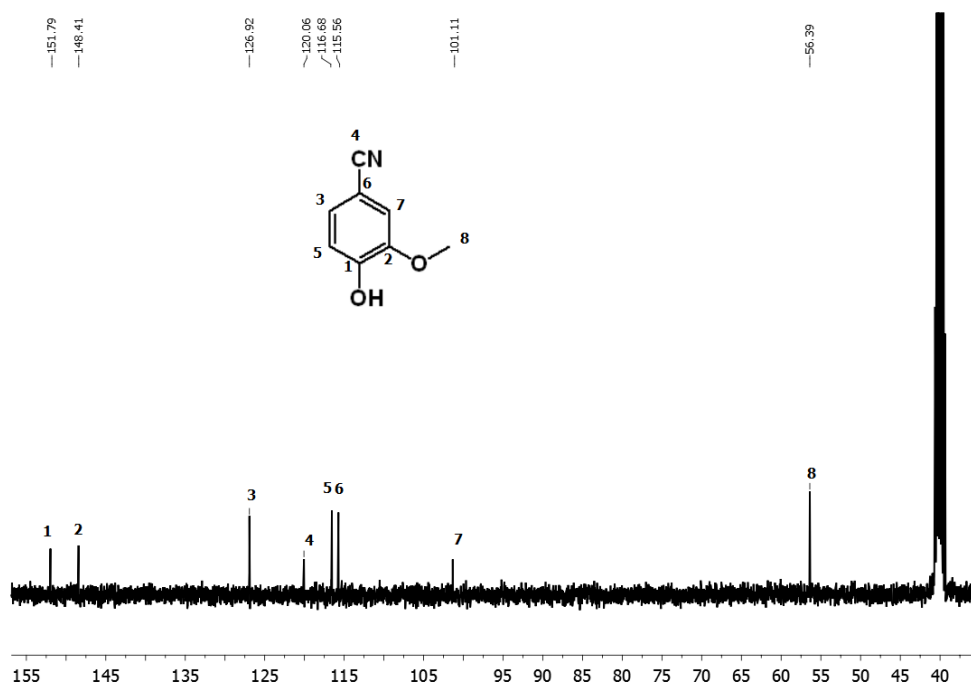


Figure 35:  $^{13}\text{C}$  NMR spectrum of 4-hydroxy3-methoxybenzonitrile in DMSO, at room temperature.

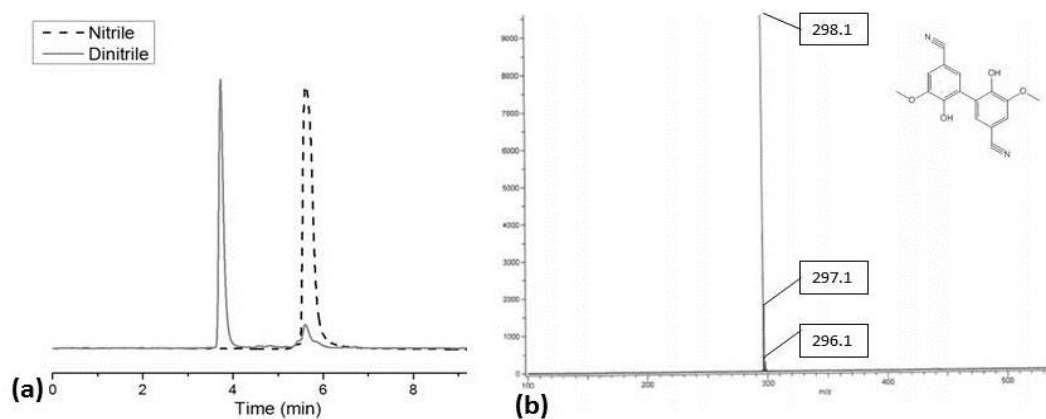


Figure 36: (a) HPLC profile of 4-hydroxy3-methoxybenzonitrile (dashed line) and 4-hydroxy3-methoxybenzonitrile dimer (2) (straight line), using a C18 grafted silica column in acetonitrile with a UV detector, (b) Mass spectrum of 4-hydroxy3-methoxybenzonitrile (2) ionized by electronic impact, positive mode, direct introduction.



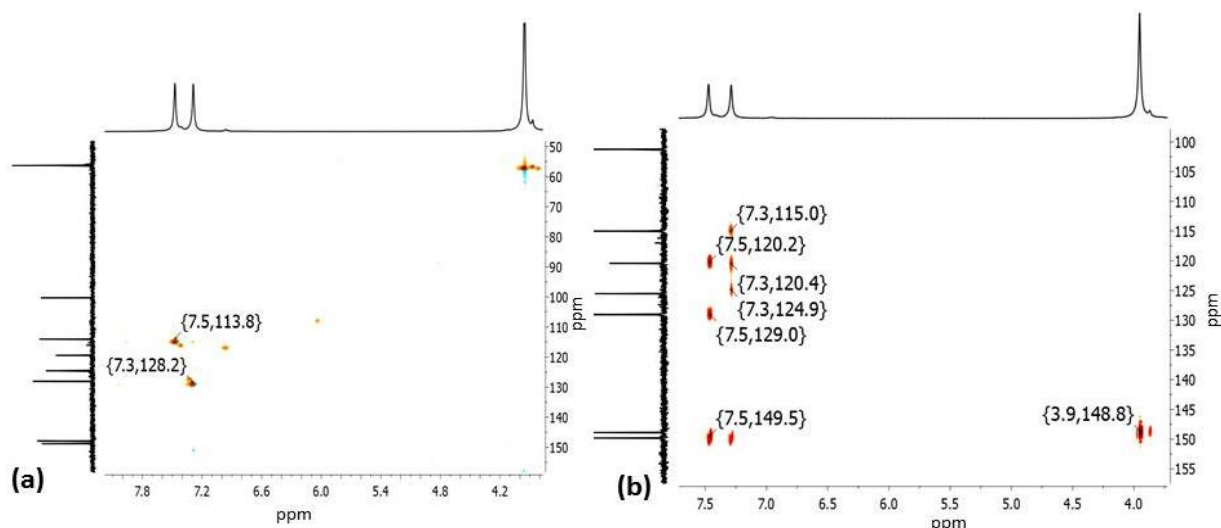


Figure 37: HSQC (a) and HMBC (b) spectra of 4-hydroxy3-methoxybenzonitrile (2) in DMSO, at room temperature.

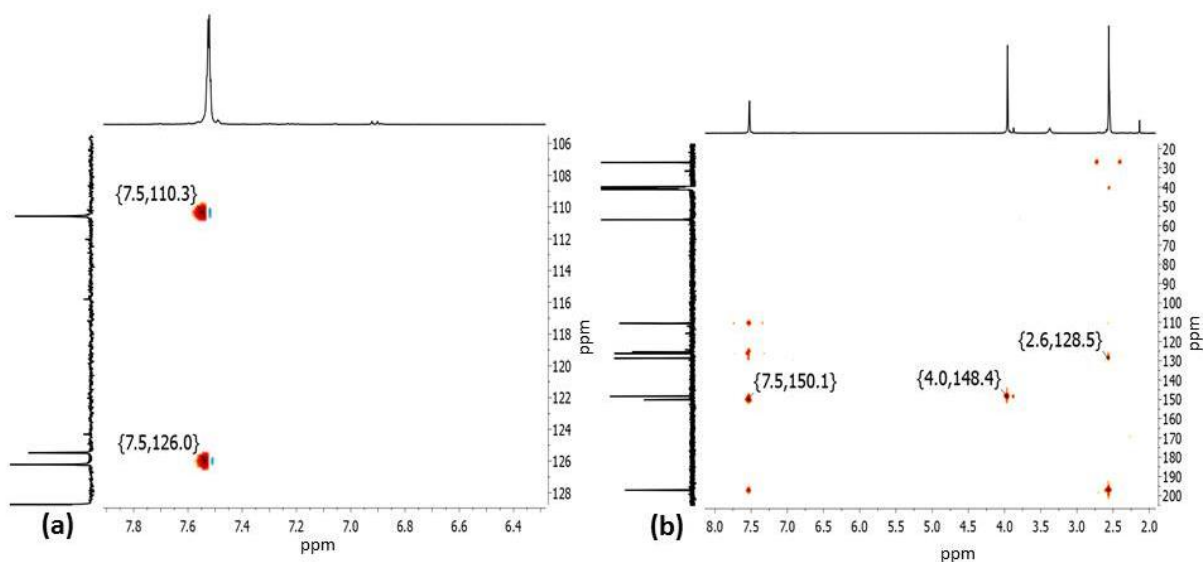


Figure 38: HSQC (zoom on the aromatic region) (a) and HMBC (b) spectra of acetovanillon dimer (3) in DMSO, at room temperature.

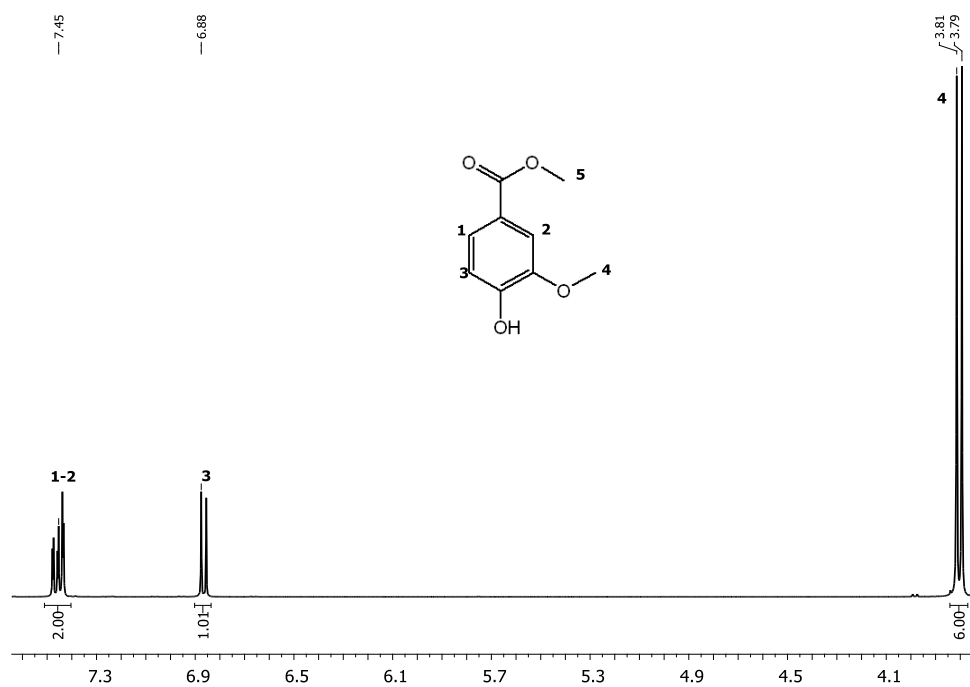


Figure 39:  $^1\text{H}$  NMR spectrum of methyl vanillate in DMSO, at room temperature.

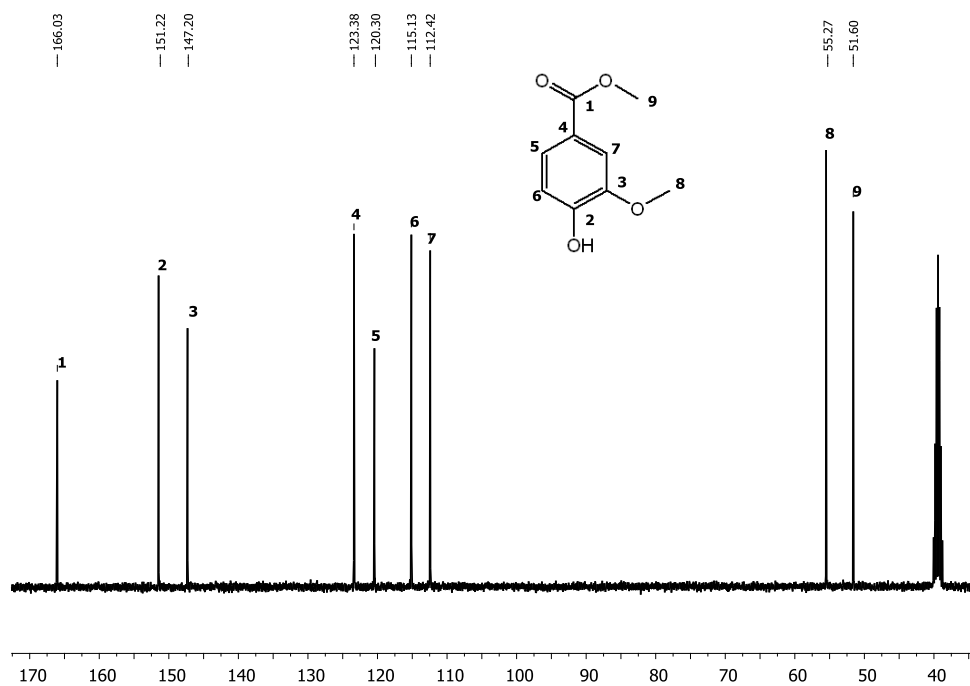


Figure 40:  $^{13}\text{C}$  NMR spectrum of methyl vanillate in DMSO, at room temperature.

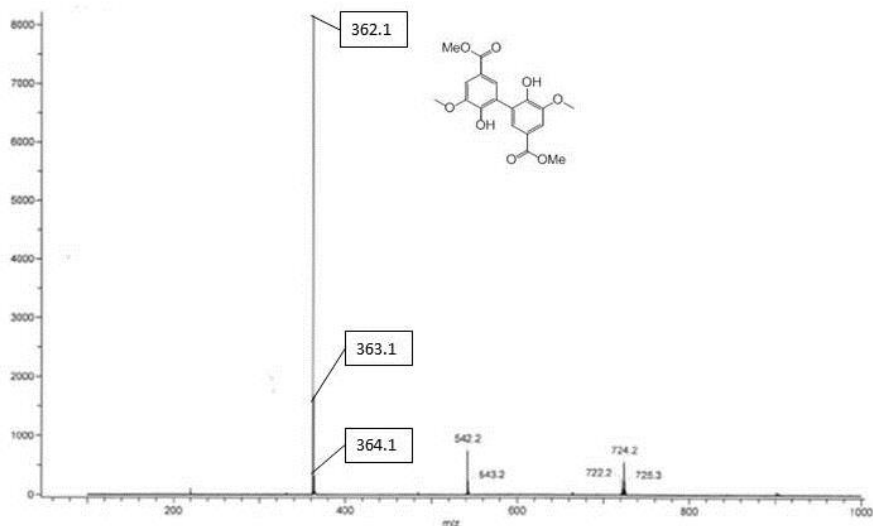


Figure 41: Mass spectrum of methyl vanillate dimer (4) ionized by electronic impact, positive mode, direct introduction.

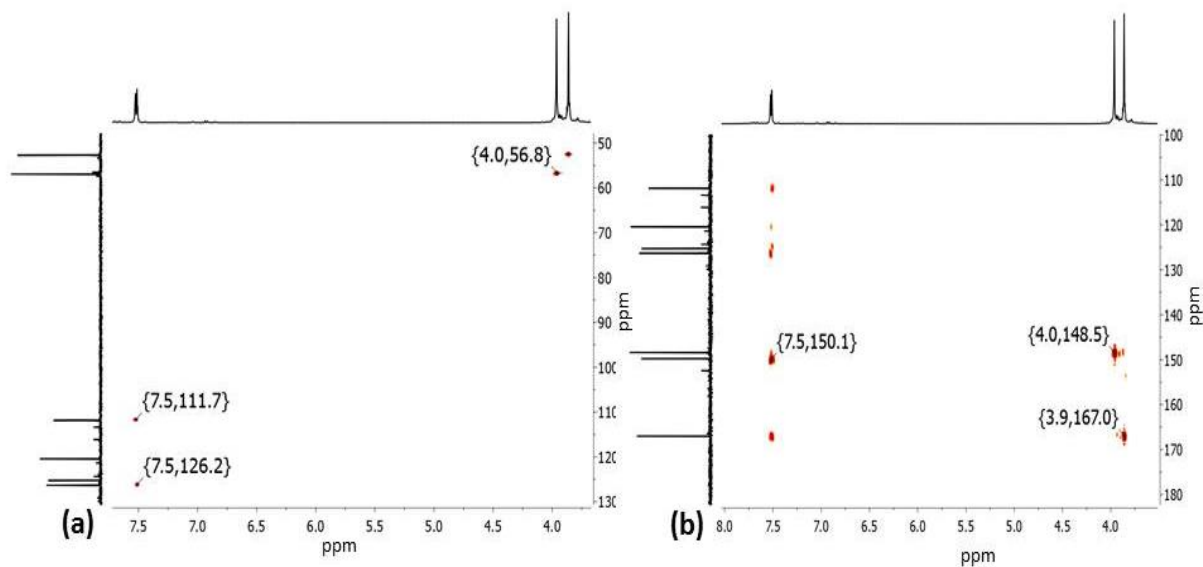


Figure 42: HSQC (a) and HMBC (b) spectra of methyl vanillate dimer (4) in DMSO, at room temperature.

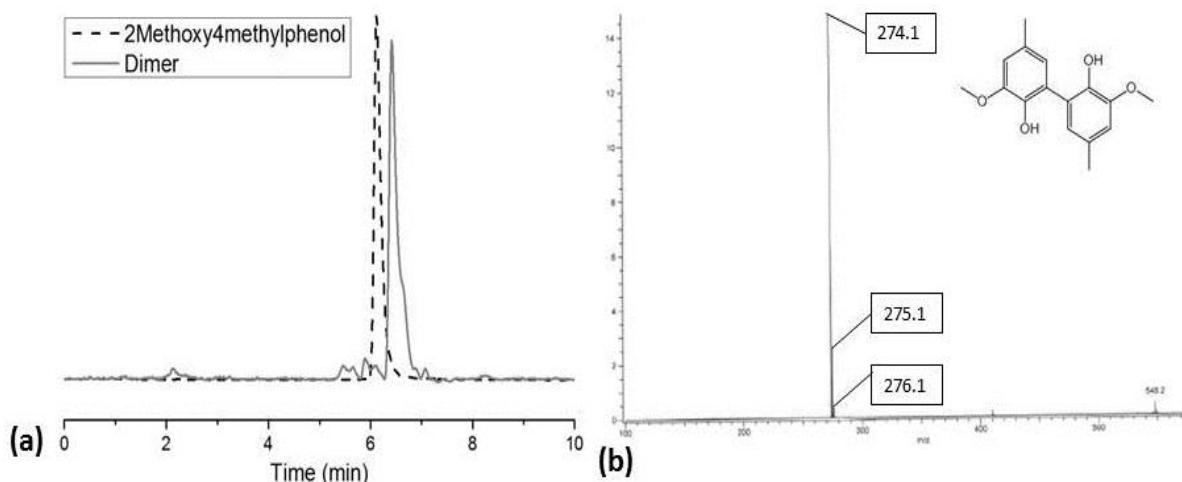


Figure 43: (a) HPLC profile of 2-methoxy-4-methylphenol (dashed line) and 2-methoxy-4-methylphenol dimer (5) (straight line), using a C18 grafted silica column in acetonitrile with a UV detector, (b) Mass spectrum of 2-methoxy-4-methylphenol dimer (5) ionized by electronic impact, positive mode, direct introduction.

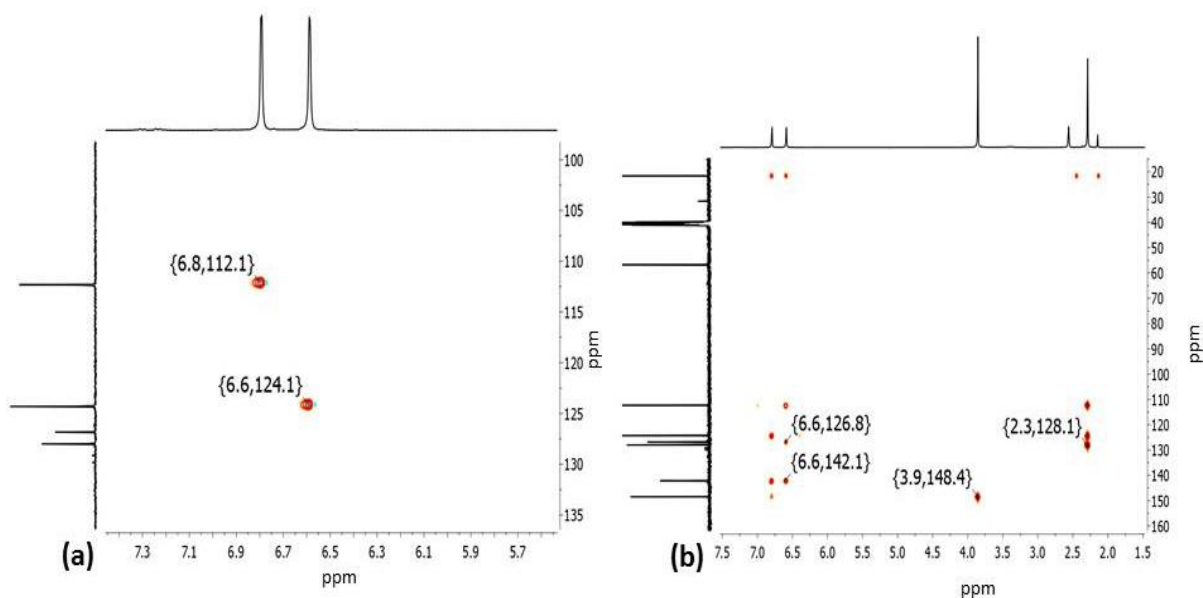


Figure 44 : HSQC (zoom on the aromatic region) (a) and HMBC (b) spectra of 2-methoxy-4-methylphenol (5) in DMSO, at room temperature.

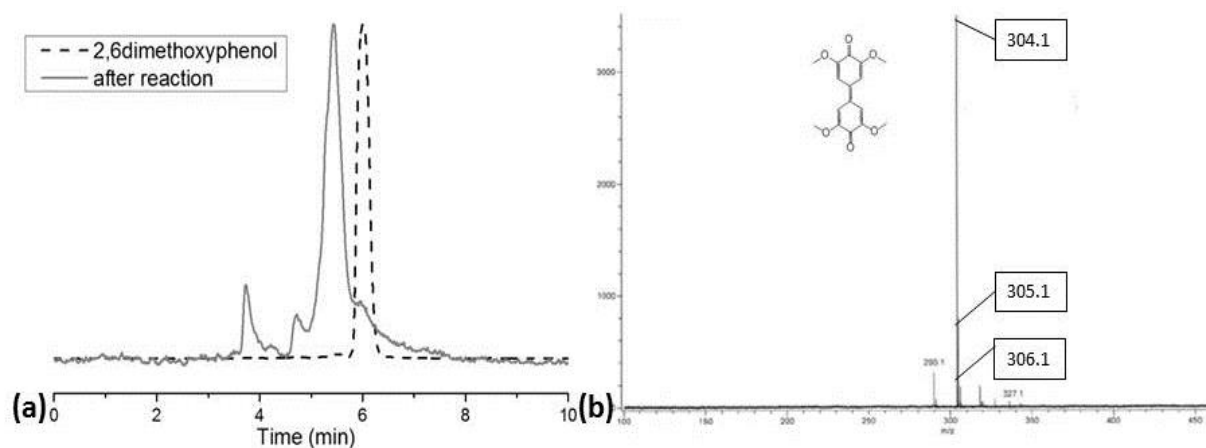


Figure 45: (a) HPLC profile of 2,6-dimethoxyphenol dimer (dashed line) and 2,6-dimethoxyphenol dimer (6) (straight line), using a C18 grafted silica column in acetonitrile with a UV detector, (b) Mass spectrum of 2,6-dimethoxyphenol dimer (6) ionized by electronic impact, positive mode, direct introduction.

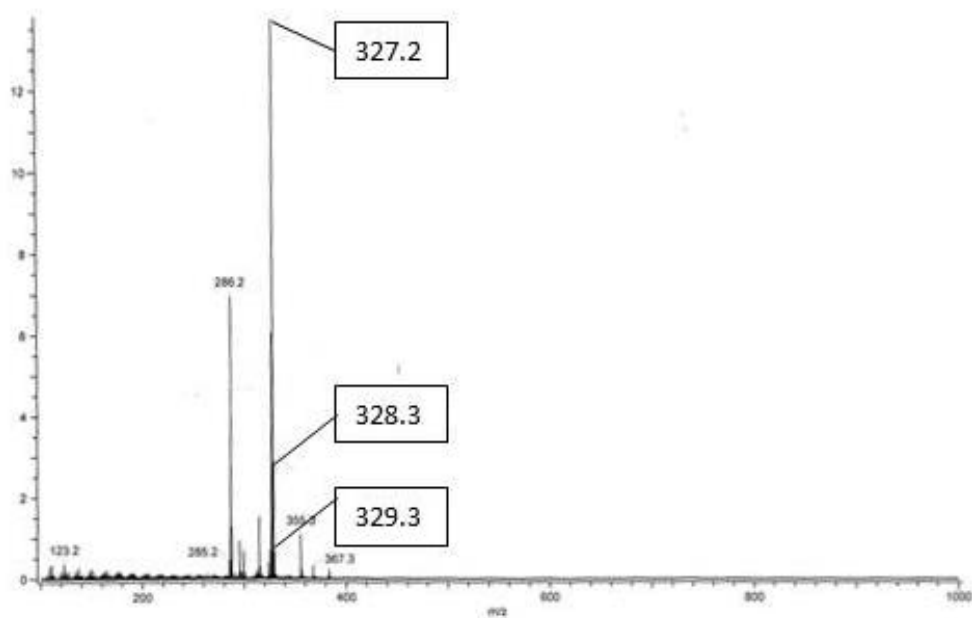


Figure 46: Mass spectrum of dieugenol (7) ionized by chemical ionization, positive mode direct introduction.

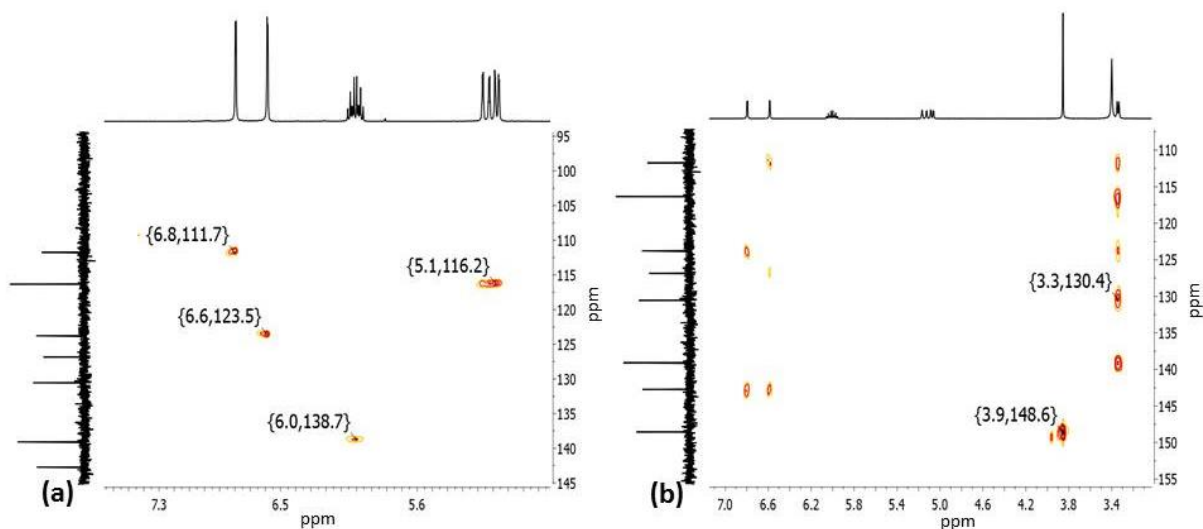


Figure 47: HSQC (zoom on the aromatic region) (a) and HMBC (b) spectra of dieugenol (7) in DMSO, at room temperature.

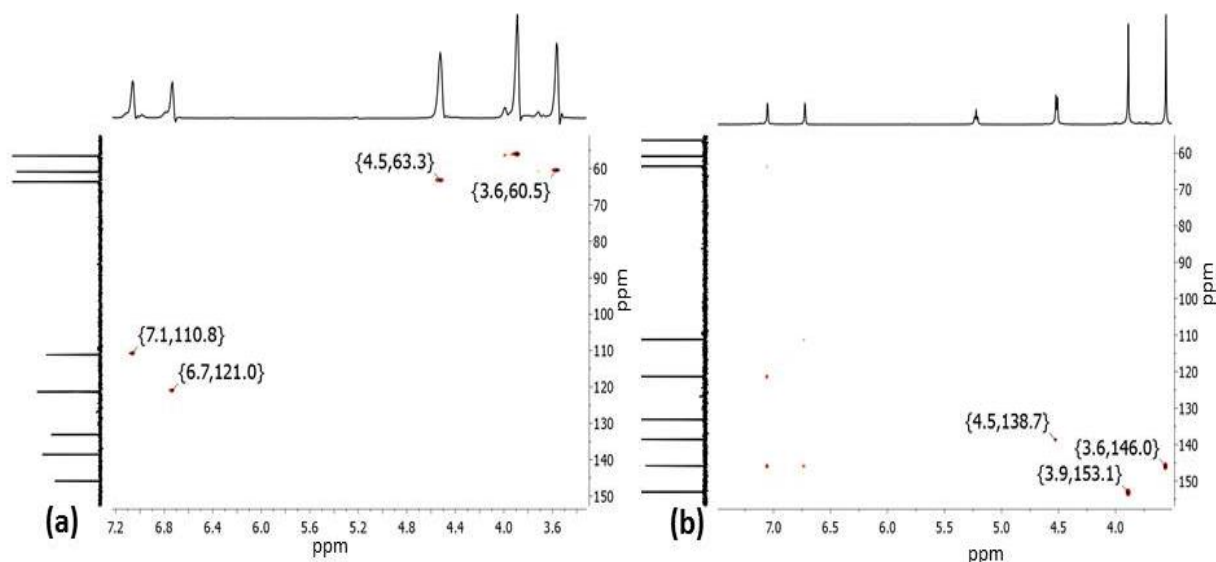


Figure 48: HSQC (a) and HMBC (b) spectra of methylated diol (10) in DMSO.

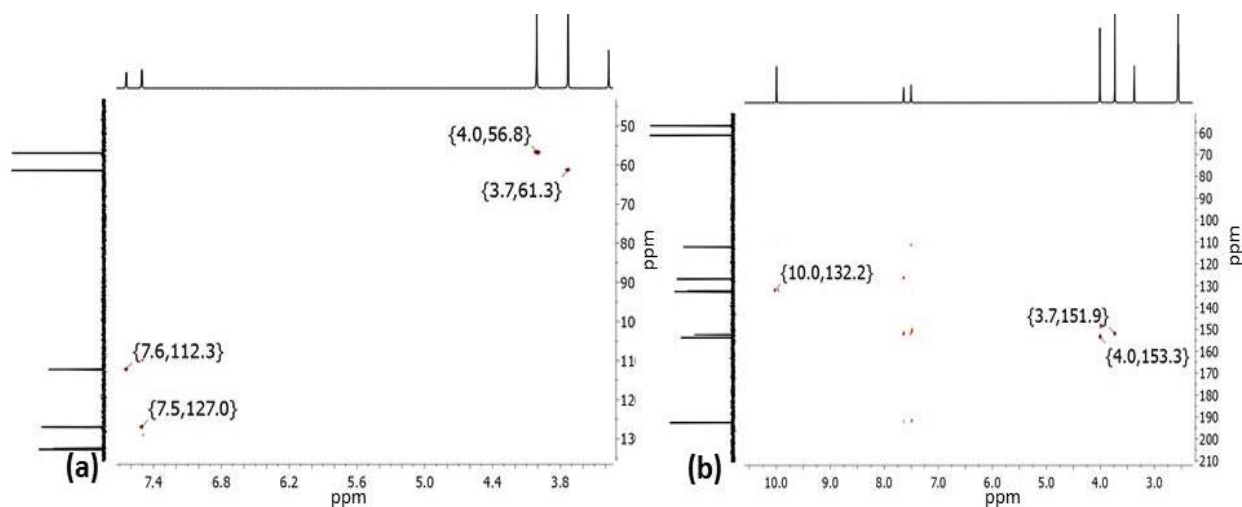


Figure 49: HSQC (a) and HMBC (b) spectra of methylated divanillin (11) in DMSO, at room temperature.

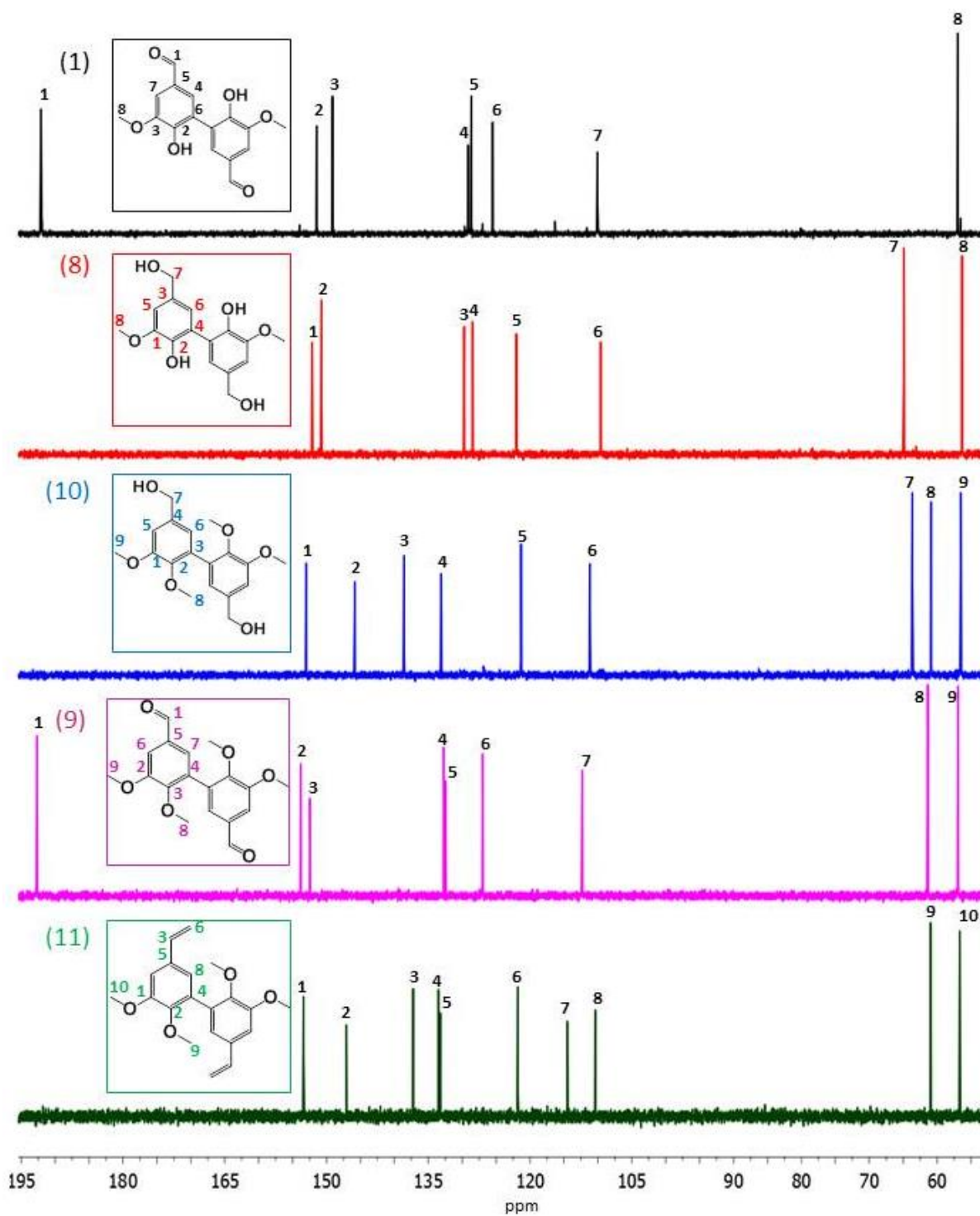


Figure 50:  $^1\text{H}$  NMR spectra of molecules (8), (9), (10), (11) synthesized from divanillin in DMSO, at room temperature.

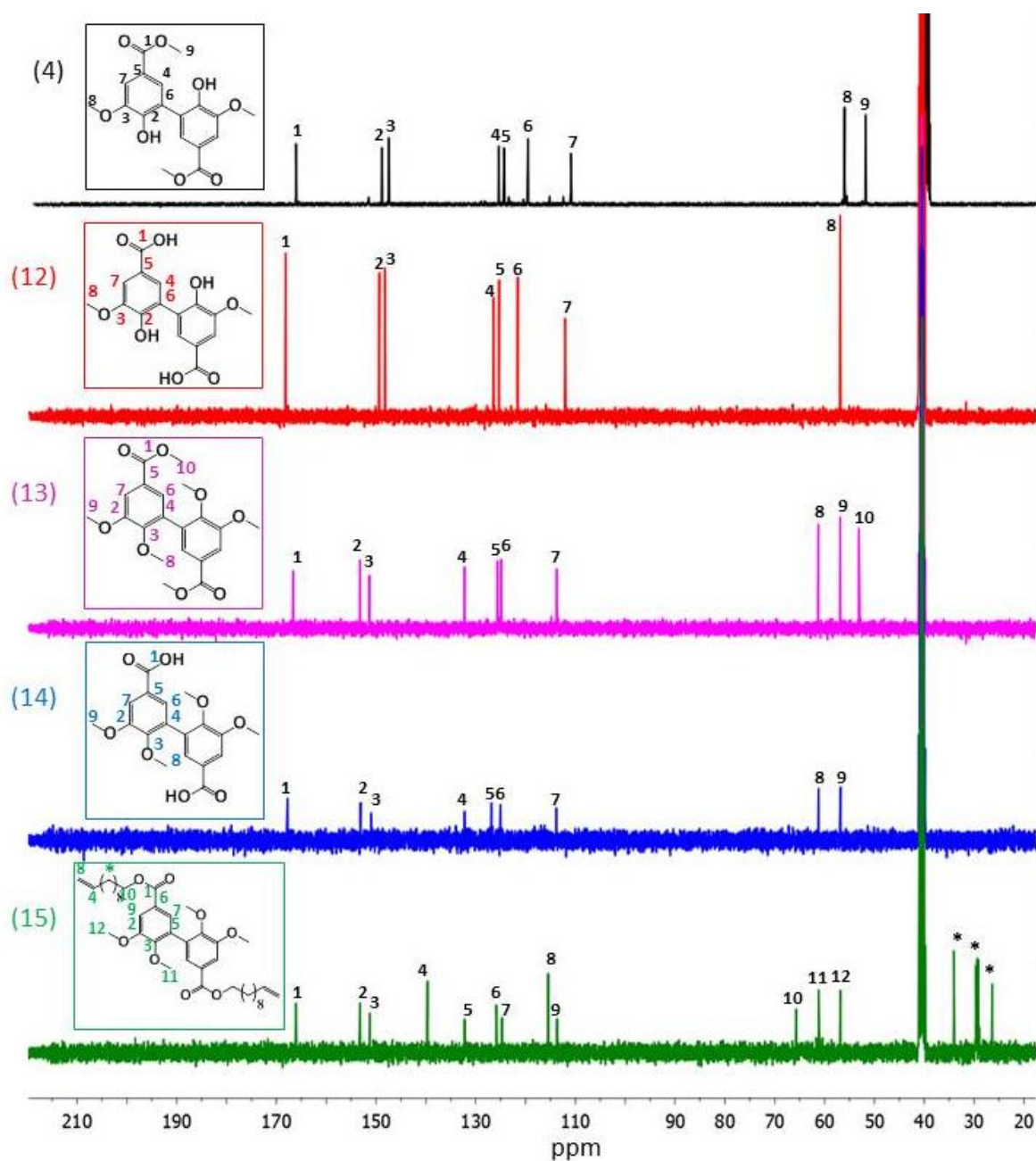


Figure 51:  $^{13}\text{C}$  NMR spectra of molecules (12), (13), (14), (15) synthesized from methylated diester (4), in DMSO, at room temperature.



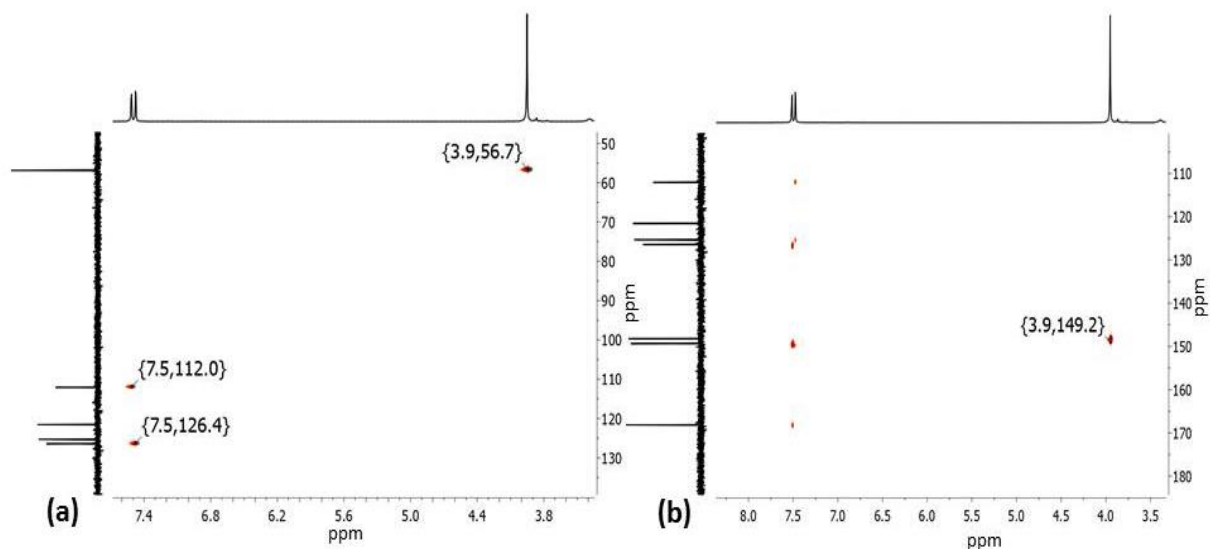


Figure 52: HSQC (a) and HMBC (b) spectra of diacid (12) in DMSO, at room temperature.

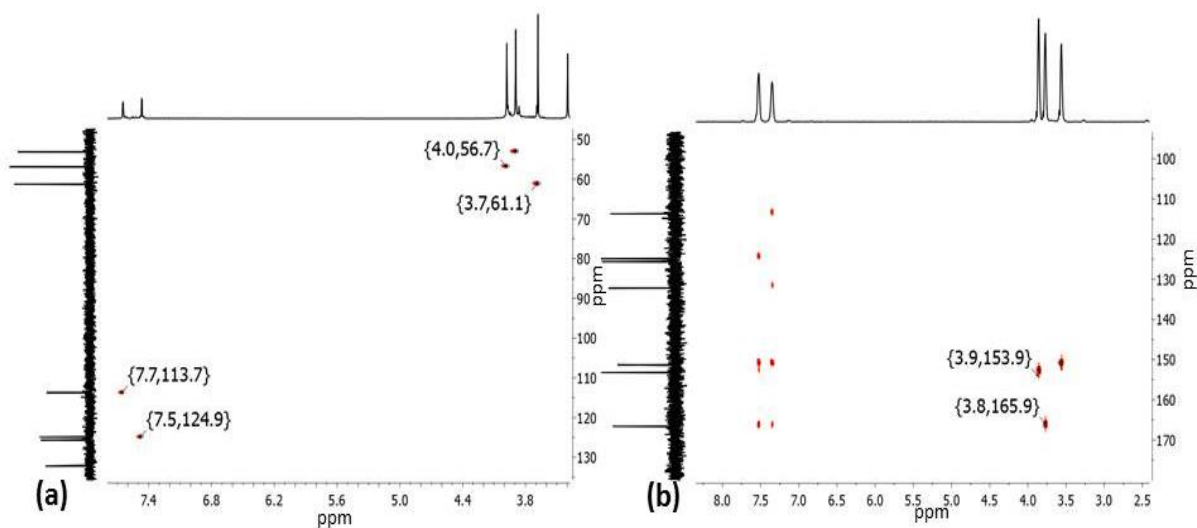


Figure 53: HSQC (a) and HMBC (b) spectra of methylated diester (13) in DMSO.

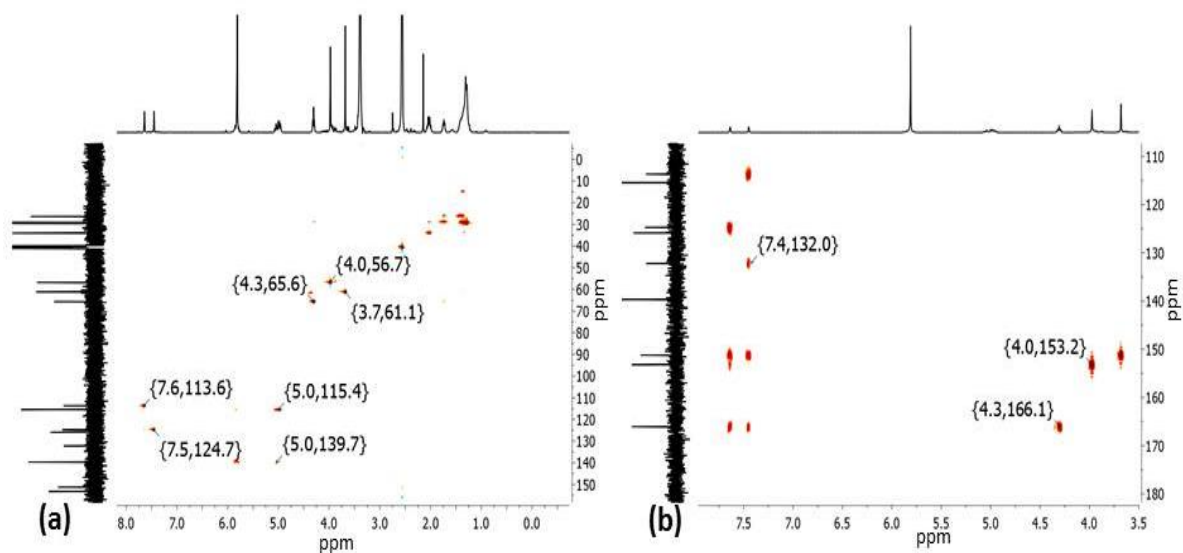


Figure 54: HSQC (a) and HMBC (b) spectra of bis-unsaturated diester (15) in DMSO, at room temperature.

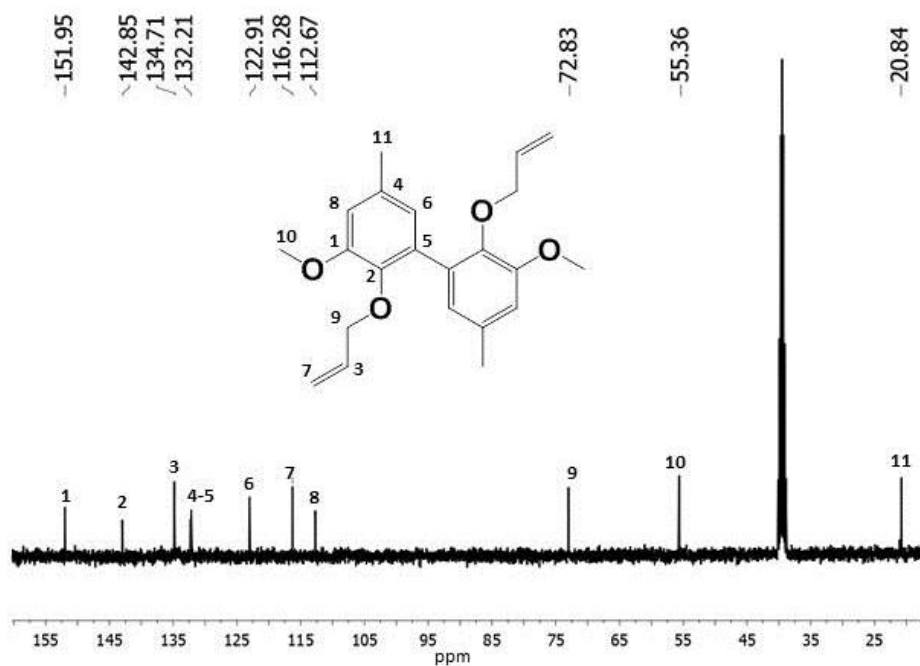


Figure 55:  $^{13}\text{C}$  NMR of allylated 2-methoxy-4-methylphenol dimer (16) in DMSO, at room temperature.

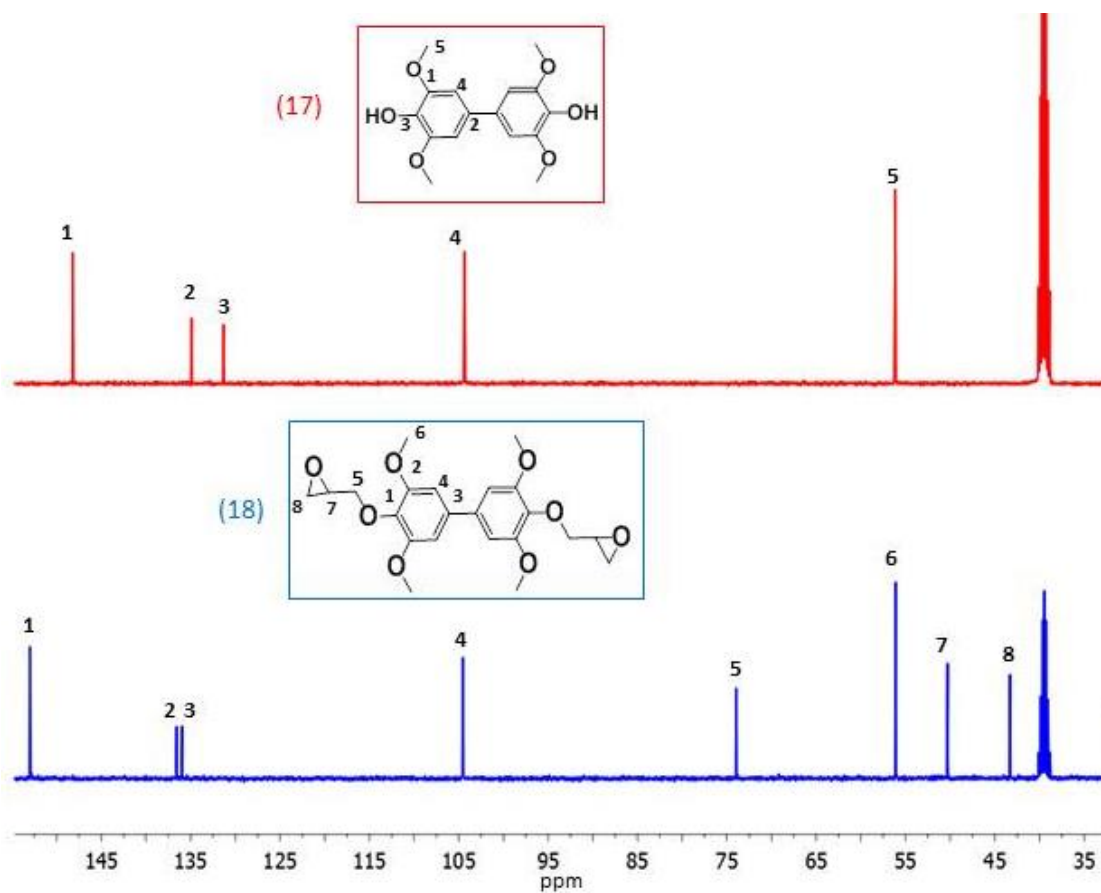


Figure 56:  $^{13}\text{C}$  NMR spectra of molecules(17) and (18) synthesized from 2,6-dimethoxyphenol dimer (6), DMSO, at room temperature.

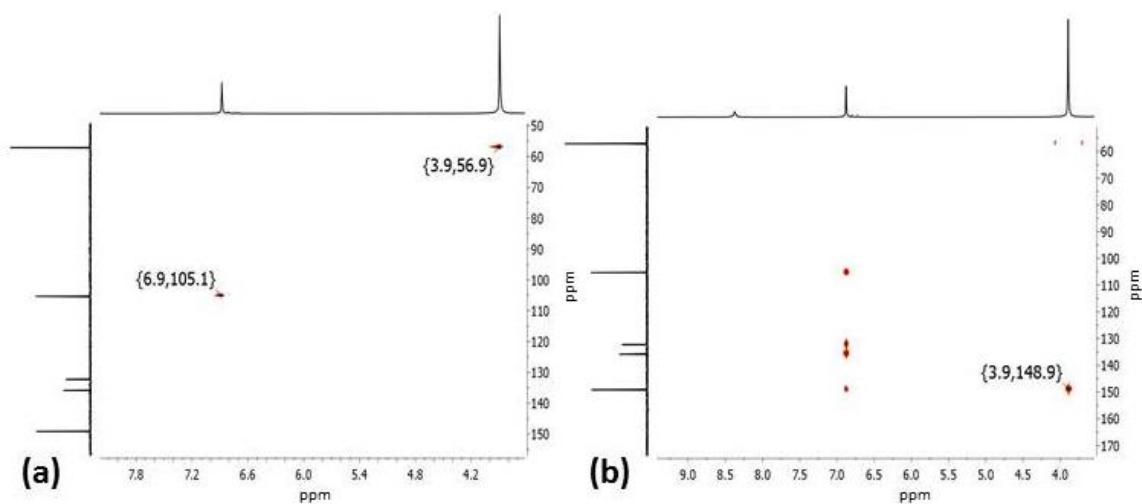


Figure 57: HSQC (a) and HMBC (b) spectra of bisphenol (17) in DMSO, at room temperature.

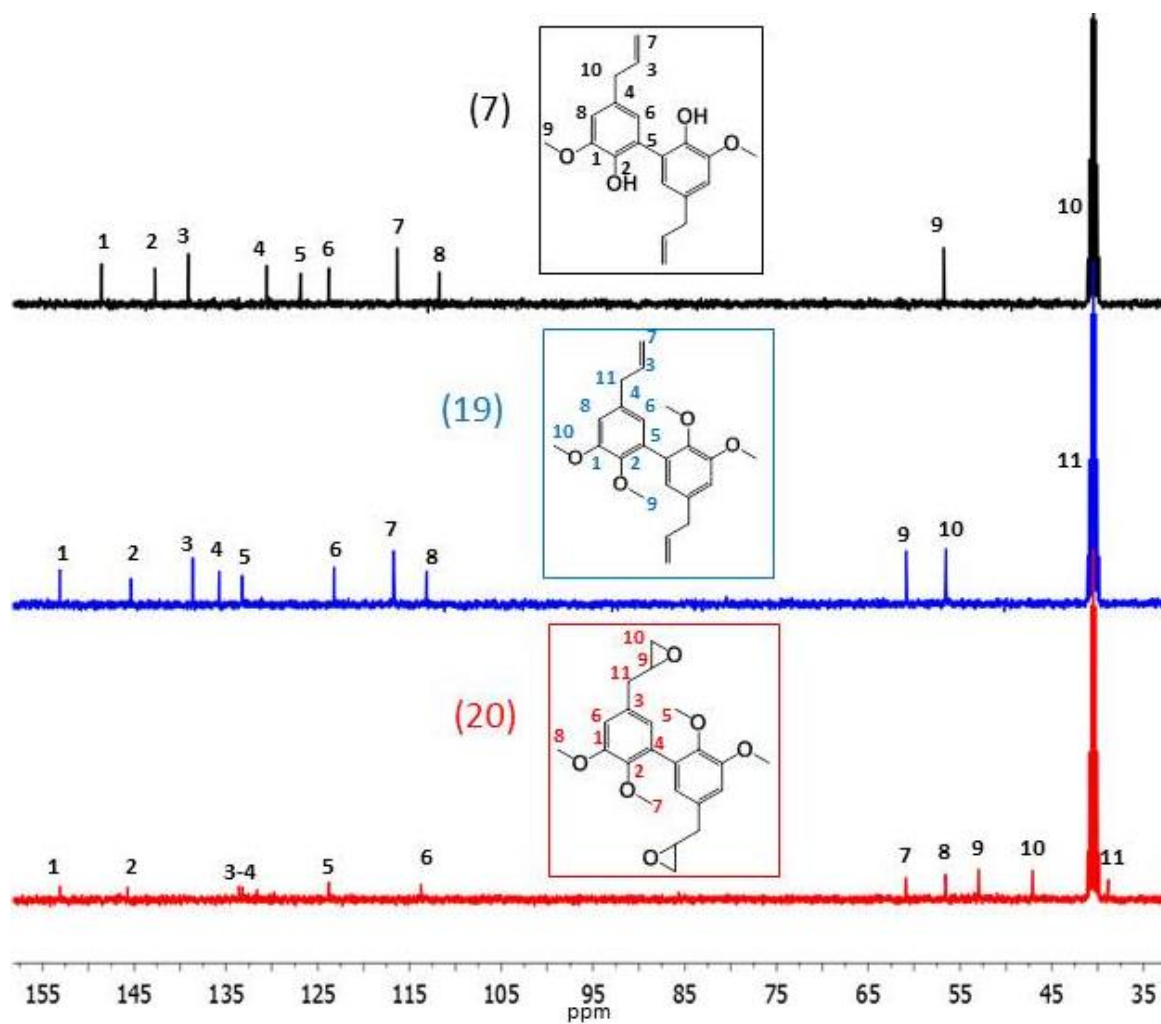


Figure 58: <sup>13</sup>C NMR spectra of molecules (19) and (20) synthesized from dieugenol.

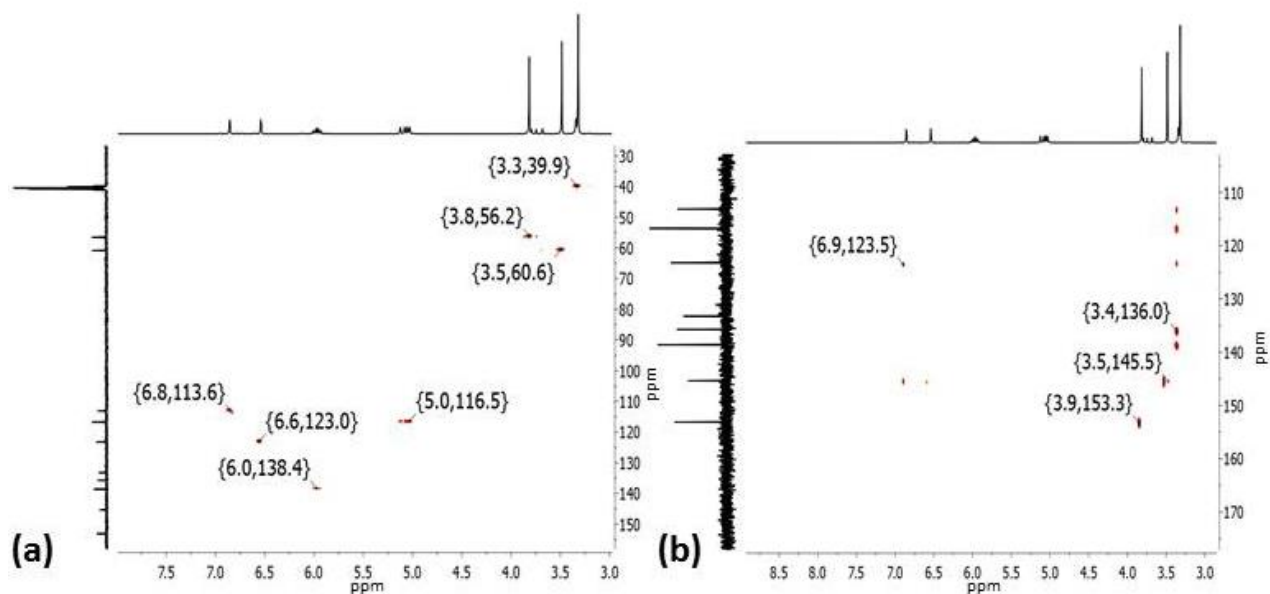


Figure 59: HSQC (a) and HMBC (b) spectra of methylated dieugenol (13) in DMSO.

Table 4: Yield and structural characteristics of dimers (1) to (7).

Dimer	Yield (%)	Mass	<sup>1</sup> H NMR	<sup>13</sup> C NMR
1	96%	302.1 (100%), 303.1 (18%), 304.1 (2%)	δ 9.85 (s, CHO), 7.50 (s, 2H Ar), 4.00 (s, OCH <sub>3</sub> )	δ 191.04 (CHO), 150.70 (Ar-C), 147.95 (Ar-C), 128.30 (Ar-C), 127.69 (Ar-C), 124.52 (Ar-C), 109.10 (Ar-C), 55.88 (OCH <sub>3</sub> )
2	95	296.1 (100%), 297.1 (18%), 298.1 (2%)	δ 9.91 (s, 2H, HO) , 7.57 (s, 2H, Ar) , 7.42 (s, 2H, Ar) , 3.93 (s, 6H, OCH <sub>3</sub> )	δ 148.63 (Ar-C), 147.85 (Ar-C), 128.05 (Ar-C), 124.56 (Ar-C), 119.45 (Ar-C), 114.03 (Ar-C), 100.30 (CN), 56.15 (OCH <sub>3</sub> )
3	92	330.1 (100%), 331.1 (18%), 332.2 (2%)	δ 7.49 (s, 4H, Ar) , 3.93 (s, 6H, OCH <sub>3</sub> ), 2.56 (s, 6H, C=OCH <sub>3</sub> )	δ 196.07 (OCH), 149.22 (Ar-C), 147.06 (Ar-C), 127.81 (Ar-C), 124.23 (Ar-C), 124.04 (Ar-C), 109.03 (Ar-C) 55.76 (OCH <sub>3</sub> ), 26.25 (CH <sub>3</sub> )
4	90	362.1 (100%), 363.1 (20%), 364.1 (2%)	δ 9.60 (s, 2H, HO) , 7.46 (s, 4H, Ar) , 3.90 (s, 6H, OCH <sub>3</sub> ), 3.80 (s, 6H, OCH <sub>3</sub> ester)	δ 166.04 (OCH <sub>3</sub> ester), 148.60 (Ar-C), 147.27 (Ar-C), 125.25 (Ar-C), 123.93 (Ar-C), 119.21 (Ar-C), 110.89 (Ar-C), 55.97 (OCH <sub>3</sub> ), 51.75 (OCH <sub>3</sub> ester)
5	92	274.1 (100%), 275.1 (18%), 276.1 (2%)	δ 6.73 (s, 2H, Ar) , 6.53 (s, 2H, Ar), 3.79 (s, 6H, OCH <sub>3</sub> ), 2.23 (s, 6H, CH <sub>3</sub> )	147.52 (Ar-C), 140.99 (Ar-C), 126.92 (Ar-C), 125.68 (Ar-C), 123.04 (Ar-C), 111.61 (Ar-C), 55.85 (OCH <sub>3</sub> ), 20.65 (CH <sub>3</sub> )
6	80	304.1 (100%), 305.1 (18%), 318.1 (2%)	δ 8.32 (s, 2H, HO) , 6.82 (s, 4H, Ar), 3.84 (s, 12H, OCH <sub>3</sub> )	Not determined
7	87	327.2 (100%), 326.2 (20%), 328.3 (10%)	δ 6.74 (s, 2H Ar), 6.52 (s, 2H Ar), 5.94 (q, 2H CH-CH <sub>2</sub> ), 5.03 (d, 4H CH-CH <sub>2</sub> ), 3.79 (s, OCH <sub>3</sub> ), 3.27 (d, 2H CH <sub>2</sub> )	δ 147.80 (Ar-C), 141.62 (Ar-C), 138.38 (CH-CH <sub>2</sub> ), 129.57 (Ar-C), 125.67 (Ar-C), 122.62 (Ar-C), 115.28 (CH-CH <sub>2</sub> ), 105.56 (Ar-C), 55.64 (OCH <sub>3</sub> ), 39.19 (CH <sub>2</sub> )

Compound	Yield (%)	<sup>1</sup> H NMR	<sup>13</sup> C NMR
<b>8</b>	80	δ 8.25 (s, OH phenol), 6.9( (s, 2H Ar), 6.73(s, 2H Ar), 5.065 (t, 2H OH), 4.46 (d, 4H CH <sub>2</sub> OH), 3.87 (s, OCH <sub>3</sub> )	δ 151.14 (Ar-C), 149.67 (Ar-C), 128.81 (Ar-C), 127.36 (Ar-C), 120.94 (Ar-C), 108.59 (Ar-C), 63.78 (CH <sub>2</sub> OH), 55.32 (OCH <sub>3</sub> )
<b>9</b>	80	δ 9.94 (s, CHO), 7.58 (s, 2H Ar), 7.55 (s, 2H Ar), 3.95 (s, OCH <sub>3</sub> ), 3.68 (s, OCH <sub>3</sub> )	δ 191.83 (CHO), 152.80 (Ar-C), 151.21 (Ar-C), 131.90 (Ar-C), 131.58 (Ar-C), 125.96 (Ar-C), 111.14 (Ar-C), 60.47 (OCH <sub>3</sub> ), 55.93 (OCH <sub>3</sub> )
<b>10</b>	85	δ 6.99 (s, 2H Ar), 6.67(s, 2H Ar), 5.15 (t, 2H OH), 4.47 (d, 4H CH <sub>2</sub> OH), 3.83 (s, OCH <sub>3</sub> ), 3.51 (s, OCH <sub>3</sub> )	δ 151.93 (Ar-C), 144.86 (Ar-C), 137.52 (Ar-C), 132.14 (Ar-C), 120.27 (Ar-C), 110.20 (Ar-C), 62.69 (CH <sub>2</sub> OH), 59.83 (OCH <sub>3</sub> ), 55.53 (OCH <sub>3</sub> )
<b>11</b>	75	δ 7.17 (s, 2H Ar), 6.83 (s, 2H Ar), 6.70 (q, 2H CH-CH <sub>2</sub> ), 5.77 (d, 2H CH-CH <sub>2</sub> ), 5.19 (d, 2H CH-CH <sub>2</sub> ) 3.87 (s, OCH <sub>3</sub> ), 3.53 (s, OCH <sub>3</sub> )	δ 152.34 (Ar-C), 145.84 (Ar-C), 136.25 (CH-CH <sub>2</sub> ), 132.66 (Ar-C), 132.01 (Ar-C), 120.82(CH-CH <sub>2</sub> ), 113.30 (Ar-C), 109.25 (Ar-C), 59.94 (OCH <sub>3</sub> ), 55.53 (OCH <sub>3</sub> )
<b>12</b>	92	δ 7.52 (s, 2H Ar), 7.48 (s, 2H Ar), 3.96 (s, OCH <sub>3</sub> )	δ 166.91 (COOH), 148.20 (Ar-C), 147.24 (Ar-C), 125.23 (Ar-C), 124.06 (Ar-C), 120.66 (Ar-C), 111.20 (Ar-C), 55.84 (OCH <sub>3</sub> )
<b>13</b>	80	δ 7.59 (s, 2H Ar), 7.41 (s, 2H Ar), 3.92 (s, OCH <sub>3</sub> ), 3.84 (s, OCH <sub>3</sub> ), 3.62 (s, OCH <sub>3</sub> )	δ 165.63 (OCH <sub>3</sub> ester), 152.16 (Ar-C), 149.95 (Ar-C), 131.19 (Ar-C), 124.44(Ar-C), 123.81 (Ar-C), 112.43 (Ar-C), 60.38 (OCH <sub>3</sub> ), 55.73(OCH <sub>3</sub> ester), 52.81(OCH <sub>3</sub> )
<b>14</b>	94	δ 7.63 (s, 2H Ar), 7.42 (s, 2H Ar), 3.96 (s, OCH <sub>3</sub> ), 3.64 (s, OCH <sub>3</sub> )	δ 166.72 (COOH), 152.21 (Ar-C), 149.91 (Ar-C), 131.06 (Ar-C), 123.86 (Ar-C), 112.88 (Ar-C), 59.89 (Ar-C), 55.84 (OCH <sub>3</sub> ), 55.86 (OCH <sub>3</sub> )
<b>15</b>	60	δ 7.37 (s, 2H Ar), 7.58 (s, 2H Ar), 4.92 (m, 3H CH-CH <sub>2</sub> ), 4.25 (t, 2H CH <sub>2</sub> -COO), 3.92 (s, OCH <sub>3</sub> ), 3.62 (s, OCH <sub>3</sub> ), 1.97 (m, 3H -CH <sub>2</sub> -), 1.67 (m, 2H -CH <sub>2</sub> -), 1.23 (m, 13H -CH <sub>2</sub> -)	δ 164.84 (COO), 152.12 (Ar-C), 150.30 (Ar-C), 138.56 (C=C), 131.26 (Ar-C), 125.08 (Ar-C), 123.50 (Ar-C), 114.34 (C=C), 112.55 (Ar-C), 64.59 (OCH <sub>2</sub> ), 60.23 (OCH <sub>3</sub> ), 56,06 (OCH <sub>3</sub> ), 25.40-32.99 (CH <sub>2</sub> )
<b>16</b>	60	δ 6.84 (s, 2H, Ar) , 6.55(s, 2H,	151.98(Ar-C), 142.92(Ar-C),

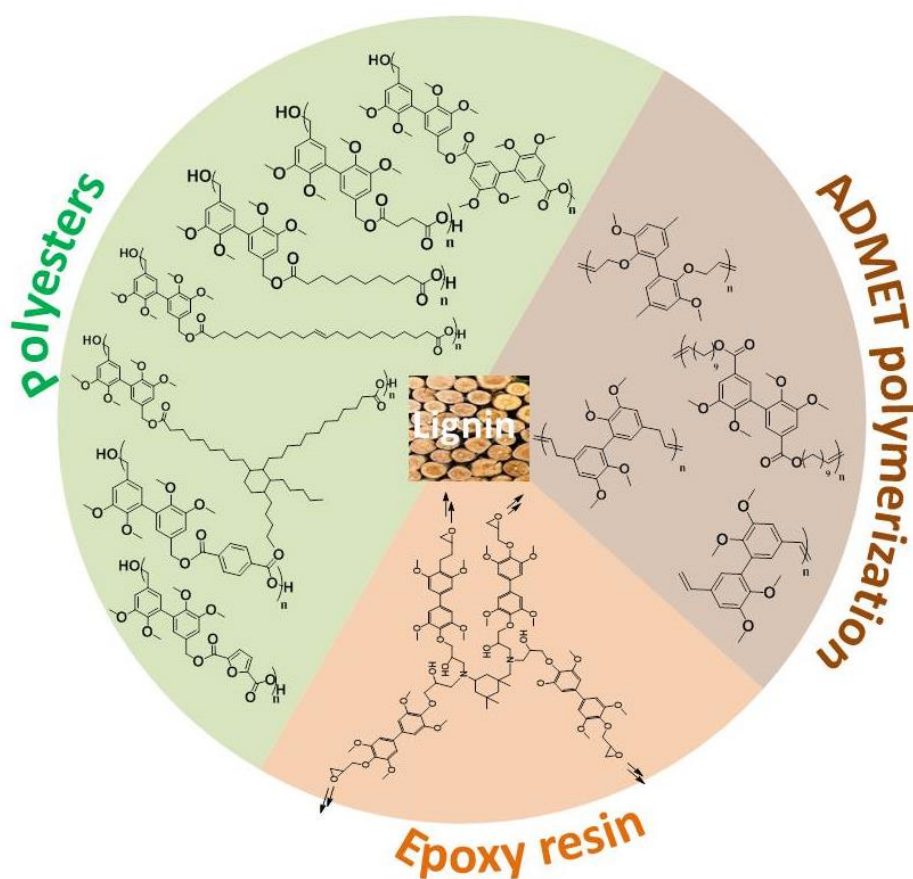
		Ar), 5.70 (m, 2H, CH-CH <sub>2</sub> ), 4.99 (dd, 4H, CH-CH <sub>2</sub> ), 4.21 (d, 4H, OCH <sub>2</sub> ), 3.80(s, 6H, OCH <sub>3</sub> ), 2.26(s, 6H, CH <sub>3</sub> )	134.95 ( <u>C</u> H-CH <sub>2</sub> ), 132.30(Ar-C), 132.17 (Ar-C), 123.03 (Ar-C), 116.43(CH- <u>C</u> H <sub>2</sub> ), 112.67(Ar-C), 73.21(CH <sub>2</sub> ), 55.36 (OCH <sub>3</sub> ), 20.78 (CH <sub>3</sub> )
<b>17</b>	78	δ 8.34 (s, 1H OH), 6.88 (s, 2H Ar), 3.90 (s, OCH <sub>3</sub> )	δ 148.13 (Ar-C), 134.98 (Ar-C), 131.00 (Ar-C), 104.12 (Ar-C), 55.98 (OCH <sub>3</sub> )
<b>18</b>	95	δ 6.89 (s, 2H Ar), 4.11 (dd, 1H OCH <sub>2</sub> ), 3.87 (s, OCH <sub>3</sub> ), 3.76 (q, 1H OCH <sub>2</sub> ), 2.74 (t, CH), 2.60 (q, CH <sub>2</sub> epoxy), 2.50 (q, CH <sub>2</sub> epoxy)	δ 152.73 (Ar-C), 136.37 (Ar-C), 135.84 (Ar-C), 104.81(Ar-C), 173.55 (OCH <sub>2</sub> ), 56.03 (OCH <sub>3</sub> ), 50.11 (CH epoxy), 43.02 (CH <sub>2</sub> epoxy)
<b>19</b>	50	δ 6.93 (s, 2H Ar), 6.61 (s, 2H Ar), 6.03 (q, 2H CH-CH <sub>2</sub> ), 5.13 (d, 4H CH-CH <sub>2</sub> ), 3.89 (s, OCH <sub>3</sub> ), 3.56 (s, OCH <sub>3</sub> ), 3.42 (d, 2H CH <sub>2</sub> )	δ 152.02 (Ar-C), 144.15 (Ar-C), 137.53 ( <u>C</u> H-CH <sub>2</sub> ), 134.73 (Ar-C), 132.29(Ar-C), 122.19 (Ar-C), 115.77(CH- <u>C</u> H <sub>2</sub> ), 112.15(Ar-C), 59.80 (OCH <sub>3</sub> ), 55.44 (OCH <sub>3</sub> ), 39.29 (CH <sub>2</sub> )
<b>20</b>	70	δ 7.01 (s, 2H Ar), 6.50 (s, 2H Ar), 3.89 (s, OCH <sub>3</sub> ), 3.58 (s, OCH <sub>3</sub> ), 3.19 (m, 2H epoxy), 2.80 (m, 6H epoxy), 2.62 (2H epoxy)	δ 151.87 (Ar-C), 144.59 (Ar-C), 133.03 ( <u>C</u> H-CH <sub>2</sub> ), 132.36 (Ar-C), 122.07(Ar-C), 112.84 (Ar-C), 59.51(OCH <sub>3</sub> ), 55.83(OCH <sub>3</sub> ), 52.23 (CH epoxy), 45.91 (CH <sub>2</sub> epoxy), 37.64 (CH <sub>2</sub> )





# Chapter 4:

## Synthesis and structure-property investigations of polymers from biphenyl building blocks



**Key words:** Polyesters, polyamides, ADMET, epoxy resins.

**Mots clés:** Polyesters, polyamides, ADMET, résines époxy.

# TABLE OF CONTENTS

<b>I</b>	<b>Introduction .....</b>	<b>199</b>
<b>II</b>	<b>Synthesis and characterization of thermoplastic polymers from biphenyl precursors <i>via</i> polycondensation .....</b>	<b>199</b>
1.	<b>Synthesis and characterization of biphenyl polyesters .....</b>	<b>200</b>
1)	<b>Optimization of the polymerization conditions .....</b>	<b>200</b>
a)	Esterification versus transesterification reactions .....	200
b)	Catalyst screening .....	202
2)	<b>Synthesis of a series of copolyester .....</b>	<b>204</b>
3)	<b>Thermomechanical properties of the copolymers .....</b>	<b>206</b>
2.	<b>Preliminary study on polyamide synthesis from biphenyl precursors .....</b>	<b>209</b>
<b>III</b>	<b>Synthesis and characterization of thermoplastic polymers from biphenyl precursors <i>via</i> ADMET polymerization .....</b>	<b>212</b>
1.	<b>Synthesis, chemical structure and molar mass determination .....</b>	<b>212</b>
2.	<b>Thermomechanical properties of the unsaturated polymers .....</b>	<b>217</b>
<b>IV</b>	<b>Synthesis and characterization of epoxy resin from biphenyl precursors .....</b>	<b>220</b>
1.	<b>Synthesis of epoxy resins from 2,6-dimethoxy phenol dimer .....</b>	<b>221</b>
2.	<b>Swelling properties .....</b>	<b>223</b>
3.	<b>Thermomechanical properties of the epoxy resins .....</b>	<b>224</b>
4.	<b>Comparison of the thermomechanical properties of several biobased epoxy resins. ....</b>	<b>228</b>
<b>V</b>	<b>Conclusion and perspectives .....</b>	<b>229</b>
<b>VI</b>	<b>References .....</b>	<b>231</b>
<b>VII</b>	<b>Experimental .....</b>	<b>233</b>

## I Introduction

In this chapter, the polymerization of the biphenyl compounds described in the previous chapter is presented. Only two examples of divanillin-based thermoplastic polymers have been reported in literature. Indeed, Razzaq and coll. reported the synthesis of *Schiff* base polymers by reaction of divanillin with alkyl diamines as well as the synthesis of polyvanillin by reductive coupling of the aldehyde group of divanillin using an electrochemical polymerization cell.<sup>1,2</sup> Additionally, Harvey and coll. prepared cyanate ester thermosets from 4-methyl-2-methoxyphenol dimer.<sup>3</sup>

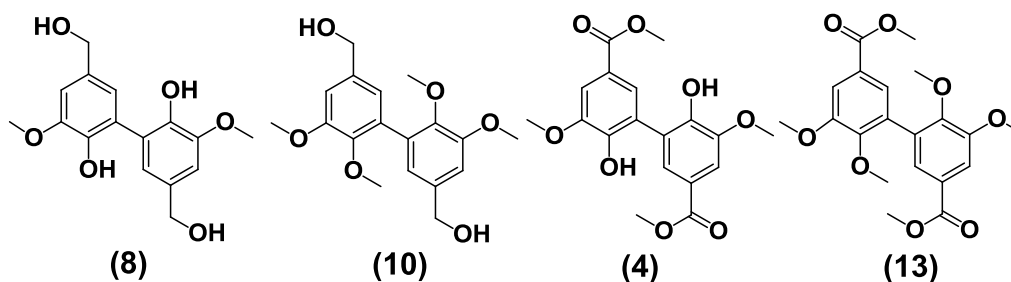
In the following chapter, several routes towards biphenyl-based polymers are presented. First, the polycondensation of divanillyl diol (**10**) with several co-monomers was investigated for the design of novel polyesters. A 100% vanillin-based polyester was notably synthesized by polycondensation of divanillyl diol (**10**) and dimethyl vanillate (**13**). Furthermore, the synthesis of polyamides is also investigated from divanillic diacid (**14**). In addition, ADMET methodology is employed to polymerize the four bis-unsaturated biphenyl monomers (**11**), (**15**), (**16**), (**19**) prepared in the previous chapter. Finally, the bisepoxide (**18**), synthesized from 2,6-dimethylphenol dimer, is compared to DGEBA for the preparation of epoxy resins with IPDA. The thermomechanical properties of the respective polymers are discussed.

## II Synthesis and characterization of thermoplastic polymers from biphenyl precursors via polycondensation

The well-defined methylated divanillyl diol (**10**) and dimethylvanillate dimer (**13**) are promising molecules to produce thermoplastic polymers. The latter were employed as starting material to the design of novel polyesters. Dimers (**8**) and (**4**) were obtained as powders with lower degradation temperatures than melting ones. For this reason, the methyl-protected biphenyls (**10**) and (**13**) which are viscous liquids at room temperature were selected for this polymerization in bulk. This protection also prevents the phenolic moiety to be involved in polymerization.

All the polycondensations described in this chapter were carried out at 160 °C for 2 h, employing a transesterification catalyst, under nitrogen flow and at 200 °C under vacuum for 6 h, in order to remove released methanol or water and to shift the equilibrium towards the

polymeric product (excepted for TBD, in this case, the reaction is performed at 120°C under vacuum for 24h).



Scheme 1: Structure of biphenyl diols (8) and (10) and diesters (4) and (13).

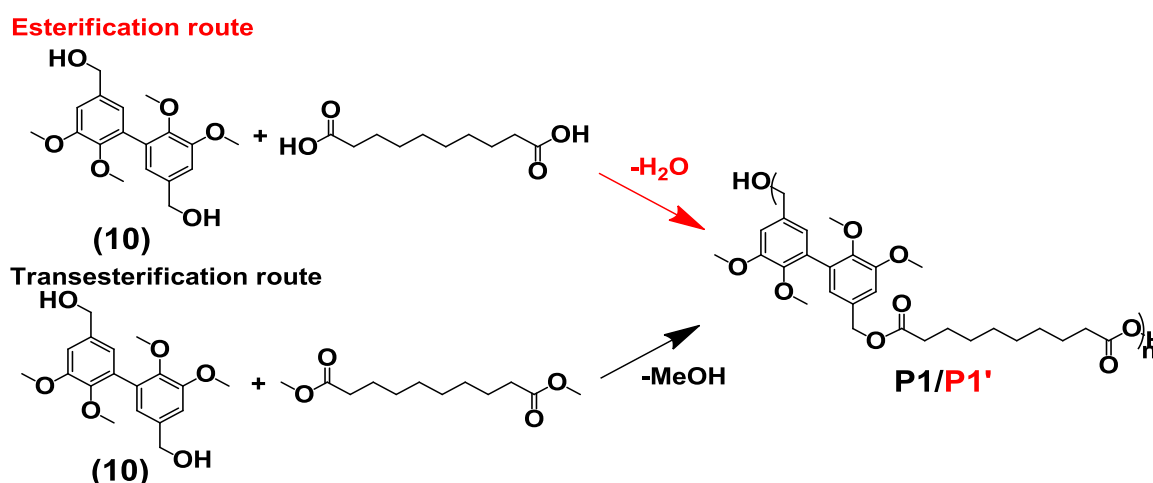
## 1. Synthesis and characterization of biphenyl polyesters

### 1) Optimization of the polymerization conditions

In this section, sebacic acid, methyl sebacate and 1,10-decanediol were employed as co-monomers to select the optimal polymerization conditions.

#### a) Esterification versus transesterification reactions

Polyesters can be produced either by esterification reaction of diols and diacids or by transesterification reaction between diols and diesters (Scheme 2). Titanium butoxide ( $\text{TiOBu}_4$ , 0.5 mol%) was employed as catalyst. The reaction of (10) with dimethylsebacate produced **P1** and, with sebacic acid, **P1'**. **P1** and **P1'** display the same co-monomer sequence but differ in terms of molar masses and thermal characteristics (Table 1).



Scheme 2: Synthesis of polyester from vanillyl diol and sebacic acid or dimethylsebacate.

**Table 1: Properties of polyesters from methylated divanillyl diol (10) and sebacic acid or dimethylsebacate.**

Polymer	Route	Co-monomer	$\bar{M}_n^a$ (kg/mol)	$\bar{D}$	Td5% (°C) <sup>b</sup>
<b>P1</b>	Transesterification	Methylsebacate	65	2.1	319
<b>P1'</b>	Esterification	Sebacic acid	20	1.7	298

<sup>a</sup>Determined by SEC in DMF/DMSO 80/20, <sup>b</sup>determined by TGA. Temperature of 5% degradation.

The chemical structures of **P1** and **P1'** were investigated by FTIR. As expected, both polymers presented similar FTIR absorption patterns (Figure 1). First, the lack of band characteristic of the alcohol moiety between 3 000 and 3 300  $\text{cm}^{-1}$  and the strong absorption of the ester carbonyl group observed at 1 729  $\text{cm}^{-1}$  indicated the conversion of alcohol into ester. The two bands at 2 931 and 2 853  $\text{cm}^{-1}$  and the two bands at 1 414 and 1 370  $\text{cm}^{-1}$  were attributed to alkane stretching and bending, respectively.

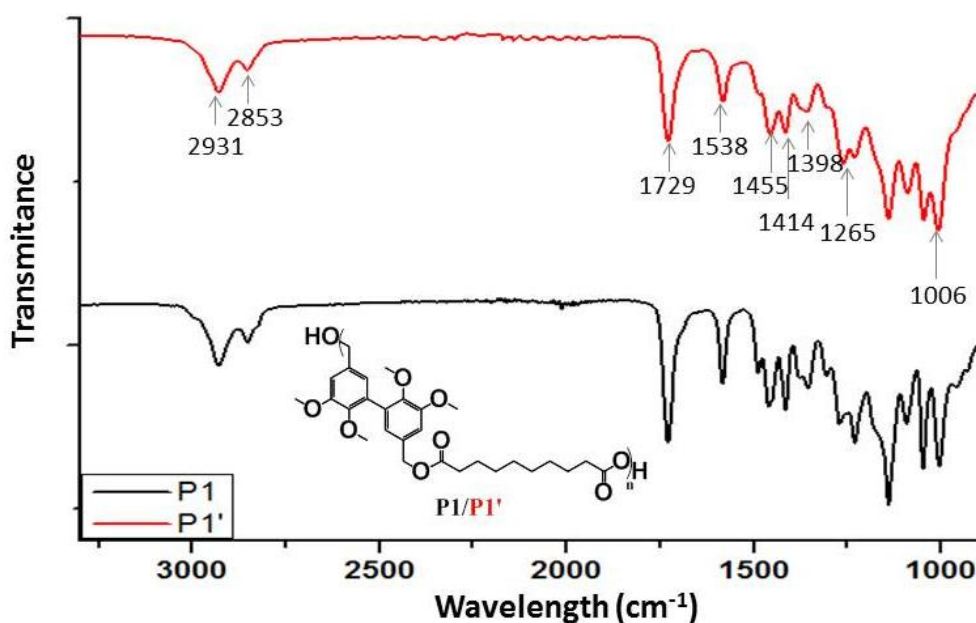


**Figure 1: FTIR spectra of methylated divanillyl diol/dimethylsebacate polymer P1 and divanillyl diol/sebacic acid polymer P1'.**

Absorption bands detected at 1 455 and 1 538  $\text{cm}^{-1}$  can be attributed to the aromatic segments in the polymer chains. The FTIR spectra also showed the characteristic signals at 1 006 and 1 265  $\text{cm}^{-1}$ , assigned to the methoxy group attached to the aromatic rings.<sup>4</sup>

The molar masses of the resulting polymers were determined by SEC analyses in DMF/DMSO 80/20 (w/w) (Figure 2). However, the molar mass values provided by SEC

should not be taken as absolute values as the SEC calibration was carried out in DMSO/DMF, using PS standards.

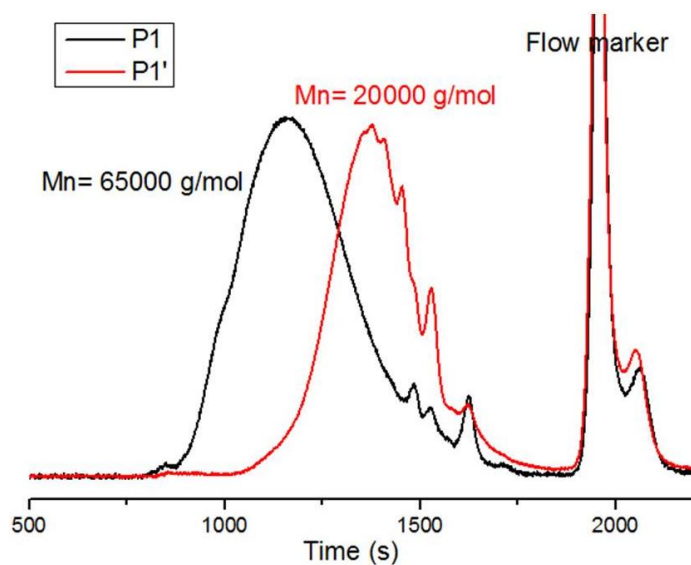


**Figure 2: SEC traces of methylated divanillyl diol/dimethylsebacate polymer **P1** and divanillyl diol/sebacid acid polymer **P1'** in DMSO/DMF 20/80, RI detection.**

**P1** exhibits a molar mass of 65 000 g/mol and a dispersity of 2.1 whereas **P1'** has a molar mass of 20 000 g/mol and a dispersity of 1.7. Degradation temperature is related to the molar mass and is also a good indicator to compare the two polymer structures. TGA analyses revealed that **P1** possess a 5% degradation temperature at 319 °C while **P1'** 5% degradation temperature was observed at 298 °C (Table 1).

While comparing the two routes, it appears that the transesterification method leads to polymers with higher molar masses and degradation temperatures. This feature can be logically explained by the easier remove of methanol in comparison to water thus shifting more efficiently the reaction equilibrium towards the polymer formed. All the polyesters described below were thus synthesized by transesterification pathway.

#### b) Catalyst screening

Several polymerization reactions of methylated divanillyl diol (**10**) with dimethylsebacate were carried out employing different catalysts: triazabicyclodecene (TBD), titanium butoxide (TiOBu<sub>4</sub>), zinc acetate (ZnAc<sub>2</sub>) and dibutyltin oxide (DBTO). Molar masses and 5% degradation temperature of the resulting polymers were compared with respect to the catalyst used (Figure 3). Thermal stability of the polymers is related to their molar mass directly connected to the catalyst employed.

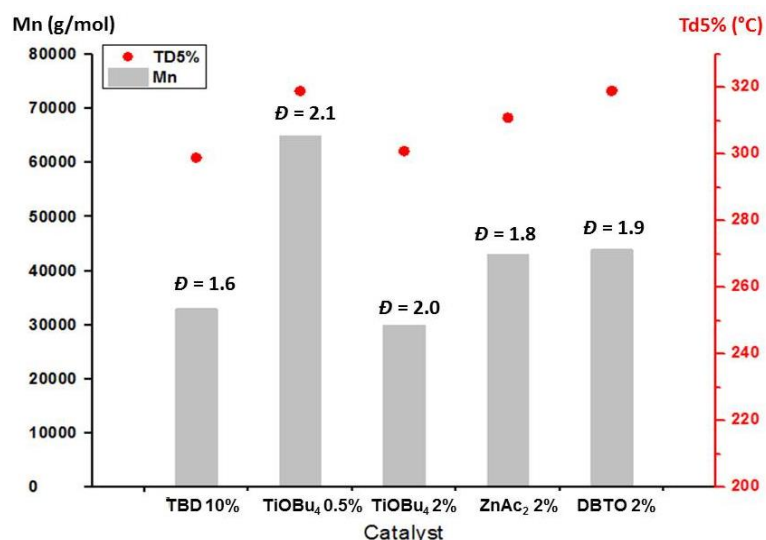


**Figure 3: Properties of polyesters from methylated divanillyl diol and methyl sebacate in the presence of different catalysts.**

Employing organocatalysts such as TBD generally requires higher catalyst loadings (10 mol%) in comparison to inorganic catalyst (2 mol%) and lower polymerization temperature (120 °C). In addition, a sample was prepared with 0.5 mol% of TiOBu<sub>4</sub>, in order to investigate the influence of the catalyst concentration on the polymerization. The polymerization with 0.5 mol% of TiOBu<sub>4</sub> afforded the highest molar mass of 65 000 g/mol and a dispersity of 2.1, and the highest 5% weight loss temperature of 320 °C. Surprisingly, it was observed that the molar mass decreased with increasing TiOBu<sub>4</sub> concentration. This reverse effect on the polymerization has already been observed in other studies reported in literature, for titanium alkoxide in general. However, no explanation was proposed.<sup>5,6</sup> ZnAc<sub>2</sub> and DBTO presented lower catalytic activities, but the molar masses and the degradation temperatures of the resulting polymers remained high, at around 45 000 g/mol and the dispersity close to 2.0 and 310 °C. TBD exhibited the lowest catalytic activity and produced polyesters with molar masses of 35 000 g/mol and a dispersity of 1.6 and the lowest 5% weight loss at around 300 °C.

The same study was conducted for the polymerization of dimethylated methyl vanillate (**13**) with 1,10-decanediol (Figure 4). In such a case, a low catalytic activity of TBD and ZnAc<sub>2</sub> was observed. Indeed, polyesters with a molar mass of 3 000 g/mol and a dispersity in the range of 1.0 to 1.2 were obtained. The use of 2 mol% of TiOBu<sub>4</sub> and DBTO showed better performance and led to the production of polyesters with molar mass in the range 11 000 to 12 000 g/mol and dispersity of 1.3 and 1.6. Finally, the polymerization with 0.5 mol% of TiOBu<sub>4</sub> afforded again the highest molar mass, 20 000 g/mol with a dispersity of 1.8. Following the same trend, the highest 5% degradation temperatures, of around 320 °C were



obtained employing DBTO and 0.5 mol% of  $\text{TiOBu}_4$  of catalyst, thus revealing the better efficiency of these catalysts.

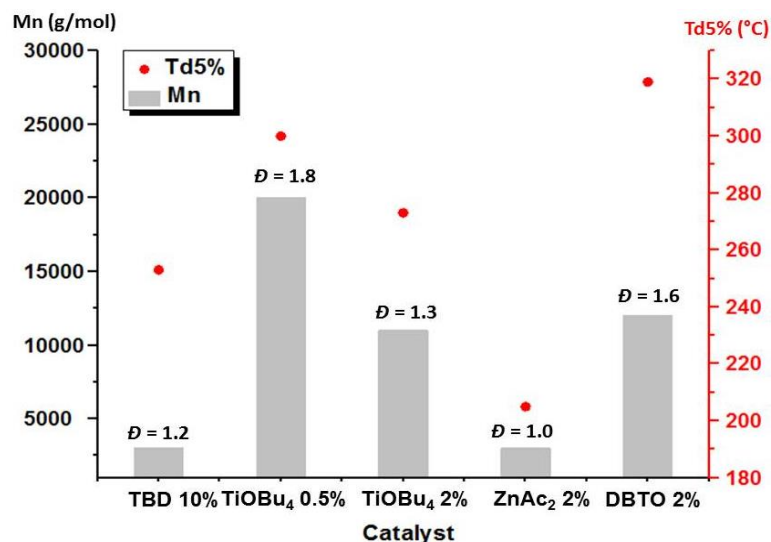


**Figure 4: Properties of polymers from methylated dimethyl vanillate dimer and 1,10-decanediol employing different catalysts.**

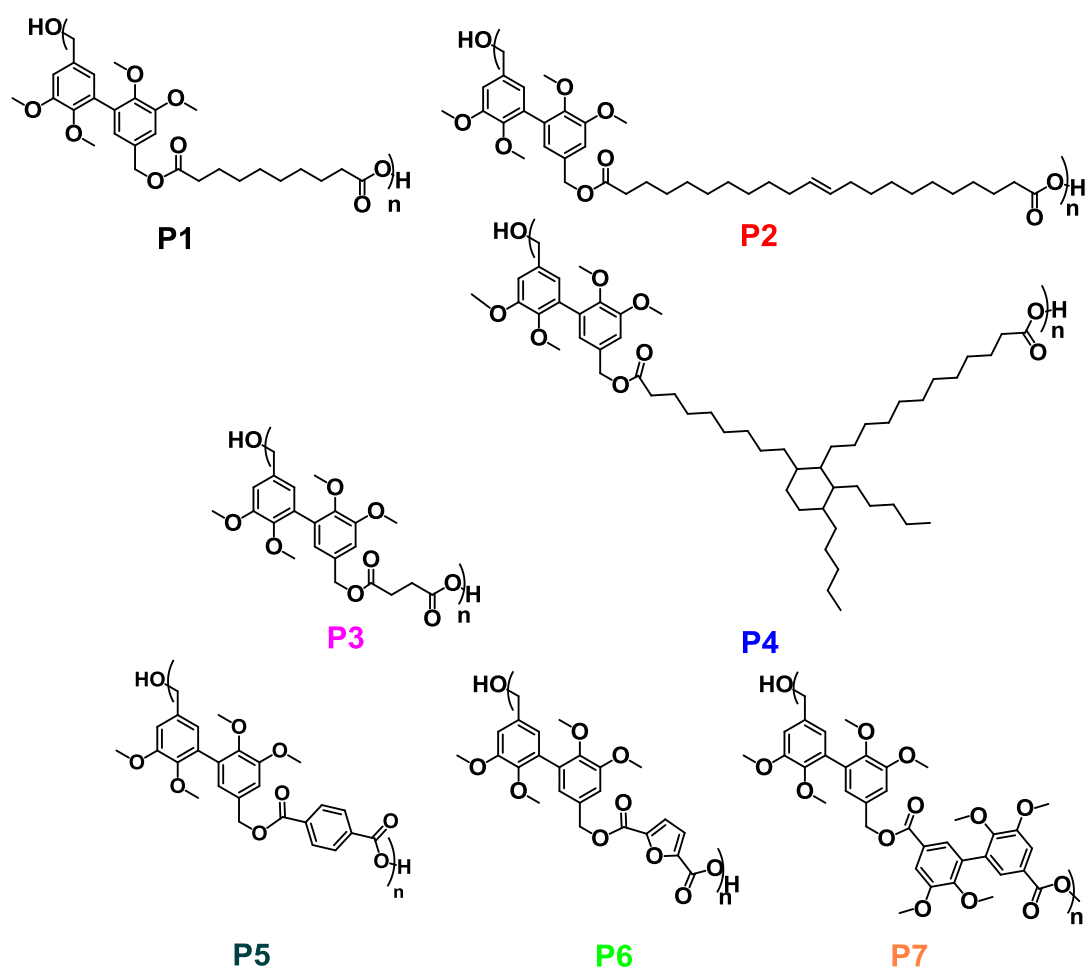
The polyesters synthesized by polycondensation of methylated dimethyl vanillate dimer (**13**) with 1,10-decanediol exhibited lower molar masses than the polyesters prepared by polycondensation of methylated divanillyl diol (**10**) with dimethylsebacate. This difference suggests that divanillyl diol (**10**) is more reactive toward polycondensation than methylated methyl vanillate dimer (**13**). Indeed, the first reaction involves an aliphatic ester and benzyl alcohol, whereas the second one involves an aromatic ester and an aliphatic primary alcohol. Under thermodynamic aspect, aromatic esters are stabilized due to the  $+\delta$  charge delocalization on the aromatic ring, which leads to a reactivity decrease in comparison to an aliphatic ester. Moreover (**10**) and (**13**) show different steric hindrance. Indeed, the ester moiety of (**13**) is closer to the aromatic ring than the benzyl alcohol group of (**10**), it is thus more hindered and logically less reactive.

Therefore, in the following studies methylated divanillyl diol (**10**) was used as biphenyl building block and  $\text{TiOBu}_4$  (0.5 mol%) was selected as catalyst. The reaction between (**10**) and (**13**) was also investigated.

## 2) Synthesis of a series of copolyester

A series of copolymers were synthesized based on methylated divanillyl diol (**10**), and several diesters with aromatic, aliphatic or cycloaliphatic structures, in order to produce polyesters with a wide range of thermomechanical properties (Scheme 3).





**Scheme 3: Structures of polyesters synthesized from methylated divanillyl diol (10) and diesters with different structures.**

The copolymerization of (10) with dimethyl sebacate, dimethyl succinate and dimethyl-11-docosenoate produced polyesters **P1**, **P2**, **P3** with alternating aromatic and aliphatic sequences, the latter having different chain lengths. **P4** was synthesized by copolymerization of (10) with a fatty acid dimer (C36), namely Pripol. The copolymerization of (10) with dimethyl terephthalate and with its common biobased substitute, 2,5-furandimethyl ester led to the aromatic polyesters **P5** and **P6**. Finally, an aromatic polyester 100% derived from vanillin, **P7**, was prepared by polycondensation of methylated divanillyl diol (10) and methylated dimethyl vanillate dimer (13).

Excepted **P1** that was previously characterized, all the polyesters were not soluble in any solvent allowing their characterization through NMR and SEC. The chemical structure of these polyesters was thus determined by FTIR analyses. Monitoring the reactions by FTIR, the success of the transesterification reaction was proved by: (i) the disappearance of broad peak between 3 000 and 3 500  $\text{cm}^{-1}$ , characteristic of the hydroxyl stretching, whereas the

typical C=C stretching vibration of the aromatic ring was found at  $1583\text{ cm}^{-1}$ , (ii) the presence of the C=O ester linkage at  $1730\text{ cm}^{-1}$  (Figure 5).

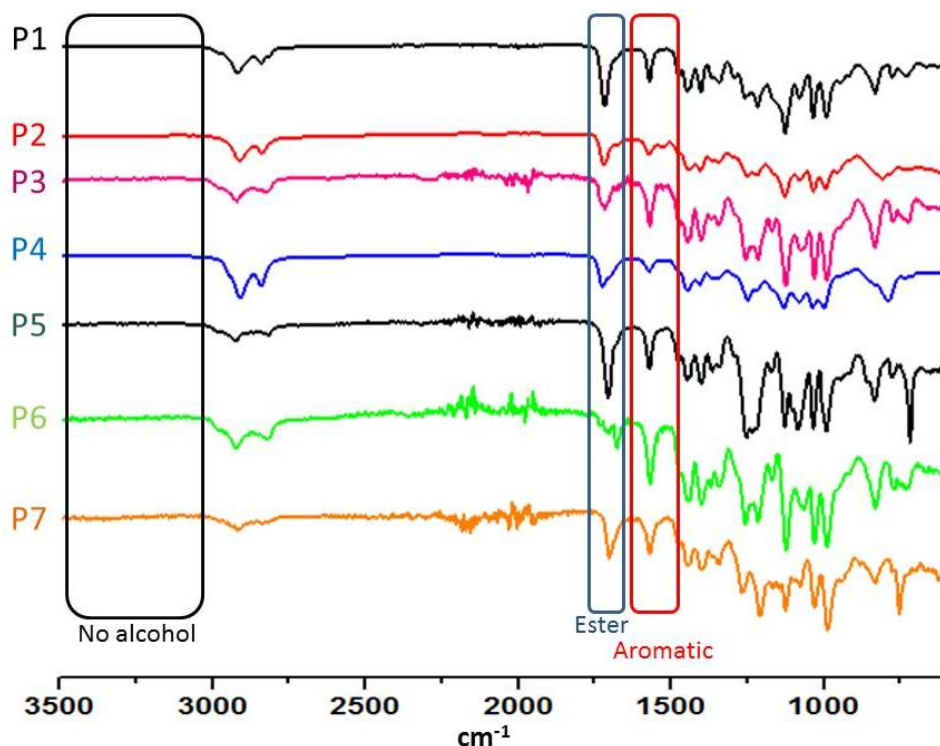


Figure 5: FTIR spectra of polyesters synthesized from methylated divanillyl diol with different diesters, P1 to P7.

### 3) Thermomechanical properties of the copolymers

The thermomechanical properties of the polyesters were determined by DSC, TGA and DMA. DSC analyses were performed by heating the sample from  $-70\text{ }^{\circ}\text{C}$  to  $180\text{ }^{\circ}\text{C}$  at a rate of  $10\text{ }^{\circ}\text{C}\cdot\text{min}^{-1}$ . Consecutive cooling and second heating runs were also performed at  $10\text{ }^{\circ}\text{C}\cdot\text{min}^{-1}$ . The glass transition temperatures were calculated from the second heating run. DSC traces showed that all the polymers were amorphous. The polyesters present a glass transition temperature ranging from  $-4.5$  to  $139.0^{\circ}\text{C}$ , influenced by the structure of the co-monomer. Miller and coll. showed the influence of methoxy groups attached to the aromatic ring on the polymer crystallinity. For instance, the authors showed that polyacetals synthesized from vanillin derivatives are semi-crystalline while polyacetals from syringaldehyde are amorphous.<sup>4,7</sup> Indeed, the presence of two methoxy groups attached to aromatic rings induces a higher free volume. This special disposition hinders the mobility and packing of the polymer chains, resulting in amorphous polymers.

The Tg value depends on the backbone flexibility of the polymer and of the free volume. As expected, **P4**, with Pripol as co-monomer, exhibited the lowest glass transition temperature.

Indeed, Pripol possesses a ring with aliphatic dangling chains, which add conformational disorder free volume, increasing the chain mobility and lowering the  $T_g$  value. The aromatic polyesters **P5**, **P6** and **P7**, exhibited the highest  $T_g$  of over 100 °C due to the inherent rigidity of the aromatic structures. On the contrary, aliphatic chains give flexibility to the resulting polymers. Thus, the  $T_g$  of the semi-aromatic polymers **P2**, **P1** and **P3** ranged from 5.2 to 68 °C. In general, shorter aliphatic chains lead to polymer with higher  $T_g$ . Indeed, **P3** synthesized from the C4 diester exhibited a  $T_g=68$  °C, value higher than the one of **P2** synthesized from the C22 diester,  $T_g=5$  °C. Varying the aliphatic co-monomer structure allowed us tailoring the  $T_g$  of the resulting polyesters.

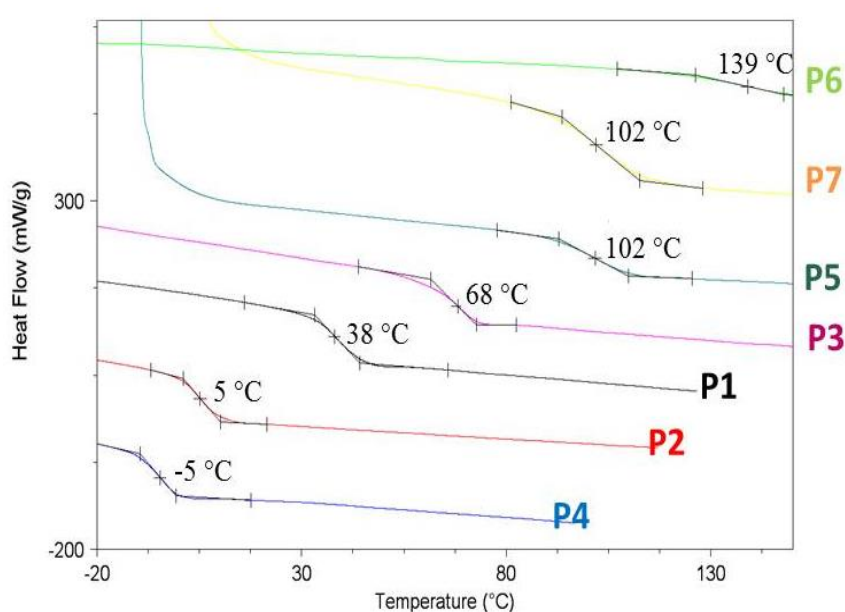


**Figure 6:** DSC thermograms (second heating cycle) of polyesters synthesized from methylated divanillyl diol (**10**) and different methyl diesters.

$T_g$  of **P5**, synthesized by copolymerization of divanillyl diol (**10**) and dimethylterephthalate, and **P7**, synthesized by copolymerization of divanillyl diol (**10**) and dimethyl divanillate (**13**) are identical. Thus, biphenyl derivatives, derived from vanillin dimerization, are potentially good substitutes for terephthalic acid in terms of thermal properties.

TGA experiments were performed under air. Besides **P3**, which 5% weight loss occurred at 270 °C, all the copolymers presented a 5% degradation temperature over 300 °C. **P4**, obtained by copolymerization of divanillyl diol and Pripol, exhibited at 340 °C the highest 5% degradation temperature.

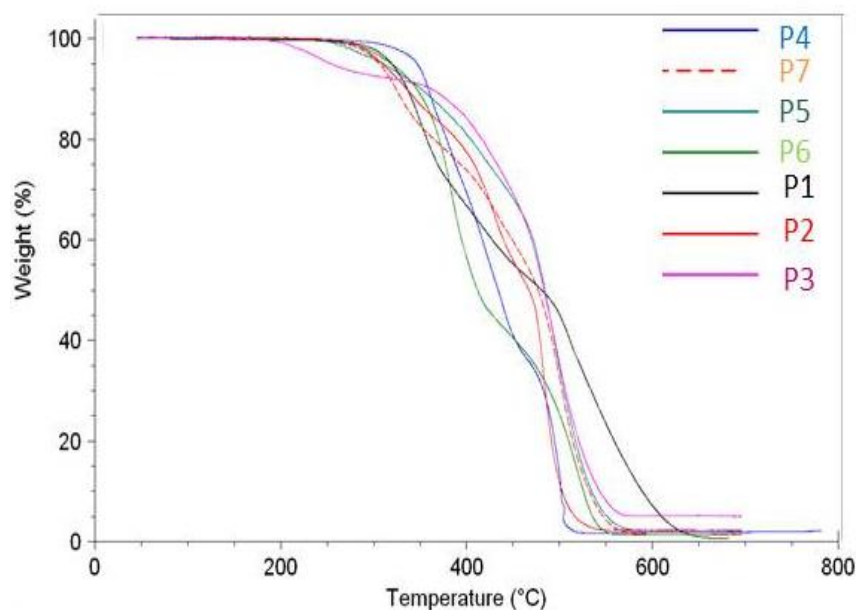


Figure 7: TGA thermogram (second heating cycle) of polyesters synthesized from methylated divanillyl diol (**10**) and different methyl diesters.

The mechanical properties of the polyesters were also investigated by dynamical mechanical analyses (DMA), performed on bar samples in a 3-point bending mode. The tensile storage modulus ( $E'$ ) versus temperature of all the copolyesters is plotted in Figure 8. The decrease of the storage modulus is characteristic of the glass transition of the material.

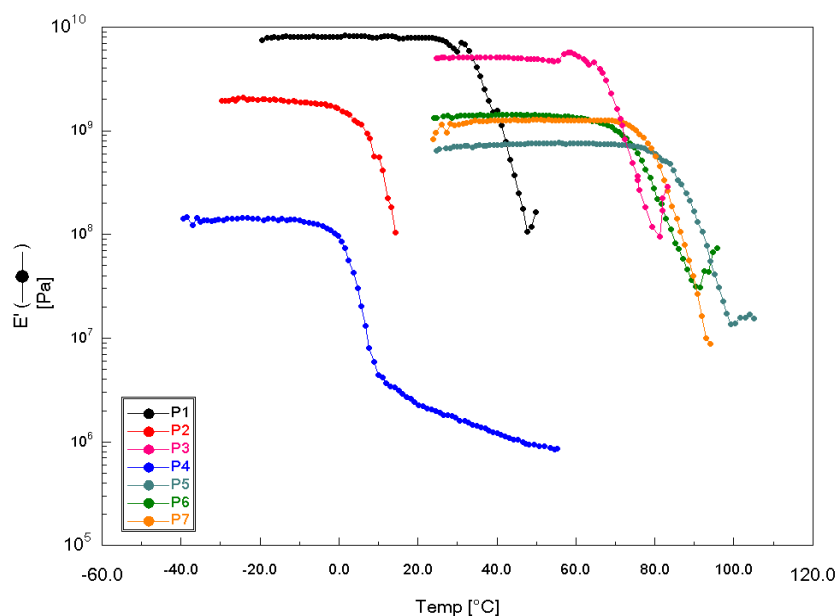


Figure 8: DMA analysis of the copolymers synthesized from divanillyl diol, using 3-point bending test at 1 Hz from -40 to 120 °C at 10 K/min.

In agreement with DSC data, the decrease of the storage modulus was observed first for **P4**, then for the semi-aromatic polyesters **P2**, **P1** and **P3** and finally for the aromatic polyesters **P6**, **P5** and **P7**. The small variations in  $T_g$  values when comparing DSC and DMA data are explainable by the way of measurement. Indeed, DSC measures the changes of the heat

capacity and DMA records the mechanical response of the polymer chains during the transition. Below the glass transition temperature, the polymer is in a glassy state whereas over the glass transition temperature, the polymer reaches a rubber state. At room temperature, **P4** and **P2** were rubber materials whereas **P1**, **P3**, **P5**, **P6** and **P7** showed a glassy behavior.

The storage modulus in glassy state ( $E'$ ) of the semi-aromatic polyesters increased when the length of the aliphatic chain decreased, i.e. **P4** < **P2** < **P1**. **P3** and **P1** exhibited similar high storage modulus, in the range of 10 GPa (Table 2).

**Table 2: Thermomechanical properties of polyesters from of methylated divanillyl diol and different methyldiesters.**

Polyester	T <sub>g</sub> (°C) <sup>a</sup>	Td5% (°C) <sup>b</sup>	E' (GPa) <sup>c</sup>
<b>P1</b>	38	319	8,1
<b>P2</b>	5	308	2,0
<b>P3</b>	68	302	5,1
<b>P4</b>	-5	347	0,1
<b>P5</b>	102	310	2,0
<b>P6</b>	140	342	1,4
<b>P7</b>	102	305	1,3

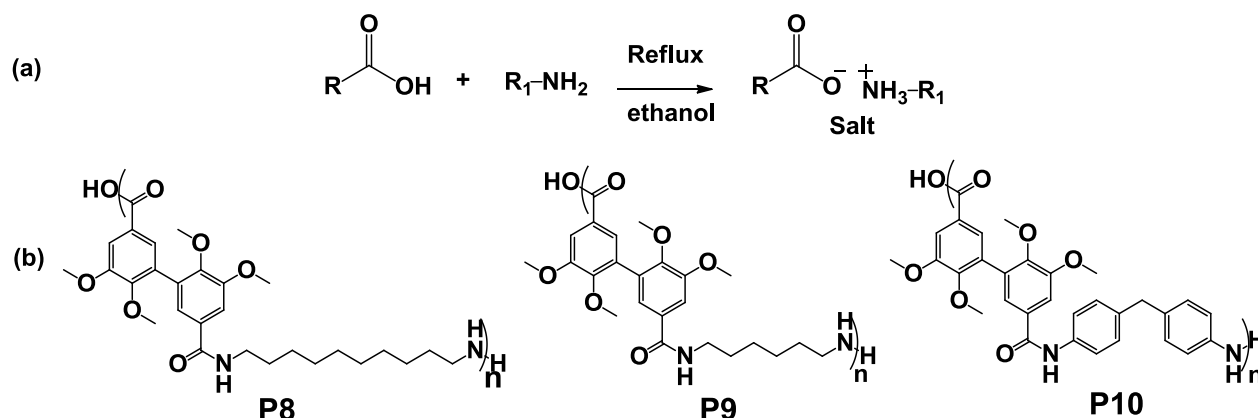
<sup>a</sup>Determined by DSC second heating cycle, <sup>b</sup>Determined by DMA 3 points flexion, <sup>c</sup>Determined by TGA. Temperature of 5% degradation.

The aromatic polyesters, **P5**, **P6** and **P7** were expected to possess higher storage modulus. However, DMA analyses revealed  $E'$  values of around 2 GPa. This lower value in comparison to  $E'$  of **P1** and **P3** might be attributed to the lower molar masses of these polyesters in agreement with the lower reactivity of the aromatic monomers explained by their steric hindrance .

## 2. Preliminary study on polyamide synthesis from biphenyl precursors

A preliminary study was carried out on the synthesis of polyamides based on methylated divanillic acid (**14**). The polyamides **P8**, **P9** and **P10** were respectively prepared by polycondensation of (**14**) with 1,10-diaminodecane, 1,6-diaminohexane and 4,4'-diaminodiphenylamine. Prior to all polymerization reactions, the diamine/dicarboxylic acid salts were prepared to ensure an exact stoichiometry of the two components. A 10% ethanolic solution of diamine was slowly added to an equimolar portion of 10% ethanolic solution of (**14**) at 60 °C, resulting in precipitation of a white solid. The mixture was refluxed for 30 min.

The salt was collected, put into a DSC capsule in order to investigate the salt behavior in temperature.



**Scheme 4:** Salt preparation (a), structures of the polyamides synthesized from methylated divanillic diacid (14) and diamines with different structures (b).

The first heating cycle of the salt prepared from (14) and 1,10-diaminododecane is displayed in Figure 9 (a). The endothermic broad peak at 70 °C was attributed to the evaporation of the remaining ethanol. The second endothermic peak at 240 °C, characteristic of the salt melting, is followed by an exothermic peak which maximum is reached at 270 °C. This peak indicates the polymerization of the sample. The same thermal behavior was observed for the two other salts which exhibited melting temperatures at 230 and 250 °C for the 1,6-diaminohexane and 4,4'-diaminodiphenylmethane. The second heating of the samples revealed the glass transition temperatures of the samples. The aromatic aliphatic polyamides, **P8** and **P9** showed a T<sub>g</sub> at 124 and 136 °C, respectively, Figure 9 (b).

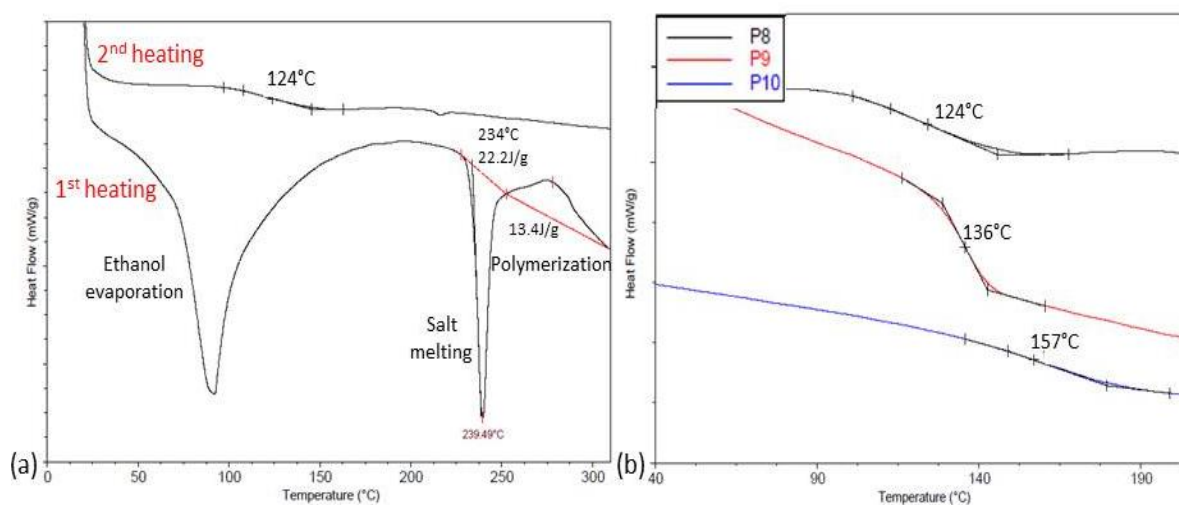


**Figure 9:** DSC thermogram of the first heating of the salt prepared from (14) and 1,10-diaminododecane(a). DSC thermogram of the second heating of the polyamides **P8**, **P9** and **P10**(b).

As expected, increasing the aliphatic chain length decreased the T<sub>g</sub> of the resulting polymers. Moreover, the T<sub>g</sub> of the aromatic polyamide **P10** reached 157 °C and was higher than the T<sub>g</sub> of the semi-aromatic polyamides. In literature, 2,5-furandicarboxylic acid (FDCA) is generally used as a bio-based substitute of terephthalic acid for the synthesis of polyamides.<sup>8</sup> The polymerization of FDCA with 1,10-diaminodecane and 1,6-diaminohexane leads to polyamides with a T<sub>g</sub> of 70 and 110 °C, respectively. T<sub>g</sub> of the divanillin-based polyamides are higher than the ones of the polyamides synthesized from FDCA. It is also interesting to compare the T<sub>g</sub> of polyamide **P8** and corresponding polyester **P1**, which exhibit the same aromatic and aliphatic sequences between the ester and amide functions. As expected, the T<sub>g</sub> of **P8** (120 °C) is higher than the one of **P1** (38 °C). Moreover, the T<sub>g</sub> of the aromatic polyamide **P10** is 50 °C higher than the one of the fully aromatic polyesters **P5** and **P6**. This difference can be attributed to hydrogen bonding due to amide linkages resulting in strong interactions between the polymer chains, requiring more energy to get the rubber state. These high T<sub>g</sub> values are in the range of T<sub>g</sub> of poly(phtalamide)s, between 90 and 140 °C. Poly(phtalamide)s are high performance polyamides and differ from aliphatic polyamides by the incorporation of aromatic dicarboxylic acid (terephthalic acid or isophthalic acid) in the polymer backbone.

However, this study constitutes only preliminary results. The synthesized polyamides should be produced in reasonable quantity, either by polymerization in bulk after screening for the best reaction parameters -such as temperature and pressure- in order to enable the salt to melt without degrading the material, or in solvent, employing a catalyst. Thus, more analyses, such as TGA, DMA, FTIR and SEC should be performed in order to better characterize the materials.

### Conclusion:

In summary, novel polyesters were synthesized by polycondensation of methylated divanillyl diol and several diesters. The optimal conditions were examined for the divanillyl diol/dimethylsebacate system. Titanium butoxide at a loading of 0.5 mol% was proven to produce the polyesters with the highest molar masses up to 65 000 g/mol, and exhibiting a T<sub>g</sub> of 38 °C, a storage modulus of 8.1 GPa and a T<sub>d5%</sub> of 318 °C. The same conditions were applied for the polymerization of methylated divanillic diol with a series of diesters. Varying the structure of the diester allowed us tailoring the thermomechanical properties of the resulting polyesters. T<sub>g</sub> of the corresponding polyesters are ranged from -4 to 140 °C. Their thermal stability is high with a 5% weight loss temperature over 300 °C. These thermal

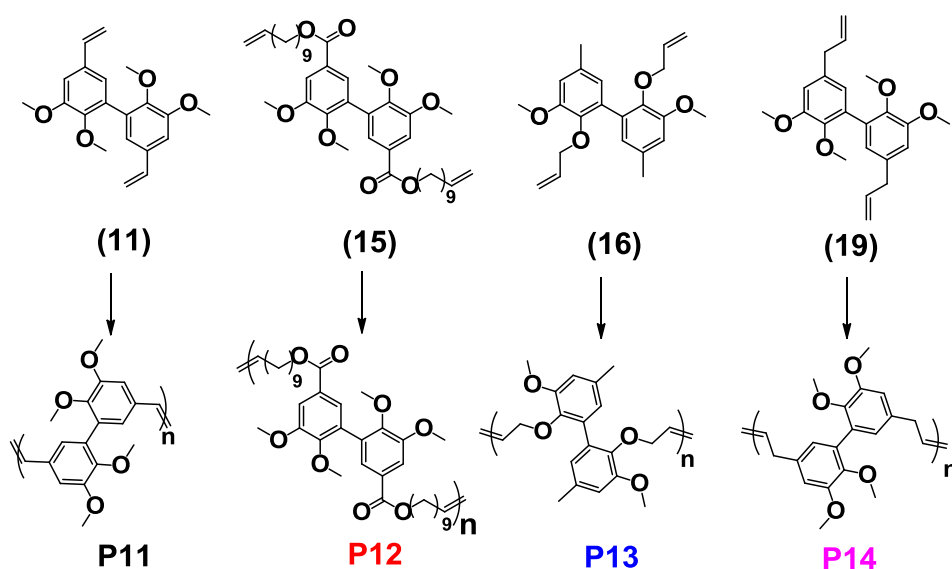


properties are similar to commodity polymers such as PET and PS which T<sub>g</sub> are around 70 and 100 °C, respectively. The potential of methylated divanillic acid in polyamide synthesis was also investigated through a preliminary DSC study. This work revealed the formation of polyamides with a T<sub>g</sub> ranging from 125 to 156 °C.

### III Synthesis and characterization of thermoplastic polymers from biphenyl precursors via ADMET polymerization

#### 1. Synthesis, chemical structure and molar mass determination

The dimers with terminal double bonds (**11**), (**15**), (**16**) and (**19**), synthesized in the previous chapter, were polymerized by acyclic diene metathesis (ADMET) polymerization resulting in **P11**, **P12**, **P13** and **P14** (Scheme 5). ADMET polymerization is a step-growth polymerisation driven by the release of a condensate, usually ethylene. ADMET is typically performed on  $\alpha,\omega$ -dienes to produce well-defined polymers with unsaturated backbones. Due to the high melting points of the monomers, the reaction temperatures of the melt were incompatible with the thermal stability of the catalyst. *Polarclean* was selected as solvent for its high boiling point, its compatibility with Grubbs catalyst and its sustainability.<sup>9</sup> Thus, the polymerizations were performed employing Grubbs catalyst (2 mol%) in *Polarclean* solvent, under vacuum, at 80 °C, for 18 h.



**Scheme 5: Structures of the polymers P11, P12, P13 and P14 synthesized by ADMET polymerization from divanillic divinyl (11), bis-unsaturated diester (15), allylated 4-methyl-2-methoxy dimer (16), methylated and dieugenol (19).**

The first step of this study focuses on the reactivity of the diene to ruthenium-based olefin metathesis catalysts. The efficiency of catalyst depends on the functional groups of the diene



to be polymerized and other factors like the melting point or solubility of the monomers.<sup>10</sup> In order to select the catalyst which leads to the polymer with the highest molar mass, each compound was polymerized employing 2 mol% Grubbs 1st (G1), Grubbs 2nd (G2), Hoveyda-Grubbs 1st (HG1) and Hoveyda-Grubbs 2nd (HG2) generation metathesis catalysts (Figure 10).

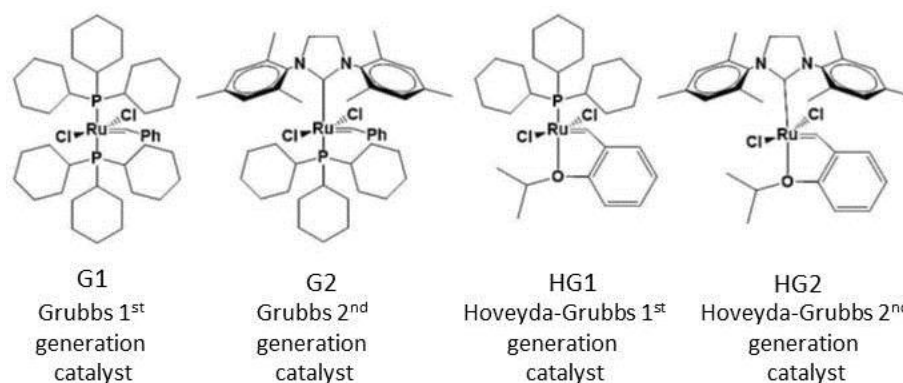


**Figure 10:** Chemical structures of the first and second generation ruthenium metathesis catalysts.

It has been reported in literature that olefin isomerization side reactions (double bond migration) can be observed in ADMET polymerization when employing G2 and HG2 catalysts. However, such a double bond isomerization can be suppressed by using quinone-type compounds.<sup>11,12</sup> Thus, when G2 and HG2 were used, 5 mol% of 1,4-benzoquinone was added to limit isomerization, for compounds **(15)**, **(16)** and **(17)**. The polymers were purified by reprecipitation in cold methanol. The polymer molar masses, determined by SEC in DMF are summarized in Table 3. The SEC profiles of **P11**, **P12**, **P13** and **P14** synthesized employing HG2, G1, HG1 and HG2, respectively are shown in Figure 11.

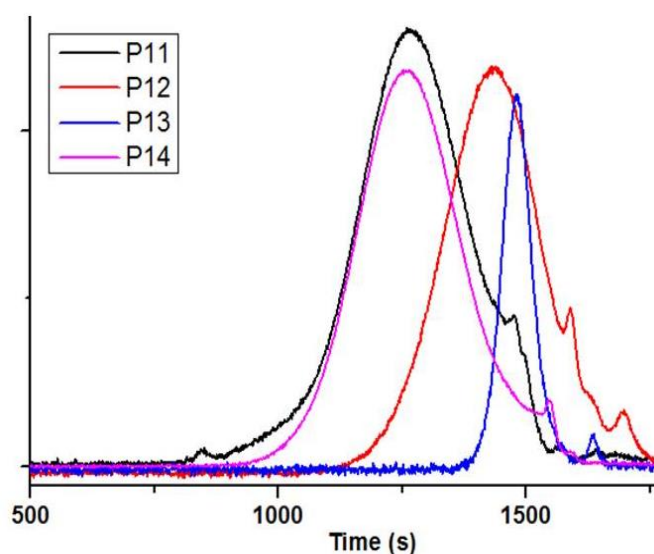


**Figure 11:** SEC profiles of **P11**, **P12**, **P13** and **P14** synthesized by ADMET polymerization of biphenyls, in DMF using PS calibration.

**P11** and **P14** respectively synthesized from divinyl (**11**) and methylated dieugenol (**19**) exhibited the highest molar mass whereas the polymerization of (**16**) leads to oligomers **P13**. More details about the polymer structures were extracted from  $^1\text{H}$  NMR analyses.

Compound (**11**) exhibits a conjugation between the double bond and the aromatic ring. In literature, the synthesis of low molar masses poly(p-phenylenevinylene)s-type polymers by ADMET in presence of molybdenumcarbene complex has already been reported.<sup>13,14</sup> In 2005, Geerts and coll. demonstrated that high molar mass, defect-free, all-*trans* poly(p-phenylenevinylene)s can be prepared employing Ruthenium-based catalysts, G2 and HG2 (Table 3).<sup>15</sup> In our study, the polymerization of (**11**) employing G2 and HG2 catalysts led to a precipitate after reprecipitation. The highest molar mass, 29 000 g/mol, was achieved employing HG2 catalyst.<sup>13,16</sup> This result is consistent with the studies reported in literature.<sup>17</sup> The disappearance of the signals at 6.68, 5.81 and 5.77 ppm attributed to the terminal double bonds on the  $^1\text{H}$  NMR spectrum of **P11** indicates the successful polymerization. The  $^1\text{H}$  NMR spectrum of **P11** also shows a signal of the methoxy protons at 3.93 and 3.61 ppm, signals of the aromatic protons at 7.04 ppm and signal of the methylene protons at 6.98 ppm (Figure 12). The results obtained prove the all-*trans* configuration of the vinylene bonds. Indeed, no signal is detected at 6.65 ppm which is the value of *cis* vinylene bonding signals found in literature.<sup>13</sup>

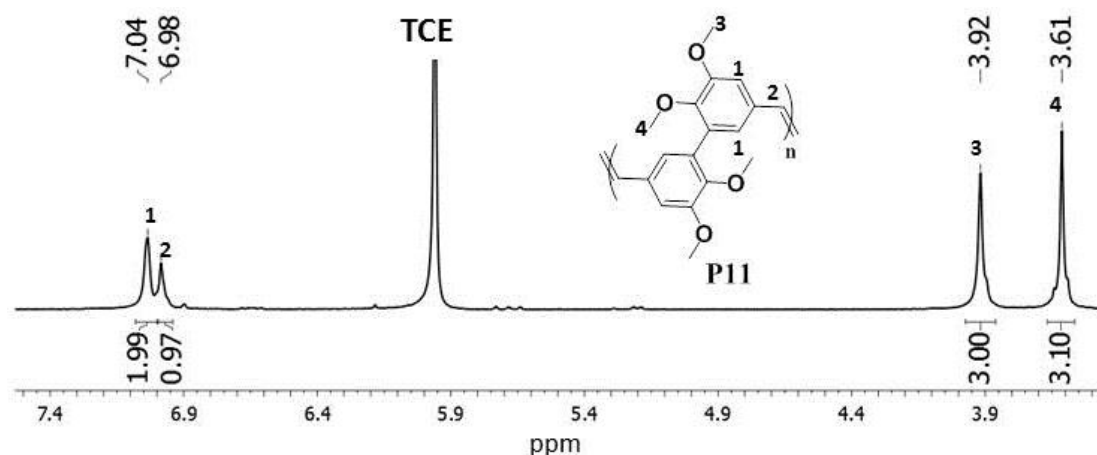


Figure 12:  $^1\text{H}$  NMR spectrum of **P11** in TCE, at room temperature.

Dimer (**15**) possesses an aliphatic chain of 10 carbons between the aromatic ring and the terminal double bond. Polymers prepared from (**15**) employing G1, HG1 and HG2 catalysts were recovered as precipitates in cold methanol (Table 3). The highest molar masses of 11 000 g/mol, were achieved employing G1 and HG2 catalysts. The  $^1\text{H}$  NMR spectrum of **P12** shows signal of the methoxy protons at 3.92 and 3.66 ppm, the signal of the aromatic

protons at 7.53 ppm and signals of the aliphatic chain between 1.00 and 2.00 ppm (Figure 13). The disappearance of the signals at 5.00 and 4.35 ppm attributed to the terminal double bonds and the appearance of a signal at 5.34 ppm assigned to internal double bonds, indicate the success of the polymerization.

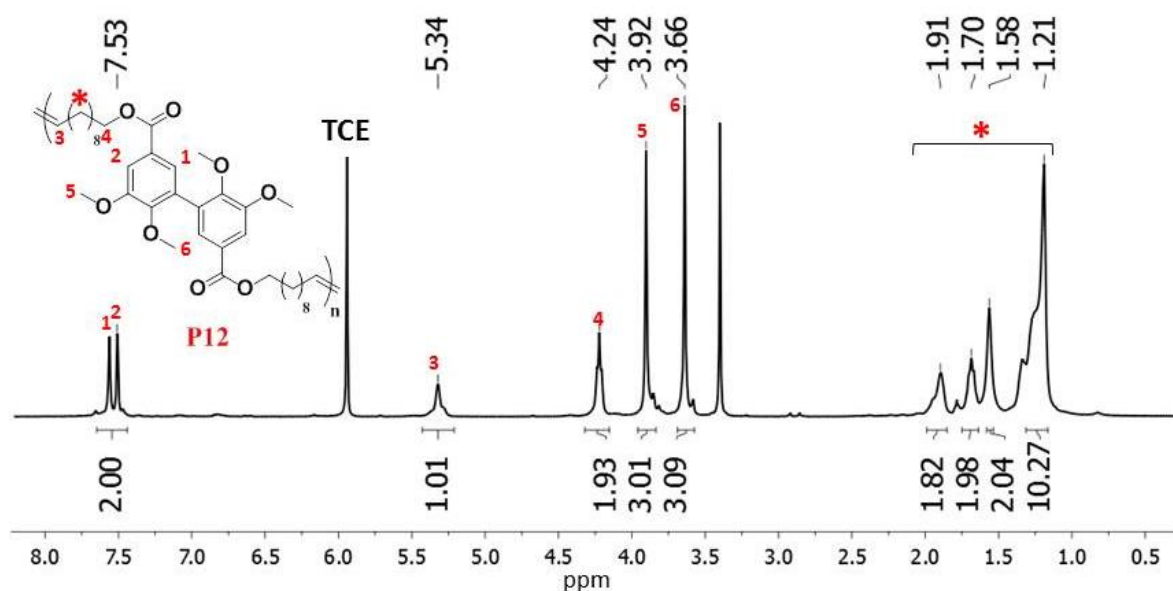


Figure 13:  $^1\text{H}$  NMR spectrum of P12 in TCE, at room temperature.

Dimer (**16**) contains a heteroatom in  $\beta$ -position of the terminal double bond. It is well-known that heteroatoms can be included in ADMET polymerization if sufficient “spacing” separates the active olefin site and the functional group containing the heteroatom itself.<sup>18</sup> The polymer prepared from (**16**) employing HG1 catalyst was recovered as precipitates in cold methanol (Table 3). **P13** exhibited the lowest molar mass of 7 000 g/mol. The  $^1\text{H}$  NMR spectrum of **P13** shows the signal characteristic of aromatic, methoxy and methyl protons, respectively at 6.60, 3.75, and 2.21 ppm. The signals at 5.42 and 4.06 ppm are assigned to internal double bonds and methylene in  $\alpha$ -position of the ether moiety. The integration below 2.00 of the signal at 4.06 ppm indicates the presence of isomerization. In addition, a doublet at 1.35 ppm can be attributed to the methyl group in  $\gamma$ -position of the ether moiety. These vinyl ether moieties are not reactive towards Grubbs catalysts and can act as chain stoppers of the polymerization.<sup>18</sup> These chain ends allowed us to calculate a degree of polymerization of 13. This value is a little lower than the value of 20 determined by SEC analyses. Thus, only oligomers were synthesized by ADMET polymerization of (**16**), probably due to complexation of the non-bonded electrons of the heteroatom with the metal center.

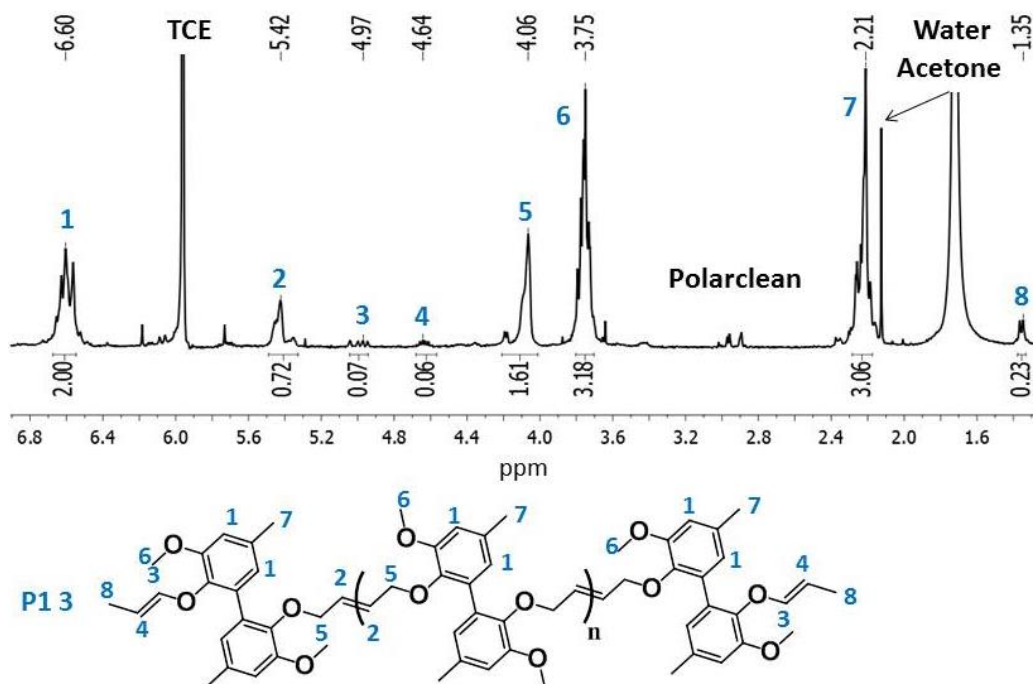


Figure 14: <sup>1</sup>H NMR spectrum of P13 in TCE, at room temperature.

The ADMET polymerization of dieugenol employing G1, HG1, G2 and HG2 catalysts did not lead to the formation of polymers. The hydroxyl moieties might deactivate the Grubbs catalysts. The polymerization was performed on methylated dieugenol (**19**). The polymers prepared from (**19**) employing HG1, G2, HG2 catalysts were recovered as precipitates in cold methanol (Table 3). The highest molar mass of 40 000 g/mol was achieved in presence of HG2 catalyst. The <sup>1</sup>H NMR spectrum of (**19**) showed 3 broad signals between 6.40 and 7.20 ppm. The signal at 7.02 ppm and 6.29 ppm were attributed to the aromatic ring and to the internal double bonds in  $\beta$ -position of the aromatic ring.<sup>19</sup> However, the signal at 6.73 ppm is characteristic of *trans* configuration the vinylene bonds of stilbenes. The integration of the signal at 2.54 ppm, commonly assigned to benzyl protons was 0.66 instead of 2. These two observations suggested the isomerization of eugenol into isoeugenol. This isomerization commonly occurs in eugenol metathesis due to the thermodynamical stability of the resulting styrene derivative and the kinetically faster subsequent metathesis to stilbene oligomers. In our case, 60% of the units were stilbene derivatives. The use of 5 mol% of 1,4-benzoquinone, was not sufficient to inhibit the isomerization.<sup>20</sup> It would be interesting to compare this polymer with a polymer synthesized by ADMET polymerization of isoeugenol dimer. However, isoeugenol dimer was not synthesized selectively by the coupling reaction catalyzed by laccase (cf previous chapter).

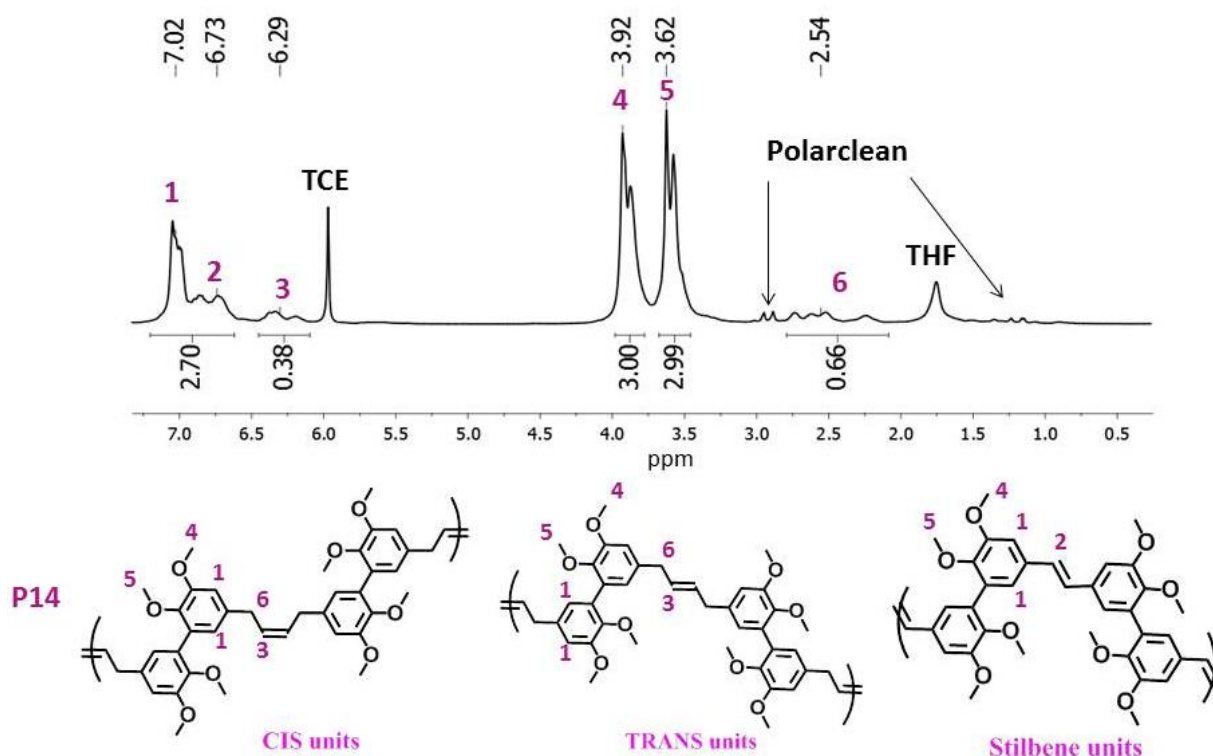
Figure 15: <sup>1</sup>H NMR spectrum of P14 in TCE, at room temperature.

Table 3: Thermomechanical properties of polymers P11, P12, P13 and P14 synthesized by ADMET of biphenyl compounds.

Monomers	Name	Catalyst	$\bar{M}_n^a$ (g/mol)	$D^a$
(11)	P11	G1	/	/
		HG1	/	/
		G2	16 000	1.4
		HG2	29 000	1.7
(15)	P12	G1	11 000	1.6
		HG1	7 000	1.6
		G2	/	/
		HG2	10 000	1.6
(16)	P13	G1	/	/
		HG1	7	1.1
		G2	/	/
		HG2	/	/
(19)	P14	G1	/	/
		HG1	6 000	1.3
		G2	28 000	1.7
		HG2	40 000	1.7

<sup>a</sup>Determined by SEC in DMF, PS calibration, RI detection.

## 2. Thermomechanical properties of the unsaturated polymers

The thermomechanical properties of the ADMET-based polymers were analyzed by DSC, TGA, and DMA (Table 4). The glass transition temperatures were calculated from the second

heating run of DSC analyses. DSC traces show that all the so-formed polymers are amorphous (Figure 16).

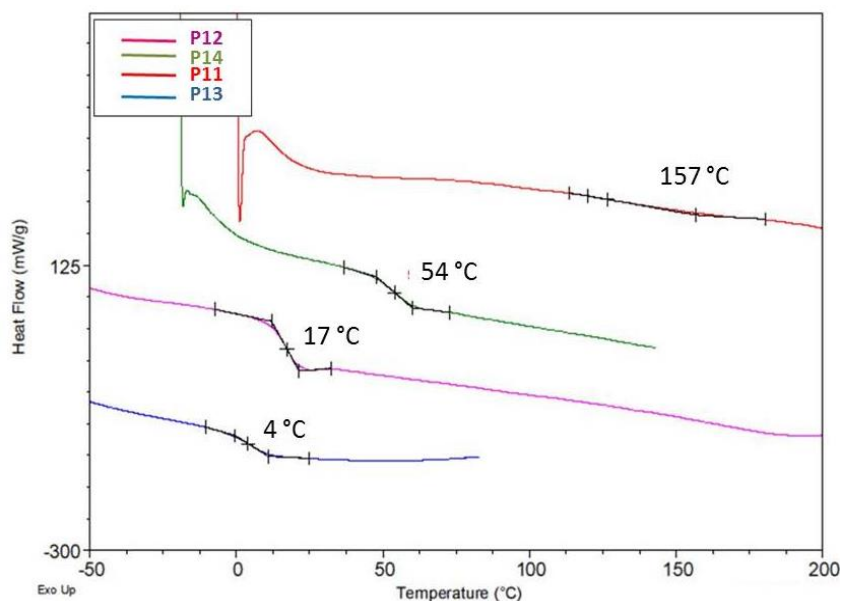
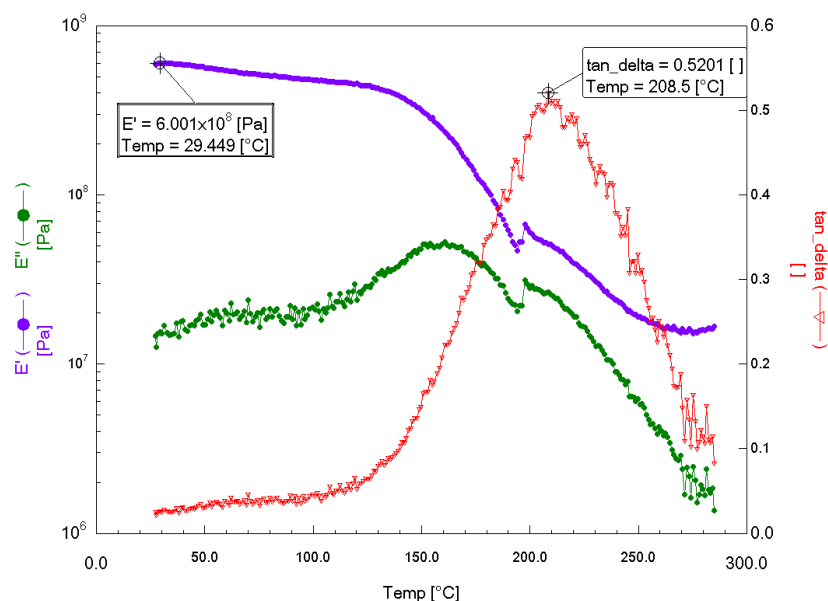


Figure 16: DSC analyses of P11, P12, P13 and P14, second heating cycle.

The polymers present a glass transition temperature ranging from 3.2 to 156.7°C. The reduction of the number of atoms between the aromatic ring and the terminal double bond of the monomer resulted in a decrease of the T<sub>g</sub>. Indeed, **P12** exhibits the lowest T<sub>g</sub> due to its C12 aliphatic chain while **P13** and **P14** constituted respectively of 2 and 3 atoms between the aromatic rings and the double bonds, show higher T<sub>g</sub> of 17.3 °C and 52 °C, respectively.

T<sub>g</sub> of **P11** seems to be at 157 °C but is difficult to detect by DSC due to the rigidity of the conjugated polymer. In order to confirm this value and to investigate the thermomechanical properties of **P11**, DMA analyses were performed (Figure 17). The end of the glassy state was revealed by the decrease of the storage modulus E' at 140 °C. The rubber state was reached when E' stop decreasing at 250 °C. The transition between the two states was spread on 110 °C due to its rigid conjugated structure. The maximum of tanδ was measured at 208 °C.





**Figure 17: DMA analysis of divinyl ADMET Polymer, P11, using 3-point bending test at 1 Hz from 20 to 300 °C at 10 K/min.**

T<sub>g</sub> of **P11** was 100 °C higher than the T<sub>g</sub> of **P14** although the structures of **(11)** and **(19)** differ by only one carbon between the aromatic ring and the double bond. The high T<sub>g</sub> of **P11** may be explained by its conjugated backbone and its all-*trans* structure, whereas the T<sub>g</sub> of **P14** is lower due to its ill-defined structure (isomerizations) and *cis-trans* configurations.

The thermal stability of the polymers was evaluated by TGA (Figure 18). 5% weight loss of **P13** appeared at 250 °C, due to its oligomeric structure. The thermal robustness of **P12**, **P13** and **P14** is high; the latter exhibit 5 wt% loss at temperatures between 310 and 380 °C.

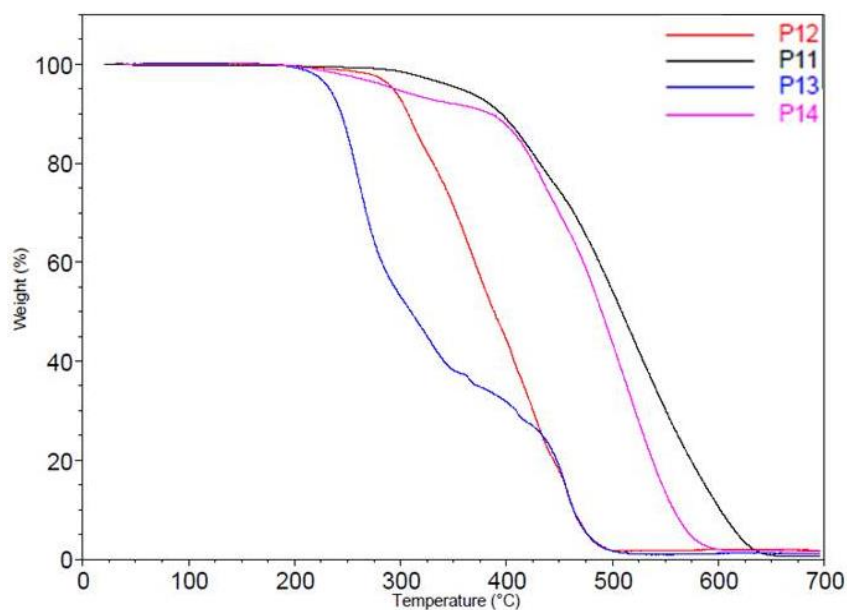


**Figure 18: TGA analyses of ADMET polymers, P11, P12, P13 and P14.**

**Table 4: Thermomechanical properties of polymers P11, P12, P13 and P14, synthesized by ADMET methodology.**

Compound	Name	Catalyst	T <sub>g</sub> (°C) <sup>a</sup>	Td5% (°C) <sup>b</sup>
(11)	P11	HG2	156	380
(15)	P12	HG2	4	310
(16)	P13	HG1	17	250
(19)	P14	HG2	54	330

<sup>a</sup>Determined by DSC second heating cycle, <sup>b</sup>Determined by TGA. Temperature of 5% degradation.

### Conclusion:

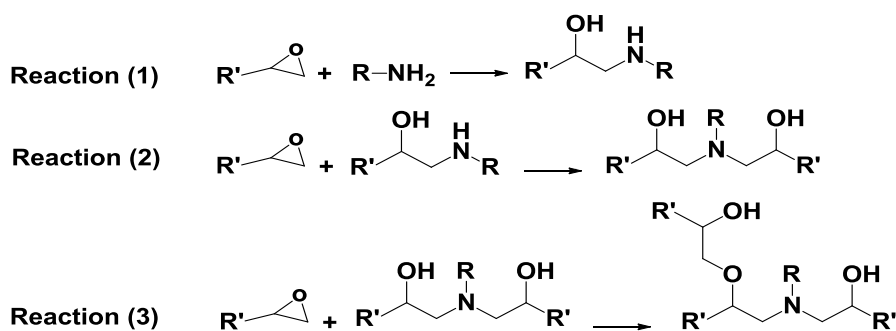
ADMET methodology allowed us synthesizing polymers from bis-unsaturated biphenyl compounds. The polymerization of four dimers was investigated. A screening of Grubbs catalyst was necessary in order to find the conditions to reach high molar masses. Only oligomers were obtained when the diallylated compound (**16**) was employed probably because the heteroatom close to the terminal double bond reduces the catalytic activity of Grubbs catalyst. Methylated dieugenol (**16**) and the bis-unsaturated diesters deriving from methyl vanillate and undecenol (**15**) exhibit good thermal stability and T<sub>g</sub> at 17 and 54 °C, respectively. **P11** synthesized by polymerization of (**11**) obtained by Wittig reaction of divanillin showed reasonably molar mass of 30 000 g/mol, a high T<sub>g</sub> at around 160 °C and an excellent thermostability with a 5% weight loss occurring at 380 °C.

## IV Synthesis and characterization of epoxy resin from biphenyl precursors

Epoxy resins constitute widely used materials, employed in many fields such as aeronautic automotive, constructions (paints, adhesives...), electronics (encapsulation) and sports (bikes, racquets...), etc.

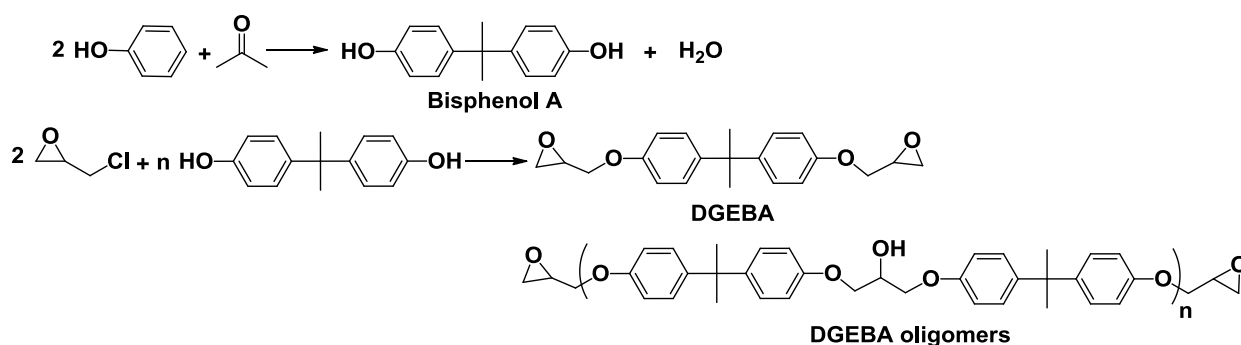
Epoxy resins are produced by polyaddition of epoxide and amine moieties (Scheme 6). The amine lone pair of electron attacks the less steric hindered oxirane carbon resulting in ring-opening and formation of an amino-alcohol. The so-formed secondary amine is able to further react with another epoxy group. The reaction between a hydroxyl group and an epoxide, reaction (3), occurs only in presence of tertiary amines generated by reaction (2) because this reaction is slower than reaction (1) and (2). It may also take place if an excess of epoxy to amine is introduced.<sup>21</sup>





Scheme 6: Reaction between an epoxy group and a primary amine (1), reaction between an epoxy group and a secondary amine (2), reaction between an epoxy and an hydroxyl group (3).

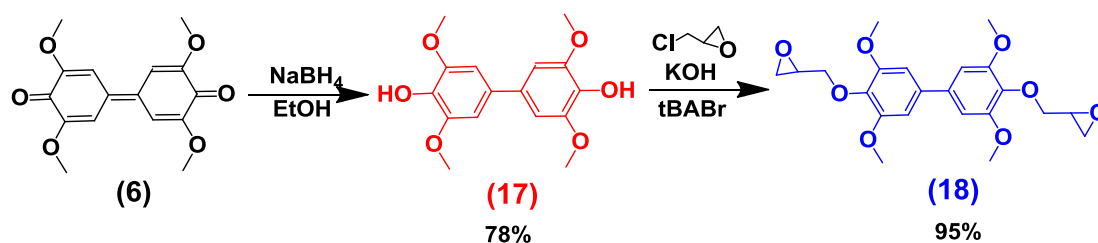
Today, 95% of epoxy resins are produced from diglycidylether of bisphenol-A (DGEBA). DGEBA is prepared by reaction between bisphenol-A and epichlorohydrin under basic conditions (Scheme 7). Bisphenol-A, which is synthesized by condensation of acetone with two equivalents of phenol, depends on fossil resources and appears to be both an estrogen receptor agonist and an androgen receptor antagonist, and to be toxic for living organisms.<sup>22</sup> Several studies related to its substitution by biobased and non-toxic molecules were recently published.<sup>21</sup>



Scheme 7: Formation mechanism of diglycidylether of bisphenol-A (DGEBA).

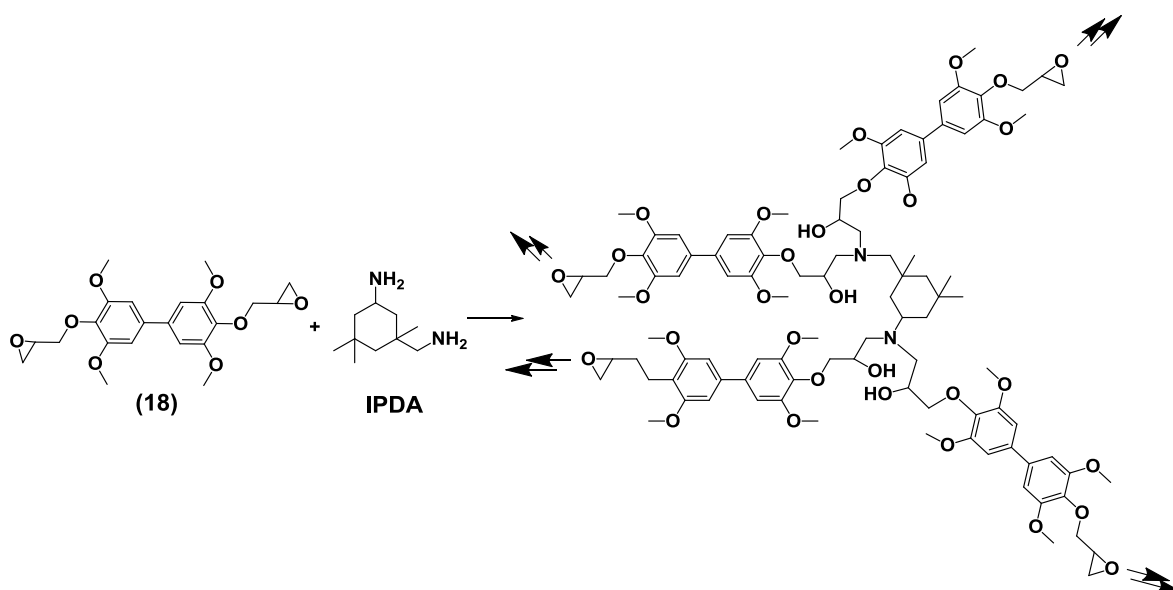
### 1. Synthesis of epoxy resins from 2,6-dimethoxy phenol dimer

The 2,6-dimethoxyphenol dimer (**6**) could be obtained by lignin depolymerization. As described in the previous chapter, the reduction of (**6**) into the bisphenol (**17**) and further reaction with epichlorohydrin led to the bisepoxide precursor (**18**) (Scheme 8).



Scheme 8: Chemical modifications of 2,6-dimethoxyphenol dimer (**6**).

Bisepoxide (**18**) was employed to produce epoxy resins with isophorone diamine (IPDA) as curing agent (Scheme 9). This cyclo-aliphatic diamine was selected for its liquid state at room temperature and good reactivity towards epoxide groups.



**Scheme 9: Formulation of epoxy resins from (18) and IPDA.**

Bisepoxide (**18**) was pre-heated to its liquid state and mixed vigorously with different amounts of IPDA ( $r$  ratio) in order to prepare the different networks. The liquid was poured into a silicon mold and heated in an oven. The epoxy/amine ratio is calculated as follow:

$$r = \frac{f_{epoxy} * n_{epoxy}}{f_{amine} * n_{amine}}$$

with  $f_{amine}$  and  $f_{epoxy}$ , the functionality of amine and epoxy, respectively equal to 4 and 2 for IPDA and (**18**) and  $n_{amine}$  and  $n_{epoxy}$  the molar quantity of epoxy and amine, respectively.

The stoichiometry of the epoxy-amine reaction,  $r$  equal to 1, generally leads to the material with the highest thermomechanical properties.<sup>23</sup> The epoxy-amine system with a ratio of 1 was taken to determine the time and temperature necessary for the completion of curing. Then, the epoxy resins with different epoxy to amine ratio were synthesized following this process in order to prepare networks with different thermomechanical properties.

The curing conditions are of crucial importance. The curing of epoxy (**18**) was investigated by DSC. After mixing (**18**) and IPDA to obtain a homogeneous mixture, the liquid was poured into a mold, heated in an oven and sampled regularly. Directly after mixing, the DSC heating reveals 2 exothermic peaks, the first one starting at 70 °C and the second one starting at 120 °C characteristic for a polymerization in two steps. These 2 peaks can be explained by the

difference of reactivity of the primary and secondary amino group of IPDA. It is essential to perform the polymerization reactions at low temperature first in order to keep the viscosity of the system enabling the chains to grow before cross-linking. Subsequently, the temperature of the oven was thus set at 70 °C. During curing, the total heat reaction ( $\Delta H$ ) decreased. After 1 h at 70 °C, the decrease of  $\Delta H$  from 139 J/g to 53 J/g and the disappearance of the first polymerization peak were observed on the DSC thermogram, Figure 19 (a). The oven temperature was increased to 120 °C. After 2 h at constant temperature, the completion of the reaction was observed. The cross-linking rate is calculated by the following calculation:

$$\%cross - linking = 100 * \frac{\Delta H_0 - \Delta H}{\Delta H_0}$$

with  $\Delta H$  the total heat reaction and  $\Delta H_0$  the initial total heat reaction.

The cross linking rate depending on time and temperature is plotted in Figure 19 (b).

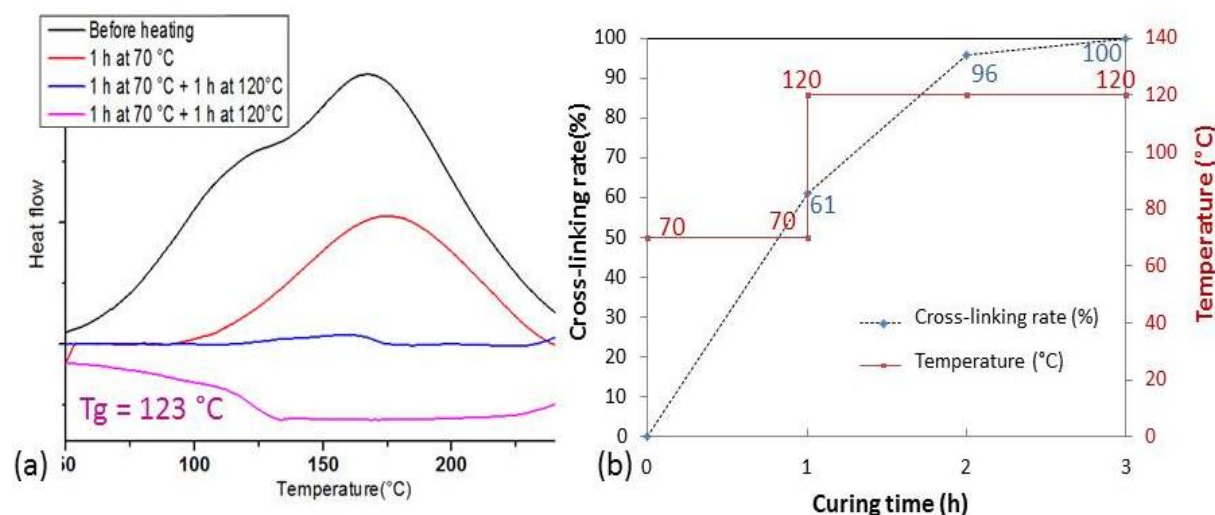


Figure 19: DSC analysis of 2,6-dimethoxyphenol-based epoxy during curing with IPDA for  $r = 1$  (a). Plot of the cross-linking percentage as a function of curing time and temperature (b).

## 2. Swelling properties

The swelling measurements of the networks were performed on the 2,6-dimethoxy-based epoxy resins for several epoxy to amine ratios. Bar samples of the cured network were weighted ( $m_D$ ) and immersed into THF for 24 h. The swollen bars were then dried between sheets of paper and weighted again ( $m_S$ ). Then, swollen bars were dried in an oven at 60 °C for 24 h and weighted again ( $m_{D0}$ ). The swelling percentage was calculated from the difference in weight between dried and swollen networks:<sup>24</sup>

$$Swelling (\%) = (m_S - m_D) / m_D * 100$$

The soluble part was calculated from the difference in weight between dried and swollen networks:

$$\text{Soluble}(\%) = 100 * \left(1 - \frac{m_{DO}}{m_D}\right)$$

The swelling percentage indicates the degree of cross-linking. Indeed, lower cross-linking density usually results in higher distances between network nodes and then a higher solvent absorption. The lowest swelling percentage of 11%, was obtained for a ratio of 1, thus corresponding to the optimum cross-linking of the material. For  $r < 1$ , amino groups are in excess which may lead to chain extension between cross-linking points and so a lower cross-linking density, characterized by a higher swelling percentage. For  $r > 1$ , epoxy moieties are in excess, less cross-linking may occur, resulting in a high swelling percentage. For  $r$  equal to 1.75, the epoxy resin was totally soluble in THF (Table 5).

**Table 5: Swelling percentage and soluble part of the 2,6-dimethoxyphenol-based IPDA networks.**

<b>r=epoxy/NH<sub>2</sub></b>	<b>0.5</b>	<b>0.75</b>	<b>1</b>	<b>1.25</b>	<b>1.5</b>
<b>%swelling</b>	23	30	11	106	ND
<b>soluble part (%)</b>	<1	<1	<1	68	100

### 3. Thermomechanical properties of the epoxy resins

The influence of the epoxy to amine ratio on the thermomechanical properties of the epoxy resin was studied. T<sub>g</sub> of the epoxy resins were determined by DSC, Figure 20 (a). As expected, the highest T<sub>g</sub>, 126 °C was exhibited by the epoxy resin formulated with an epoxy to amine ratio equal to 1. This maximum value suggested that the only mechanism occurring during the cross-linking of the reactive systems is the amine-epoxy addition and no side reaction such as etherification occurs during the cross-linking.<sup>23</sup> Indeed, for  $r > 1$ , epoxy moieties are in excess, less cross-linking may occur and the T<sub>g</sub> of the resulting epoxy resin dropped drastically. For  $r < 1$ , a slight decrease of the T<sub>g</sub> was observed. For these ratios, amino groups are in excess which may lead to chain extension between cross-linking points resulting in a decrease of T<sub>g</sub>. DGEBA-based epoxy resins were also synthesized in order to compare their properties to the one of epoxy resins based on 2,6-dimethoxyphenol. The variation of T<sub>g</sub> with the stoichiometric ratio of 2,6-dimethoxyphenol and DGEBA-based epoxy resins is plotted in Figure 20 (b).

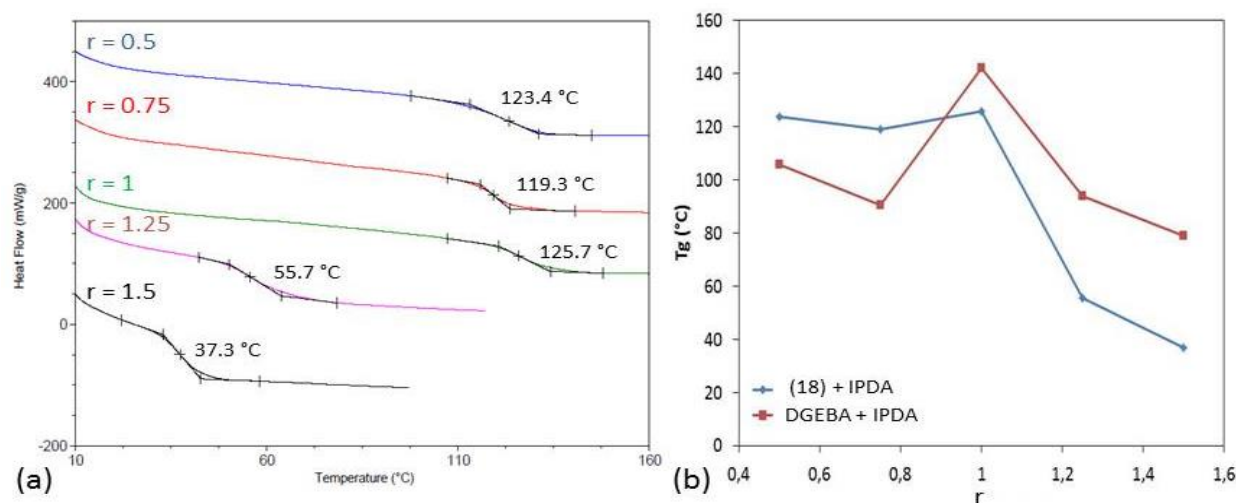


**Figure 20: DSC of 2,6-dimethoxyphenol/IPDA-based epoxy resins (second heating cycle) (a), Glass transition temperature versus  $r$  for networks based on DGEBA and of 2,6-dimethoxyphenol combined with IPDA (b).**

For  $r$  equal to 1 or  $r > 1$ , the  $T_g$  of 2,6-dimethoxyphenol/IPDA-based epoxy resins were lower than the  $T_g$  of the conventional DGEBA/IPDA epoxy resins. This observation cannot be attributed to incomplete curing because no residual heat was observed by DSC (Figure 19). This difference can be explained by the chemical structure of the two systems. DGEBA exhibits one more carbon in the bisepoxide backbone in comparison to 2,6-dimethoxyphenol derivative and, as a result, a lower cross-linking density. The  $T_g$  value generally increases with the cross-linking density, so the difference in  $T_g$  cannot be attributed to this parameter. However, the four methoxy groups of the 2,6-dimethoxyphenol derivative may increase the free volume of the chains and thus decrease the  $T_g$  value. For  $r = 1$ , the  $T_g$  of the 2,6-dimethoxyphenol-based network was  $16\text{ }^\circ\text{C}$  lower than the one of conventional DGEBA/IPDA epoxy resin.

The thermomechanical properties of the epoxy networks were investigated by DMA, performed on bar sample in a 3-point bending mode. In Figure 21 (a) is plotted the change of storage modulus ( $E'$ ), the loss tangent ( $\tan\delta$ ) and the loss modulus ( $E''$ ) against temperature. The tensile storage modulus of networks based on 2,6-dimethoxyphenol derivative with different epoxy to amine ratios are displayed on Figure 21 (b). The storage modulus in the glassy state was around 1 GPa which is similar to the one of DGEBA/IPDA epoxy resins. The decrease of the storage modulus is characteristic of the glass transition  $T_\alpha$  of the material. Values of  $T_\alpha$  follow the same trend as  $T_g$  values measured by DSC (Table 6). For  $r = 1$ ,  $T_\alpha$  of the 2,6-dimethoxyphenol-based epoxy resin reached  $123\text{ }^\circ\text{C}$ , that being  $32\text{ }^\circ\text{C}$  degrees lower than the one of DGEBA/IPDA epoxy resins. (Table 7)

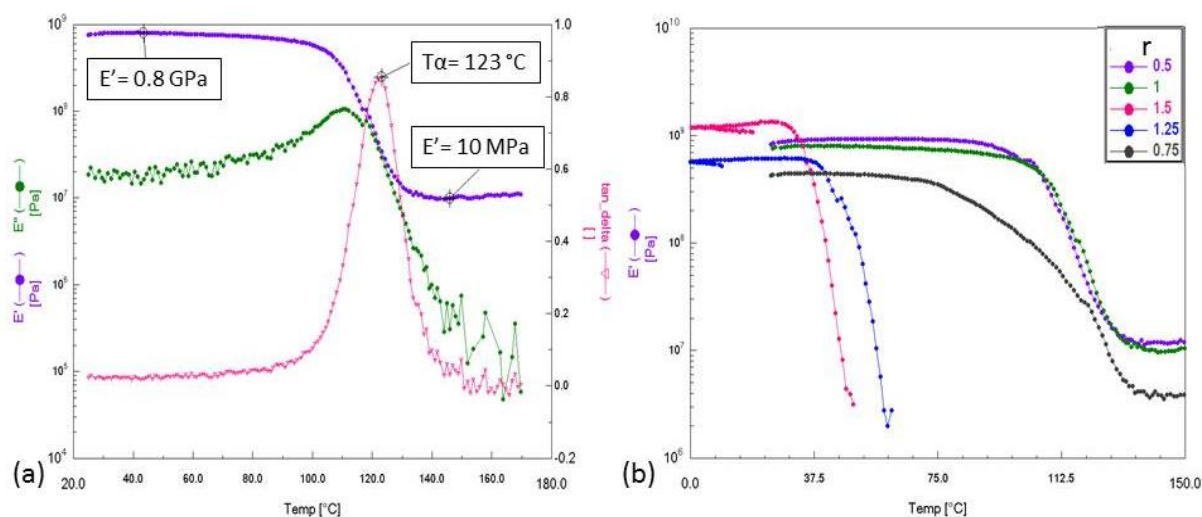


**Figure 21: DMA analysis of 2,6-dimethoxyphenol-based epoxy resin  $r = 1$  (a) and storage modulus of 2,6-dimethoxyphenol-based epoxy resin for several  $r$  ratios (b), using 3-point bending test at 1 Hz from 0 °C to 150 °C at 10 K/min.**

The cross-linking density of the networks can be calculated from the DMA data, according to the rubber elasticity theory:<sup>25</sup>

$$\nu = \frac{E'}{\phi * R * T}$$

with  $E'$  the storage modulus of the thermoset at the rubbery plateau ( $T\alpha + 30$  K),  $R$  the gas constant ( $8.314 \text{ J} \cdot \text{mol}^{-1} \cdot \text{K}^{-1}$ ),  $\phi$  the front factor (approximately 1 in the Flory theory)<sup>26</sup> and  $T$  the temperature in K.

The cross-linking density of the DGEBA and 2,6-dimethoxyphenol-based epoxy resins synthesized with an epoxy to amine ratio equal to 1 were compared. A value of  $8.3 \cdot 10^{-3} \text{ mol/m}^3$  was calculated for the 2,6-dimethoxyphenol-based epoxy resin. This value is slightly lower than the one of  $4.5 \cdot 10^{-3} \text{ mol/m}^3$  commonly obtained for DGEBA/IPDA epoxy resins.<sup>27,28</sup> This difference was consistent with the chemical structure of the two networks.

The thermal stability of the networks was investigated by TGA under nitrogen (Figure 22). The epoxy resins showed a single step degradation profile with a residue of around 17% at 600 °C. For comparison, the DGEBA/IPDA network residue is about 8%. Highest residue values indicate better flame retardancy properties of the material. Dyakonov and coll. showed that the char formation is related to the cross-linking density.<sup>29</sup> Thus, the higher crosslinking density of the 2,6-dimethoxy-based epoxy resin may be responsible for higher thermal char formation than for the DGEBA/IPDA network. The epoxy resin with an epoxy to amine ratio of 1 exhibited the highest thermal stability with a 5 wt% loss at 312 °C and 30 wt% loss at 337 °C. These values are lower than the ones of DGEBA/IPDA network which are 346 and 368 °C for the 5 wt% and 30 wt% loss, respectively Figure 22 (b).

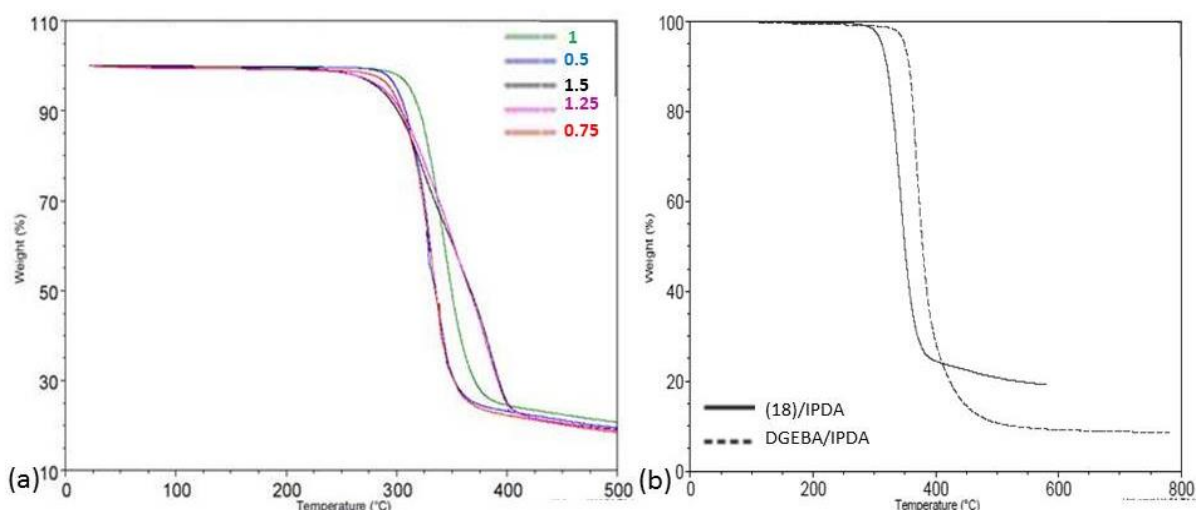


**Figure 22: TGA analyses of epoxy resins from 2,6-dimethoxy-bisepoxy+IPDA with different r values (a), epoxy resins from 2,6-dimethoxy-bisepoxy+IPDA and from DGEBA/IPDA or r = 1 (b).**

The statistic heat-resistant index ( $T_s$ ) is calculated from the temperature of 5 wt% loss ( $T_{d5\%}$ ) and of 30 wt% loss ( $T_{d30\%}$ ) of the sample by the following equation:<sup>30</sup> It is characteristic of the thermal stability of the cured epoxy resins.

$$T_s = 0,49 * (T_{d5\%} + 0,6 * (T_{d30\%} - T_{d5\%}))$$

The value of statistic heat-resistant index for the 2,6-dimethoxy-based epoxy resin is 160 °C, 16 °C lower than the one of DGEBA/IPDA network.

The thermomechanical properties of the epoxy resins synthesized from 2,6-dimethoxyphenol dimer with different epoxy to amine ratio and of the epoxy resin synthesized from DGEBA with an epoxy to amine ratio equal to 1 are summarized in Table 6.

**Table 6: Thermomechanical properties of 2,6-dimethoxyphenol based epoxy resins synthesized with different epoxy to amine ratio, comparison with traditional DGEBA/IPDA network.**

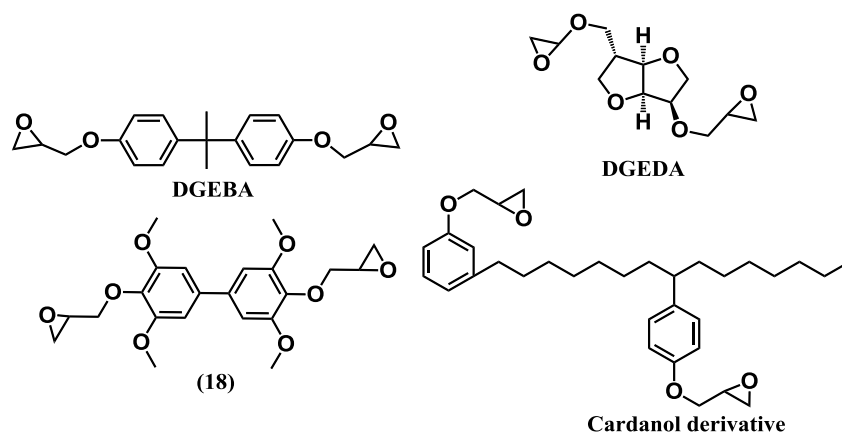
r	2,6-dimethoxyphenol dimer					DGEBA
	0.5	0.75	1	1.25	1.5	1
$T_g$ (°C) <sup>a</sup>	123.8	119.2	125.9	55.6	37.1	142
$T_a$ (°C) <sup>b</sup>	116.3	137.8	123.1	/	/	155
$T_{d5\%}$ (°C) <sup>c</sup>	300	295	312	287	284	340
$T_{d30\%}$ (°C) <sup>c</sup>	325	324	337	338	334	365
$T_s$ (°C) <sup>d</sup>	154	153	160	156	154	176

<sup>a</sup>Determined by DSC second heating cycle, <sup>b</sup>Determined by DMA 3 points flexion, <sup>c</sup>Determined by TGA. Temperature of 5% degradation. <sup>d</sup>Calculated from TGA analyses.



#### 4. Comparison of the thermomechanical properties of several biobased epoxy resins.

In literature, several biobased molecules have been employed for the formulation of epoxy resins.<sup>21</sup> Among them, epoxy based on cyclo-aliphatic molecules such as isosorbide<sup>28</sup> (DGEDA) and aromatic compounds such as cardanol were cured with IPDA (Scheme 10).<sup>27</sup> The thermomechanical properties of the resulting networks can be compared to the epoxy resin based on molecule (18) prepared in our study (Table 7).



**Scheme 10:** Structures of some epoxy used for the synthesis of epoxy resins with IPDA as curing agent.

Epoxy resins based on (18) exhibited  $T_g$  and thermal stability slightly lower than DGEBA-based epoxy resins. This difference can be attributed to the presence of the four methoxy groups in the structure of (18). However, the aromatic structure of (18) provides higher thermomechanical properties than DGEDA-based epoxy resins (Table 7). Logically,  $T_g$  of cardanol-based epoxy resin is lower due to the presence of long aliphatic chains but the latter exhibit good thermal stability.

**Table 7:** Thermomechanical properties of epoxy resins from DGEBA, (18), isosorbide, cardanol and gallic acid cured by IPDA.

Monomer	$T_g$ (°C)	$T_a$ (°C)	$T_{d5\%}$ (°C)	$\nu$ $10^{-3} \text{mol.m}^{-3}$	Reference
DGEBA	142	155	330	4.5	28
(18)	125	123	312	8.3	
DGEDA	100	112	305	4.8	28
Cardanol	50	59	325	1.5	27



**Conclusion:**

The 2,6-dimethoxyphenol dimer was produced by the laccase-catalyzed process described in the previous chapter. Chemical modifications of this dimer with epichlorohydrin led to the bisepoxide (**18**). Curing time and temperature of (**18**) with IPDA were determined by DSC. Epoxy resins with different epoxy to amine ratio were synthesized and compared in terms of thermomechanical properties, swelling behaviors and cross-linking densities. As expected, the highest properties were achieved for a ratio 1/1. This network exhibited high T<sub>g</sub> of 123 °C, a high thermal stability with a 5 wt% loss of 312 °C, a high cross-linking density of  $8.3 \cdot 10^{-3} \text{ mol} \cdot \text{m}^{-3}$ . While their thermomechanical properties are slightly lower than the ones of equivalent DGEBA-based network, these new epoxy resins are very promising materials.

**V Conclusion and perspectives**

In this chapter, polymers were synthesized from the dimers produced by laccase catalysis. Linear thermoplastic polymers were prepared by transesterification or ADMET polymerizations. The copolymerization of methylated divanillic diol with diesters having different structures, employing 0.5 mol% of titanium butoxide as a catalyst, allowed us tuning of the glass transition temperature of the resulting polymers, between -4 to 140 °C. Due to solubility issues, only the molar mass of the copolymer with dimethylsebacate was investigated and found close to 65 000 g/mol. The thermal stability of all the copolymers was high with a 5 wt% loss over 300 °C. These thermal properties are similar to commodity polymers such as PET and PS which T<sub>g</sub> are around 70 and 100 °C. Furthermore, the ADMET polymerization of four bis-unsaturated bisphenyl monomers prepared by chemical modifications of dimers produced by laccase catalysis was investigated. Methylated dieugenol and the bis-unsaturated diester derived from methyl vanillate and undecenol exhibited good thermal stability, reasonable molar masses and T<sub>g</sub> at 17 and 54 °C, respectively. The polymerization of the divinyl compound obtained by Wittig reaction of divanillin show a molar mass of 30 000 g/mol, a high T<sub>g</sub> of around 160 °C and an excellent thermostability with a 5 wt% loss occurring at 380 °C. For both polymerization methods, polymers with high thermal stability were synthesized. Changing the diester for polycondensation or the structure of the bisunsaturated substrate for ADMET polymerization enables to tailor the T<sub>g</sub> of the resulting polymers.

The 2,6-dimethoxyphenol dimer produced by the laccase-catalyzed process exhibits a structure similar to bisphenol-A. The bisepoxide produced by reaction of this dimer with epichlorohydrin was employed for the synthesis of epoxy resin cured with IPDA and compared with DGEBA-based resins. The network prepared with a 1/1 epoxy to amine ratio exhibits a high T<sub>g</sub> of 123 °C, a high thermal stability with a 5% weight loss of 312 °C, a high cross-linking density of  $8.3 \times 10^{-3} \text{ mol.m}^{-3}$ . These thermomechanical properties are slightly lower than the one of DGEBA-based network.

In this chapter, preliminary studies on the synthesis of polyamides from methylated divanillic diacid also showed promising results. The reaction conditions have to be investigated in more details and the resulting polyamides characterized further.

All the thermoplastic polymers were produced with methylated phenols. In the future, it would be interesting to deprotect totally or partially these moieties and to compare the properties of these polymers. Epoxy resins were synthesized only from 2,6-dimethoxyphenol dimer derivatives. In the previous chapter, we reported the synthesis of the epoxidized dieugenol (**20**); the latter could be advantageously employed to synthesize new epoxy resins. Moreover, the epoxidation of the bis-unsaturated compounds (**11**) (**16**) and (**15**) employed for ADMET polymerization was not performed and could also lead to valuable bisepoxy substrates for the formulation of novel epoxy resins.

## VI References

1. A. S. Amarasekara, B. Wiredu and A. Razzaq, *Green Chemistry*, **2012**, 14, 2395-2397.
2. A. S. Amarasekara and A. Razzaq, *ISRN Polymer Science*, **2012**.
3. B. G. Harvey, M. E. Wright, S. Compel, A. J. Guenthner, K. Lamison, L. R. Cambrea, H. A. Meylemans and S. McCormick, *polymer preprint*, **2011**, 52, 282-283.
4. C. Pang, J. Zhang, G. Wu, Y. Wang, H. Gao and J. Ma, *Polymer Chemistry*, **2014**.
5. K. Pang, R. Kotek and A. Tonelli, *Journal of Polymer Science Part A: Polymer Chemistry*, **2006**, 44, 6801-6809.
6. N. Kolb and M. A. R. Meier, *Green Chemistry*, **2012**.
7. A. G. Pemba, M. Rostagno, T. Lee and S. Miller, *Polymer Chemistry*, **2014**.
8. O. Grosshardt, U. Fehrencacher, K. Kowollik, B. Tübke, N. Dingenouts and M. Wilhem, *Chemie Ingenieur Technik*, **2009**, 81, 1829-1835.
9. T. Lebarbé, A. S. More, P. S. Sane, E. Grau, C. Alfos and H. Cramail, *Macromolecular Rapid Communications*, **2014**, 35, 479-483.
10. H. Mutlu, L. M. de Espinosa and M. A. R. Meier, *Chemical Society Reviews*, **2011**, 40, 1404-1445.
11. P. A. Fokou and M. A. R. Meier, *Macromolecular Rapid Communications*, **2010**, 31, 368-373.
12. S. H. Hong, D. P. Sanders, C. W. Lee and R. H. Grubbs, *Journal of the American Chemical Society*, **2005**, 127, 17160-17161.
13. E. Thorn-Csányi and P. Kraxner, *Macromolecular Chemistry and Physics*, **1997**, 198, 3827-3843.
14. R. Peetz, A. Strachota and E. Thorn-Csányi, *Macromolecular Chemistry and Physics*, **2003**, 204, 1439-1450.
15. K. Nomura, Y. Miyamoto, H. Morimoto and Y. Geerts, *Journal of Polymer Science Part A: Polymer Chemistry*, **2005**, 43, 6166-6177.
16. H. Weyhardt and H. Plenio, *Organometallics*, **2008**, 27, 1479-1485.
17. S. N. Liss, P. A. Bicho and J. N. Saddler, *Canadian Journal of Microbiology*, **1997**, 43, 599-611.
18. K. B. Wagener, K. Brzezinska, J. D. Anderson, T. R. Younkin, K. Steppe and W. DeBoer, *Macromolecules*, **1997**, 30, 7363-7369.
19. S. Günther, P. Lamprecht and G. A. Luinstra, *Macromolecular Symposia*, **2010**, 293, 15-19.
20. H. Bilel, N. Hamdi, F. Zagrouba, C. Fischmeister and C. Bruneau, *RSC Advances*, **2012**, 2, 9584-9589.
21. R. Auvergne, S. Caillol, G. David, B. Boutevin and J.-P. Pascault, *Chemical Reviews*, **2013**.
22. R. E. Chapin, J. Adams, K. Boekelheide, L. E. Gray, S. W. Hayward, P. S. J. Lees, B. S. McIntyre, K. M. Portier, T. M. Schnorr, S. G. Selevan, J. G. Vandenberg and S. R. Woskie, *Birth Defects Research Part B: Developmental and Reproductive Toxicology*, **2008**, 83, 157-395.
23. J. Galy, A. Sabra and J.-P. Pascault, *Polymer Engineering & Science*, **1986**, 26, 1514-1523.
24. C. Aouf, H. Nouailhas, M. Fache, S. Caillol, B. Boutevin and H. Fulcrand, *European Polymer Journal*, **2013**, 49, 1185-1195.
25. T. Iijima, N. Yoshioka and M. Tomoi, *European Polymer Journal*, **1992**, 28, 573-581.
26. P. J. Flory, *Polymer*, **1979**, 20, 1317-1320.

27. F. Jaillet, E. Darroman, A. Ratsimihety, R. Auvergne, B. Boutevin and S. Caillol, *European Journal of Lipid Science and Technology*, **2014**, 116, 63-73.
28. M. Chrysanthos, J. Galy and J.-P. Pascault, *Macromolecular Materials and Engineering*, **2013**, 298, 1209-1219.
29. M. M. Sain and C. Daneault, *Polymer Degradation and Stability*, **1996**, 51, 67-75.
30. Y.-C. Chiu, I. C. Chou, W.-C. Tseng and C.-C. M. Ma, *Polymer Degradation and Stability*, **2008**, 93, 668-676.

## VII Experimental

### *Polyester synthesis*

Methylated divanillyl diol (1 equivalent) and diacid or diester (1 equivalent) were stirred at 160 °C for 2 h under nitrogen flow and at 200 °C under vacuum for 6 h in the presence of 2 mol% of catalyst (titanium butoxide, zinc acetate or dibutyltin oxide) or in the presence of 0.5 mol% of titanium butoxide or stirred at 120 °C for 24 h in the presence of 10 mol% of TBD.

### *Polyamide synthesis*

A 10% ethanolic solution of diamine was slowly added to an equimolar portion of 10% ethanolic solution of diacid (**14**) at 60 °C, resulting in precipitation of a white solid. The mixture was refluxed for 30 min. The salt was collected, put into a DSC capsule.

### *ADMET polymerization*

Unsaturated dimer (0.22 mmol) was dissolved in 1 mL of Polarclean. Grubbs catalyst (2 mol%) was added to the flask. The flask was heated at 80°C under vacuum for 18h. Then 1 mL of ethyl vinyl ether was introduced to the flask to quench the reaction. The final polymer was dissolved into 1 mL of THF and reprecipitated in cold methanol.

### *Epoxy resins*

Compound (**18**) was pre-heated to its liquid state and mixed vigorously with different amounts of IPDA (ratio r). The liquid was poured into a silicon mold and heated in an oven at 70 °C for 1 h followed by 120 °C for 2 h.



# General conclusion and perspectives

---

Petrol depletion and environmental concerns lead the chemical industry to consider renewable resources as source of building blocks for the synthesis of polymers. Although renewable aliphatic polymers can be widely synthesized from vegetable oils, the incorporation of biobased cyclo-aliphatic or aromatic units in the polymer backbone, in order to increase the material rigidity, remains a challenge. The aim of this thesis was to investigate new polycyclic and aromatic biobased monomers for the synthesis of polymers with high thermomechanical properties. A polycyclic biobased molecule, i.e resinic acids, and phenolic compounds potentially derived from lignin, such as vanillin and other *o*-methoxy or *o*-dimethoxy phenols were selected for this study. Both classes of substrates were dimerized in order to get difunctional symmetric synthons. These dimers were then tested for the synthesis of thermoplastic polymers by polycondensation and ADMET methodology or for the synthesis of epoxy resins.

On the one hand, this study focused on the synthesis of abietic acid dimers. Abietic acid was dimerized by a cationic mechanism using sulfuric acid. However, the dimerization of abietic acid dimer proved to be a complex mechanism of proton addition, transfer and proton elimination resulting in the formation of not only one dimer but several different structures. As the mixture obtained after reaction contained 60% of dimers, 30% of monomers and 10% of trimers, we developed a method to isolate the abietic acid dimers. Indeed, Flash chromatography allowed us to collect a fraction composed mainly of dimers (91%) and of some traces of trimers, in a reasonable yield (35% wt). With a functionality of 2 in acidic functions, this fraction can be polymerized. This work afforded the development of new biobased rigid difunctional synthons, which for the best of our knowledge were polymerized for the first time.

Direct polycondensation of the dimers only led to low molar mass polyesters, probably due to the presence of sterically hindered compounds and to the presence of a lactone moiety. The promising thermal properties of these polymers encouraged us to develop another way of polymerization. To avoid reactivity issues, dimers with reactive terminal double bonds were successfully synthesized by esterification of abietic acid dimers with undecenol and polymerized by ADMET methodology. Random copolymers of bis-unsaturated abietic acid with undecenyl undecenoate showed a semi-crystalline structure with a melting temperature between 40 °C and 50 °C. A demixtion phenomenon was

observed for incorporation of abietic acid dimers over 50 mol%. However, the objective of this part was fulfilled with the obtention of polymers exhibiting excellent thermal stability, over 300 °C and of a homopolymer of bis-unsaturated abietic ester dimers with a high glass transition temperature of 102 °C. Moreover, by esterification of sterically hindered molecules with undecenol (or other aliphatic molecules) followed by ADMET polymerization, we provided a polymerization method of low reactive compounds.

On the other hand, this study focused on the synthesis of biphenyl compounds from lignin derivatives by enzymatic catalysis and their further polymerization. We developed a “green” process to dimerize phenolic compounds in large quantity and high yield. The main advantage of this method is that the phenolic monomer is soluble in the reaction medium while the dimer precipitates out of the solution. Moreover, after filtration of the dimer, the filtrate is filled with monomer and oxygen again. This process was repeated 8 times and yields higher than 90% were obtained. This method was applied to several substrates and depending on the aromatic ring substitution, provided oligomers, mixture of dimers or selectively one dimer. Seven phenolic substrates led to the synthesis of pure dimers with yields over 80%: vanillin, methyl vanillate, eugenol, 2,6-dimethoxyphenol, acetovanillon, 4-hydroxy-2-methoxybenzotrile and 4-methyl-2-methoxyphenol. From chemical modifications of these dimers, we built a bio-platform of biphenyl molecules, including diols, diacids, bis-unsaturated diesters, divinyl compound and bisepoxides.

In the last chapter, polymers were synthesized from the biphenyl dimers produced by laccase catalysis and chemically modified. The polyesters synthesized from methylated divanillic diol and different diesters presented excellent thermal stability and glass transition temperature ranging from -4 to 140 °C. These thermal properties are higher than the ones of commodity polymers such as PET and PS which T<sub>g</sub> are around 70 and 100 °C, respectively. Preliminary studies on polyamide synthesis showed promising results and thermal properties similar to the poly(phtalamide)s. ADMET polymerization was also performed on four bis-unsaturated compounds of different structures, allowing the synthesis of polymers with T<sub>g</sub> ranging from 3 °C to 160 °C. Among them, the polymerization of the divinyl dimer obtained by Wittig reaction of divanillin should be highlighted. Indeed, this polymer constitutes a high performance material with a molar mass of 30 000 g/mol, a high T<sub>g</sub> of around 160 °C and an excellent thermostability with a 5% weight loss occurring at 380 °C. Finally, the bisepoxide produced by reaction of 2,6-dimethoxyphenol dimer with epichlorohydrin was employed for the synthesis of epoxy resin cured with IPDA and compared to DGEBA. The epoxy network prepared with a 1/1 epoxy to amine ratio exhibits a high T<sub>g</sub> of 123 °C, a high thermal stability



with a 5% weight loss of 312 °C, a high cross linking density of  $8.3 \cdot 10^{-3} \text{ mol.m}^{-3}$ . These properties are close to the ones of the DGEBA/IPDA epoxy resins.

To conclude, the main objective of the thesis which was to investigate new biobased aromatic and polycyclic synthons was fulfilled by the isolation of the abietic acid dimers and the development of a new promising biphenyl platform derived from lignin. Although the abietic acid dimers show some reactivity issues, the biphenyl molecules proved to be good substitutes for terephthalic acid and bisphenol A. Some examples of polymerizations were studied but this palette of biobased biphenyl molecules afford a large range of possibilities for their polymerization that will require further works.



# Materials and methods

---

## 1. Materials

Methyl 10-undecenoate (98.0%), 2,5-furandicarboxylic acid (98.0%), 1,10-diaminodecane , dimethylsebacate (97.0%) and epichlorohydrine (99.0%), were supplied by TCI Europe.

10-undecenol (99%), abietic acid (85%), N,N'-Diisopropylcarbodiimide (DIPC 99%), p-toluenesulfonic acid monohydrate (99%), 1,5,7-triazabicyclo[4.4.0]dec-5-ene (TBD, 98%), zinc acetate (99.999%), sodium acetate (99%), acetic acid (99.7%), laccase from *Trametes Versicolor*, hydroxylamine hydrochloride (99%), sulfuric acid (95%), iodomethane (99%), dibutyltin oxide (98%), Grubbs 1<sup>st</sup> generation catalyst, Grubbs 2<sup>nd</sup> generation, Hoveyda Grubbs 1<sup>st</sup> generation, Hoveyda Grubbs 2<sup>nd</sup> generation, succinic acid (99%), dimethyl succinate (98%), dimethyl terephthalate (98%), 4,4'-methylenedianiline (98%) were purchased at Sigma Aldrich.

Sulfuric acid (98%), 4-dimethylaminopyridine (99%), isophorone diamine (99%) and titanium butoxide (99%) were bought from Fisher.

*Polarclean* (methyl-5-(dimethylamino)-2-methyl-5-oxopentanoate) and Pripol were supplied by Solvay and Croda respectively.

Antimony trioxide (99.6%), sodium borohydride (98%), potassium hydroxide (85%), triphenylphosphine (99%), allyl bromide (99%), and 1,6-diaminohexane (98%) were bought from Alfa Aesar.

4-dimethylaminopyridine (99%) was bought from Acros organic.

Potassium carbonate (99%) and terephthalic acid (98%) were supplied by Prolabo.

Potassium tert-butoxide (97%) was purchased at ABCR.

All products and solvents (reagent grade) were used as received otherwise mentioned.

## 2. Methods

### Nuclear Magnetic Resonance (NMR)

All NMR experiments were performed at 298 K on a Bruker Avance 400 spectrometer operating at 400MHz. CDCl<sub>3</sub>, DMSO, acetone and TCE were used as solvent depending on the sample and are mentioned in the legends of the NMR spectra.

### Gas chromatography (GC)

Analytical GC characterization was carried out with a TRACE GC instrument equipped with 2 different columns and programs: column 1 : CP Sil 8CB (25 m × 0.32 mm × 0.12 μm), oven temperature program: initial temperature 200 °C, ramp at 15 °C.min<sup>-1</sup> to 300 °C, hold for 10 min, ramp at 2 °C.min<sup>-1</sup> to 310 °C, hold for 10 min, or column 2: CP Sil 5CB (25 m × 0.32 mm × 0.40 μm), oven temperature program: initial temperature 155 °C, ramp at 15 °C.min<sup>-1</sup> to 300 °C, hold for 10 min, ramp at 2 °C. min<sup>-1</sup> to 310 °C, hold for 10 min, hold for 10 min, using flame ionization detection. The injector transfer line temperature was set to 280 °C. Measurements were performed in split mode using helium as the carrier gas (flow rate 10 mL.min<sup>-1</sup>). The samples were methylated using TMSH (trimethylsulfonium hydroxide) 0.2 M in methanol from Macherey-Nagel before GC analysis.

### Fourier Transformed Infra-Red-Attenuated Total Reflection (FTIR-ATR)

Infrared spectra were obtained on a Thermoscientific Nicolet iS10 spectrometer using the attenuated total reflection (ATR) mode. The spectra were acquired using 16 scans.

### Size exclusion chromatography (SEC)

Size exclusion chromatography (SEC) analyses were performed in THF (40°C) on a PL-GPC 50 plus Integrated GPC from Polymer laboratories-Varian with a series of four columns from TOSOH (TSKgel TOSOH: HXL-L (guard column 6.0mm ID x 4.0cm L); G4000HXL (7.8mm ID x 30.0cm L) ;G3000HXL (7.8mm ID x 30.0cm L) and G2000HXL (7.8mm ID x 30.0cm L)). The elution of the filtered samples was monitored using simultaneous refractive index and UV detection. The elution times were converted to molar mass using a calibration curve based on low dispersity (M<sub>w</sub>/M<sub>n</sub>) polystyrene (PS) standards.

Size exclusion chromatography (SEC) analyses were performed in DMF or DMSO/DMF (20/80) (80°C) on a PL-GPC 50 plus Integrated GPC from Polymer laboratories-Varian with a series of three columns from PLgel (PLgel 5μm Guard (guard column 7,5mm ID x 5,0cm L); PLgel 5μm MIXED-D (7,5mm ID x 30,0cm L) and PLgel 5μm MIXED-D (7,5mm ID x 30,0cm L)). The elution of the filtered samples was monitored using simultaneous refractive index and UV detection. The elution times were converted to molar mass using a calibration curve based on low dispersity (M<sub>w</sub>/M<sub>n</sub>) polystyrene (PS) standards.

### **Differential Scanning Calorimetry (DSC)**

Differential Scanning Calorimetry (DSC) measurements were performed on DSC Q100 (TA Instruments). The sample was heated from  $-70\text{ }^{\circ}\text{C}$  to  $200\text{ }^{\circ}\text{C}$  at a rate of  $10\text{ }^{\circ}\text{C}\cdot\text{min}^{-1}$ . Consecutive cooling and second heating run were also performed at  $10\text{ }^{\circ}\text{C}\cdot\text{min}^{-1}$ . The glass transition temperatures and melting points were calculated from the second heating run.

### **Thermogravimetric analysis (TGA)**

Thermogravimetric analyses (TGA) were performed on TGA-Q50 system from TA instruments at a heating rate of  $10\text{ }^{\circ}\text{C}\cdot\text{min}^{-1}$  under nitrogen or air atmosphere as mentioned in the manuscript.

### **Dynamic Mechanical Analysis (DMA)**

DMA RSA 3 (TA instrument). The sample temperature was modulated from  $-80\text{ }^{\circ}\text{C}$  to  $220\text{ }^{\circ}\text{C}$ , depending on the sample at a heating rate of  $5\text{ }^{\circ}\text{C}/\text{min}$ . The measurements were performed in a 3-point bending mode at a frequency of 1 Hz, an initial static force varying between 0.1 and 0.5 N and a strain sweep of 0.1%.

### **Optical microscopy**

Optical images were obtained using a Leitz Laborlux K polarizing microscope equipped with a digital camera (moticam 2 000 2.0 M pixels) connected to the computer. The spherulite morphology was observed in thin films prepared between microscope coverslips.

### **High-performance liquid chromatography (HPLC)**

HPLC was performed using a Spectra system instrument fitted with a Phenomenex Luna  $5\mu\text{C}18$  100A column and compounds were detected with a Sedere Sedex 85 LT ELSD detector at  $40\text{ }^{\circ}\text{C}$  (G=4, filter OFF). These analyses were performed with a methanol/water gradient in the second chapter and in acetonitrile in the third chapter at a flow rate of 1 mL/min.

### **Flash chromatography**

Flash chromatography was performed on a Grace Reveleris apparatus, employing C18 reversed-phase cartridges from Grace and a water/methanol gradient solvent (cf chapter 2) equipped with a ELSD and UV detectors at 254 and 280 nm.

### **Mass spectroscopy**

(FD) spectra were performed by the Centre d'Etudes Structurales et d'Analyses des Molécules, CESAMO (Bordeaux, France). The measurements were carried out on a TOF mass spectrometer AccuTOF GCv using an FD emitter with an emitter voltage of 10 kV. One to two microliters solution of the compound is deposited on a 13mm emitter wire.

## **Dimères d'acides résiniques et de dérivés de la lignine : nouveaux précurseurs pour la synthèse de polymères bio-sourcés**

### **Résumé :**

Ces travaux de thèse traitent de l'utilisation d'une molécule polycyclique, l'acide abiétique, issu de la colophane, et de dérivés phénoliques potentiellement dérivés de la lignine, pour la synthèse de polymères rigides bio-sourcés. Dans les deux cas, des monomères symétriques et difonctionnels sont élaborés par réaction de dimérisation des précurseurs bio-sourcés puis testés en polymérisation. D'une part, les dimères de l'acide abiétique obtenus par un mécanisme cationique possèdent des structures mal définies qui compliquent leur polymérisation. Ces dimères ont alors été estérifiés avec de l'undécénol afin d'obtenir un composé bis-insaturé qui est ensuite polymérisé par ADMET. D'autre part, un procédé de dimérisation de molécules phénoliques, potentiellement issues de la lignine, a été développé par voie enzymatique utilisant une laccase. L'avantage majeur de ce procédé 'vert' réside dans la séparation très simple entre le monomère, soluble, et son dimère, insoluble. Ces dimères ont ensuite été modifiés chimiquement afin de constituer une bio-plateforme de composés biphenyles fonctionnels. Ces composés ont été utilisés pour la synthèse de polyesters, polyamides et résines époxy qui présentent des propriétés thermiques et thermomécaniques remarquables.

**Mots clés :** Acide abiétique, dimères, vanilline, dérivés de la lignine, laccase, polycondensation ADMET, résines epoxy.

## **Resinic acid and lignin derivative dimers : new precursors for the synthesis of biobased polymers**

### **Abstract :**

The aim of this thesis is to investigate new biobased rigid synthons for the synthesis of polymers with high thermomechanical properties. A polycyclic biobased molecule, i.e resinic acids, and phenolic compounds potentially derived from lignin, such as vanillin were selected. Both classes of substrates were dimerized in order to get difunctional symmetric synthons. On the one hand, abietic acid dimers synthesized *via* a cationic mechanism presented an ill-defined structure. To avoid reactivity issues, dimers with reactive terminal double bonds were successfully synthesized by esterification of abietic acid dimers with undecenol and polymerized by ADMET methodology. On the other hand, we developed a "green" process to dimerize phenolic compounds derived from lignin in large quantity and high yield *via* enzymatic catalysis using a laccase. The main advantage of this method is that the phenolic monomer is soluble in the reaction medium while the dimer precipitates. After chemical modifications of the dimers, we built a functional bio-platform of biphenyl derivatives. The latter were then used for the synthesis of polyesters, polyamides and epoxy resins which exhibited remarkable thermal and thermomechanical properties.

**Keywords :** Abietic acid, dimer, vanillin, lignin derivatives, laccase, polycondensation, ADMET, epoxy resins.